DIRECT CONTACT HEAT TRANSFER BETWEEN AN EVAPORATING FLUID AND AN IMMISCIBLE LIQUID

MARTYN JOHN LENCH

A thesis submitted in partial fulfilment of the requirements of the Council for National Academic Awards for the degree of Doctor of Philosophy

August 1991

The Polytechnic of Wales in collaboration with British Steel

Direct Contact Heat Transfer Between An Evaporating Fluid And An Immiscible Liquid.

Abstract of thesis submitted for PhD by M.J. Lench, August 1991.

An investigation has been conducted into the process of cooling water by the evaporation of droplets of isopentane in direct contact. The research has potential industrial application to a pickling acid recovery crystalliser. In order to minimise industrial equipment size a counter current flowing apparatus was developed and studied. Studies of optimum column height were carried out over a wide range of flow and drop size values.

Several computer based models have been developed to predict optimum column height. The results of initial models were used to modify experimental work and gave rise to the measurement of initial drop size using a high speed video camera technique.

A more sophisticated version of the computer based model has been developed and is the major product of this research. This included the development of a dimensionless correlation for instantaneous heat transfer to an evaporating droplet. This is based on existing correlations which are compared and modified empirically. The correlation produced is:

$$Nu = 2 + 0.76\ Re^{1/3}\ Pr^{1/2}$$

The computer model with this correlation is accurate to within 22%. The model assumes an average vapour half opening angle (β) of 135^{o} based on published work. Drop velocities are based on terminal values and rigid sphere behaviour of 2-phase droplets is assumed. The final model assumes that the

vapour and liquid dispersed phase remain attached as they rise through the column.

Reynolds number of the continuous phase is found to have no independent effect on minimum evaporative height.

The pinch temperature difference in the temperature profiles through the evaporative column is found to be significant in determination of minimum evaporative height. An approximate relationship of the form:

$$\text{Minimum evaporative height} \propto \Delta T_{pinch}^{-0.5}$$

is proposed.

Acknowledgements

I wish to thank Dr H. Worthington and Dr W.H. Granville for their guidance and supervision of the work performed for this thesis.

I also wish to thank the staff of the Department of Science and Chemical Engineering for the assistance they have provided and my immediate family for their tolerance and support. Finally I wish to thank British Steel Welsh Laboratory for their collaboration.

Contents

Contents

Contents

Contents

Contents

List of Figures

List of Figures

1. Introduction

1.1 Background

High energy costs, particularly present since 1973, give a financial incentive to reduce energy consumption in many processes. Initially the more straightforward means to reduce energy usage (e.g. improved insulation) were undertaken by the process industries, but as energy costs continue to remain high and the simple means of conservation have been implemented it becomes necessary to undertake research into the application of more involved systems.

In general terms, when a process requires cooling to a temperature below that easily achieved by water or air based heat exchange, energy and capital costs are likely to rise substantially. Refrigeration plants are both high in energy use and high in capital cost compared to a simple heat exchanger based system. Thus a low temperature cooling system which is more efficient and has a low equipment requirement has considerable practical application. The subject of this research relates to such a system. The work on this project was carried out on a part-time basis and was completed in 1991.

Greater efficiency of cooling is achieved by having the refrigerant in direct contact with the hot fluid which simultaneously simplifies the equipment requirement.

A cooling operation which requires no heat exchanger surface area has a greater practical application in unit operations in which the exchanger surface becomes rapidly fouled or clogged, corroded, or is otherwise difficult to operate, for example for reasons of thermal sensitivity. Scraped surface heat

exchangers are often a problematical design solution due to the scraping mechanism becoming fouled, clogged, etc. along with the exchanger surface. Just such an operation inspired the direction of the research into direct contact heat transfer between an evaporating fluid and an immiscible liquid.

1.2 Practical Application To An Acid Recovery Operation

An offstream from the steel making process consists of sulphuric acid which has been used to remove iron oxide scale (pickle liquor). The removal process produces a 60-70 g l^{-1} solution of ferrous sulphate in aqueous sulphuric acid which is pre cooled to around 42°C . The ferrous sulphate needs to be removed to allow recycling of acid, which is more economic and environmentally desirable than the alternatives. This is carried out in the Lurgi system by a chilling crystalliser which uses a steam ejector system to reduce the pressure of the pickle liquor in a large vacuum evaporator plant. Heat is removed as latent heat by evaporation of water from the liquor, which thereby cools to 6°C. The concentrating and cooling effectscause crystallisation of the FeSO4.7H2O which is removed by centrifuge as a saleable item. Sulphuric acid solution is recycled via a preheater. This evaporation process hinges on the hard vacuum induced by the steam ejectors. This gives a considerable energy cost for steam used at a rate of 2200 kg h^{-1} (a cost of around £20 per hour). A process based on direct injection of a suitable immiscible volatile liquid droplet to the liquor, which would then itself evaporate and be drawn off as a vapour is likely to give a saving in running costs of around 87%[1], and a relatively low capital cost. At the present time alternatives such as ion exchange produce large scale disposal problems. Therefore research into the practical feasibility and theoretical mechanism for such a direct contact evaporative cooling has a practical and potentially economic application.

At inception the process of direct contact heat transfer was thought to be entirely novel. Subsequent literature searches however found that work had been done in this field, mostly for application to water desalination by crystallisation. This did limit the anticipated scope of the study slightly in order to ensure originality, however the potential applications and configuration of the process are wide, as this study of a counter current process related to acid recovery shows.

British Steel have collaborated with this project, providing support with equipment and advice via the Welsh Laboratory. Further research is being carried out on a pilot plant scale into the practical application of a butane refrigerant system with condensation of refrigerant.

1.3 The Study Of Direct Contact Heat Transfer

The practical and safety aspects of the system and laboratory workspace put several constraints on the study. Firstly the selection of an appropriate refrigerant had to be made. For reasons which are detailed later this favoured a low molecular weight hydrocarbon, initially proposed as n-butane. In limited laboratory space a direct simulation, even on a small scale, of the pickle liquor industrial system has potentially serious safety risks. Considering that the system contains hot sulphuric acid under agitation with a flammable hydrocarbon vapour/liquid mixture, the potential dangers to personnel in the event of an accident are self evident. For this reason it was decided that water would be substituted for the pickle liquor since the study of the mechanism was still valid, differences in physical properties being allowed for during any subsequent scale up to pilot plant. In order to minimise risk of hydrocarbon vapour explosion it was required that the equipment be ventilated in a fume cupboard, to maintain at all times a vapour concentration below the lower

flammability limits. This would also prevent the "creeping" effect of a denser-than-air flammable vapour which can lead to localised high concentrations in low level pockets. This size was limited by available fume cupboard space, and this scale limitation eventually had a consequential effect on selection of refrigerant.

The system under study is inherently complex since it is a three phase-system (2 liquid phases, 1 vapour phase) involving heat transfer and simultaneous phase change by mechanisms which are so far not well theoretically understood. In order to reduce the number of variables and gain a meaningful result therefore it is desirable to simplify the system as far as possible. This consideration also justifies the selection of water as a hot medium, and also has led to the study requiring steady state conditions and initial refrigerant injection as a single phase (liquid droplets).

1.4 Mechanisms Involved In Direct Contact Heat Transfer

The water in the column is usually referred to as the continuous phase, or CP, and the immiscible refrigerant as the dispersed phase or DP.

The heat transfer between a droplet of immiscible liquid injected into a water column of higher temperature can be divided for simplicity into several regions:
1. Sensible heat transfer between the two liquids (up to the boiling point of the refrigerant droplet).
2. Evaporative heat transfer between the droplet liquid and vapour phases.
3. Heat transfer between the water column and the refrigerant vapour.

(1) is initially straight forward. (2) is likely to give the greatest heat transfer coefficients. (3) is likely to give a relatively very low heat transfer coefficient

due to the poorer thermal properties of a vapour. However, in reality these 3 stages are not necessarily separate and consecutive. Work done by Sideman and Taitel [2] on a static water column shows a considerable amount of vapour surrounds the liquid droplet as it rises. This will cause insulation of the droplet, replacing the relatively high heat transfer coefficients present by mechanisms (1) and (2) with the lower value in (3). The vapour attachment or detachment from the liquid and disruption of heat transfer under flowing CP conditions is an important part of the heat transfer process. For this reason, as well as practical considerations, a counter current flowing system is studied in this work, as opposed to the static water column of Sideman and Taitel. The flow and potential for turbulence in the column is therefore important for its effect on heat transfer film coefficients but also for its effect on distorting the vapour bubble and inducing detachment from the liquid bubble. The important parameters governing the fluid mechanisms of the system are therefore those that will affect Reynolds number i.e.:

a Droplet / bubble diameter

b Fluid density

c Fluid viscosity

d Fluid relative velocity

e Column diameter

(d) is affected by several factors:

(i) The injection rate of the droplet

(ii) The flowrate of the water in the column

(iii) The flotation affect caused by density difference between refrigerant (in both phases) and water, given by Stokes Law.

Note that (iii) also will therefore include (b) and (a) as important parameters. Finally there is some mass transfer going on in the system, although in its

effect on heat transfer much of it can be neglected:

(i) Immiscibility is a relative term which means very low miscibility. Refrigerants immiscible with the cooling water are selected to prevent contamination, however care must be taken to prevent addition of emulsification agents in processes such as foodstuff preparation, where small amounts of contamination are critical.
(ii) A typical hydrocarbon refrigerant vapour is slightly soluble in the water. This is a small but measurable effect.
(iii)The refrigerant vapour will become saturated with water vapour.

The effects of (i) and (ii) are small except that they may be sufficient to provide low level contamination of the water which could prevent use of the system in a sensitive area e.g. production of hydrated crystals for consumption as a foodstuff. The effect of (iii) is small, but can be allowed for and its significance depends on vapour rate.

Thus it can be seen that the mechanisms are complex. Further discussion and simplification of the system is dealt with in the theory section.

1.5 Scope Of The Study

The practical research carried out can be divided into the main areas of effort:
(i) Heat transfer measurements.
(ii) Droplet size measurements.
(iii) Computer model development.

This involved the construction and development of two experimental apparatuses and the use of a fast digital microcomputer to model the results

gained.

Theoretical work is based on the results of the above, although, given the industrial collaboration and practical application of this process, a large degree of emphasis is placed on practical utility rather than intensively theoretical study.

2. Theoretical Considerations And Literature Review

2.1.1 Introduction To The System Under Review

Direct contact heat transfer between immiscible liquids is heat transfer via a liquid to liquid interface without an intervening surface. To achieve high surface area for transfer, one liquid (the dispersed phase or DP) is broken up into droplets and contacted with the other liquid, which is usually kept as a continuous liquid medium (continuous phase or CP). The DP is usually that present in the lower quantity, and if evaporation is to take place then this will inevitably be of the dispersed phase due to relative heat capacity effects. The dispersed phase is often selected as a refrigerant liquid which has the necessary boiling point and immiscibility and is chemically inert.

The direct contact heat transfer process between liquids has the advantage of eliminating heat transfer surfaces which are prone to corrosion and fouling particularly in a hot acid crystallised process (see section 1.2). In addition, if phase change occurs, a larger capacity for heat absorption is available. In order to maximise surface area the evaporating phase is introduced as droplets which become bubbles in a dispersed phase (DP). The mechanism of heat transfer between two immiscible liquids and dynamics of a vaporising drop are fairly complex when compared to a single phase DP where the droplet or bubble is of constant diameter.

In the system studied droplets of isopentane of various diameters were injected into a continuous phase (CP) consisting of hot distilled water flowing counter current to the rising droplets. The inlet temperature of the CP is varied as are flowrates of both phases. The selection of isopentane was made for practical reasons discussed later (section 3.1). Sideman and Taitel [2] found

only small differences between related systems with sea water / butane and distilled water / pentane and distilled water / butane.

2.1.2 Aims Of The Study

The research carried out was planned with consideration for the potential practical aspects of the process already described (see section 1.2). For this reason when discussions of direction and choice of parameter were made it was with a view to making the results of practical utility rather than following interesting but more theoretical avenues of investigation. Thus the main parameter examined is that of minimum column height to achieve total evaporation of DP since this is crucial to optimum sizing of practical equipment whilst still being a very useful measurement which incorporates the combined effects of the various mechanisms involved.

In addition it is important that the contribution of this research should be original. Some studies of theoretical aspects of direct contact heat transfer were published in the duration of this study. Many potentially interesting areas of study were therefore not prosecuted where they were found to have been already studied. A consequence therefore of preserving originality so far as is possible is that the corroborative value of other work, and vice versa,is limited. As is described below, much work in the field is being carried out on the theoretical production of equations to describe the evaporative (and condensing) mechanisms of direct contact heat transfer, and so avoiding duplication steers this study toward a more practical vein.

In order then to meet the aims of practicality and originality this study uses a DP which has undergone some other studies, in a counter current flowing environment, which is of practical utility but makes theoretical study more

difficult and inevitably leads to simplified modelling of the system. Considerable development of the computer program based on simple models is carried out since these form a useful end product and incorporate the most accurate form of the simple model for prediction of MEH. Literature surveys have found no other instances of study of a counter current isopentane / water system with computer model development.

2.2 Review Of Other Direct Contact Heat Transfer Work

2.2.1 Practical Application Studies

A great number of studies have been reported on practical applications of direct contact heat transfer where no phase change takes place. These can be related to bubble columns [3], [13] which are often used for 2 phase reaction processes and for which study of heat transfer mechanism is still being carried out [14], [15]. This 2 phase system is simpler than the evaporating liquid system yet is still not well described.

Much work on the evaporating liquid process has been done in order to provide an economic desalination process, however reverse osmosis is now the preferred process, accounting for 85% of new desalination capacity in 1990 [16]. Multi stage flash is the less favoured option since it is energy intensive. Wilke et al [17] carried out economic study of a direct contact desalination plant where cold sea-water was evaporated by direct contact with a hot liquid in order to gain the practical benefits of the process. They concluded that the process had favourable total costs. Most other studies use evaporative cooling of the dispersed phase to freeze sea water producing crystals of desalinated sea water [28] for recovery. The energy relationships were studied by Weigandt [18] based on DP refrigerants which gave a suitably

low boiling point (n-butane, isobutane and methylene chloride). He concluded the energy relationships made the freezing process look attractive. Many of the references quoted in later sections refer to studies which find practical application in desalination processes.

7 000 lb / day and 20 000 lb / day desalination plants at A.E.R.E. Harwell, U.K. were used by Denton et al [19], [20] to study on a pilot plant scale the feasibility of a process using butane to induce freezing. One interesting conclusion was that crystal quality improved with higher butane flowrates because of the higher agitation effect. The practical aspects of the apparatus were investigated and found to be largely trouble free. However the use of butane did cause performance problems at high throughput after long operating periods when it accumulated in the post freezing wash column. This shows that in a butane based crystalliser, build-up of butane in crystal slurries must be monitored carefully because it may impair performance.

Cosmodyne Inc. have patented a direct contact crystalliser which uses butane to crystallise Glauber salt from sodium sulphate solution [22].

Mobil Oil have patented a direct contact crystalliser invented by Fowles et al [21] in order to remove crystals of durene from an aromatic fraction using n-butane as evaporating DP. This shows that other crystallisation processes have been tested using direct contact heat transfer. Despite this a recent review of types of crystalliser [55] made no mention of direct contact systems.

Kisakurek et al [22] have studied the liquid-liquid direct contact heat transfer without phase change between salt-water and a heat transfer oil and refers to earlier (pre 1983) work in this area. They quote practical applications as desalination and nuclear reactor cooling. The study is very specific to the

system used.

Raina and Grover [41] refer to a potential application in power generation utilizing geothermal energy. Battya et al [44] refer to a potential application in ocean energy conversion and thermal energy storage.

Finally some study has been done on direct contact condensation heat transfer which is currently under study at British Steel. Sideman has published wide ranging work with a view to desalination processes in 1965 [23] and 1982 [24], Tamir et al [25] study condensation of CS_2CCl_4 in water, and Pattantyus-h [26] investigates the collapse time of vapour bubbles.

The potential application of this research to acid recovery appears to be novel.

2.2.2 Studies In Heat Transfer

This section deals with published work in the area of direct contact heat transfer with the emphasis on theoretical application. Some studies inevitably also include bubble / droplet movement investigation but where practicable this is left to the next section.

The mechanism of heat transfer and the dynamics of a vaporising two phase bubble / droplet are highly complex [29], [30], [31]. After the drop is injected sensible heat transfer takes place to raise the drop temperature. After reaching the DP boiling point evaporation will begin to take place. Klipstein [32] found that the dispersed liquid droplet did not evaporate even when the temperature of the CP medium in which it formed was much higher than the boiling point of the liquid. This is attributed to nucleation problems with the vapour bubble. Moore [33] reported that liquid droplets had to be greatly superheated in order

to initiate vaporisation. The effect of superheat was manifested as an "explosive" evaporation. The amount of superheat required depends on the initial diameter of the dispersed liquid droplet.With highly pure systems as much as 100°C superheat was found [2], [33], [36].

Nucleation is more difficult with droplets of smaller initial diameter and is assisted by the presence of gas bubbles, impurities and increased turbulence which are likely to be present under normal industrial conditions [2]. For experimental work various methods to avoid superheat have been used. Sideman and Taitel introduce small (below 0.1 mm) gas bubbles into the continuous medium [2]. Klipstein [32] used an electric power pulse through a nichrome wire. Prakash and Pinder [34] inject each droplet with a tiny air bubble. Raina and Grover [31] use a Teflon tip which has a surface tension higher than the DP and lower than the CP media. This latter method has been found to be ineffective for small drops.

These findings had some impact on experimental design. Since the study was intended for industrial scale up where nucleation problems were unlikely (as mentioned earlier) it would be advantageous to avoid problematical nucleation regimes where possible. Use of a Teflon tip is possible but unreliable and adds complexity to the equipment. Using impure water for the CP was ruled out as this may have indeterminate effects in other areas. However there is scope for specifying drop diameter and temperature driving forces. Mean initial drop diameter is always significantly above the 2 mm threshold for nucleation difficulty proposed by Raina and Grover [31]. This threshold is not derived for a flowing CP column but it is based on a range of systems including isopentane / distilled water.The CP inlet temperature in my study is kept fairly high. Its minimum value is around 9°C above the DP boiling point. It is therefore anticipated that applying these limits together with the improved nucleation due

to CP motion should avoid nucleation problems. This is borne out by the experimental observation that, whilst "explosive" evaporation (noisy, 'thumping' agitation behaviour) is sometimes observed during warm-up of the apparatus, it is not present at steady state operation. It is ironic that the line boiling behaviour of n-butane which proved so problematic (see section 3.1) in this research study could actually be of some benefit industrially as the vapour injected would aid evaporative nucleation.

When evaporation is initiated, heat transfer to the bubble / droplet will continue. The heat transfer mechanism will depend on the geometry and relative distribution of attached vapour in the bubble / drop. Transfer can take place from via CP liquid film to the DP liquid film direct or to the DP vapour film and thence to the DP liquid. Once evaporation is initiated transfer rates will depend on relative areas of vapour and liquid DP in contact with the CP and on the size of heat transfer film coefficients for the three films involved. All reported work makes two assumptions about the process:

(i)The resistance of the CP / DP interface is negligible - all resistance to heat transfer lies in the fluid film. This assumption is common in heat transfer two film models and is well supported by applications of these models to empirical measurements.

(ii)The heat transfer between the CP and DP vapour bubble is negligible. This is justified by considering typical values of film coefficient of heat transfer for liquid / liquid and liquid / vapour heat transfer:

Fluid	Approximate heat Transfer Coefficient ($W\ m^{-2}\ K^{-1}$)
Water	1700 -11350
Organic Solvents	340 - 2840

Evaporating Organic Solvents	850 - 2840
Gases	17 - 280

It can be seen that the value of film coefficient is likely to be much lower with the liquid / vapour films than with the liquid / liquid films.

Both of these assumptions were first made by Sideman et al [2], [3] and since they are reasonable have been accepted by other subsequent research workers and are made herein.

Study of heat transfer broadly lies in two areas then: calculation of appropriate heat transfer coefficient, and evaluation of the appropriate heat transfer area. The following literature review will therefore concentrate on the main findings in these areas.

The earliest literature review of literature relevant to this subject was made by Sideman and Shabtai [3] in 1964 and this report is used instead of making an individual survey into pre 1960 literature. Thus the earliest theoretical reference directly accessed is 1958. The following review is made in chronological order.

Bird, Stewart and Lightfoot [35] quote the following relationship for mean heat transfer coefficient for forced convection applied to a non-evaporative submerged sphere in an infinite flowing fluid:

$$h\,D / kc = 2.0 + 0.60\,(D\,uc\,\rho c / \mu c)^{1/2}\,(Cpc\,\mu c / kc)^{1/3} \qquad \{eqn\ 2.2.1\}$$

this is similar to that of Rowe et al [11], discussed later.

In their 1964 review of other work Sideman and Shabtai [3] discuss the many

relationships for non evaporating systems based on dimensional analysis for CP Nusselt no.. They find many relationships of the form:

$$Nu = f\ (Rec, Prc, Wec, \rho d / \rho c\ , \mu d / \mu c\ , ad / ac) \qquad \{eqn\ 2.2.2\}$$

and describe some work of a limited nature to determine the empirical coefficients, however this is handicapped by the interrelational nature of the dimensionless groups. This work has produced the equation:

$$Nuc = 2.44 \times 10^{-12}\, Red^{0.9}\, Rec^{0.2}\, Prd^{0.5}\, Prc^{0.5}\, Fo^{-0.14}\, Gr^{1.8}\, K^{-0.5}\, L^{-1.5} \qquad \{eqn\ 2.2.3\}$$

where:

Fo = Fourier No ($a \times time / D^2$)

Gr = Grashof No ($D^3\, g\, \rho c\, \Delta\rho / \mu c^2$)

K = log mean average distribution coefficient

L = a geometrical factor

which serves to illustrate the complexity of the system. This equation applies to a non-evaporating droplet - thus any comprehensive study of the evaporating droplet system must be even more involved.

Furthermore, Sideman and Shabtai divide drops into two main practical size categories: "small", below 1 to 3 mm diameter and "large" 2 to 7 mm diameter. The larger drops exhibited higher heat transfer coefficients and although the transition diameter depends to some extent on the system, the transition from lower to higher heat transfer coefficient is abrupt. This is attributed to internal circulation in the large drops whilst small drops behave rigidly. Thus although it may be thought advantageous to minimise drop diameter in order to maximise heat transfer area, there is a diminishing advantage below 2 to 3 mm diameter. On a larger scale process with higher flowrates then drops of the range 2 to 7 mm are likely to be more practicable and this range is therefore studied in this thesis. Sideman quotes an equation for larger drops (>2 to 3 mm) for

$$Nuc = 0.42 (\Delta\rho\ \rho c\ g\ D^3 / \mu c^2)^{1/3} Prc^{1/3} \qquad \{eqn.\ 2.2.4\}$$

although he recommends it is treated cautiously since it indicates that h is independent of D.

In 1964 Sideman and Taitel [2] reported their own work on evaporating immiscible drops of butane and pentane in sea water and distilled water. This involved high speed cine photography of bubbles / droplets rising through a static column, and analysis of heat transfer rates. The cine work forms a basis for later work in the area and shows the way liquid DP sinks to the bottom of a two phase bubble yet remains attached in a static CP environment. The geometric model and coordinates of a two phase droplet defined in this paper have been widely adopted and are shown in fig 2.1. In later literature these have been slightly modified to take account of sloshing effects (see later) but are still relevant and have been adopted in this study. Time and evaporation level, drop velocity and heat transfer coefficient analysis is reported for the static column systems for drops of 1.9 to 3.7 mm. To summarise these findings:

1.There is little difference between any of the pentane or butane / sea water or pentane / distilled water systems. Butane / distilled water indicates different behaviour, probably due to localised freezing.

2.Level of drop evaporation is inversely proportional to the temperature difference between CP and DP (ΔT).

3.The order of magnitude of instantaneous heat transfer coefficient based on actual area are 1 000 to 2 000 kcal $m^{-2}\ h^{-1}\ {}^{o}C^{-1}$ for D^* (initial diameter) = 3.5

mm and 2 500 to 3 500 kcal m^{-2} h^{-1} $^{o}C^{-1}$ for D^{*} = 2.0 mm.

4.h is largely independent of ΔT for the range 4°C to 15°C.

5.The rising velocity of the DP is proportional to the amount evaporated, increasing moderately above 1% evaporation. Average velocities in this range are 25 cm s^{-1} for D^{*} = 3.5 m and 22 cm s^{-1} for D^{*} = 2.0 mm.

6.This equation can be used to evaluate average instantaneous heat transfer coefficients:

$$Nu = ((3\cos\beta - \cos^{3}\beta + 2) / \pi)^{0.5} Pe^{0.5} \qquad \{eqn.\ 2.2.5\}$$

where 2β is the vapour opening angle (see fig 2.1), Peclet number, Pe is used instead of separating Re and Pr, of which it is the product. This therefore implies that exponents to Re and Pr are both 0.5 so the terms can be combined. It is suggested that $\beta = 135^{o}$ (pre-Peclet group = 0.272) gives a good approximation to the heat transfer coefficients obtained.

This work provides something in the way of measurements for comparison and corroborative purposes albeit in a different i.e. static CP system. The motion of the CP present in my study will have an effect on the validity of all comparisons.

The specification of an average value of vapour opening angle has been useful in my model development (see later). The conclusion that there is little difference between hydrocarbon systems where freezing is not present assisted in the decision to choose isopentane as a refrigerant (see section B) since results can be applied to similar systems.

A review of published data by Rowe et al in 1965 [11] assesses the results of many researchers on heat and mass transfer to spheres and reports on corroborative experimental work. A relationship based on the CP is recommended for rigid spheres in size range 12.5 to 38mm and $10 < Re < 10^4$ is recommended:

$$Nu = 2 + B\, Pr^{1/3}\, Re^{1/2} \qquad \{eqn\ 2.2.6\}$$

where B = 0.69 in air and 0.79 in water. The Re exponent increases slowly from about 0.4 at Re = 1 to about 0.6 at $Re = 10^4$ but can be assumed constant at 0.5 in the range $20 < Re < 2000$.

This is a fundamental relationship for CP heat transfer and has been widely used. Therefore this expression is used and evaluated in the modelling work herein, where an appropriate value of B for the system is one parameter to be determined. Prior to this determination the value of 0.79, that for water, is used.

Prakash and Pinder [34] used a cine camera technique to study droplets of furan, cyclopentane and isopentane rising in a static column of distilled water. Measurements are made both of the initial 10% of evaporation and of full evaporation using a dilatometric technique. The relationships for isopentane / water with total evaporation is of more direct relevance to this study. They confirm that in a static column the bulk of the heat transfer appears to take place via the DP liquid section of a 2 phase droplet / bubble, and hypothesise that bulk heat transfer takes place in the turbulent wake region of the bubble / drop. Free convection is thought to be insignificant compared to forced convection at Re > 1000. The rate of rise of an evaporating drop was found to be nearly equal to the instantaneous terminal velocity.

They compare their results with those of Klipstein [32] and Sideman et al [2] and for the isopentane / water system find their correlation closer to Sideman's model. Discrepancies in Sideman's work are attributed to the difficulty of visually determining complete evaporation when the remaining liquid film is small and thin, even with high speed cine.

The best equation for isopentane water is given as:

$$Nu = 0.304\ Pe'^{0.5}\ ((\rho c - \rho d) / \rho c)^{1.78} \qquad \{eqn.\ 2.2.7\}$$

where Pe' is a viscosity modified Pe (see nomenclature, appendix 3). Weber number (We) was also considered in their dimensional analysis but was found to be insignificant. The equation is more conservative then Klipstein [32] and Sideman's [2], giving lower coefficients.

They also propose an equation for average heat transfer rate:

$$Qave = 2.84\ D^{*2}\ \Delta T \qquad \{eqn\ 2.2.8\}$$

The conclusions of Prakash and Pinder's work also have some input to this research. Their conclusion about free convection being insignificant at Re > 1000 leads to it being neglected in my work with a flowing CP. Their use of high speed cine measurements of drop velocity and conclusion that rising velocity is almost equal justifies the use of terminal velocity correlations for velocity prediction in my computer based models. The insignificance of We in the analysis (as is implied but not specified in other work) leads to its ready omission as a simplification in my work. Their isopentane - distilled water work in a static column is therefore a useful precursor to my flowing column work.

Their caveat about the difficulty of visually determining complete evaporation in a single droplet has been noted but is not a problem in my work since it is the net result of many bubbles incompletely evaporating which is visually determined in my work (see later) a method which is not so readily applicable to a static column.

Sideman and Isenberg [42] proposed an expression of the form:

$$Nuc = 0.977\, Pec^{1/2} (Cos\ \beta-(Cos^3\beta / 3)+(2 / 3))^{1/2} \qquad \{eqn\ 2.2.9\}$$

which has formed a basis for later work modified by others [38], [40], [41] but did not itself give a very good agreement with prior experimental work [2].

Adams and Pinder [37] use a dilatometric method to study the evaporation of isopentane and cyclopentane drops in static columns of glycerine- water solution. They propose the following empirical correlation for his own work and that of Sideman and Prakash:

$$Nud = 7550\, Prc^{-0.75} (\mu c / (\mu c+\mu d))^{4.3} Bo^{0.33} \qquad \{eqn\ 2.2.10\}$$

where Bo = Liquid Bond number $(\rho c-\rho d)D^{*2}\, g / \sigma$). It is interesting in that it uses DP Nusselt number and is based on initial droplet dimensions. Pr for the DP is reported not to be significant.

Simpson et al [38] studied butane drops evaporating in a brine and water column with a view to desalination equipment development. The butane was refrigerated prior to injection. His most important observation, made with cine techniques, was that when a spherical droplet evaporated it gave an ellipsoidal bubble in which remaining liquid 'sloshed' from side to side. Eventually the

bubble adopted the mushroom cap shape reported by other experimenters. The sloshing of the liquid film appeared to leave a film of liquid butane on the inside surface of the butane vapour bubble, having implications of increased film coefficient and heat transfer area. This observation led to the incorporation of 'sloshing effects' into the heat transfer models of Simpson and later experimenters. Since the sloshing model fits his own and Sideman's data well, Simpson concludes that it is an improvement on prior theories. Since this is a specific desalination study, most of Simpson's analytical results are specific to the butane / brine system and are not therefore quoted here.

Sloshing behaviour is an important point to consider in direct contact evaporative work. The mechanisms are not easy to determine but it is thought that with a flowing CP a greater degree of sloshing will occur. This sloshing effects DP film coefficient, making it large due to the thinness of the layer of DP on the inside of the vapour surface. If the layer covers all of the vapour bubble then vapour insulation of the heat transfer disappears. Alternatively the sloshing may only cover a proportion of the surface which can be described by the use of an average vapour opening angle and (as suggested by Sideman, see earlier) high internal film coefficients. The sloshing effects and heat transfer area results are reported by other experimenters (see later).

Pinder [39] uses three dimensional photography and a system of a more volatile and less volatile DP in a water CP to derive relationships for the inter surface areas. Unfortunately, the fairly complex empirical relationships rely on knowledge of instantaneous vapour opening angle to not take into account sloshing effects so if one agrees that sloshing is present these are of limited value.

Smith et al [46] developed the following correlation for single drop evaporation

using cyclopentane / water in a static column:

$$Nu = C\ Re^{x}\ Pr^{1/3} \qquad \{eqn\ 2.2.11\}$$

where the value of the constant C depends on initial drop diameter and the value of the exponent x. This work reflects the Rowe et al [11] equation 2.2.6.

Raina and Grover propose a theoretical model in 1982 [40] which is updated to incorporate sloshing effects in 1985 [41]. The 1985 model is reported to give reasonable agreement with the Sideman and Taitel 1964 [2] results, and assumed a rigid bubble obeying Stokes law for velocity calculation. The expression is a development of the work by Sideman and Isenberg [42] and Tochitani et al [43]. It is based on the CP and assumes that 'sloshing' of the unevaporated DP liquid in the 2 phase bubble causes an extension of the thin film above the level of the top of the liquid layer (see fig 2.2). This extension is such that the whole of the vapour inner surface is covered which is an assumption that is most accurate during the early stages of evaporation. It is further assumed that frequency of renewal of the film by sloshing is sufficient to prevent dry patch formation at the top (leading surface) of the bubble. Since the film is very thin it is assumed to have negligible inside resistance to heat transfer. It is reported that sloshing effects are non-existent in the case of small drops less than 2mm diameter. Comparison work is done on a pentane / water system which is therefore of direct application. They mention the significant point that interfacial and surface tensile forces are important in film attachment effects, and thus it is of benefit that their pentane / water system is close to that studied herein, since these forces are not readily evaluated.

The expression for the model incorporating sloshing effect is:

$$Nuc = 0.4629\ Pec^{1/3}\ (\beta-(\sin 2\beta / 2)^{2/3} \quad \{eqn\ 2.2.12\}$$

where 2β is the vapour opening angle. No average value for β which describes the overall system is recommended.

The assumption made in this model to enable sloshing to be dealt with are important for this work also. Firstly, since droplets over 2mm are studied, sloshing effects will be present. Secondly, the assumption that inside film resistance is negligible, which seems reasonable given thin layers in motion, allows analysis based on the greater resistance i.e. CP film resistance. Whilst it is accepted that sloshing is present, the assumption that it is sufficient to cover the whole vapour inner surface is not well justified. It is consistent with the observations of Simpson et al [38] but this was for a butane / water system. However, this assumption is more valid for a system such as that herein where CP motion induces additional turbulence to promote sloshing. It is interesting to note that Sideman suggested an empirical value of $\beta = 135^{\circ}$ to reproduce measured heat transfer coefficients, which remained approximately constant after initial evaporation. If the sloshing theory is correct this angle, which delineates the DP liquid drop, may still represent that which is available to heat transfer, the heat transfer taking place through the 270° (2β) arc of vapour sphere lined with liquid film rather than the remaining 90° arc of liquid. Equation 2.2.12 is supported by a relatively limited set of results and is therefore considered tentative.

Battya et al [44] review direct contact work in 1984 and finds that there is no generalised theoretical analysis of direct contact evaporation in immiscible liquids in the literature. Building largely on the work of Sideman and Taitel [2] and using pentane drops in a static distilled water column a parametric regression analysis for a range of dimensionless groups is carried out with

refrigerant R113 and n-pentane in a countercurrent water column. A maximum volumetric heat transfer coefficient of about 120 kW m^{-3} $^{o}C^{-1}$ for n-pentane water was found. The assumption is made that heat transfer takes place in the liquid-liquid interface only. The n-pentane drop size range is from 2 to 4 mm and ΔT between 1.5 ^{o}C and 15 ^{o}C. He reports some discrepancies in droplet velocity and evaporation height measurements when compared to equations 2.2.5 and 2.2.13, but does not suggest an alternative.

The system and analysis is quite relevant to this thesis and some overlap is present. However, the system used is n-pentane, not isopentane, drop size and ΔT are different and the treatment is analytically mathematical rather than a distributed finite difference computer model as used herein.

Shimizu and Mori [48] report work on droplets on n-pentane and refrigerant R113 in a static water column under elevated pressure. CP temperatures are taken up to 88^{o}C and pressures up to 0.48 MPa. "Small" initial drop sizes of 1.4 to 1.7mm are used. They are critical of the Battya et al relationship of eqn 2.2.13 and accompanying analysis, preferring that of Sideman and Taitel eqn 2.2.5 in their own analysis, when modified to take in to account a temperature difference accounting for water vapour effects. They recommend the equation:

$$Nu = 0.169\ Pe^{1/2} \qquad \{eqn\ 2.2.15\}$$

and report a fairly constant rise velocity of 20.3 cm s^{-1}.

Certain aspects such as the constant rise velocity and different correlation constants for this work can be attributed to the small drop size and consequent lack of sloshing and minimal bubble distortion. However, this paper is significant in that it generally supports the form of equation 2.2.5 rather than

drop diameters around 3 to 4mm and ΔT values up to 8°C. They report the following correlation for instantaneous Nusselt number:

$$Nu = 0.64\ Pe^{0.5}\ Ja^{-0.35} \qquad \{eqn\ 2.2.13\}$$

with Pe and Ja (Jakob number, $\rho c\ Cp\ (Tc-Td) / \rho dv\ \lambda$) being the major system dependents. In a later paper (1985) Battya et al [45] again based on regression analysis, relate the results from 2.2.13 to an average value of β of 90°, as opposed to the value of 135° proposed by Sideman and Taitel [2]. This recommendation is based on the Ja exponent and constant term in eqn 2.2.13 which is produced when the Pe exponent is mathematically forced to 0.5.

This work presents an alternative value for overall average β to that recommended by Sideman, based on a different heat transfer equation. No confirmation for either value has been found reported by other experimenters in the field, so the correct value cannot yet be chosen with any certainty. This is unfortunate as an appropriate value is of practical importance in sizing a system based on many theoretical relationships.

Raina and Wanchoo [30] report further work done on the sloshing model, eqn 2.2.12, based on evaporation time work. They also find that total evaporation time depends mainly on temperature gradient and initial bubble diameter for a given system. The work is based on experimental analysis by Sideman and Taitel [2]. Assuming as in ref [40] that the whole vapour surface is permanently covered by a thin film of liquid due to sloshing, and that it is this area only which is used for heat transfer,this relationship is proposed:

$$Nu=1.347(ud\ D / 2\ ac)^{1/3} \qquad \{eqn\ 2.2.14\}$$

Tadrist et al [47] report on the vaporisation of single and multiple droplets of

2.2.13. Thus in the absence of definitive corroborative work one would tend to prefer the equation 2.2.5 and 2.2.15 forms. The water vapour pressure effects would be expected to be more significant in pressure-related studies.

Mochizuke et al [51] report that electrical fields can enhance direct contact heat transfer.

Raina and Grover give details of their experimental technique in a 1988 paper [31]. Based on an overview of this literature simplifications and assumptions can be made to aid in the analysis of heat transfer in section 2.3.2 below. The literature also has an effect on determining the originality of research. Counter current studies are limited. The work of Tadrist et al [47] corresponds closest to the system under study, but in my study the refrigerant is isopentane not n-pentane, the drop size range studied is larger, the ΔT driving force range studied is greater and the experimental apparatus different. Mathematical analysis of theoretical models is common but incremental computer modelling has not been reported.

2.2.3 Bubble Droplet Size And Dynamics

The subject of predicting droplet size is a large one. A great deal of literature is available on the subject, which is not yet well theoretically described and understood. In the interests of brevity therefore most available space is devoted to the more significant heat transfer literature in the above section. Review of literature was made and the calculation of initial droplet size was attempted from equation such as:

$$v\rho = (F / 100)[(0.02155\ \rho\ do / \Delta\rho) + (1.356\ \mu c\ Vo\ do^3 / dp^2\ \Delta\rho) - (3.26\ \rho d\ do^2\ Vo^2 / \Delta\rho) + 4.80\ do^2\ (Vo\ \rho d\ \sigma / \Delta\rho^2)^{1/3}] \quad \{eqn\ 2.2.16\}$$

as given in reference [5].

The solution of this equation is by trial and error and is fairly involved. The interfacial tension, σ, is a property not readily available in data sources and recourse has been made to a values quoted in a publications, e.g. by Ito et al [6] who studied droplet size in an isopentane / water system. Given this accuracy limitation and the involved nature of the calculations, physical properties for the equation were calculated at an average temperature condition and sizes evaluated depending on the value of the major variable Vo.

The results of this equation were unreliable. Due to the importance of initial drop diameter to heat transfer as reported in the literature and the sensitivity of the computer model to the value (see section 6) it was decided to measure mean initial drop size empirically by a photographic method (see section 3). A review of methods for measuring drop / bubble size was consulted. Therefore, the rest of this section summarises drop dynamics rather than droplet size prediction.

Due to the interrelational nature of drop dynamics work and heat transfer, some dynamics work is covered in heat transfer sections and is not repeated here.

Literature reports already cited lead to the conclusion that droplet rising velocity can be calculated from terminal velocity equations with good accuracy. This is the method adopted in modelling work (see section 6). However, the assumption that a 2 phase bubble droplet can be treated as a rigid sphere when in reality it will distort merits discussion. Interfacial tension between DP (mainly vapour phase) and CP will determine the sphericity of the bubble / droplet as it rises and as already stated, these are difficult to determine. The bubble drop will be subject to these forces shown in fig 2.3. Drag forces at

Redc above 500 will be due to skin friction and form drag. The bubble will oscillate and distort to a shape which is determined by the balance between distortive drag forces and interfacial tension. In the absence of data we can only speculate based on literature [12] that at high vapour / liquid ratios the deformation may be sufficiently great that drag forces increase at the same rate as velocity and terminal velocity therefore becomes size independent. Qualitatively this would tend to give lower film coefficients than a spherical shape model, leading to the model under predicting MEH for this reason. However, this shape distortion would also tend to give higher area than the spherical shape model, leading to the model over predicting MEH. These two effects would tend to cancel out in direction, although magnitude remains unknown and must be accepted as a source of error.

Internal circulation will be present in the vapour DP bubble due to its low viscosity relative to the CP. This will tend to reduce velocity gradient at the surface, reducing drag and increasing velocity up to a theoretical maximum of 1.5 times terminal velocity [12]. The presence of liquid moving in the vapour bubble will however reduce this effect below the maximum by an indeterminate amount. This effect is not allowed for in the model, so directionally the model will assume a lower velocity and film coefficient and under predicting MEH.

The CP velocity is taken at its average value in the model. However, whilst the CP is flowing in laminar flow there will be a pronounced velocity profile in the column with a point value at the centre of double the mean velocity. Thus since the model takes into account both velocities the accuracy of the MEH predicted will in fact depend on the position the bubbles take in the column. For CP turbulent flow the velocity profile is not so pronounced with a central flow of 1.22 times the mean. In laminar CP flow CP velocity varies quickly with position in the column. The computer model uses mean velocity in all cases

since it is most readily available and is impractical to allow for droplet position in the column. However, the effect of CP flowrate is studied later. Quantitatively, since CP injection is to the centre of the column the effects of this assumption will be that whilst residence time may be accurately determined, the conversion into column height will be based on a uc value which is too low. This will lead to a prediction of MEH which is too low. However, since film coefficient calculation in the model is also a function of uc then this would tend to be under evaluated leading to a prediction of MEH which is too high. Again the effects oppose each other in direction and the magnitude of the resultant effect on the prediction cannot be determined. If this effect is marked it would show up by an improved accuracy of prediction in turbulent CP studies.

In the light of these indeterminate effects on velocity and with no recourse to practical measurement it is therefore assumed that terminal velocity relationships provide sufficiently accurate calculation procedure for heat transfer work, and the model uses this method. There is some support for this approach as previously mentioned by Prakash and Pinder [34].

Specific work on classification of the bubble / droplet or "two phase bubbles" in various configurations is reported by Mori [52]. The motion of evaporating droplets for a n-pentane / glycerol solution is examined by Raina et al [53], who later goes on to develop a rather involved relationship for 2-phase bubble velocity [29]. No comparison is made with terminal velocity relationships.

2.3 Development Of Theoretical Model

2.3.1 Assumptions On Simplification For The Heat Transfer System

This section summarises decisions about theoretical development based on the literature survey describing other work in the field and experience gained in the course of the study. The following key points are relevant:

1. Choice and range of refrigerant(s). N-butane was desirable from the point of view of approach temperature but proved impractical (see section 3.1). Isopentane proved practical and literature showed that a range of hydrocarbon refrigerants gives similar performance. An expanded study of a single refrigerant was adopted as a better use of time than a lesser study of several different types.

2. Orifice / drop size regime. The most interesting drop size regime appears to be the "larger" range i.e. 2mm and above. This is for reasons of avoiding nucleation problems and that such drops are reported as exhibiting internal circulation and vapour / liquid sloshing behaviour. Both effects would tend to improve heat transfer performance which is of practical value and offsets the usual choice which is to make drop as small as possible to increase surface area. For these reasons, and reasons of better visibility the injection orifice was sized to give drops of initial diameter >2mm at the appropriate flowrates. This was a trial and error procedure. The 1mm orifice chosen gave mean initial drop sizes in the range 2.8mm to 6.5mm over the full range of flowrates, with smaller injection pump. This enables a study of the 2mm range with some smaller drop work for comparison purposes.

3. Free convection heat transfer is likely to be swamped by forced convection.

Therefore only forced convection is studied. This is a good assumption at Re >1000.

4. Rising velocities can be calculated with good accuracy from terminal velocity relationships. Because of bubble vapour deformation this is likely to be a better assumption at lower percentage evaporation. A terminal velocity approach is adopted, noting that any inaccuracy is likely to give an under-estimation of velocity (and hence calculated MEH).

5. Sloshing effects. Sloshing of unevaporated liquid DP inside the rising vapour bubble has been reported but not fully described analytically. At its optimum effect for heat transfer, sloshing is thought to coat the whole of the bubble inner surface with a thin film of liquid. Work based on this then assumes that the major portion of heat transfer takes place via this thin film and that the amount of bubble surface remaining covered by bulk DP liquid can be assumed not available for heat transfer (see fig 2.2). This is an inversion of the heat transfer area assumption of the non-sloshing model in that in non-sloshing models it is the liquid bulk area rather than the vapour bulk area which is assumed to be significant for heat transfer. In a simplified study it is helpful to use an 'average area' for general use application over the evaporation process. This has only been supplied by Sideman and Taitel [2] who suggest an average vapour opening angle, 2β of 270^{o}. This work was based on reserved heat transfer before the data observations of sloshing behaviour. This value is still applicable if one assumes that sloshing was present in Sideman and Taitel's work, giving heat transfer enhancement but was not observed in photographic work.

If we assume that the simplified form of Sideman and Taitel's equation (eqn 2.2.5) applies for an average β:

$$Nu = 0.272\ Pe^{0.5} \qquad \{eqn\ 2.3.1\}$$

and compare this with the sloshing model equation of Raina and Grover (eqn 2.2.12):

$$Nuc = 0.4629\ Pec^{1/3}\ (\beta-(Sin\ 2\beta\ /\ 2))^{2/3}$$

Then if this latest sloshing model adequately represents the heat transfer of Sideman and Taitel we can equate both expressions for Nu. If we further assume that the different exponent for Pe can be neglected (i.e. $Pe^{0.33}$ approx. $=Pe^{0.5}$) then:

$$0.4629\ (\beta-(sin2\beta\ /\ 2)^{2/3} = 0.272 \qquad \{eqn\ 2.3.2\}$$

In the sloshing model (see section 2.3.3) this angle represents the sector unavailable to heat transfer. Thus the angle available for heat transfer is $360-(2 \times 53^{o}) = 254^{o}$. This would be equivalent to a value of β for Sideman's non-sloshing model of 127^{o}, close to the 135^{o} assumed.

The applicability of an 'average heat transfer area' as a percentage of that available does not rely on adoption of either a sloshing or non-sloshing model if it is based on heat transfer measurements. Heat transfer area and film coefficient calculation are interrelational and assumptions made about one will inevitably effect calculation of the other from rate equations. Therefore, whilst the average value of $\beta = 135^{o}$ is taken as best available in this study, it is necessary to link the film coefficient relationship work to this assumption, and to consider sloshing and area effects when discussing the results.

6. It is widely assumed with some justification that heat transfer is liquid / liquid

and that the bubble / droplet inside film resistance is negligible. This is assumed to be due to internal circulation, small amounts of DP liquid present and the presence of 'sloshing' providing turbulence and very thin film. Thus most work is based on outside film heat transfer coefficients which are assumed to be the lowest and thus rate limiting. In a turbulent CP outside film resistance is likely to be lower but the effects of turbulence on sloshing and circulation in the droplet would tend to decrease DP inside film resistance as well. It therefore is reasonable to base heat transfer work on the CP outside film coefficient, which is the approach adopted.

7. Form of dimensional analysis relationship. Dimensional analysis for heat transfer involving Nu is well known and there is little point in reproducing the theoretical derivation and dimensional analysis herein. Weber number, We, has been reported to be insignificant and most relationships are in the form:

$$Nu = f(Re, Pr)$$

for which the specific form can be analysed for any system. Some workers prefer to use Pe (= Re Pr) which implies that any exponent for Re and Pr is equal.

In this work the separated form was chosen so it could be related to a large volume of earlier work as summarised by Rowe et al [11]. The weight of this volume of work leads to the study of equation 2.2.6 to determine the correct value of β appropriate of direct contact heat transfer. Other derived equations are also studied but this one gives the best to fit experimental data (see section 7.3.3).

8. Development of results. The isopentane / water system has had some study

but not in an equivalent counter current flowing system. Reports in literature are limited to a theoretical treatment arriving at relationships based on dimensional analysis. No other workers report development of an incremental heat transfer model incorporating a relationship for instantaneous heat transfer coefficients, so this course was adopted to develop a model of the experimental results.

The basic theoretical model then is as follows. DP is injected through the orifice where it forms a liquid droplet. Mean diameter is related to flowrate based on experimental measurements.

The droplet rises under buoyancy forces at its terminal velocity. The distance taken to accelerate to terminal velocity is assumed negligible. The CP liquid flows downwards at a velocity less than the rising velocity. No heat is lost to atmosphere. Heat is transferred to the liquid droplet at a rate based on total surface area of droplet, outside film coefficient and temperature difference between the CP and lower temperature DP droplet at any point during the rise of the drop. The drop will increase in temperature until its boiling point is reached. This will depend on absolute pressure but an average value based on atmospheric pressure plus mean hydrostatic head pressure due to the appropriate column height is used in boiling point calculations. On reaching this temperature vapour nucleation takes place and the bubble / droplet continues to rise, DP vapour will either detach from the droplet or remain attached. (Both are considered). The effects of vapour attachment and sloshing are assumed to have a net effect of producing an average heat transfer area of 25% (corresponding to the $\beta = 135^{o}$ value) of the total spherical surface area of the DP vapour / liquid.

For surface area and velocity purposes the bubble / droplet is assumed to

have the same characteristics as a sphere i.e. distortion effects are negligible. As heat is transferred to the DP liquid, more evaporates until all of the DP is vapour phase. At this point the most significant heat transfer process is complete and the column height at which this occurs is of major practical significance.

The theoretical considerations involved in developing the computer based model are discussed either in this section or where more apposite, in section 6.

The following points are noted here. The incremental model makes an assumption about the temperature driving force for heat transfer. The column is divided into small increments of time (see fig 2.4). The appropriate mean driving force for counter current heat transfer is the log mean, which is derived by integration of the equation for a small element of heat transfer surface [49]. This would apply to the incremental heat transfer also. However, as the increment becomes smaller the temperature gradient over the increment for both phases becomes less steep (see figs 2.5 and 2.6). In this case
Tc(A) -> Tc(B) and Td(A) -> Td(B)
therefore LMTD -> (Tc(A) - Td(A)) = (Tc(N) - Td(N)) = simple ΔT
where A and B represent boundary values for the increment and N is the increment number. When the increment size becomes as small as a calculus increment this relationship is exact, being the equation from which LMTD is derived by integration. Even with finite sized small increments the simple ΔT can be used with good accuracy. This approach is taken in the more advanced computer models, with a checking routine imposed which reduces increment size if the inaccuracy of the simple ΔT assumption is above a tolerance value. In the simple overall model which has no such accuracy check, this assumption will lead to inaccuracy (see section 6).

The model assumption for the behaviour of the droplet as it boils and rises through the column represents a simplification. Real behaviour of the 2 phase droplet / bubble is not completely known but is thought to be as follows. When the droplet reaches its boiling point, it will nucleate immediately for drops above 2 mm diameter and begin to boil. The boiling point necessary will be that which applies at the droplet absolute pressure i.e. atmospheric plus hydrostatic head. When boiling has begun the hydrostatic head will reduce as the DP rises, causing the DP boiling point to decline with increasing height. This will cause the unevaporated liquid to flash. The DP bubble / drop temperature reduces as it rises, keeping to the prevailing hydrostatic boiling point. The latent heat for this evaporation is provided by cooling the remaining liquid. It is likely that inter phase heat transfer and mixing are sufficient to maintain a homogenous temperature for the DP liquid and vapour phases. Additional heat transfer from the CP will provide further latent heat of vaporisation for evaporation to DP liquid. The rate of heat transfer will depend on film resistances and ΔT driving force. As the DP rises its temperature reduces and so heat transfer from the CP will increase. ΔT driving force increases due to the imposed increase in CP temperature and the decrease in DP temperature, assuming coefficients do not vary significantly. Eventually all DP liquid is evaporated.

It is interesting to note that the reduction in DP temperature even while evaporating improves heat transfer and could lead to direct contact exchangers operating at low apparent driving forces.

It greatly simplifies the computer models to assume a constant boiling point for the DP. This is reasonable for the low MEH values in this work with the chosen refrigerant system. The constant value taken,which has to be calculated by iteration, is the atmospheric plus mean hydrostatic head for the MEH (see

section 6.3.2). The variation in boiling temperature between maximum and minimum MEH values in this work is 2.7 K. The effect of this assumption made in the model will vary with MEH and is illustrated in fig 2.7.In the diagram it is assumed that the MEH predicted from the model is close to the true case, which is a better assumption at low MEH values. Note the model assumes onset of boiling takes place earlier, giving smaller predicted MEH. However, since the sensible heat transfer is small compared to evaporative, this effect will be small. The deviations in driving force will tend to cancel out. The net effect of this amount will therefore be that true MEH will be slightly larger than that predicted by the model.

2.3.2 Bubble Drop Dynamics

The development of a model for heat transfer area has been discussed in section 2.3.1. This covered the use of an average value of half opening angle, β in the model derived from Sideman and Taitel's work [2] and its relationship to the sloshing model of Raina and Grover [41].

In order for the heat transfer model to work a choice does not have to be made between sloshing or non-sloshing models, provided the values used for average value of heat transfer area as a fraction of total area is accurate for either condition. A discussion of published models and diagrammatic representation of my model for heat transfer area is therefore brief. The best way to show the models concisely is by diagrams.

The range of models published are often very similar and can be shown by three generalised diagrams with nomenclature converted to a uniform basis.

The first diagram, fig 2.8, represents the simplified planar model which has

been used by Sideman and Isenberg [42] and as a reference point for Raina and Grover [41] and Tadrist [47]. This model is geometrically straightforward. Net heat transfer area is assumed to be liquid phase and arc subtended by $2\pi - 2\beta$. This model assumes no sloshing or interfacial tension distorting the plane upper surface of the liquid phase.

The second diagram, fig 2.1, represents the models of Sideman and Taitel [2], Battya et al [45] and Tadrist et al [47]. This shows a curved surface to the liquid portion which extends its area. This may be due to sloshing of the liquid up the sides or interfacial tension effects or both. The value of β will quantify the extent of these effects. The angle $2\pi - 2\beta$ subtends the whole of the liquid surface area and it is assumed that this is the net area available for heat transfer. Tadrist et al [47] reports that the angle β in this model was 75 to 85% of the value it would have if the planar model above applied.

The third diagram is fig 2.2. This represents the sloshing model of Raina and Grover [41]. This differs from the other two in that β is redefined. β in this case represents the half opening angle which would apply in a planar model (as in fig 2.8). Sloshing is assumed to coat the inner surface up to the radial limiter of angle γ. The net available heat transfer area is redefined as the surface subtended by the angle $(2\beta-2\gamma)$ i.e. the sloshed film only. Heat transfer to the bubble DP liquid subtended by angle $(2\pi - 2\beta)$ is discounted. This assumption differs from other models and is justified by noting that the sloshed film in angle $(2\beta-2\gamma)$ is very thin. In fact in their model development Raina and Grover go on to incorporate the observation of Smith et al, that sloshing covers the whole inner surface of the bubble and put γ equal to zero.

The assumption in my modelling is that average heat transfer area available for heat transfer = 25% of the total spherical surface area of the bubble /

droplet. This relates to the second model above with angle β of 135^{o} (as suggested by Sideman and Taitel [2]). Battya et al [45] suggests a β value of 90^{o} is appropriate, but this work has been criticised by Shimizu and Mori. I find the assumption that no heat transfer takes place to the bulk liquid in a situation where it is sloshing about questionable, and therefore have not adopted a model similar to Raina and Grover. This is not, however, to rule out the presence of sloshing. It is quite possible to achieve a mean heat transfer area of 25% of the total spherical area using the Raina and Grover model if by their definitions $\gamma = 0$ and $\beta = \pi / 2$ (45^{o}). Therefore whilst the second geometric model is taken as my basis the assumptions in the computer model are not geometric-model dependent. The only modification in the computer model is that the area would be reduced if there were insufficient DP liquid left to cover the surface, however, in fact this represents such a small proportion of total evaporative amount it is not really significant and the area reduction routine is not normally initiated in the iterative computer program.

The magnitude of error likely due to deviation from spherical shape on the models with large bubbles makes detailed analysis of the precise internal geometry rather impractical in application. This is another reason for adopting a simplified approach.

All of the models assume vapour remains in contact with its evaporating liquid. Whilst this is the most likely behaviour, in a flowing CP vapour disengagement is a possibility. For this reason a computer model including total vapour disengagement is developed and tested.

Initial droplet diameter measurement was carried out by direct measurement in a photographic method. Although the range of drops from initial diameters from just over 1mm to 6.5 mm was measured, data below 2 mm and above 6.3 mm

was later discarded for reasons of accuracy. It was found that diameter depended mainly on injection rate though the orifice, the experimental range of variations in CP velocity and temperature having a small discernible effect on drop initial diameter when compared with normal deviation around the mean (see fig 5.1). To characterise the drop diameter measurements made from replay of the video recordings of drop size were entered into a spreadsheet to calculate mean and standard deviation. Sufficient data points were entered successively until it was found that for the worst case (i.e. highest standard deviation) data set, additional data did not significantly reduce the standard deviations or change mean diameter (see fig 5.2). This led to a sample size of 20 measurements being selected as sufficient for the measurement analysis. Sample printout from the spreadsheet is used to illustrate the calculation of mean and standard deviation figures reported in the results section (see fig 5.1).

2.4 Heat Transfer Calculations

2.4.1 Introduction

Some heat transfer calculations are necessary to enable the design of equipment and to determine the expected magnitude of experimental error. The most relevant to practical measurements are summarised below. Calculations are generally based on convective heat loss, radiation and conduction being comparatively small.

2.4.2 Column Heat Loss And Insulation Thickness

Insulation thickness was chosen such that in the worst case:

1.The insulation resistance to heat transfer would be greater than other film

resistances in the heat loss process.

2.CP temperature losses should be below 1°C.

Film coefficients for the inside (CP) film is calculated using the Sieder and Tate equation for water [49] using the turbulent flow form which gives the higher coefficient (worst case):

$$hi = 1063\ (1 + 0.00293\ Tcb)\ uc^{0.8} / Dcol^{0.2} \quad \{eqn\ 2.4.1\}$$

where Tcb is the bulk temperature in K.

Thermal conductivities in W / m K are:

Perspex 0.2

Urethane foam insulation 0.03

Film coefficient for transfer to air, assuming turbulent flow due to the fume cupboard air flow, (worst case) is given by the Saunders equation [49]:

$$ho = 1.65\ \Delta T^{1/4} \quad \{eqn\ 2.4.2\}$$

Taking worst case values for all figures (this is a conservative case as all of these will not necessarily apply to single run):

at $uc = 4.4 \times 10^{-3}$ m s^{-1}, $Fc = 328 \times 10^{-6}$ m^3 s^{-1}

$md = 13.24 \times 10^{-4}$ m^3 s^{-1}, and Tcb = 353 K

for which $himax = 45.1$ W m^{-1} K^{-1}

and at a minimum ambient temperature of 289 K:

$homax = 4.7$ W m^{-1} K^{-1}

Now $$(1 / U) = (1 / ho) + (y / kw) + (1 / hi) \quad \{eqn\ 2.4.3\}$$

where wall thickness is comparatively small. Therefore, taking an insulation thickness of 15 mm:

$$1 / Umax = (1 / 45.1) + (0.003 / 0.2) + (0.015 / 0.03) + (1 / 4.7)$$

or $$1 / Umax = (1 / 45.1) + (1 / 66.7) + (1 / 2) + (1 / 4.7)$$

Umax can never be greater than the lowest coefficient, i.e. lowest right hand denominator term. This is 2 W m^{-1} K^{-1} i.e. the insulation term is limiting. In fact Umax = 1.3 W m^{-1} K^{-1}.

We can use the fact of limiting insulation thickness to make the simplifying assumption that the worst case (i.e. maximum) U under all circumstances will be 2 W m^{-1} K^{-1}, and use this conservative value in calculating heat losses.

Outer Surface area of column = 0.296 m^2= A

Heat balance for heat losses:

$$Q = U A \Delta T = mc Cpc \Delta T \qquad \{eqn\ 2.4.4\}$$

in the case already considered:

$$Qmax = 2 \times 0.296 \times 64.1 = 37.9\ W$$

which gives a CP temperature drop, ΔTc, of 2.8 x 10^{-8} K. Not very significant due to the high CP flowrate.

At lower flowrates the temperature drop will be greater. Assuming the limiting U value of 2 W m^{-1} K^{-1} then equation 2.4.4 can be solved to give the minimum mc such that ΔTc is less than or equal to 1 K. The worst case will be when Tc1= 80 °C and md is small, which keeps CP bulk temperature high. In the limiting case:

$$mc\ min = 2 \times 0.296 \times 62.5 / 4200$$

$$= 8.81 \times 10^{-3}\ kg\ s^{-1}$$

Hence

$$Fc\ min = 8.96 \times 10^{-6}\ m^3\ s^{-1}$$

This sets the lower value of Fc flowrate in experimental work, taken as 1×10^{-5} $m^3 s^{-1}$. Insulation thickness for the experimental rig is to be 15mm of urethane foam.

2.4.3 ΔTc Compared To Heat Losses

To have an accurate CP temperature drop compared to the temperature drop resulting from heat loss the criterion that:

$$\Delta Tc > 2 \times \Delta Tc \text{ heat loss} \qquad \{eqn\ 2.4.5\}$$

is applied. A simplified approach is used to calculate the DP flowrate appropriate to this limit.

From section 2.4.2, the heat loss rate Qmax = 37.9 W.
From heat balance between CP and DP, assuming evaporative heat transfer of the DP outweighs sensible heat transfer (a conservative assumption):

$$\Delta Tc = md\ \lambda / mc\ Cpc \qquad \{eqn\ 2.4.6\}$$

$$\Delta Tc \text{ heat loss} = Qmax / mc\ Cpc$$

therefore applying eqn 2.4.5

$$md\ \lambda / mc\ Cpc > 2 \times 37.9 / mc\ Cpc$$

therefore $md\ \lambda / > 75.8$

hence $md > 2.26 \times 10^{-4}$ kg s^{-1}

Thus acceptable DP mass flowrates are above 2.26×10^{-4} kg s^{-1}. The lowest experimental value usable is 65% greater than this value.

2.4.4 CP / DP Flowrate Ratio

The ratio of CP / DP flowrate when MEH has been achieved sets the size of the CP temperature drop (neglecting heat loss effects), ΔTc. Although insulation (see section 2.4.3) reduces the effect of heat loss, it is desirable also to the absolute value of ΔTc is of a measurable size.

From equation 2.4.6 to obtain at least 1 K ΔTc, then approximately:

$$md\ \lambda \geq mc\ Cpc$$

hence $80 \geq mc / md$

The application of this criterion is discussed in section 5.2.2.

2.4.5 Heater Duty

Maximum heating duty for the water bath heater is calculated by adding total maximum cooling duties.These are approximately:

Maximum DP cooling, md $\lambda = 13.81 \times 10^{-4} \times 334.7 =$	0.46 kW
Max heat loss	0.04 kW
Total	0.50 kW

therefore a 1.5 kW heater should be adequate for all the reported flowrates herein. Additional heating was available if required, see section 3.2.1.

2.4.6 Temperature Rise In Injection Tube

The insulated copper tube used for injection carries DP into the column before it is expelled through the injection orifice, see fig 3.3 and section 3.2.1.

Temperature of DP is measured prior to entry to the tube and thus any heat gained in the tube as sensible heat will be removed from the CP and taken into account with the MEH analysis. It is necessary therefore to check if this has a significant effect on the column heat duties.

Tube dimensions are:
i.d. 7.3 mm, o.d. 8.7 mm, insulation thickness 10 mm.

The worst case basis is for highest temperature rise in the tube at lowest md (3.74 kg s^{-1}). DP flow effects on film coefficient are of lesser effect. ho will be greatest at highest Fc (328 x 10^{-6} $m^3 s^{-1}$).

The external film coefficient is calculated from:

$$Nu = 0.26\ Re^{0.6}\ Pr^{0.3} \qquad \{eqn\ 2.4.7\}$$

and the internal film coefficient from:

$$Nu = 1.62\ (Re\ Pr\ Dt / l)^{0.5} \qquad \{eqn\ 2.4.8\}$$

for laminar flow heat transfer [49], where Dt = tube internal diameter and l = tube length.

Film coefficients generated by equation 2.4.7 and 2.4.8 are found to be insignificant in the calculation for temperature rise since the resistance of the insulation dominates the overall heat transfer coefficient. The insulation is 10 mm of foam, thermal conductivity 0.03 W m^{-1} K^{-1}.

Example values for the worst case are:

hi	396 W m^{-2} K^{-1}
ho	1906 W m^{-2} K^{-1}
Cu wall conductance	133000 W m^{-2} K^{-1}
Insulation conductance	3 W m^{-2} K^{-1}
U overall	2.97 W m^{-2} K^{-1}

Therefore heat gained in the tube will be based on a maximum value of U of 3 W m^{-2} K^{-1}. This value is used in a trial and error calculation to establish DP outlet temperature and hence LMTD, with a maximum CP upper temperature of 79.5°C and DP inlet temperature at a minimum value of 15.9°C (worst case values for max driving force) to give:

Qt max = 0.0192 W

maximum temperature rise in tube = 0.02 K

This value is small enough to be neglected.

3. Development Of Apparatus

3.1 The Selection Of Fluid For Dispersed Phase Refrigerant

The factors affecting choice of refrigerant / DP have already been outlined in section 1. The initial industrial application proposed for the apparatus required cooling to around 6°C. Given that the refrigerant must be immiscible with water and have the correct boiling point characteristics, it was decided that n-butane was very suitable. The normal boiling point of n-butane is -0.6°C, providing adequate temperature driving force.

For this reason n-butane was initially selected as refrigerant / DP. One point to note however if going from hot water to hot sulphuric acid in the industrial application is that potential for chemical reaction with a hydrocarbon refrigerant has not been completely assessed. For analytical reasons (although not necessarily affecting the practical application of the system in an industrial setting) it was considered vital that the refrigerant enter the column as a single phase i.e. liquid. A large proportion of the time spent on this project has therefore been in developing apparatus to ensure this. Safety considerations led to a necessity for the equipment to be enclosed in a fume cupboard to enable the removal of the inevitable spillages and leakages which occur when commissioning, using and operating a newly designed apparatus. The imposed ventilation would keep vapour concentration of the hydrocarbon low and facilitate removal of fumes from the flare. The equipment therefore is limited to a fairly small scale.

The various designs of equipment tried are detailed below. Appendix 6 contains diagrams and photographs relevant to this section. These trials took up a lot of the time available for this project. It is true to say that this research

project has been one involving a lot of practical work compared to analysis time.

Eventually, after the limitation of scale had meant that none of the apparatus trials had been successfully achieved, time pressure led to the decision to abandon n-butane and try other refrigerant / DPs which had higher normal boiling points and so would allow single phase injection. After trial work isopentane was selected.

Chlorofluorocarbon refrigerants were tried but as they are denser than water the flow situation would require major modification. However the chemically inert nature of these compounds plus their low toxicity and non-flammable nature make these attractive candidates for consideration in the practical application of the process, provided design takes account of their tendency for droplets to sink in water - they may be of considerable use for cooling higher density continuous phase systems (above 1600 kg m^{-3}) or water based systems with modified apparatus. It should be noted however that use of these refrigerants may be restricted in future due to the atmospheric ozone layer depletion and greenhouse effects.

Isopentane has been found to give good cooling and provides data for theoretical and practical study, although only producing cooling in an atmospheric rig down to around 32°C with a normal boiling point of 27.88°C. There have been positive advantages in terms of experience and equipment and operation familiarity from the several redesigns necessary. As these designs form a large part of the scoping work, and will be of use in any further work in this area carried out by other investigators, the several major equipment modifications are dealt with here in chronological order.

3.2 Description And Development Of Heat Transfer Apparatus

For reasons of brevity only major stages in modifications are detailed here.

3.2.1 Equipment Common To All Apparatus Designs

The following equipment is common to all apparatus designs (except where qualified later):

1) Column.

This is a perspex cylinder one metre high, 100 mm in outside diameter with a wall thickness of 3 mm. Water inlet and outlet tappings are at top and bottom of the left hand side and the injection nozzle enters 91 cm down from the water inlet on the right. The column has tappings for temperature probes along its height. The perspex top is open and is capped by an O-ring sealed aluminium top which has a segmental plate in to prevent excessive droplet carryover, and a temperature probe (tp). Perspex is selected for visibility and safety reasons. A tp is anchored to the outside of the column to measure ambient temperature. Eventual crazing of the perspex reduces visibility, so that the column has a finite useful life.

2) Injection Nozzle.

This consists of a sealed copper tube insulated along the majority of its length to minimise heat gain in the tube. A 1 mm orifice is drilled in the cylinder side. This is so placed that the orifice is in column centre, opening upwards. A tp is situated in a reservoir upstream of the copper tube. For photographic work the insulation is removed where feasible to allow clarity. In this case it is easy to visually determine any tube boiling on video tape, and measurements show no measurable difference between insulated and non insulated initial drop size

provided the liquid phase is maintained.

3) Injection pump.

This pump and the water circulation pumps are peristaltic pumps giving accurate flow at low values, with drives operating from a reversible calibrated drive control. The only difference between the pump units is in the bore and type of tubing, as the injection pump has a hydrocarbon resistant tubing. Both pumps are calibrated using the usual "mass delivered in a certain time" method, as measured by a receiver and stopwatch.

4) Water circulation pumps.

The first set of these are as described in (3) except the drive has two pump units attached - one for water inlet and one for outlet. This ensures both operate at the same stroke rate and matches inlet and outlet rate fairly closely, with fine adjustment to ensure steady column height by means of a tube clamp. The second set are higher flowrate centrifugal pumps operating at constant speed and controlled by outlet throttle valves. The valves require more adjustment to maintain column height than for the first set of pumps. Water mass flow is measured independently for each experiment when it is being varied since the clamp affects the calibration to a varying degree. Water outlet from the pump has a tp fitted. Pumps are used in reverse to initially fill the column.

5) Thermostatic water bath.

This serves two functions. Firstly as a source of constant temperature hot water for which temperature can be set as required. Secondly by means of a mercury in glass thermometer and tp as a hot reference temperature for tp calibration, since this will be the highest temperature in the equipment. In order to cope with high heating loads, additional heating coils were available to be

placed in the bath. This gave a maximum of 5.1 kW heating in total, which will cope with bath temperatures up to 80°C at higher flowrates than those reported in section 5.

6) Cold reference temperature ice bath. This is a dewar flask containing ice and water with a mercury in glass thermometer and tp fitted for tp calibration at low reference temperature (0°C). The flask is fitted with a magnetic stirrer to maintain uniform temperature and requires occasional replenishment with ice and removal of water. This was checked hourly which was an adequate frequency for prevailing ambient temperatures.

7) Temperature probes (tp).

These are miniature thermocouples which are adequate for non-corrosive environments when closely calibrated. They are mounted in sealing bushes where necessary and connected to (8) with compensating cable, ensuring no intervening junctions. They are calibrated against accurate mercury in glass thermometers across as small a temperature range as is practicable, at each measurement if desired.

8) Analogue to digital converter (ADC).

This device converts the analogue voltage from the tp's to a digital signal necessary for a digital computer. The device is not temperature compensated hence another need for the continuous calibration approach explained in (7). Up to 16 inputs can be used although to date only 7 are in use. These channels are:

Channel	tp measurement
0	cold reference (ice bath)
1	hot reference and water inlet (water bath)
2	water outlet

3	refrigerant / DP inlet (liquid)
4	refrigerant / DP outlet (vapour)
5	ambient air temperature
15	shorted channel

Channel 15 is shorted to provide a measure of the "chatter" due to signal noise in the system. Digital output is sent to the computer (9).

9) Pet computer.

The Commodore Pet computer system used is of a somewhat old standard but is adequate for the task here. The computer is attached to a floppy disk drive and has a printer for producing hardcopy results (see fig. 3.5). It is situated away from the "wet" equipment for safety reasons. The digital signals from the ADC are analysed by software (10) and a set of temperatures is printed out.

10) Software for temperature measurement.

The Commodore BASIC program for conversion of the digital signal from the ADC via calibration to a temperature readout is based on an initial program provided by the ADC manufacturers. However, this program as supplied was inadequate and incorrect for the pet 8-bit digital input handling. Extensive reprogramming was necessary and the program was finally complete and proven in its twenty third version. The program listing is given in Appendix 4 and is entitled ADC23. In brief, subroutine 5000 is for titling of output, subroutine 2000 is for input of calibration data, subroutine 1000 reads the digital input, performs necessary binary operations on the input, and records the result in an array. Subroutine 4000 checks to see if system "chatter" is unacceptable, and prints a warning message and program interrupt if so. Subroutine 3000 calibrates the digital values stored in array and prints out the temperatures thus produced. Subroutine 1500 interrupts the program until

further measurement is required. The main program runs the subroutines in the order given above. Subroutine 10000 is a convenient development tool only, added to the end .

For clarity the above items are (1) to (10) labelled, where appropriate, in fig. 3.3 only. See also figs. 3.4 and 3.5.

3.2.2 Apparatus 1: n-Butane Injection

For a sketch of apparatus see fig. 3.1. This version was an initial attempt to achieve single phase butane injection by means of a cylinder dipleg and flash vessel. Offgas was burnt in a flare in the next door fume cupboard i.e. isolated by a partition. The very low butane mass flowrate, the relatively high surface area of tubing from flash vessel via pump to column, the ambient temperature driving force and the energy input to the butane by the pump all combined to evaporate a portion of the butane at injection even in a cold water column.

The following apparatus was used in addition to that detailed in section 3.2.1:

11) n-butane cylinder and valve.
This is a cylinder of high purity, instrument grade n-butane plus a specialised reducing valve fitted with display to produce a liquid stream. This feeds through a pressure tube to the flash vessel (12).

12) Flash vessel.
This is a device to depressure the n-butane, causing it to flash and cool. Vapour is removed from the top and liquid taken off the bottom for pumping. The vessel was metal with a plastic sight glass to show liquid level. A clamp on the liquid line provided shutoff from the column to prevent backflow when not

in use.

13) Butane vapour flare.

Vapour offtake was routed via tubing into a separate fume cupboard through a non return valve and tube in tube heat exchanger to a flare. The non return valve was a welding grade anti blowback device. The tube in tube exchanger had tap water flowing from tap to drain through the outer tube and prevented heat conduction from the flame from weakening upstream joints. Flame ignition was accomplished by having a lit bunsen burner adjacent to the flare.

3.2.3 Apparatus 2: n-Butane Injection

This design attempted to achieve single phase butane injection by the addition of upstream cooling and insulation. The apparatus was essentially the same as in 3.2.2 with the following additions:

14) Cooling Bath, see fig. 3.2.

The flash vessel was placed in a large insulated perspex vessel (perspex so the level gauge and flowmeter could be read). The vapour offtube was throttled with a valve to provide pressure for injection. The liquid offtake was also valve throttled, then passed through a copper cooling coil and a gap type flowmeter to measure flow rate. All these items were immersed in the cooling bath which was filled with antifreeze solution and cooled to -10^{o}C using cubes of frozen antifreeze solution. A magnetic stirrer agitated the cold solution. The bath was provided with a mercury in glass thermometer.

15) Insulation and pump bypass.

On exit from the gap meter the butane injection tube was connected directly to the injection orifice tube via a tp. The need for an injection pump with its

associated heat input was obviated. All tubing from the cooling bath (14) to injection orifice tube was insulated and kept short.

This apparatus was unsuccessful in providing single phase liquid n-butane. Subsequent heat transfer calculations showed that to effect the degree of cooling with the cold bath temperature achievable would take a copper cooling coil of many metres length, due to the very low mass flowrate of n-butane involved.

3.2.4 Apparatus 3: n-Butane Injection

This apparatus applied pressure up to the safe column limit (2 bar gauge) in order to prevent vaporisation of n-butane by increase of boiling temperature. In addition to the apparatus in 3.2.3 above and much leak repairing and reinforcement at various points the following modifications were made to give cold injection pressurisation:

16) Closing of vapour offtake from flash vessel.
In order to enable pressurisation, the valve in the vapour offtube from the flash vessel was almost completely closed after the vessel had been filled from the cylinder.

17) Sealing of the column cap.
The column cap had a rubber gasket fitted to compress against the top rim of the cylindrical column. A strong metal clamping bar was then fitted which forced the cap down onto the column top, compressing the gasket and preventing the cap from being forced upwards by internal pressure.

18) Pressure gauge.

A T-piece was fitted to the column top vapour offtake and a bourdon pressure gauge was fitted (accurate to 0.1 bar).

19) Throttle valve.

A throttle valve was fitted between the T-piece in (18) and the non return valve in (13) to enable a back pressure to be built up.

When this apparatus failed to provide required conditions at 2 bar gauge it was decided that the limitations of scale and equipment were insurmountable in the time available and other refrigerants were considered.

3.2.5 Final Heat Transfer Apparatus: Isopentane Injection

The apparatus is sketched in fig. 3.3. It is essentially that detailed in 3.2.1 plus the following:

20) Column insulation.

Calculations (see section 2.4.2) show that heat loss from the bare column at elevated temperature would be significant. The column was therefore insulated with a 1.5cm thickness of foam / plastic insulating material, leaving a small strip clear for visual determinations. Because of restricted visibility, a high intensity 1kW photographic light was often used to aid in observation.

21) Holding vessel.

The isopentane for injection is kept in a glass vessel with a high top vent and valve upstream of the pump (3). Isopentane of Analar grade is used.

22) Isopentane recovery condenser.

Offcoming vapour from the column top is routed to a cooling condenser

operating from the cold water tap. Isopentane vapour plus some water is condensed therein and runs in to a decanting vessel with a high top vent. To reduce isopentane usage, isopentane is thereby periodically recovered by decanting off the water then storing the isopentane.

Liquid injection of refrigerant / DP is clearly achieved with this apparatus, which is photographed in figs. 3.4 and 3.5.

3.3 Description And Development Of Photographic Apparatus

The photographic apparatus was designed as far as possible to replicate the heat transfer apparatus, but with modifications to allow the clear photography and measurement of initial droplet size. for this reason pumps, tubing and valves were identical to the heat transfer rig but the column itself was modified and a rule inserted in the column. The apparatus is sketched in fig 3.6 and the numbers in following description refer to this diagram. Photographs of the apparatus are included in figs 3.7 and 3.8, without and with camera and light.

23) Photographic Column.

This column is 1.2 m high in total to completely accommodate item (24). To maintain mean velocity / flowrate relationships the column was kept to the same cross sectional area as column (1), but to remove distortion was constructed of square cross section. Internal dimension is 8.3cm x 8.3cm. Other dimensions are as for column (1). The front wall is glass for good visibility, and the other three walls, top and bottom are 1cm thick perspex. The top and bottom are sealed with rubber gaskets and the walls with silicone rubber. The glass is held in place by aluminium brackets. The same injection tube, (2) and overhead apparatus (22) is used as for column (1). Visual distortion is very small although it must be accepted that there will be some

deviation in flow characteristics from column (1).

24) Rule.

An aluminium metre rule graduated in mm is attached as closely as possible along side ignition point where it can be clearly photographed. In calibration work, ball bearings of measured diameter were suspended above the injection nozzle to ensure accuracy of the camera / ruler combination. No measurable parallax distortion was found.

25) Video Camera.

A Sony Video 8 PRO video camcorder with a fast shutter speed of 1 / 4000 s is mounted in a tripod close in to the column. This camera also has a short focal length facility which was necessary to get as close to the column as possible. Depth of focus was small so to get sharp images of droplet and ruler these had to be the same distance from the camera. The results were recorded on a VHS C format cassette for later replay, which gave a much quicker result turn around then high speed cine.

26) Lighting.

With the fast shutter speed used to enable 'freezing' of the droplet, the camera required a well lit subject. This was achieved with a mounted 1kW photographic light angled to give best definition and mounted as far back as practical to reduce heating effects.

27) Background Screen.

A white card background was mounted behind the column to provide contrast. This is omitted in fig 3.7 for clarity.

For measurement work the video film was replayed on a high resolution Philips

CM 8833 video monitor. A photograph of the screen is included in fig 3.9. The picture on the screen is better quality than would be suggested by this photograph due to the usual difficulty of adequately photographing a TV screen.

4. Experimental Procedure

4.1 Heat Transfer Experiments

The heat transfer experiments followed the set procedure set out below. Numbered equipment refers to fig 3.3, appendix 6. Initial set up of the apparatus involved heating up of the water bath, filling up the column and then circulating the water. When this was almost complete ice was placed in the bath cold reference bath (6). The equipment calibration was set by entering hot and cold reference temperatures to the monitoring software ADC23 (see appendix 4). Temperature measurements could then be taken by pressing a key on the keyboard. After the CP fluid had circulated for five residence times (typically about 1 hour, depending on CP pump in use), temperature measurement was taken and the ambient valve checked against a mercury in glass thermometer. 'Chatter' produced by signal noise was also checked at this time by checking for the appropriate printed error message.

The procedure was followed for a predetermined range of flows and Tc1 values. Flowrates of CP, Fc, proved the most difficult to reproduce so this variable was primarily set for each run. Setting Tc1 and MEH variations accurately was somewhat limited by practical considerations and these values only approximate to the predetermined targets.

The experimental variables were changed in the following way for each run of constant Fc.

Fc is set close to a predetermined value and held constant for the run.
md is set initially to its lowest value then increased over the specified range.
Tc1 is set initially to its lowest value then increased over the specified range.

Column height is set initially to highest value then reduced by steps of 10 cm at first, then later by 1 cm. Values <10 cm are not taken due to their limited accuracy. This is in terms of % error being larger with a low absolute height, and the need to allow the establishment of drop velocity and CP temperature profile after injection.

The procedure below was followed until the full range of variables were covered. The procedure is as follows after initial apparatus warm up and calibration:

A) Set Fc via pump speed (pump set 1) and / or throttle valves (pump set 2). Measure flowrate. Adjust outlet valve marginally as necessary to maintain constant column height.

B) Set md via pump speed. Refill DP reservoir as necessary.

C) Set Tc / on water bath thermostat.

D) Set column height using a ruler with CP and DP flows temporarily shut off to still the surface. Height is measured to the top of the water surface. Temporary shut off of CP and DP is achieved by cutting off pump power and blocking CP outlet as necessary to avoid disturbing the settings.

E) Wait until steady state is reached, as evidenced by no significant change in temperature readings over ten minutes. This typically took about 5 CP residence times, on average about 1 hour.

F) Measure temperatures. Quickly cut off CP and DP flows to still the surface as in (D), then immediately examine top water surface for evidence of a visible

(approx. 5 mm deep) pool of DP. Any DP build up caused by pooling should be removed.

G) If pool is absent, reduce column height by appropriate amount, down to the limit of 10 cm minimum height, and repeat from (D).

H) If a pool is present, flush the pool into the overhead collector by blocking the CP outlet to temporarily flood the column, with DP flow temporarily turned off.

I) If column height is being reduced by 1cm at a time then record the height as the result and continue from C with next Tc1 value. Note that if Tc1 is being increased it will help to flash off the DP pool and flushing as in (H) may be unnecessary.

J) If column height is being reduced by 10 cm at a time then increase column height by 9 cm and repeat from (D) using reduction steps of 1 cm.

In this way pooling heights (MEHs) to within 1cm were determined. As a checking procedure temperatures could be taken with no DP flow as an indication of heat losses.

4.2 Photographic Drop Size Experiments

4.2.1 Procedure

The procedure for these measurements are straightforward. Initially the apparatus is calibrated by suspending a ball bearing of known diameter above the injection orifice, operating the rig and measuring its diameter on the video

tape produced. Then comparative work was done to see if removing insulation from the copper injection tube had any measurable effect on initial drop size.The insulation was consequently removed for clarity. Flow rates were set up to duplicate those in heat transfer experiments. Drops were photographed for an average time of one minute per run, initially with cold CP then with temperatures equivalent to the heat transfer runs. In the absence of temperature sensors the rig was left to reach thermal equilibrium for five CP residence times or one hour, whichever was the longer time. In fact CP temperature was found to have little effect on initial drop size. Video tapes were made and replayed later for analysis.

The greater visibility of this rig showed an interesting effect not noticed in the heat transfer work. At high CP flow rates, when a pool of DP formed the CP turbulence at column top would break this up and the smaller drops, with smaller buoyancy force, would be entrained by the CP and carried down the column. This means that it is important not to allow a pool to be present for too long when making measurements. However, practically speaking this effect, which would produce further cooling, could be desirable in an industrial unit and would tend to favour high CP flowrates.

4.2.2 Tape Analysis

Tapes were replayed in freeze-frame on the monitor and drop diameters measured on screen. The drop diameter was determined by comparing the diameter of the drop image taken with callipers, with the image of the metre rule. Calibration work with ball bearing showed accuracy to be well within the 1mm rule accuracy (see fig 3.9, appendix 6).

Some oscillation occurred in diameter and this was visible in successive

frames, which allowed an average value to be taken. Analysis of initial run showed that a sample size of 20 drops was sufficient to reasonably describe the mean drop size for a run (see section 2.3.2).

Finally, an approximate measurement of initial velocity of the drop could be made by timing the tape replay speed and comparing it to the distance a drop travelled whilst in freeze frame. This gave support for the terminal velocity calculation method (see section 2.2.3).

5. Experimental Results

5.1 Introduction

This section presents results based on experimentation. In the interests of brevity only pertinent major results are presented, rather than a full reproduction of every measurement taken. To this end sets of MEH versus Tc1 data that are sufficiently accurate for analysis are presented in full since these are major results of the study. Other data for the experimental runs are only presented if significant. Drop size results are presented as the mean value determined for each DP mass flowrate, rather than as every individual measurement for calculation of a simple mean value.

Figures for this section are generally contained in appendix 16 for spread sheet output and appendix 17 for graphical results.

5.2 Heat Transfer MEH Analysis

5.2.1 Introduction

These results are categorised by a run number which is arbitrarily assigned, having no particular chronological or other significance. The results of run 1 were expected to be among the most accurate, and triplicate runs were carried out on this set to determine reproducibility. These three runs are designated A, B and C. The reasons for selecting run 1 are:

1. A good range of MEH values is present.
2. The run has a mid range value of Fc which avoids the problems of high Fc (low ΔTc and higher heat loss with difficulty of observation at high degree of

turbulence) and low Fc (high column heat loss at high CP temperatures). These problems are discussed below.

For these reasons one would expect run 1 to be a better set of results for reproducibility and modelling.

Tc1 temperatures for the runs were set on the bath thermostat to be 40, 42, 45, 50, 55, 60, 65, 70, 75, 80 ^{o}C consecutively, although the actual values showed calibration deviations. The greater concentration of values around 42^{o}C reflects the sensitivity of the data and the importance of 42^{o}C to the acid recovery application.

5.2.2 Selection Of Data

More experimental runs were carried out than are presented here. Selection of data, given that there was scope for a significant reduction in bulk, was made on the grounds of likely accuracy. Data was discarded if calculations showed that it was likely to be inaccurate. In the case of heat losses, the data was rejected if high heat loss would be anticipated even if temperature drop measurement appeared acceptable. The criteria for selection were as follows:

1. Calculated maximum temperature drop due to heat losses for the column (see section 2.4.2) is to be < 1K. The maximum heat loss would occur at maximum Tc1 (around 80^{o}C).
Given that the insulation thickness is chosen to make heat loss rate insensitive to CP film coefficient, the size of heat loss induced temperature drop from the CP depends on residence time in the column. For heat loss to be <1K at Tc1=80^{o}C, CP flowrate, Fc, must be >9 x 10^{-6} m^3 s^{-1}. Experimental data with a lower Fc is rejected.

2. Size of ΔTc compared to heat losses. At high CP : DP flowrate ratios the CP temperature drop, ΔTc, becomes small and the CP temperature profile consequently poorly established. Error in temperature measurement becomes more significant and heat loss error proportionately greater. For this reason data runs where $\Delta Tc < 2$ x (temperature drop due to heat losses) were discarded. This criterion was again more applicable at high Tc1 values, and ruled out low DP flowrates (see section 2.4.3).

3. Absolute size of CP temperature profile (see section 2.4.3). In order to measure the absolute size of ΔTc with some accuracy, data runs where $\Delta Tc <$ 1 K were normally discarded. Exceptions to this are the high Fc flowrate work for investigation of the effect of CP turbulence. In this work violations of this criterion were inevitable, but the runs selected were those with highest available ΔTc with a full set of results acceptable on other criteria. In analysis of this work it is necessary therefore to make note of this caveat which applies to runs 26, 32, 33, 35, 36, 37, 38 and 39.

4. MEH Range. If more than half of the Tc1 values in a set gave an MEH of >90 cm or <10 cm then that run of values was discarded on the grounds of insufficient data.

5.2.3 Run Numbering Key

The following table gives the significant parameters for each run number. Note that initial drop diameter for a given md can be found in section 5.3.2 below. md is derived from pump calibration measurements.

Run number	Fc (10^{-6} m^3 s^{-1})	md (10^{-4} kg s^{-1})	Mean ambient temperature (°C)
1A,B,C	10	8.60	17.9
2	10	3.74	16.9
3	10	5.42	18.2
4	10	7.01	17.7
5	10	10.24	17.5
6	10	11.87	18.5
7	10	13.24	19.0
8	10	13.81	17.9
9	32	7.01	16.8
10	32	8.60	17.9
11	32	5.42	18.0
12	32	10.24	15.5
13	32	11.87	16.5
14	32	13.24	17.2
15	32	13.81	18.3
16	51	7.01	18.1
17	51	8.60	18.7
18	51	10.24	19.2
19	51	11.87	19.3
20	51	13.24	18.0
21	69	8.60	17.9
22	69	10.24	18.1
23	69	11.87	18.1
24	69	13.24	18.2
25	69	13.81	18.0
26	150	13.24	18.0
27	90	11.87	18.0

28	90	13.24	15.8
29	90	13.81	16.5
30	106	13.24	18.1
31	106	13.81	18.5
32	120	13.24	18.8
33	134	13.24	18.6
34	7.50	13.81	18.3
35	172	13.24	19.0
36	210	13.24	18.8
37	251	13.24	18.7
38	297	13.24	18.7
39	328	13.24	18.1
40	2.11	3.74	15.9
41	4.51	3.74	18.0
42	4.51	5.42	16.5
43	4.51	7.01	17.8
44	4.51	8.60	17.9
45	4.51	10.24	18.0
46	4.51	11.87	18.1
47	4.51	13.24	18.0
48	7.50	3.74	18.1
49	7.50	5.42	18.2
50	7.50	7.01	18.5
51	7.50	8.60	18.3
52	7.50	10.24	18.6
53	7.50	11.87	19.0
54	7.50	13.24	18.1
		Overall mean=	17.97 °C

Note that the mean ambient temperature is equivalent to the DP temperature

prior to injection.

5.2.4 Tc1 And MEH Results

For the key to the run numbers, see previous section.

Units are Tc1: °C, MEH: cm.

Run no.1A		Run no.1B		Run no.1C	
Tc1	MEH	Tc1	MEH	Tc1	MEH
41.7	82.4	41.4	85.6	40.9	87.4
42.7	82.2	40.4	63.9	42.0	80.0
45.0	48.7	43.1	62.3	45.8	57.0
49.9	30.0	50.0	36.3	49.8	35.6
53.4	30.6	55.7	26.0	53.1	23.6
60.2	22.1	62.6	25.7	61.6	24.2
65.6	18.8	62.1	21.4	66.2	19.6
68.7	14.4	68.0	17.3	72.3	13.5
76.1	14.3	72.9	15.0	77.9	15.6

Run no.2		Run no.3		Run no.4	
Tc1	MEH	Tc1	MEH	Tc1	MEH
-	-	38.1	>90	40.0	87.5
40.1	>90	40.2	83.5	40.7	76.5
46.1	86.9	43.8	61.2	46.4	47.1
49.0	64.0	50.8	45.3	51.2	38.8
56.5	48.2	56.0	28.1	54.6	32.4
61.7	37.5	59.7	20.2	61.2	21.7
65.1	27.0	64.4	22.5	65.6	20.3
68.7	25.3	71.6	18.8	71.6	15.4
76.4	19.7	74.4	15.4	73.2	12.4
81.7	17.8	82.0	12.5	80.9	11.7

Run no.5		Run no.6		Run no.7	
Tc1	MEH	Tc1	MEH	Tc1	MEH
38.6	>90	40.9	78.1	38.1	>90
41.2	73.3	41.1	68.1	42.8	77.9
46.3	42.4	45.3	36.6	44.8	33.9
49.1	30.3	50.4	25.8	51.3	27.0
54.3	17.7	55.7	18.2	54.8	17.0
59.9	14.2	60.4	19.4	61.4	18.1
64.4	16.3	63.4	16.4	65.6	15.3

71.1	12.1	70.9	11.7	70.3	11.7
73.1	<10	75.3	<10	75.3	10.7
-	-	-	-	79.6	<10

Run no.8		Run no.9		Run no.10	
Tc1	MEH	Tc1	MEH	Tc1	MEH
38.1	>90	41.5	51.6	38.1	62.5
42.8	60.0	43.7	60.4	40.4	46.0
46.8	26.9	44.6	48.6	44.8	35.2
48.7	22.0	49.2	33.3	48.5	25.6
54.0	14.3	53.1	26.0	53.3	22.9
60.2	13.2	58.2	17.2	58.7	22.9
63.7	10.8	65.6	19.4	64.2	15.4
71.5	<10	69.5	14.9	69.4	13.0
-	-	74.5	13.1	76.4	14.4
-	-	78.5	13.3	81.3	13.0

Run no.11		Run no.12		Run no.13	
Tc1	MEH	Tc1	MEH	Tc1	MEH
40.6	77.8	39.5	57.3	39.0	38.2
40.9	62.1	44.0	41.9	42.1	42.1
43.3	50.7	46.9	34.2	44.2	27.1
48.7	30.1	48.6	26.6	48.3	20.9
53.8	31.8	56.6	18.7	56.7	14.4
61.1	26.6	59.6	14.3	61.8	12.4
65.0	23.8	63.6	10.7	63.1	11.1
70.0	17.8	71.8	12.7	70.0	<10
73.8	15.0	76.0	11.1	-	-
81.4	11.1	81.5	<10	-	-

Run no.14		Run no.15		Run no.16	
Tc1	MEH	Tc1	MEH	Tc1	MEH
38.3	39.8	40.6	27.0	41.3	67.3
42.0	33.0	40.9	26.2	42.9	42.8
43.5	27.2	44.6	23.5	45.6	41.3
49.7	23.8	48.2	12.7	50.8	28.2
55.5	18.5	57.0	10.8	54.3	23.1
60.4	14.6	61.1	10.1	60.4	19.5
65.6	11.6	66.3	<10	66.9	14.4
71.7	<10	-	-	68.6	17.0
-	-	-	-	75.8	14.7
-	-	-	-	81.4	10.4

Run no.17

Tc1	MEH
39.4	52.7
40.3	43.4
44.3	39.9
50.2	23.1
56.9	19.2
61.1	17.3
64.9	16.4
71.2	12.2
74.7	10.1
78.3	10.8

Run no.18

Tc1	MEH
38.3	45.9
43.4	37.3
46.7	25.6
49.2	26.8
56.0	20.8
59.3	16.4
63.1	10.2
69.9	12.2
76.1	10.2
80.8	<10

Run no.19

Tc1	MEH
40.7	36.1
41.2	34.8
46.6	23.2
50.9	24.7
55.4	14.0
60.2	15.9
64.5	10.9
71.0	10.4
76.7	10.1
79.4	<10

Run no.20

Tc1	MEH
39.0	45.3
43.9	27.7
45.9	25.7
49.8	21.4
53.9	18.5
58.6	13.8
64.8	<10
-	-
-	-
-	-

Run no.21

Tc1	MEH
38.4	58.9
42.1	46.9
43.6	39.0
51.4	26.1
55.2	26.3
60.8	18.3
64.2	18.8
70.4	14.2
76.4	13.2
80.1	26.3

Run no.22

Tc1	MEH
38.0	42.8
42.7	42.2
46.6	29.8
48.7	23.3
55.8	16.3
61.7	17.7
66.8	10.7
69.2	<10
-	-
-	-

Run no.23

Tc1	MEH
47.1	42.0
42.4	33.4
44.7	32.9
49.5	18.7
53.6	13.6
58.9	11.4
66.1	11.8
69.2	10.0
76.0	<10

Run no.24

Tc1	MEH
39.4	37.8
42.7	35.5
44.2	25.9
51.0	17.1
53.7	15.5
61.4	13.4
66.5	<10
-	-
-	-

Run no.25

Tc1	MEH
39.8	29.2
41.1	24.2
43.4	15.1
50.9	13.8
55.2	11.2
58.6	<10
-	-
-	-
-	-

Run no.26

Tc1	MEH
41.7	41.9
42.0	27.1
44.9	25.1

Run no.27

Tc1	MEH
40.0	48.7
43.6	35.2
45.4	27.1

Run no.28

Tc1	MEH
40.4	46.7
41.6	30.1
46.0	22.9

49.4	22.1	48.6	22.6	50.4	21.6
56.8	17.6	56.8	19.9	55.4	18.2
58.5	13.6	58.4	14.4	61.4	16.8
63.2	<10	64.6	11.7	64.1	11.8
-	-	68.8	<10	68.4	11.7
-	-	-	-	74.0	<10

Run no.29		Run no.30		Run no.31	
Tc1	MEH	Tc1	MEH	Tc1	MEH
39.3	27.3	40.3	45.9	38.5	26.4
42.1	19.7	42.4	35.4	42.8	23.7
43.9	15.7	43.1	29.1	45.2	18.7
49.1	11.5	48.6	20.8	51.1	10.9
53.8	12.6	56.5	13.7	54.7	12.3
60.0	<10	58.7	11.0	58.7	<10
-	-	64.2	11.1	-	-
-	-	68.6	10.3	-	-
-	-	76.5	<10	-	-

Run no.32		Run no.33		Run no.34	
Tc1	MEH	Tc1	MEH	Tc1	MEH
41.0	34.4	40.8	39.0	-	-
41.9	25.1	41.8	34.0	43.4	>90
46.0	27.3	44.8	29.0	44.1	47.3
51.7	20.1	49.7	16.3	51.6	20.1
55.5	16.9	56.0	17.4	53.7	17.0
61.8	12.5	61.7	14.5	58.8	11.9
65.3	11.3	65.8	12.2	65.2	10.7
69.6	<10	70.2	<10	68.9	<10

Run no.35		Run no.36		Run no.37	
Tc1	MEH	Tc1	MEH	Tc1	MEH
40.3	42.6	38.2	38.5	39.8	41.8
41.0	28.8	44.0	32.9	40.6	27.2
46.0	23.6	43.4	24.4	44.0	23.1
50.8	17.5	51.6	15.2	50.1	16.1
54.6	12.5	54.8	12.6	54.6	12.1
58.3	10.3	59.4	11.4	60.9	11.6
63.7	10.7	63.4	<10	64.9	10.9
71.3	<10	-	-	68.2	<10

Run no.38		Run no.39		Run no.40	
Tc1	MEH	Tc1	MEH	Tc1	MEH
40.6	33.3	39.6	28.1	-	-
42.8	32.5	44.0	26.1	-	-
44.8	22.2	45.6	21.9	46.5	>90
50.1	21.3	51.6	16.2	51.5	89.1
56.8	16.7	53.7	15.7	53.8	62.9
58.9	11.2	61.3	13.7	60.5	46.7
63.9	<10	65.1	<10	66.0	32.4
-	-	-	-	71.2	31.6
-	-	-	-	76.2	20.7
-	-	-	-	81.6	19.3

Run no.41		Run no.42		Run no.43	
Tc1	MEH	Tc1	MEH	Tc1	MEH
-	-	42.1	>90	-	-
44.4	>90	44.0	78.5	45.8	>90
50.4	83.4	49.5	56.7	49.9	43.1
55.1	55.3	54.7	31.7	55.3	38.1
58.4	46.9	59.2	33.8	60.7	33.9
66.8	32.0	65.9	29.7	64.8	26.7
69.8	28.5	69.1	19.8	68.2	19.8
74.3	27.8	75.5	21.1	74.5	16.7
79.6	25.4	81.2	15.8	78.5	13.6

Run no.44		Run no.45		Run no.46	
Tc1	MEH	Tc1	MEH	Tc1	MEH
46.0	>90	46.7	>90	-	-
49.6	54.1	50.1	54.1	51.0	>90
53.4	32.0	56.3	29.2	53.1	37.6
59.9	25.1	60.0	22.0	61.0	27.8
65.9	14.4	64.4	16.1	65.5	21.9
69.0	13.1	70.8	15.7	68.6	13.9
76.1	14.7	74.5	15.6	74.3	12.9
78.3	<10	78.2	11.8	79.8	12.6

Run no.47		Run no.48		Run no.49	
Tc1	MEH	Tc1	MEH	Tc1	MEH
-	-	39.9	-	41.3	>90
-	-	41.0	-	42.3	84.6
-	-	43.3	>90	45.5	69.6
50.1	>90	48.7	73.3	48.7	44.3
55.3	52.2	56.5	50.8	54.7	26.9

58.7	26.1	59.0	41.0	61.8	24.6
65.5	23.2	63.9	33.7	66.0	24.1
69.8	18.3	70.9	31.6	71.0	21.9
75.8	12.6	76.8	22.8	74.9	18.9
81.2	12.0	81.2	24.8	79.2	13.2

Run no.50		Run no.51		Run no.52	
Tc1	MEH	Tc1	MEH	Tc1	MEH
40.0	>90	-	-	-	-
42.6	87.6	40.8	>90	43.2	>90
44.7	61.7	43.7	64.7	46.4	45.2
50.8	31.8	48.3	47.0	48.9	34.1
55.2	25.9	55.0	26.5	56.8	23.4
60.3	19.2	61.3	21.9	58.9	20.9
66.0	18.0	66.0	21.2	63.5	17.7
69.9	17.3	71.8	18.9	70.9	10.0
76.4	13.2	73.2	13.3	73.4	11.8
79.2	11.1	79.1	13.8	80.6	10.3

Run no.53		Run no.54	
Tc1	MEH	Tc1	MEH
43.4	>90	41.9	>90
46.3	52.3	43.7	36.4
49.4	28.3	48.6	39.0
56.4	21.8	55.5	20.3
59.8	20.8	60.1	19.5
64.0	14.8	64.7	17.3
70.4	12.2	68.7	14.2
76.4	12.0	75.3	11.4
79.4	<10	79.2	10.6

These results are presented graphically (in all cases except Run 1, together with a line representing the best model fit as discussed in section 7.3.5. These graphs are figures 5.4 to 5.31, appendix 17. In order to fit a polynomial curve using a least squares method a log-linear plot is used. It must be borne in mind that this has a coarsening effect on the scatter at the highest MEH regions. This means that scatter is generally greater than these graphs suggest. As long as this effect is borne in mind, the log-linear graph is the best way to plot these results to give a smooth and appropriate graph (see section 7.1.2 for a further discussion). For comparison purposes a linear plot for Runs 1A, B and

C (triplicate runs) is shown in figure 5.3 so that scatter can be judged without logarithmic compaction.

5.3 Drop Size Measurement

5.3.1 Introduction

Statistical analysis of drop size using computer spreadsheets found that over the range of CP temperatures and flowrates used in the heat transfer work, initial DP drop size could be considered independent of these CP conditions. Since a constant injection orifice size and DP initial condition was used, initial DP drop size was found to be a function of DP flowrate. In the interests of brevity only a simple table of initial drop size versus DP injection rate, md, is presented here.

An example of the spreadsheet for four of the photographic runs for injection pump speed 3 ($md = 3.74 \times 10^{-4}$ kg s^{-1}) is shown in figure 5.1, appendix 16. Note that photographic run numbers are entirely independent of heat transfer run numbers. Also the spreadsheet has been truncated to four runs to fit on the page - in actuality more runs were done at different CP conditions, which gave an eventual overall mean diameter of 6.22 mm for this run with a similar standard deviation. This example shows that the variation in mean diameter between the different CP conditions for each run is small compared to the standard deviation, justifying the use of DP flow as the only significant determinant of initial drop size in these tests. For convenience the drop sizes are sorted after transcription into ascending order in figure 5.1. Measurements were taken to the nearest 0.5 mm.

Figure 5.2 is an example of the spreadsheet used to determine appropriate

sample size to give accurate measurement without incurring a prohibitive time overhead. This is discussed in Section 2.3.2. A sample size of 20 was selected since above this number the mean diameter does not vary significantly when considering the measurement accuracy and standard deviation values.

5.3.2 Mean Drop Size Measurements

The following table reports the results obtained from drop size measurement analysis. Standard deviation for the whole range of drop measurements for a particular md is also shown.

Injection pump setting	md (10^{-4} kg s^{-1})	Mean D (mm)	Standard deviation(mm)
3	3.74	6.2	0.97
4	5.42	4.8	0.70
5	7.01	4.4	0.58
6	8.60	4.3	0.55
7	10.24	3.7	0.56
8	11.87	3.6	0.41
9	13.24	3.5	0.41
10	13.81	2.8	0.40

5.4 Drop Velocity

Approximate measurements were made from seven sets of video recordings to check initial velocity. The results are included for completeness, but are of confirmatory value only, and are insufficiently accurate to merit close analysis. The values measured were constant after 1 cm of rise. No evaporation occurred to these drops during measurement.

Drop size for measurement (mm)	Velocity (m s^{-1})
4.5	0.20
4.5	0.20
4.0	0.19
5.5	0.22
4.0	0.21
3.0	0.20
6.5	0.18

5.5 Experimental Error

5.5.1 Introduction

Experimental error can be estimated either from appreciation of the scatter produced or by accumulation of accuracy values in individual measurements. In order that a model can be independently fitted to the MEH results, given that there is as yet no proven theoretical basis which tells us conclusively how the results should look, no data which appears erroneous at this stage is omitted in reporting the results, unless it is subject to experimental verification. Thus estimation of scatter is limited as an error assessment method, and recourse is made to the estimation of measurement accuracy. This will tell us the error in measurement but will provide no evidence on the validity of the experimental method.

5.5.2 Measurement Accuracy

The following accuracies apply to the MEH measurement. The percentage figures are the mean percentage error.

Measurement of Tc1 within 1°C (1.6%)

Measurement of MEH within 1 mm (0.2%)

Evaluation of MEH within 10 mm (2%)

Heat Loss Effects within 1°C (1.6%)

Flow Measurement Reproduction estimated within 5%

Ambient Temperature fluctuates within 2°C (11%)

Thus if the errors have a cumulative effect, which is the worst case, experimental error is estimated at within 22% for the MEH values. This is not an unacceptable figure for heat transfer correlations. Work with the model suggests that ambient temperature fluctuation effects are small and not directly cumulative which would reduce the overall error considerably. The best estimation then is that percentage error for MEH is in the range 11 to 22%.

Consider the graph figure 5.3 and examine the Run 1A point 60.2, 22.1 which is near the mean value. Applying 22% error to the ordinate gives a range of 5 cm. Points for other runs scattered around this temperature all fall within the delineated band of 18 to 27 cm, so the upper error figure is supported by comparison to experimental scatter.

For the drop size measurement, calibration work shows that the method is accurate to within the readable accuracy of the rule i.e. 0.5 mm. Given the wide range of drop diameters, this gives a percentage error of 18% in 20 measurements for the smallest drop, and 8% in 20 measurements for the largest, with a mean variation of 12%. This value is comparable with the variation in drop size around the mean as quantified by the standard deviation, which is 12.8% for the case where mean D = 4.3 mm.

The drop velocity method is rather crude and accuracy for these results is

estimated as within 25%. This is adequate for the purpose of confirmation, but is low since the apparatus was not specifically designed for this measurement.

6. Computer Model Development

6.1 Introduction

6.1.1 Overview

Computer models of the heat transfer taking place in the column were developed with the following aims:

(i) To measure the applicability and accuracy of the instantaneous heat transfer coefficients calculated from dimensional analysis relationships.

(ii) To provide a program of practical value to allow initial design of a cooling column (e.g. potential computer aided design use).

Because of the difficulty in prediction of drop size as mentioned earlier, the computer models concentrate on prediction of heat transfer capabilities with appropriate drop diameter retained as a parameter requiring specification. This has some advantage in that the model is not limited to experimental injection orifice dimensions.

The computer models aim to predict the minimum column height for complete evaporation (MEH) for a given range of conditions, with a specified heat transfer coefficient calculation algorithm. All models were written in BBC Basic 5 on an Acorn Archimedes microcomputer which has a fast processor. For very long programs particularly in the highly interactive final versions, the program was compiled to cut down run time.

6.1.2 Stages In Development

The first simple overall model was developed early to allow interactive experimental design. The model was run many times to carry out a sensitivity analysis to investigate how the major parameters (e.g. drop diameter, viscosity of continuous phase) affected MEH when they were varied between their maximum and minimum values appropriate to the experimental range. The resulting analysis gave information important in two areas:

(i) Indicating which experimental parameters were likely to have a large effect on the MEH. As a result of this analysis for example, it was found that variation in drop diameter had a large effect and this eventually led to the decision to measure drop size directly with the photographic apparatus (after concluding that a theoretical prediction would not be appropriate).

(ii) Indicating which derived parameters could be assumed constant without greatly affecting the accuracy of the predicted MEH. This analysis enabled more accurate development of subsequent models, for example, continuous phase viscosity showed a 12% variation in predicted MEH when flexed between its maximum and minimum values appropriate to the potential continuous phase temperature range. For this reason later computer models incorporate an algorithm calculating this viscosity at the appropriate temperature through the column.

Using this information improved simple models were developed. Based on these models the incremental stage to stage interactive computer programs were developed which calculate parameters in each increment and check for eventual convergence to boundary conditions and accuracy limits. The development of the models followed the procedure below:

(i) Manual calculation of parameters.

(ii) Add refinement to the program. Debug until the program works.

(iii) Check against the manual calculation. Debug until the parameters agree and the results are 'reasonable'.

(iv) Check sensitivities of major parameters using this program to see if further refinement is required.

(v) Repeat from (i) until program is complete and correct.

To aid in this the programs were coded as a set of subroutines using the "Procedure" form of BBC Basic 5. The procedures are concerned with the performance of a specific task, as indicated by their title, and are called in the necessary sequence by the main program which supervises the iterative processes as necessary. Procedures may also be called from within a procedure. This method of coding is often used to allow ease of debugging for a large program, which can have each subsection debugged and tested as a separate program. The form was adopted for this reason plus the relative ease with which the sophistication of the program could be increased by addition of procedures in a 'building block' approach.

When this process was complete (requiring over 115 versions of the final program version eventually) the program was compared with experimental data. Various means of calculating increment heat transfer coefficient were used until the best fit to the experimental data was obtained, giving the most accurate practical computer model. Up until this last stage, heat transfer

coefficients were calculated using equation 2.2.6 suggested by Rowe et al [11] with the coefficient B set at 0.79.

6.1.3 Presentation Of The Computer Models

It is inappropriate to describe all versions of the computer models in full throughout their development in this thesis. As the later models build on the prior version, the earlier programs contain much material which is repeated in the later model. The presentation of the model herein is therefore a compromise between avoiding repetition of subset material and yet giving a complete picture of the model development which can be easily understood by showing the simple version with a sequential approach to its subsequent evolution. For this reason the most sophisticated program is presented in detail, with earlier models also presented but in less detail.Three models are presented:

(i) The simple overall model which treats the whole column as a single evaporative heat transfer stage. This is the basis for future models.

(ii) The incremental model which assumes complete disengagement of vapour from the liquid droplet (version 77).

(iii) The incremental model which assumes vapour attachment to the liquid droplet resulting in a degree of insulation of some drop area, and droplet surface area modification. This is the most complex model which comes closest to reproducing experimental results (version 115).

All three programs have a full listing in the appendices. These programs have line numbers which are numbered according to the following convention:

Lines	1 to 99	Remark statements
Lines	100 to 109	Data statements
Lines	109 to 999	Main program
Lines	1000 onwards	Subprogram procedures

The procedures are all called with the 'PROC' statement and defined later in a DEFPROC ... ENDPROC construction.

6.2 The Simple Overall Model

6.2.1 Overview

This model was developed at an early stage and is basically a program to carry out a fairly involved heat transfer calculation which needed to be repeated many times. The program was written with the anticipation of its subsequent development into the more sophisticated models which use iterative and incremental methods. It is included here for reasons of completeness, because of its relevance to experimental and program design, and as an aid to explaining the other programs in a stepwise fashion.

The results of this program are evaluated by comparison with the later models to investigate the accuracy which could be achieved in a simple model but its use is not recommended in design work as the approach is somewhat simple and inaccurate.

As this program was developed at an early stage, before the conclusion of much of the experimental work, data input to this program is less accurate than was later determined e.g. drop diameter experiment work was initiated partly because of this models predictions, therefore accurate drop diameter information could not be input to the program at its time of development; some

column conditions were also not accurately known therefore some physical property data are approximations later found to be inaccurate.

The program listing (appendix 7), calculations and flexibility results reflect this early data, although for later comparison purposes the program was run with the same data as later models.

The program is described in less detail than the final version of the incremental model, consistent with providing relevant information without too much repetition.

To understand the following sections it is necessary to study the program listing (appendix 7) and make reference to the computing symbol index (section 6.6).

6.2.2 Calculation Methods And Theoretical Basis

The best way to show how the program operates is to show manual calculations upon which it is based. Appropriate theory is discussed as it is applied and reference made if the relevant point has been covered in more detail in the theory section, chapter 2.

Consider the schematic diagram of the process, figure 2.4 (appendix 1). For all the injected DP to be evaporated, heat is removed from the CP in an amount which can be determined by heat balance. Assuming the column is well insulated and heat losses are negligible we can easily calculate Tc2 for any given Tc1 and DP mass flowrate, md. This assumption is justified and discussed in section 2.4.2.

Firstly a data set was determined which, given that all the experimental work had not been completed at the inception of this model, would adequately represent the system properties at average conditions.

These were as follows:

(i) Density of continuous phase (assumed constant)

$$\rho c = 994 \text{ kg m}^{-3}$$

(ii) Viscosity of continuous phase (assumed constant)

$$\mu c = 718 \times 10^{-6} \text{ kg m}^{-1} \text{ s}^{-1}$$

These values are for water at 35°C, 1 atm. Pressure effects are small over the range 1 to 1.1 atm. (due to hydrostatic pressure in the column), but the assumption that a constant temperature value can be used in the continuous phase, particularly for viscosity, is poor and gives rise to inaccuracy in the important Reynolds number and Prandtl number dimensionless equations used in the model. The inaccuracy due to the assumed temperature being incurred will become greater as continuous phase temperatures depart from 35°C. This will be most apparent at high CP inlet temperatures (Tc1) and low continuous phase temperature drop (ΔTc) i.e. low mass flowrate of dispersed phase (md). The assumption that any constant value is applicable will be less accurate at high ΔTc i.e. low CP flowrates (Fc) and high md. Hence this approximation is likely to be inaccurate over a range of operations. This is shown in sensitivity analysis and corrected for in later models.

(iii) Density of dispersed phase (assumed constant)

$$\rho d = 612.3 \text{ kg m}^{-3}$$

This is taken for isopentane at 301.03 K, 1 atm. The assumption that it stays

constant relies firstly on the hydrostatic pressure effects being negligible, which over the range 1 to 1.1 atm. gives less than 0.05% variation in density, and secondly the assumption that the temperature of the drop is constant at its boiling point at 1 atm. (i.e. 301.03 K).

This second assumption is less accurate for two reasons:

a) The simplification in the model derivation is that once the droplet starts to boil its liquid temperature remains constant at that boiling point, regardless of any reduction in boiling point that would be due to hydrostatic pressure reduction as it rises through the column. This simplification is discussed in the theory (section 2.3.1) and is necessary to prevent extreme complexity in the modelling calculations. The exact magnitude of error involved in this assumption is difficult to ascertain and will be greater with dispersed phase liquids which have a higher tendency to flash under reducing pressure. The vapour pressure relationships of isopentane compared to n-butane show that the implication is more justified in the isopentane case. As explained in section 2.3.1 the net effect is likely to be that the program over estimates MEH. The effect on ρd however is small, the 2 K difference in boiling point which occurs between pressures of 1 atm. and 1.1 atm. gives a variation of 2 kg m^{-3} in ρd, about 0.3%.

b) The assumption in the model is that sensible heat transfer to the drop, to increase its temperature from injection temperature to boiling point, is negligible compared to the evaporative heat transfer. Subsequent calculation shows this assumption to be a poor one, requiring correction in later models. In actual fact the DP will begin to heat up as soon as it enters the injection tube, and will need to gain typically 12°C before it will boil. It has been shown in the theory section that heat transfer to the insulated injection tube is negligible

(section 2.4.6).

As it rises through the column, drop temperature (TDROPd) will increase and as pressure reduced DP boiling point (TBPd) will reduce until at a certain height which cannot be simply determined, boiling will take place. This model takes no account of the sensible heat transfer. This has an affect on the drop temperature and heat balance which is significant. However the consequences for the assumption of constant density are the same as those given in (a) above, i.e. <0.3% variation.

As a result of both these reasons the boiling temperature varies with operating conditions and cannot be strictly assumed constant (see later). Thus the assumption of a constant density at an assumed constant boiling point is not accurate. Fortunately sensitivity of density to temperature over the experimental range is low so error is small (0.3%) and a constant density is itself a reasonable approximation.

(iv) Specific heat capacity of continuous phase (assumed constant)

$$Cpc = 4178 \text{ J kg}^{-1} \text{ K}^{-1} \ (35^{\circ}\text{C, 1 atm}).$$

The assumption of constant Cpc is good for hydrostatic pressure effects and over the continuous phase temperature range concerned varied by less than 0.5%.

(v) Thermal conductivity of the continuous phase (assumed constant)

$$kc = 0.625 \text{ W m}^{-1} \text{ K}^{-1} \ (35^{\circ}\text{C, 1 atm}).$$

The assumption of constant kc is a poor one since the variation of kc over the relevant temperature range is 7%. This value is really therefore only valid where the continuous phase temperature is close to 35°C. This will typically be when Tc1 is around 40°C. The value of kc affects Prandtl and Nusselt

numbers (Pr and Nu) and at higher Tc1 values, kc should be higher. Having a kc value too low will make calculated heat transfer coefficient (h) too high, since in the form of the equation used h is approximately proportional to $kc^{0.7}$. This will lead to an underestimation of MEH.

(vi) Specific latent heat of evaporation of dispersed phase (assumed constant)

$$\lambda = 334.7 \times 10^3 \text{ J kg}^{-1}.$$

This value is for isopentane at the conditions 303.8 K, 1.1 atm. The assumption of constant λ relies on the same assumptions of DP boiling temperature given in (iii) (a) and (b) above. Over the range of hydrostatic pressure and temperatures present the variation in value of λ is between 334.7 and 336.8 kJ kg^{-1}, an acceptable variation of <1%.

Data is taken from the PPDS program (see appendix 5) for isopentane and from steam tables for water.

Secondly a set of variables for use in developing the model were chosen. These were:

(i) Droplet diameter D = 5 mm.

This model is based on initial drop diameter only. Velocity and heat transfer characteristics are all based on this initial value. This assumption is a fundamental approximation which separates this model from its more sophisticated antecedents. Comparison of this model with others gives an indication of its accuracy.

(ii) Continuous phase volume flowrate Fc = 7.59×10^{-6} $m^3 s^{-1}$

(iii) DP mass flowrate md= 8.6×10^{-4} kg s^{-1}

All 3 variables are not directly applicable to actual experimental values but are those estimated at time of development.

Calculations can now proceed as follows:

(i) Calculation of rising velocity.

This is based on the method of force balancing between drag, gravitational and flotation forces on the droplet as shown in ref [12]. This makes the assumption that the effect of internal circulation on drag is negligible, the drop remains spherical. These assumptions are better for small drops where scope for circulation and distortion is less due to the greater relative effect of surface tension. The consequences of these assumptions which are made to simplify the model are discussed in the theory section (2.2.3 et seq). Considering the validity of these assumptions note that experimental measurement (section 5.4) shows that the initial rising velocity calculated agrees with that measured to within experimental error of 25% which shows that the assumption is not grossly inaccurate.

A further assumption is that the drop will accelerate to its terminal velocity so quickly, that lower velocities can be ignored. Experimental work (section 5.4) shows this to take place within 1 cm of injection so in most cases is justified as long as column heights are large which reduces the significance of the error.

For a droplet moving upwards under the effects of buoyancy, drag force and gravity act downwards, and the droplet will accelerate until these forces are balanced.

$$\text{Upthrust} = \text{drag force} + \text{gravity force}$$

$$(\rho c \times \pi \times D^3 \times g) / 6 = (R \times \pi \times D^2) / 4 + (\rho d \times \pi \times D^3 \times g) / 6$$

$$(R \times \pi \times D^2) / 4 = ((\rho c - \rho d)\, \pi \times D^3 \times g) / 6$$

$$R = 2((\rho c - \rho d)\, D \times g) / 3 \qquad \{6.2.1\}$$

this equation allows drag force coefficient R to be calculated thus:

$$R = (994 - 612.3) \times 5 \times 10^{-3} \times 9.81 \times 0.6667$$

$$= 12.5 \text{ N m}^2$$

To calculate ud is a trial and error method since the relationship to calculate ud is dependent Reynolds number (Re) which also depends on ud. However, for droplet diameters of the initial values used it can be shown that Re will lie in the range 500 to 10000 so only this region needs consideration in this simple model. The value of Reynolds number considered here is that based on relative velocity between DP and CP, no continuous phase velocity is involved. For this region the equation:

$$R / \rho c\, ud^2 = 0.22 \qquad \{6.2.2\}$$

applies.Therefore: $12.5 / 994\ ud^2 = 0.22$

$$ud = 0.239 \text{ m s}^{-1}$$

Check Re:

$$Re = D\, ud\ \rho c / \mu c = (5 \times 10^{-3} \times 0.239 \times 994) / (718 \times 10^{-6}) = 1653$$

which is >500 and < 10000.

Having calculated ud the heat transfer calculations can now proceed. The heat transfer relationship of Rowe [11] is used and this is based on Reynolds number. The Reynolds number chosen for this is slightly different to the one based on relative motion of DP and CP as measured by ud. The value of Re used includes continuous phase velocity uc. The reason for including this is based on the premise that Re for film coefficient of heat transfer relationships is present to characterise turbulence and hence film thickness. Thus, whilst recognising that in a dimensional analysis approach which is non analytical

such premises can only be empirically proven, it is decided to include CP velocity, uc, into the Re value for heat transfer, since uc undoubtedly affects turbulence at its higher values. The lower values of uc are so small compared to ud that it is of small consequence, particularly when it is noted that Reynolds number is raised to a fractional power in the Rowe relationship.

$$Fc = 7.59 \text{ ml s}^{-1}$$

Cross sectional area of column = $\pi \times (4.7 \times 10^{-2})^2$

$$= 6.93 \times 10^{-3} \text{ m}^2$$

$$uc = 7.59 \times 10^{-6} / 6.93 \times 10^{-3} = 1.09 \times 10^{-3} \text{ m s}^{-1}$$

$$Redc = 5 \times 10^{-3} (1.09 \times 10^{-3} + 0.239) \times 994 / 718 \times 10^{-6}$$

$$= 1661$$

Rowe [11] relationship:

$$Nu = 2 + 0.79 \, Pr^{1/3} \, Re^{1/2} \qquad \{eqn\ 2.2.6\}$$

$$Pr = Cpc \, \mu c / kc = 4178 \times 718 \times 10^{-6} / 0.625$$

$$= 4.80$$

$$Nu = 2 + 0.79 (4.80)^{1/3} (1661)^{1/2}$$

$$= 56.31 = h \, D / kc$$

$$h = 0.625 \times 56.31 / 5 \times 10^{-3} = 7.04 \times 10^{3} \text{ W m}^{-1} \text{ K}^{-1}$$

$$\text{drop surface area} = \pi \times D^2 = 7.85 \times 10^{-5} \text{ m}^2$$

Overall heat balance, basis one seconds operation at steady state:

For total evaporation of all DP:

$$Q = md \, \lambda$$

$$= 8.6 \times 10^{-4} \times 334.7 \times 103 = 288 \text{ W}$$

$$= mc \, Cpc \, \Delta Tc$$

$$mc = 994 \times 7.59 \times 10^{-6} = 7.54 \times 10^{-3} \text{ kg s}^{-1}$$

$$\Delta Tc = 288 / (4178 \times 7.54 \times 10^{-3}) = 9.14^{\circ}C$$

If $Tc1 = 42^{\circ}C$ (water inlet temperature)

$$Tc \text{ average} = (42 - 9.14 / 2) = 37.4^{\circ}C$$

Taking mean boiling point of isopentane as 30.6°C (1.1 atm) then driving force ΔT is approximated as (Tc mean - TBP mean). This is an approximation since the appropriate driving force for this countercurrent system is the log mean driving force. This assumption is not very accurate and a much better approximation method is made in the incremental models. In this case taking the assumption of negligible sensible heat transfer as valid

$$LMTD = ((42 - 30.6) - (32.9 - 30.6)) / (\ln ((42 - 30.6) / (32.9 - 30.6)))$$
$$= 5.7^{\circ}C$$

whereas the taken: $\Delta T = 37.4 - 30.6 = 6.8^{\circ}C$

which is a 19% error. This was a simplification made for the benefit of later models and has no other justification. In this case the model will overestimate Q and therefore underestimate MEH due to this assumption.

Heat transferred to drop,

$$Q = \text{“}h\ A\ \Delta T\text{”}$$
$$= 7.04 \times 103 \times 7.854 \times 10^{-5} \times 6.8$$
$$= 3.78\ W$$

hence mass evaporated per second $= q / \lambda = 3.78 / 334.7 \times 10^{3}$

$$= 1.13 \times 10^{-5}\ kg\ s^{-1}$$

mass of one drop = volume of drop x ρd

$$= 4\ \pi\ r^{3}\ \rho d / 3 = 4 \times \pi \times (2.5 \times 10^{-3})^{3} \times 612.3 / 3$$
$$= 4.01 \times 10^{-5}\ kg$$

evaporation time for one drop $= 4.01 \times 10^{-5} / 1.13 \times 10^{-5} = 3.55\ s$

equivalent column height necessary for 3.55 s contact time = MEH

$$MEH = 3.55\ (ud - uc)$$
$$= 3.55\ (0.239 - 0.001)$$
$$= 0.845\ m$$

Note that the effect of uc is to reduce column height necessary for a given

contact time. If uc becomes as large as ud heights will approach zero as drops are carried down the column relative to the column wall. In actual practice however near zero column heights would not be achievable since the column area would be overloaded with DP droplets / bubbles at the injection point which would impede good mixing and heat transfer in the column. Vapour slugging and droplet entrainment in the vapour could well occur and hence column heights below 10 cm were not examined (see experimental section 4.1).

The above calculation and discussion illustrate the way the simple overall model achieves its calculation of MEH and the drawbacks involved.

6.2.3 Procedural Analysis

A description of the main program and subprogram procedure tasks now follows. Reference should be made to the program listing, appendix 7, list of variables 6.6 and example calculation in the previous section 6.2.2.

Line 10 Contains program title.
Line 20 Is a remark to aid identification of data markers in line 100.
Line 100 Contains the main data list in the order given in lines 20 and 1010. Tc1 is specified at the end of the list.
Line 110 Procedure READ_DATA is called.

PROCREAD_DATA reads value for variables in the READ statement from the DATA list in line 100.

Line 120 Procedure FALLING_V is called.

PROCFALLING_V calculates uc as in section 6.2.2.

Line 130 Procedure FORCE_BAL is called.

PROCFORCE_BAL This calculates ud as shown in section 6.2.2. If Reynolds number (Redc) is outside the assumed range the program is stopped and an error message printed. Redc is then modified for the heat transfer calculation.

Line 140 Procedure hCALC is called.

PROChCALC Calculates Nusselt and Prandtl numbers then heat transfer coefficient h as in section 6.2.2.

Line 150 Procedure O_HEAT_BAL is called.

PROCO_HEAT_BAL This calculates continuous phase temperature drop from an overall heat balance (Dtc).

Line 160 Procedure MASS_EVAP is called.

PROCMASS_EVAP The mean CP temperature, TcMEAN is calculated by subtracting half of Dtc from the Tc1 specified. The mass of DP evaporated in 1 second is calculated (MEVAP).

Line 170 Procedure TIME_HT is called

PROCTIME_HT This procedure calculates contact time and equivalent MEH (COLEVAPHT) as shown in section 6.2.2.

Line 180 Prints a blank line to give separation.

Line 190 Prints out the value of ud and Tc1.

Line 200 Prints out h and the MEH as "CHT".

Line 210 Prints out CP temperature drop.

Line 220 Ends the main program.

6.2.4 Typical Program Output

The output of this program is virtually self explanatory. Appendix 8 shows a typical hard copy printout produced by the program listing in appendix 7.

The program produces predicted MEH for the value of Tc1 specified in the data statement in °C. MEH values, printed out as "C HT" are in metres. It can be seen that the value for Tc1 = 42°C is 0.844 m which corresponds within round off error to the calculation shown in section 6.2.2, as do the other variables printed out. Units are omitted in printout since this would only serve to extend the program. The units are however, strict SI except that °C are used instead of Kelvin (Prefixed units are not used unless they are fundamental quantities i.e. kg and kmol).

6.2.5 Results Of Sensitivity Analysis

The following table summarises the results gained from the simple overall model when various parameters were varied to determine the corresponding sensitivity of predicted MEH. The MEH predictions at Tc1 = 42°C were used in all the sensitivity analysis in this and subsequent sectors as being the more practically relevant and more sensitive to change than higher temperatures. Other analyses at different Tc1 values were carried out but for brevity are not shown here, the results supporting those shown below.

The variable range is anticipated maximum and minimum values for the experimental system at time of program development.

Variable	Range	% Variation in MEH
D	3 to 8 (mm)	149
μc	351 to 718 (x 10^{-6} kg m^{-1} s^{-1})	12
λ	334.7 to 336.8 (x 10^{3} J kg^{-1})	1.1
Cpc	4178 to 4198 (J kg^{-1} K^{-1})	0.5
kc	0.625 to 0.670 (W $m^{-1}K^{-1}$)	4.8
ρc	994 to 972 (kg m^{-3})	1.6
ρd	609.4 to 612.2 (kg m^{-3})	0.3
TBPd	27.9 to 30.6 (^{o}C)	40

As explained earlier experimental modification was implemented to improve measurement of D since this was crucial. Any variable showing more than 2% variance was not assumed constant in later models. Later models also had to allow for changes in D due to evaporation as this was likely to have a large effect on the accuracy of the models.

6.3 Common Points In Both Incremental Models

6.3.1 General Overview

This program is based on dividing the column into increments in the time domain. Increments of distance were considered but time was selected since it is easier to handle in a steady state model and is likely to give a more uniform temperature profile through the column. Using this approach, column height equivalent to the time increments was calculated from velocity information.

After carrying out an overall heat balance to establish boundary conditions the programs divide the column into a number of time increments the initial size of which is specified by the user in the program. The programs begin at column bottom and calculate incrementally upwards.

The programs calculate heat transfer coefficients using the equation supplied by the user in terms of dimensionless groups and then heat transfer rates for the increment. After initial injection the DP droplet will increase in temperature until it reaches its boiling point temperature. In this range drop temperature increase is calculated and the temperature of the continuous phase at inlet (i.e. the 'top') of the increment is calculated. The programs then move on to the next increment and progress up the column. When the DP droplet reaches its boiling point no further temperature rise takes place and the program continues, calculating the mass of the DP in vapour and liquid phases at each increment. When total evaporation has been calculated the progress stores the results of the first run through, halves the increment size and runs through the calculation again until total evaporation is calculated.

Column height for the two consecutive runs is calculated (by reference to velocities of both phases) and compared to an accuracy tolerance limit (0.3%). If they vary by more than this limit then the increment size is halved again and the process repeated until the tolerance is met. The inaccuracy of temperature driving force approximation is then measured at its greatest point, and compared to a tolerance limit (1%). If the tolerance is exceeded then the increment size is further reduced, which improves the approximation, until the tolerance is met.

The column height thus calculated is then used to calculate a new DP boiling

point, averaged over the new column height with its appropriate hydrostatic pressure effect. If the difference between the new boiling point and the old is less than a tolerance (0.05 ^{o}C) then the whole process is repeated with the new DP boiling point.

Eventually a column height for MEH is calculated which meets all the accuracy tolerances. If desired, a column profile can be printed of all major parameters for each increment. This is likely to be very large and of limited use due to the sheer bulk of data - however it is of use for debugging purposes.

6.3.2 Calculation Procedure And Rationale

Calculation procedure follows the outline given in the general overview section above. This section details the program bases in heat transfer and fluid mechanics calculation and theory. Assumptions and approximations are detailed when made and summarised in a later section.

A. Factors Affecting General Model Development.

Time or distance increments to be used.
The main choice was between these two parameters which are related by drop velocity. Other incremental possibilities such as temperature were ruled out on the grounds of complexity. As stated in section 6.3.1 time was chosen for reasons of simplicity although distance could equally well have been used. When an expression for heat transfer rate measured in Watts is used, it is easier to calculate an amount of heat by multiplying by time than a more involved procedure involving velocities.

Direction of stagewise calculations.

The calculations could proceed downward from the top or upwards from the bottom. Both have advantages and disadvantages, since the column is countercurrent so for each medium starting conditions are better specified at opposite ends.

The decision was made to make the interactive programs start at column bottom and work up to the top since this gives more straightforward approach when considering the DP boundary conditions. These are known at the column bottom, and because of simplifying assumptions discussed later, are not of great significance at column top. Since this is a countercurrent column however, CP conditions are known at column top but column bottom temperature has to be calculated. This disadvantage is outweighed by the advantages for the DP which is the more complex to describe as it is undergoing phase change, and it is a relatively simple matter to calculate CP outlet temperature at column bottom by overall heat balance assuming total evaporation of the DP. For the simple overall model direction is not critical.

Having made these decisions the programs could be developed, bearing in mind which parameters could be assumed constant and which needed to be varied for each increment as a result of sensitivity analysis using the simple overall model.

B. Incorporation of Sensitivity Analysis Results

Drop diameter, D.

The initial size of drop diameter is specified for the program as data resulting from experimentation. This is seen to be more accurate than any prediction formula found in literature (see theory section 2.2.3). Given the high sensitivity

to drop diameter the large amount of work involved in measuring drop size was felt to be justified and even so drop size still exhibited scatter which will effect the models results. In a practical development of the models it is clearly not very appropriate to require a drop size to be input to the program and a predictive technique would be desirable based on the usual specification of orifice size, flowrates, interfacial tension, etc, but this will be limited by lack of data for the latter property and lack of a definitive formula reproducing experimental work. This is an area for future development of the models if so desired, but will require experimentation and research in the area of drop size and form to achieve a degree of confidence in the results. Such studies have formed the basis for complete PhD theses in the past.

It is better when investigating the accuracy and application of the models to supply the drop diameter and not introduce a high level of inaccuracy at a fundamental stage, hence measurement and specification of drop diameter is used to limit the inaccuracy. Nevertheless it must be borne in mind that we would expect experimental scatter due to drop size variation about the mean when comparing experimental results and model results.

The degree of variation will depend on the validity of the mean initial drop diameter used when the experimental rig is left to run at steady state for a period of time, compared to the assumption of constant initial drop diameter made in the models.

The incremental approach of the models, calculating variation in drop size with each increment is the second way that the sensitivity to D is incorporated. This is a much more realistic approach than in the simple overall model.

Incremental size is reduced until predicted MEH shows no significant change

with further reduction. This method therefore compensates for the sensitivity to drop diameter as it changes in the heat transfer process.

CP viscosity, μc.

The temperature dependence of μc is allowed for by calculating μc for each increment at the increment temperature. Viscosity for a given temperature is calculated in a user defined function, FNVISCOc. The algorithm for calculating viscosity as a function of T was generated by feeding data from steam tables over the appropriate temperature range into the curve fitting program PLOTER (on the Polytechnic VAX mainframe) and obtaining a best fit polynomial for μc versus Tc. The program (see graph and printouts, figs 6.1 and 6.2, appendices 9 and 10) gave the following fifth order polynomial:

$\mu c = 1720.31 - 50.4985Tc + 0.90707Tc^2 - 0.010014Tc^3 + 6.09509 \times 10^{-5}Tc^4 - 1.5383 \times 10^{-5}Tc^5$

where Tc is in °C and μc is multiplied by 10^{-6} to get kg m^{-1} s^{-1}. Mean error of fit is 0.15 or less than 0.03%.

CP thermal conductivity, kc.

This was allowed for in the same manner as μc above. The PLOTER program (see graph and printouts, figs 6.1 and 6.3, appendices 9 and 10) gave the following sixth order polynomial:

$kc = 1177.06 - 74.1296Tc + 3.8319Tc^2 - 0.100445Tc^3 + 0.14376Tc^4 - 1.0698 \times 10^{-5}Tc^5 + 3.24181 \times 10^{-8}Tc^6$

where Tc is in °C and kc is multiplied by 10^{-3} to get W m^{-1} K^{-1}. Mean error is 9.90 or less than 0.02%. The program function FNTHERMKc calculates kc at increment temperature using this relationship.

DP boiling point TBPd.

The direct effect of this on heat transfer driving force is shown in the sensitivity

analysis, despite the fact that the maximum possible variation in TBPd is less than 3°C (around 10%). The method of incorporating the variation of TBPd due to hydrostatic pressure changes in the column into the incremental models was the subject of some thought. The most desirable means would be to recalculate a new TBPd at each increment. This would prove difficult however since the MEH is not known until the final increment is reached. The program would have to use an assumed value then reiterate with a new value based on the predicted MEH. This would greatly increase an already considerable run time for the program as convergence would be quite slow. Development time for such a complex procedure would be large. A compromise between these time factors was therefore made to include TBPd variation in a simpler way which is consistent with the modelling assumption in the theory section (2.3.1) that TBPd does not vary much when boiling commences. Both models calculate a MEH using a typical mean TBPd of 28.6°C. This is the average of 91 cm and 20 cm hydrostatic head values for TBPd. After calculation of MEH, the value of TBPd is modified by interpolation to the new mean value, and if this is significantly different (0.05°C or above) then the program is rerun with this value. This procedure is continued until the TBPd variation is no longer significant.

This approach uses a single TBPd based on mean hydrostatic pressure for the whole column rather than an incrementally calculated one but represents a good compromise between the need to modify TBPd, the time constraints mentioned earlier and the accuracy required.

Linear interpolation was used to calculate TBPd at various column heights between the maximum and minimum values generated by the PPDS program (appendix 5), since it gave a maximum error of only 0.07%.

The tolerance value of 0.05% was partly determined by successive runs of the base case program with various values. As the tolerance has a great effect on run time it needs to be as small as is acceptable. If we compare base case runs of model 115VAMODEL at Tc1 = 42°C:

Predicted MEH with tolerance of 0.05°C = 0.7199 m

Predicted MEH with tolerance of 0.005°C = 0.7228 m

-an increase in MEH "accuracy" of 0.4% or 3 mm with an increase in run time of 55% (53 seconds). When we consider that measured temperatures are likely to be at the very best accurate to ± 0.1°C then 0.05°C tolerance seems a good value.

Further calculation points are described in detail for the vapour attachment model section 6.5.3.

6.4 The Incremental Model With Vapour Disengagement

6.4.1 General

This version of the model, 77VDMODEL, was developed after the simple overall model, 38SOMODEL, and prior to the more complex vapour attachment model, 115VAMODEL. To avoid repetition this model is not described in as much detail as the later model, which is the most vigorously tested and is considered the best description of real behaviour based on the work of Sideman and Taitel [2] (see below sections 6.4.2 and 6.5.2). The following 6.4 section should therefore be read in conjunction with section 6.5 to get a detailed picture of the vapour disengagement model. However, this model is important both as an intermediate step in developing the later version, and as a means to study the relative importance of vapour bubble / liquid droplet behaviour on MEH determination.

6.4.2 The Assumption Of Vapour Disengagement

This assumption is the major difference between this model and the later model shown herein. The assumption is that as the liquid droplet evaporates, vapour thus formed quickly detaches from the droplet and leaves a wholly liquid surface area for heat transfer. Thus any effect of a joint bubble / droplet on heat transfer area or on velocity due to increased buoyancy is neglected.

The likely effect of vapour attachment on heat transfer is to considerably reduce film coefficient for heat transfer due to the low values typical for the vapour relative to liquid phases. However liquid / liquid surface area is also modified, and is likely to increase due to sloshing effects.

The likely effect of vapour attachment on drop velocity is to increase buoyancy force due to the lower density, but increase drag force due to the increased diameter of the bubble / droplet. By comparing the two models it can be shown that the predicted net result of the two opposing effects is that vapour attachment increases velocity i.e. the buoyancy effect predominates. The increase in velocity would tend to increase film coefficients of heat transfer so to an extent the effect of vapour insulation is compensated for. It is difficult to predict what the implications of the assumption of vapour disengagement are without recourse to comparison of the two models. This comparison is discussed later (section 7.3.2).

Turbulence of the CP is likely to help vapour bubbles to break up and leave the droplet so it might be expected that vapour disengagement is potentially a better assumption at high CP flowrates.

6.4.3 Calculation Basis And Rationale

The calculation basis for this model is essentially the same as for the vapour attachment model so rather than reproduce that section (6.5.3) this section outlines the growth from the overall simple model, and summarises the differences between the two incremental models.

A. Development from prior model. The adoption of an incremental approach allows the incorporation of sensitivity results as detailed in section 6.3.2. The calculations for one increment correspond to those made for the whole column in the overall simple model, with modifications made to certain parameters based on this sensitivity analysis.

Initially increment size is set to a specified value (0.005 s) which is chosen to be fairly close to that necessary for program accuracy convergence. The increment size is reduced as the program recalculates, and choosing a too large initial value would merely extend program run time. The incremental calculations are carried out in a stage to stage manner, with the final MEH equivalent to the sum of the increments calculated. This procedure is done again and subsequent calculations checked for accuracy. If this is sufficient then a loop testing for correct TBPd is initiated. MEH is indicated when the calculated mass of the liquid droplet becomes zero or (slightly) negative due to evaporation. The program contains three sets of convergence tolerances to be met before completion. Printout of results is improved with either a final printout or an increment-by-increment printout possible - the latter very verbose except for debugging work. Hardcopy printout is selectable. Arrays are set up to store major incremental parameter values which can be printed out as a column profile. Internal limits are set via the variable M to prevent the program running past maximum number of increments in order to trap errors in data

entry which may result in an infinite loop occurring.

B. Summary of major program differences between 77VDMODEL and 115VAMODEL. The major extension to 77VDMODEL occurs in the procedure PROCMASS_EVAP. In this model this procedure is only concerned with calculating how much the mass of the liquid droplet is reduced by any evaporation in the current increment. In 115VAMODEL the additional task of working out the overall density and available liquid heat transfer area is done in this procedure. Other changes are largely to do with handling the extra 18 program variables necessary to the additional calculation.

Other minor changes to 77VDMODEL were made on the grounds of better programming technique e.g. removal of some printing job coding from the main program into a subprogram procedure.

6.4.4 Procedure Analysis

Again to avoid repetition a simple analysis of the main differences of 77VDMODEL from 115VAMODEL is given here. This is most apparent in the way PROCMASS_EVAP operates. This procedure is called from the main program after the droplet temperature has reached boiling point (see appendix 11).

Line 3040 Defines procedure start
Line 3050 Calculates drop surface area ASURFd from the formula "πD^2"
Line 3060 Calculates increment temperature driving force DT (= increment temperature - drop temperature)
Line 3070 Calculates heat transferred from CP to DP (by "$Q = h A \Delta T$") per drop per second, QDROPcd

Line 3080 Calculates mass evaporated per drop per second by dividing by specific latent heat of vaporisation
Line 3090 Calculates mass evaporated per drop, MEVAPDROP, by multiplying by the size of the time increment in seconds
Line 3100 End procedure definition.

6.4.5 Typical Program Output

A typical hardcopy printout is shown in appendix 12. On screen printout is slightly different to this in that the computer prints the current increment number for each iteration on screen as it progresses through the calculation. This is useful as an indication that the computer or program has not 'hung up' in some way and as a measure of progress towards completion. This screen printout is determined at line 380.

The hardcopy printout is fairly self explanatory. One set of results is produced for the final interaction of each value of mean DP boiling point (TBPd). In appendix 12 only one modification of TBPd was necessary so the final output shows values for the initial TBPd of 28.6°C and the final value of 28.82°C. The phrase "NOW ITERATING FOR CORRECT MEAN B PT" serves to split up the relative results.

It is always the lower result set which is the final answer matrix. In the first section is a reprint of specified data and fixed variables, uc, mINJECTEDd, etc, to identify the corresponding data set. Next comes the most significant result, the column height for MEH in metres for the given Tc1 in degrees C. This is highlighted by 'arrows'. Program operational data and important temperatures follow. In the third section is a printout of important variables averaged over each increment. A more detailed description of the printout identical to this for

the program 115VAMODEL is given in section 6.5.6. Operations for getting increment by increment printout and a column profile are also detailed therein.

6.5 The Incremental Model With Vapour Attachment

6.5.1 General

This program, 115VAMODEL, is the most sophisticated of the three presented. It is not only the most rigorously tested and most systematically coded, but it is based on the model which is most accurately represents the physical situation, as far as can be determined. As such this program represents the end result of a large part of the work done in this project. The program and its calculation basis is therefore presented in some detail.

Relative points made in earlier subsections to chapter 6, particularly section 6.3, are not repeated in detail here, so section 6.5 should be seen as following on in sequence rather than as a completely stand alone description. Relevant theoretical points are discussed in section 6.5.3 where this is more appropriate than referral to the theory discussion, chapter 2.

6.5.2 The Assumption Of Vapour Attachment

Unlike program 77VDMODEL the model for program 115VAMODEL assumes that vapour formed from the liquid droplet remain in contact with the droplet until all liquid has evaporated. Thus it is assumed that cohesive vapour-liquid tensile forces are stronger than the forces which would tend to produce separation. The difference in buoyancy forces between vapour and liquid due to their differing density is the major force for detachment. However this is opposed by greater drag forces for the vapour bubble due to its larger size and

hence larger projected area. CP turbulence is applied to both phases so its absolute effect as a precursor to disengagement may be small, however it is likely that the resultant distortion and flexing of the bubble / droplet would assist in bringing about disengagement should it be driven by other forces. This assumption is justified by consideration of the high speed photographic work originally done by Sideman and Taitel [2] as discussed in the theory section (2.2.2). This work was done in a static CP column which also leads to the validity of the model possibly being lower at high CP flowrates.

The model assumes then that, based on Sideman's [2] work, after about 1% evaporation takes place the liquid droplet distorts from the spherical and forms a lens shape at the lower part of the vapour bubble. This is a complex process to describe mathematically and certain simplifications have been made to model this behaviour (see figures 2.1 and 2.2).

Firstly it is assumed that the vapour bubble is an insulating layer with no heat transfer taking place to the vapour from the CP. This assumption has been discussed earlier (section 2.2.2). All heat transfer takes place from CP to the remaining liquid DP via the appropriate heat transfer surface area. This area therefore needs estimation. Then we assume the vapour bubble and liquid droplet remains spherical in shape. This is an approximation since it is known that the bubble will distort to give a larger surface area, particularly after about 20% evaporation. The liquid will spread to form a layer at the lower side of the bubble due to gravitational forces. The area of the liquid liquid interface at the bottom of the 2 phase sphere must therefore be estimated. This is done by taking Sideman and Taitel's [2] conclusion that a good average value of vapour opening angle, i.e. the angle subtended at the centre of the 2 phase sphere by the spherical segment of vapour (2β in figures 2.1 and 2.2), is 270°. The conclusion was based on heat transfer work, therefore this value would

incorporate any sloshing effects of the liquid inside the vapour. Thus the liquid-liquid heat exchange area is one quarter of the surface area of the 2 phase sphere. This assumes however that there is sufficient liquid DP phase to cover this area. By assuming a minimum liquid thickness based on the molecular size of isopentane as 6×10^{-10} m then any allowance for reduction in the area due to insufficient liquid volume for coverage can then be made. In the average case this procedure results in an increase in heat transfer area over the vapour disengagement case.

In order to calculate droplet and bubble velocities for each increment it is assumed that the velocity will be the same as that calculated by the prior methods used for liquid droplets alone, (section 6.2.2) substituting an average density and appropriate diameter into the relationships in ref [12]. The implicit assumption of a rigid sphere will not be very good when an appreciable amount of vaporisation has taken place since some distortion of the bubble is inevitable. This is discussed in the theory chapter (section 2.2.3).

6.5.3 Calculation Basis And Rationale

The calculation determines the MEH for a given set of flowrates and droplet size and any Tc1 chosen.

Firstly a set of data is determined for the physical properties which can be assumed constant. This is based on sensitivity analysis as described earlier (section 6.2.5). Differences from prior models lie in the way DP density is treated. Two simplifying approximations are made:

(i) Hydrostatic pressure effects do not vary the density of vapour or liquid phase DP significantly.

(ii)The size of the temperature changes to the DP as it rises through the

column will produce a negligibly small change in densities of vapour and liquid phase DP.

These approximations allow a single average value of density to be used for each phase of the DP component.

The consequences of these approximations are as follows:

a) For liquid phase:

Approximation (i) is good -data shows no change in liquid density (to 6 figure accuracy) over the pressure range anticipated. Approximation (ii) is not so good. DP liquid is injected at an average of 18°C and rises to its boiling point, 30.7°C at 1.1 atm. The values of ρd for this range is 622.3 and 609.4 kg m^{-3} respectively. This is a variation of 2%. This density figure is used for velocity calculations throughout the whole of the column. Since for the large majority of the time and for the largest proportion of the heat transfer process the DP is at its boiling point, the liquid density value at boiling point is taken as representative. Since boiling point does not vary much with hydrostatic pressure, and it has been assumed constant (see prior models), this assumption is reasonable in the boiling region, but is less accurate during sensible heat transfer. Using 622.3 instead of 609.4 in the program gives a 1.4% increase in predicted MEH when run with the standard data set (1) at Tc1 = 42°C. This shows that the model is not too sensitive to this approximation.

Note that future sensitivity comparisons will be made to this data set unless otherwise stated.

b) For vapour phase:

Vapour phase density is much more susceptible to pressure variation than liquid phase. However since vapour phase only exists at the boiling point and this is close to constant, temperature effects are small. At the boiling point at

1.1 atm. the DP vapour density (ρdv) is almost 3.2 kg m^{-3}. At 1 atm. it is about 3.1 kg m^{-3}, so again variation is not great. Since conditions at column bottom are likely to have a larger consequential effect on the model the higher of these figures was chosen for the constant value in the model. Comparing the MEH results by sensitivity analysis gives a 1.2% reduction in MEH if 3.1 kg m^{-3} is used.

Other items in the physical property data set are as discussed previously. The program assumes an initial TBPd of 28.6°C based on an average hydrostatic head. Injection temperature of the DP is taken as 18°C which is an average figure for the experimental runs. This is a simplification to avoid repeated input of this temperature value which has little effect on the final result. An injection temperature of 15°C which is the most extreme variation from the mean, gives a 2.1% increase in predicted MEH on sensitivity analysis.

Calculations of increase in DP droplet temperature over an increment are carried out based on a similar procedure to that used for the simple overall model (section 6.2.2), but applied to a single increment rather than the whole column. The calculation of drop velocity is more sophisticated. Whilst the droplet is gaining temperature its diameter will not vary appreciably, but at boiling point the attached vapour will affect diameter and droplet / bubble density. For this reason the range of velocity and Reynolds number based on this condition is greater than that for the simple overall model which used only initial droplet diameter. For this reason the incremental models incorporate the full range of correlations given in reference [12] for calculation of velocity. These can be summarised as follows:-

For Re up to 0.2, $R / \rho c \; ud^2 = 12 / Re$

For Re between 0.2 and 500, $R / \rho c \; ud^2 = 9 / Re^{0.6}$

For Re between 500 and 10000, $R / \rho c\ ud^2 = 0.22$

For Re above 10000, $R / \rho c\ ud^2 = 0.05$

Use of these relationships is subject to the same limitations and approximations discussed in section 6.2.2.

Analysis of velocity profiles through the column produced by the program show inevitable step change as Reynolds number changes from one region to another. There is no experimental work to confirm or refute whether a real step change in velocity exists, however it is assumed that while individual velocity values may not be accurate, the average picture represents reality fairly well. There is evidence (previously discussed) that the relationships used are quite good in the lower column as discussed in section 6.2.2.

The equations above are calculated as before by rearrangement, then a trial and error basis where an Re regime is assumed, ud calculated and then Re checked to see if it is correct. If Re is incorrect then another Re regime is taken until a correct ud value is determined.

Using these values of velocity in the Rowe [11] relationship allows calculation of h as in section 6.2.2 for the increment in question.

In the pre-boiling point section where the DP droplet is single phase and its temperature is increasing, heat transferred to the droplet is calculated by:

$$Q = h\ A\ \Delta T$$

where A is the spherical droplet surface area (πD^2) which will be constant for all increments in this section.

ΔT should strictly be the LMTD for the increment.The discussion of LMTD

AMTD in section 2.3.1 is briefly reprised in terms of computer variables: If we consider the first increment where 'inlet' and 'outlet' Tc values are Tc(B) and Tc(A) and the drop temperature rises from TDROPd(A) to TDROPd(B) then the LMTD for the increment will be given by:

$$LMTD = ((Tc(B) - TDROPd(B)) - (Tc(A) - TDROPd(A))) / \ln((Tc(B) - TDROPd(B)) / (Tc(A) - TDROPd(A)))$$

If the increment is made very small then:

$$Tc(B) = Tc(A) \text{ and } TDROPd(B) = TDROPd(A)$$

The two ΔTs: (Tc(B) - TDROPd(B)) and (Tc(A) - TDROPd(A)) become nearly equal and therefore the LMTD approximates to the arithmetic mean temperature difference which is equal to Tc(A) - TDROPd(A) (or its (B) equivalent).This simplified driving force is arithmetically much more convenient to use for each increment and thus it is used by the incremental programs e.g. for increment 1 the driving force is Tc(0) - TDROPd(0). To ensure that the increments are small enough an additional accuracy limit is set.

The error in the assumption LMTD = AMTD is greatest in the sensible heat section of the column since the DP temperature profile becomes horizontal in the evaporative section increments and hence only the CP has the approximation applied to it. The accuracy limit is applied to the LMTD / AMTD figures calculated for the first increment, since we can be certain that no evaporation will be taking place in his increment. Whilst error may be greater in later increments, it can be examined and shown to be a small effect (see below). AMTD and LMTD are calculated for the first increment once the program has already converged to the overall accuracy in MEH calculation by successive reduction in increment size. If the tolerance on the LMTD or AMTD is exceeded then the increment size is halved and further iteration carried out, with the process repeated until the tolerance is met. The value of tolerance chosen in the final version is so that the ratio of the difference between LMTD

and AMTD to the LMTD (LMAC) is no greater than 1%. Considerations in selecting tolerances is discussed below. In fact the LMTD tolerance is usually superseded by the accuracy tolerance in MEH, so a typical LMAC is 0.2%.
If we consider the following table produced from profile values for the 115VAMODEL standard data set we can see that the approximation using this method is good for the whole column. Increment size is 6.25×10^{-4} s.

Increment No. (comment)	AMTD, (°C)	LMTD, (°C)	LMAC (%)
1st	16.555	16.519	0.219
11th	15.846	15.812	0.219
220th (just before boiling)	6.341	6.327	0.220
225th (just after boiling)	6.2512	6.2514	0.003

It can be seen that the error introduced by this approximation is small, and the calculation of tolerance appropriate to the column as a whole.

In the evaporative heat transfer section, heat transferred is calculated in the same manner, with ΔT being approximated in the same way as (Tc increment - TDROPd increment). Area however in the equation is calculated using the method outlined in section 6.5.2. This simplifies to one quarter the area of the two phase droplet / bubble surface area as the liquid surface available for heat transfer. Should this give a liquid film thickness less than the minimum specified, the area will be reduced to correspond to film thickness at the minimum.

From the heat transferred several incremental values are calculated:
(i) Continuous phase temperature for the next increment, calculated as an "increase" over the current increment using "$Q = m\ Cp\ \Delta T$" with CP values to

find ΔT.

(ii) In the sensible heat section, DP drop temperature for the next increment using "$Q = m\ Cp\ \Delta T$" with DP values to find ΔT for the droplet.

(iii) In the evaporative section, DP amount evaporated from "$Q = m\ \lambda$" and subsequent droplet / bubble dimension.

These calculation results are stored and allow the calculations for the next increment to begin with velocity calculation based on any drop / bubble size change (in the evaporative region) and so on through heat transfer calculations. The height equivalent of each time increment is calculated and stored based on CP and DP velocities.

When the mass of DP remaining as a liquid becomes zero (or a calculated negative) then the accuracy limits for convergence and log mean approximation are calculated. The accuracy of MEH limit requires that the incremental iteration be carried out at least twice so that the current value of MEH can be compared to the prior value which would have been produced at double the increment size. Thus the program automatically carries out 2 iterations before applying the accuracy tests. If the variation in subsequent MEH calculations (AC) vary by more than the tolerance, then increment size is halved and a further iteration carried out, the process being repeated until the MEH accuracy is met. Then the LMTD accuracy is tested and a similar procedure followed if necessary (see earlier) until both limits are met.

The determination of accuracy limits represents a compromise between achieving the highest accuracy and constraints on computer memory and program run time. In order to converge to higher accuracies in LMAC and AC, the program would need to iterate to smaller increment sizes. This means run time will increase with the number of increments to be calculated. Since all the

major increment values are stored as arrays in memory, there is an upper limit to the number of increments that will fit into the computer memory. The variable M in the program is used to set an upper limit on array size to prevent "endless loop" calculation. In fact the likely size of experimental error in parameters which the program calculates set a realistic target for accuracy. Limits giving accuracy greater than that measurable are of little use for comparison work but may be of some value in predictive design work at a later stage. Several program runs of the incremental models were carried out to determine run time and memory limitations and the following program parameters were set.

Tolerance for MEH accuracy (AC) = 0.003. This gives a maximum variation of 2.7 mm for the highest MEH, so error in MEH prediction will be something less than this in the worst case. Experimental measurements are typically accurate to within 5 mm.

Tolerance for log mean accuracy LMAC = 0.01. As explained earlier this was usually exceeded. However for a typical maximum ΔT of 16.6°C this accuracy give a maximum variation of 0.17°C which is less than the experimental error in temperature of 0.2°C.

Maximum array size, M is set at 5000 which is adequate for convergence to the above tolerances for all the experimental data sets. In any reduction in accuracy it should be noted that M may have to be increased, which has a large effect on run time and memory usage.

The selection of a tolerance for boiling point recalculation, for hydrostatic effects, was determined in a similar way. The tolerance value of 0.05°C is somewhat lower than the experimental temperature error of 0.2°C reflecting

the high sensitivity of MEH prediction to the value of TBPd. This tolerance has an effect on run time but little additional effect on memory usage.

Having converged to the AC and LMAC tolerances the program then proceeds to check if TBPd is within tolerance, and will repeat calculations if this is not so as described in section 6.3.1. Finally a calculation of MEH is produced which meets the three tolerances. The initial increment size of 0.00125 seconds is chosen based on experience of the eventual values necessary to give convergence. Any other value could be chosen between the limits of the maximum, which must be no greater than the residence time of the DP in the column (the program checks this is the case) and the minimum which, via interaction with the variable M, will be set by memory limitations of how many increments can be stored.

The program has various printout options: hard copy or screen, printout of each increment in the calculations or just final results, and hardcopy printout of major parameter arrays for each increment as a column profile.

6.5.4 Summary Of Significant Assumptions And Approximations In Model

This table is included to tie together the significant assumptions and approximations relative to the model distributed through this thesis.

Assumption / Approximation	Reference to Discussion	Effect
Column is well insulated and heat loses negligible	6.2.2 & 2.4.2	MEH will be smaller than calculated, particularly at high Fc and Tc1. Effect small due to insulation.
Density of continuous phase is constant	6.2.2 & 6.2.5	Effect varies with Tc1. Effects ud calculation and hence h. MEH max variation 1.6%

Density of dispersed phase constant in either phase	6.2.2, 6.2.5 & 6.5.3	Effect varies with Tc1 and column height. Typical MEH max variation 1.4%.
Droplet / bubble stays at constant boiling point when rising.	6.2.2 & 2.3.1	MEH will be larger than calculated by an indeterminate (but probably small) amount.
Cpc is constant over temperature range	6.2.2 & 6.2.5	Effect varies with Tc. Typical MEH max variation 0.5%.
λ of DP is constant over temperature range	6.2.2 & 6.2.5	Effect varies with Tc. Typical MEH max variation 1.1%.
Droplet and droplet / bubble behave as rigid spheres for velocity calculation (negligible distortion or internal circulation effects)	6.2.2, 6.5.3 & 2.2.3	Effect not readily quantifiable. More inaccurate after evaporation and large drops. Velocity calculation quite good when it can be compared to measurement. Likely to give MEH smaller than calculated.
h calculation based on Re for combined CP and DP velocities.	6.2.2	Small effect at low Fc. If assumption were erroneous then MEH would be larger than calculated.
LMTD for increment = AMTD for increment	6.2.2 & 6.5.3	Very small effect due to program design. Small increment size needed to justify assumption.
DP droplet / bubble travels at terminal velocity	6.2.2 & 2.2.3	Small effect as drop rapidly accelerates. Would result in MEH larger than calculated.
Mean drop diameter value represents scatter in real values	6.3.2	Effect not quantifiable. MEH over a long time period involving several hundred drops should agree with calculated.

TBPd does not vary after boiling commences	6.3.2	Effect small due to program design which selects a mean TBPd for the column height.
Vapour attachment / disengagement	6.4.2 & 6.5.2	Partial disengagement of vapour due to random effects may occur. Effect on MEH would be variable depends on position when disengaged.
Vapour opening angle fixed at 90°	6.5.2	Effect difficult to determine. Based on Sideman's [2] work.
Injection of DP temperature a constant 18°C (with no temperature rise in nozzle)	6.5.3	Effect depends on ambient DP temperature. Typical MEH max variation 2.1%. Temperature rise in nozzle is small, in the worst case 0.5°C.
Validity of step change in ud when Re changes regime	6.5.3	If this does not replicate real behaviour effect will be small due to 'averaging' over a large number of increments.

6.5.5 Procedural Analysis

A description of the main program 115VAMODEL and it's subprogram procedure lists now follows. Reference should be made to the program listing, appendix 13, and the list of variables, section 6.6.

Line 10 Contains the program title

Line 20 Identifies basis

Line 30 Is a remark to aid identification of data numbers in line 100

Line 100 Is the main data list in the order given in lines 30 and 2900

Line 110 Sets the value of M which sets the maximum number of increments.

This can be varied -see section 6.5.3. The value of 5000 is used (see line 2670)

Line 120 Assigns a value to the string PCOPY$. If the value is "Y" then a hardcopy of the results is made

Line 130 Sets the initial value of TBPd to 28.6 °C for the first set of iteration

Line 140 Calls the procedure F_KEYS.

This procedure PROCF_KEYS (lines 2560 - 2590) defines function key one to rise the command PROCPROFILE and function key 3 to rise the command PROCCOND_PRO. These make it easier to call these two procedures, which give additional printout options, (see later) when the main program is complete.

Line 150 Sets a print format variable

Line 160 Initialises FLAG5 which flags the need to reiterate for a new TBPd (see lines 620, 630, 4500, 4530)

Line 170 Requests input of Tc1 in degrees C, for the run

Line 180 Requests whether a full (i.e. increment by increment) printout is required. The variable diag$ stores the response string (see lines 290, 360, 490, 1630)

Line 190 Initialises the TIME variable which measures run time - a development tool (see line 650)

Line 200 Calls procedure DIM_ARRAYS

PROCDIM_ARRAYS (lines 2660 - 2810). This procedure dimensions the arrays which are used to store incremental values of important parameters for subsequent use, or printout as a profile via PROCPROFILE. This is an initialisation which only takes place once per program run. The size of the array is set by the variable M - specified in line 110, which can be user specified. Line 2670 evaluates the array size variable, size AR, which is equal

to M plus 1 to allow for an additional increment without overflow. The rest of the procedure sets up 13 arrays of this size, one for each important parameter which is identifiable by its array name. Procedure definition ends.
Line 210 Start of the main REPEAT-UNTIL loop contained between lines 210 and 630. This loop continues until full convergence with correct mean TBPd is achieved.

Line 220 Calls procedure ZERO_ARRAYS.

PROCZERO_ARRAYS (lines 1850 - 2010). This procedure sets all of the values in the thirteen arrays dimensioned in PROCDIM_ARRAYS to zero so that prior values from previous TBPd iterations are deleted. This is to prevent error and confusion by possibly having a smaller data set overwriting a larger one and making the values ambiguous. The zeroing takes place in a FOR NEXT loop construction using an integer loop counter (Y%) for speed.

Line 230 Sets the initial value of S, the increment size in seconds, prior to the iterative loop at line 280 (see lines 600, 2840, 3430)
Line 240 Sets FLAG1 to zero. This flag is used to ensure that iterations for accuracy are carried out twice before the accuracy test is made (see line 550). This is because the accuracy test needs to compare 2 successive iterations with S modified FLAG1 reset when the first iteration is complete (see line 570)
Line 250 Initially sets FLAG4 to zero. This flag will be reset to 1 when the accuracy iterations have converged to a result (see line 1320). It must be re-zero'd within the TBPd iterative loop, lines 210 to 630
Line 260 Sets a print format variable
Line 270 Zeros the variable NOIT which counts the number of accuracy iterations.

Line 280 This is the start of the REPEAT-UNTIL loop which controls the accuracy iterations. This loop requires that the iterative procedure converges to the accuracy limits before the TBPd loop in which it is rested (lines 210 to 630) can precede. The until statement is at line 610
Line 290 Calls procedure PRINT_LINE if full incremental printout has been specified.

PROCPRINT_LINE This procedure simply prints a line of dots as a layout boarder and an increment count on screen. One is added to NOIT to make the count start from one rather than zero.

Line 300 Increments the accuracy iteration counter NOIT by 1 to count number of these the REPEAT-UNTIL loop at lines 280 / 610 is executed
Line 310 Calls procedure READ_DATA

PROCREAD_DATA (lines 2880 - 2910) This procedure reads in the data specified in line 100 to the variables in the order in line 2900. The first time this is called the variables have not been set. On subsequent calls some of the variables will have had their values modified in the stagewise calculations so the re-READing of them serves to reset them to their initial values. Because the procedure is reused, the data reading position is first reset with a RESTORE command.

Line 320 Calls procedure INITIALISE

PROCINITIALISE (lines 3680 - 3920) This procedure initialises important variables which need to be reset at this point in the program before stagewise calculation starts or restarts. These may be variables whose values are changed in the stagewise calculations or just

require being given an initial value for the first calculation. Variables set in PROCREAD_DATA have already been similarly set (see above). Also several important figures are set to zero here since this is an important point in the performance of the program.

Most initialised variables are those which relate to droplet / bubble parameters or incremental values. Column height counter COLHT and pinch ΔT variable PINCHDT are also zero'd here, TDROPd is set to the initial mean injection temperature of 18°C. Calculations of initial drop mass from drop diameter and density are carried out and drop size rolling variables are initialised. The number of drops injected per second, NDROPPSd is calculated here from injection mass flowrate and initial droplet mass for later use (see line 2840). The flags zero'd at lines 3810 to 3840 all have remarks in the listing to explain their function. Two other procedures are called from within this procedure these are:

at Line 3900, procedure FALLING_V

PROCFALLING_V (lines 3150 - 3180) This calculates cross sectional area of the column, CSATUBE from "πr^2" then the downward (or "falling") velocity of the CP, uc,by volume flowrate / cross sectional area.

and line 3910, procedure O_HEAT_BAL

PROCO_HEAT_BAL (lines 3320 - 3370) This carries out an overall heat balance on the column to calculate CP temperature drop Dtc. Line 3330 contains the value for DP latent heat, LATHTd. The heat gained by the DP, Q overall is calculated by "$Q = m \lambda + m Cp \Delta T$" then the ΔT for the CP is calculated from "$\Delta T = Q / m Cp$".

After calling the above procedures, PROCINITIALISE is complete.

Line 330 Switches off the screen cursor for speed and convenience.
Line 340 Prints a blank line for layout.
Line 350 This is the start of the stagewise calculations which is carried out in a FOR-NEXT loop (see line 530) with each execution of the loop representing one increment. The maximum number of increments calculated is set by the variable M, although the loop is usually terminated at line 540 before this number is reached.
Line 360 If full or incremental printout has not been specified at line 180 then the procedure PRINT_INC is called.

PROCPRINT_INC (lines 1090-1120) This prints a message on the screen counting number of interactions and increments. The VDU11 command in line 1110 moves the cursor position up one place to save screen space. This message is an indication that the computer is calculating and would show up a program halt or endless loop situation. It also gives an indication of progress towards solution.

Line 370 The boundary temperature at CP outlet, Tc(0) is calculated from the input value Tc1 and the CP ΔT, Dtc calculated in PROCO_HEAT_BAL.
Line 380 If the calculated Tc(0) is below the DP boiling point then this would be equivalent to a temperature crossover in the countercurrent temperature / enthalpy diagram. Whilst this is marginally possible, because DP sensible heat gain is small compared to the evaporative heat gain the temperature approach pinch is far to one side. Consequently if Tc(0) is below TBPd it is certain that the pinch approach is very small, and likely that it has become zero or negative. In this case a column would have to be larger to achieve total evaporation. In the majority of cases this crossover occurs because, due to the

difference in CP and DP flowrates, it requires more heat to evaporate the DP than can be removed from the CP by cooling to its minimum temperature. For this reason if Tc(0) is calculated to be below TBPd an error message is printed and the program terminated. This avoids the need to check driving forces each increment, which is a needless complication considering the likelihood of its necessity. To further check on this the pinch approach temperature is calculated in line 2430.

Line 390 Viscosity of the CP, MUc is calculated by calling the user defined function VISCOc with the increment temperature as a parameter.

FNVISCOc (lines 1000-1010) This calculates CP viscosity from a fifth order expression in terms of temperature, which is passed to the function as a parameter (T) in degrees C.

Line 400 Thermal conductivity of the CP, kc is calculated by calling the user defined function THERMKc with the increment temperature as a parameter.

FNTHERMKc (lines 1030-1040) This calculates CP thermal conductivity from a sixth order expression in terms of temperature, which is passed to the function as a parameter (T) in degrees C.

Line 410 Calls procedure FORCE_BAL

PROCFORCE_BAL (lines 2930-3130) This procedure calculates DP velocity, ud by means of trial and error method described in section 6.5.3. Firstly (line 2940) the drag coefficient R is calculated for current density and diameter values. Then starting with the highest Re regimes, ud is evaluated using the formula appropriate to that regime. The unchanging factor for Re, ReFACT is determined to simplify coding, then Redc is calculated. If it

falls into the same regime, the procedure branches to line 3110. If not, the next regime is calculated. Regime areas are delineated by REM statements for clarity. At line 3110, by which time ud has been determined, Redc is modified for heat transfer calculations to take into account CP turbulence Re based purely on the CP, Rec is also calculated in line 3120. This procedure requires recalculation wherever D or ROd changes, i.e. every increment after evaporation begins but it is called every increment since the number of unnecessary calls is too small to justify additional code.

Line 420 On the very first execution of this line, as indicated by FLAG1 and NOIT, the procedure CHECK_S is called. It is called at this point since ud which has just been calculated and will be at a minimum, is necessary for the procedure.

PROCCHECK_S (lines 4020-4050) This evaluates the maximum value increment size, S, can have, Smax. This is equal to one residence time or 1 / ud when ud is a minimum. The user specified value of Smax is checked to be greater than S. If it is not then an error message is printed and the program stopped.

Line 430 This stores the current value of drop temperature TDROPd in the variable TDROPdO, for later use.
Line 440 If drop temperature is below the DP boiling point procedure hCALC_SH is called. Otherwise procedure hCALC_EV is called.

PROChCALC_SH (lines 3260-3300) This procedure calculates heat transfer film coefficient, h, using a formula appropriate to the sensible heat region of the column. Prandtl number, Pr, is calculated, then Nusselt number, Nu, from the Rowe [11] relationship. Finally h is calculated

from Nu. This separate form of procedure for sensible heat transfer allows separate calculation equations for h to be used from the evaporative heat transfer. However in this model the same is used in both procedures.

PROChCALC_EV (lines 3200-3240) Since the same equation is used in this model to calculate h for evaporative heat transfer as for sensible heat transfer, this procedure is identical to PROChCALC_SH. If a different calculation were required for evaporative transfer as a refinement to the model, it would be specified in this procedure.

Line 450 If drop temperature is below boiling temperature TBPd procedure DROP_TEMP is called. If evaporation has began, then drop temperature will be equal to or larger than TBPd and procedure MASS_EVAP is called.

PROCDROP_TEMP (lines 3570-3660) This procedure calculates the new value of droplet temperature, TDROPd, after heat is gained in the current increment. Droplet surface area is calculated ("π D^2") and this is equated to the heat transfer surface area, HTAREAd, for this non evaporating region. The variable MEVAPDROP is zero'd. The driving force for heat transfer, DT is calculated then the heat transferred to one drop calculated in line 3620 by "Q = h A ΔT". This gives QDROPcd in Watts per drop. Temperature gain for the drop is calculated in line 3630 by taking the number of Joules transferred per drop (QDROPcd x S) and dividing by drop mass and specific heat capacity. This gain is added to the old value of DROPd to get the new value. Finally, to prevent the possibility of round off error making it appear that the drop temperature can become larger than its boiling point, this is checked for and corrected in line 3560.

PROCMASS_EVAP (lines 3390=3550) This handles the

changing droplet / bubble characteristics when evaporation has commenced. Surface area of the drop / bubble is calculated based on the latest value of D (which has been updated in line 3950 of PROCNEW_PARAMS, see below). DT is calculated as above. Now the mass evaporated per drop per second MEVAP, is evaluated "Q / latent heat" in line 3420, and this is converted to a mass per drop, MEVAPDROP by multiplying by increment size S in seconds. This value is used to calculate the current mass of DP in the liquid and vapour phases as stored by the rolling variables MASSliqd and MASSvapd. Equivalent volumes are calculated using density data and a total volume, VOLlv of the 2-phase droplet / bubble is calculated. A diameter equivalent to this volume, Dlv, assuming a spherical shape is calculated at line 3500. Flag 7 is used to branch around line 3520 the first time it is reached, so that heat transfer surface area, HTAREAd, is not modified for vapour shielding / liquid puddling until the first increment after evaporation begins. Line 3520 checks that the volume of DP liquid remaining is sufficient, then modifies the heat transfer area to 25% of the vapour / liquid sphere surface area (see section 6.5.2), representing the liquid surface area. If liquid volume remaining is insufficient HTAREAd is set to the maximum achievable. The test relies on an approximation to the relationship between volume and minimum film thickness which is quite good for thin films and large bubbles. In fact this limit has not yet been reached with current data runs and increment sizes.

QDROPPcd, heat transfer rate per drop is then evaluated based on the latest area HTAREAd, ready for use next increment. The drop density rolling variable ROd is updated for use in velocity calculations next increment.

Line 460 Stores the old value of mdropremd (droplet liquid mass) as mdropremdO for future use.

Line 470 Calculates new value of the rolling variable mdropremd by subtracting

mass evaporated in this increment.
Line 480 Calls the procedure Q_VALUES.

PROCQ_VALUES (lines 2830-2860) This procedure calculates outstanding values of Q i.e. heat amounts / flowrates. Firstly QINC, the heat transfer rate per increment is calculated by multiplying the h.t. rate per drop by the number of drops in an increment. Number of drops in an increment is number of drops per second, NDROPPS, times increment size in seconds, S. Finally the running total of QINC, sum QINC is updated here.
Line 490 If full printout for each increment has been requested in line 180 then the controlling procedure PRINTOUTI is called.

PROCPRINTOUTI (lines 1620-1830) This procedure prints out firstly constant properties for the run, as a means of run identification, then key incremental values for each increment as it is calculated. This is a large volume of printout due to the large number of increments. The print is normally to VDU, the user having to arrange echo to the printer if hardcopy is required. FLAG2 is used to prevent repetition by making sure that constant data is only printed out at the first call of the procedure per accuracy iteration rather than every increment. This is achieved in lines 1640 and 1820, FLAG2 being given the value zero in PROCINITIALISE. Increment printout is separated by printed lines and spaces.

Line 500 Calls procedure SET_ARRAYS

PROCSET_ARRAYS This procedure is quite straightforward. It sets the array storing 12 of the 13 important incremental parameters for profile study. The exception is the Tc array which is set later (line 3960, PROCNEW_PARAMS). In two cases, the mdropremd and

TDROPd arrays, the value at this stage in the program has been modified ready for the next increment, so these arrays are set to the values for the increment stored in variables for this purpose, named with last character "O".

Line 510 This tests to see if all liquid phase DP has been evaporated by testing if the variable mdropremd is zero or negative. If this is the case the program branches out of the stagewise loop to line 540.
Line 520 Calls procedure NEW_PARAMS

PROCNEW_PARAMS (lines 3940-4000) This procedure evaluates outstanding new parameters for the next iteration of the stagewise loop (lines 350-530). Drop diameter is set to the value calculated in PROCMASS_EVAP (Dlv) based on vapour / liquid criteria should evaporation have started. Before evaporation Dlv is set at initial liquid diameter. The increment CP temperature array value for the next increment, Tc(N) is calculated (based on the increment counter N) by adding a temperature difference calculated by "$\Delta T = Q / m Cp$" (where "m = velocity x cross sectional area x density") to the current value. In the first execution the current value has been set by boundary conditions. The height equivalent (CHINC) to the time increment (S) is then calculated from the two velocities ud and uc in line 3970 by the equation CHINC = S(ud - uc). A check is made that CHINC cannot become negative if uc is greater than ud. In this instance CHINC is set to zero. Finally the running total column height, COLHT is updated by adding on the height equivalent of this current increment.

Line 530 This is the stagewise FOR-NEXT loop terminator. If the test in line 510 is not met then this line sends control back to line 350.
Line 540 If this line is not branched to from 520 then this means that the stagewise loop has gone to completion with the maximum (M) number of

iterations without complete evaporation of the liquid phase taking place. This line tests for this and after confirming this is the case, prints a message to show that M is insufficient for this case and halts the program.
Line 550 This line branches around the convergence tests if only one run of the accuracy iteration loop (between lines 280 and 610) has so far been completed. FLAG1 controls this branching, which is sent to line 570.
Line 560 When there has been at least 2 runs of the accuracy iterative loop this line is accessed and calls procedure TEST_AC.

PROCTEST_AC This procedure tests convergence of the accuracy iterative loop to within limits set by accuracy of successive MEH predictions (COLHT) with the increment size reduced by half. Accuracy in the approximation of LMTD = AMTD for an increment is also tested here.

The variable AC is defined which is the fractional variation in two successive stagewise calculations of MEH, COLHT and COLHTOLD. COLHTOLD is the value of COLHT produced in the previous run of the stagewise calculation loop which has been stored (see later, line 590 and PROCSTORE_VAR). If the value of AC is greater than the tolerance specified in line 1250, 0.003, then the procedure branches to the end, line 1330, without further tests or without FLAG4 being set to 1. If this test is met, the test for LMTD will take place starting at line 1260. LMTD is calculated for the first increment in the usual way in lines 1260 to 1290 using variable names DF1 and DF2 for the temperature driving forces. The variable LMAC is calculated in line 1300, this being the fractional variation between LMTD and AMTD (arithmetic mean temperature difference for heat transfer driving force) for the first increment. If the value of LMAC is greater than the tolerance specified in line 1310, then the procedure branches to line 1330 without FLAG4 being set to 1. Line 1320 is therefore only executed if both accuracy tolerances are met, and this line set FLAG4 to

1. This value shows convergence for the given TBPd value.

Line 570 This line sets FLAG1 to 1 (on the initial run of the accuracy iteration, see line 240)
Line 580 This line tests if FLAG4 is set to 1. If it is it carries out two things: firstly it calls procedure FINAL, then it branches to line 610.

PROCFINAL (lines 1140-1170) This procedure calls two other procedures: firstly the procedure CALC_AVES then the procedure PRINTOUTF.

PROCCALC_AVES (lines 2300-2540) This procedure calculates values of important incremental parameters stored in arrays, averaged over the column. Firstly a loop count maximum is set up (J) which is one less than the increment counter (N). This is because the test value of N will usually correspond to a negative value of mdropremd which is unrealistic. The increment before, number (N-1), will therefore be the last increment just before total evaporation takes place. As increments are very small this corresponds well to the MEH. A loop is set up to count through the array up to the value of J calculating running totals of the incremental arrays in variables with names ending in "tot" (lines 2320-2440). Then average values are calculated by dividing these totals by the number of values. This is J+1 since counting began with zero, and is equal numerically to N. Average values have variable names ending in "A".

PROCPRINTOUTF This procedure prints out answers for the converged results of the accuracy iterations for the current value of TBPd. Line 1360 turns the screen cursor back on. There then follows a fairly standard set of print statements to give input data reprint, calculation results

and mean (or average) values over the column. If hard copy is requested via the variable PCOPY$ in line 120 then the printer is turned on as a VDU echo and off in lines 1390 and 1590. TBPd is printed in the first line to show how it is iterating within the TBPd iteration loop and a set of "arrows" highlight the important column height (MEH) printout. Printouts of this kind are produced every time this procedure executes which is for every TBPd iteration. The latest or 'lowest down' printout will correspond to the final answers produced by the program.

Line 590 Calls procedure STORE_VAR

PROCSTORE_VAR This procedure stores the current value of calculated MEH produced by the stagewise loop, COLHT, as the variable COLHTOLD for use in PROCTEST_AC in the next iteration of the accuracy iteration loop (see line 1240).

Line 600 This halves the size of the increment for the next iteration of the accuracy iterative loop. Halving the size is a compromise between making increments too small, giving memory capacity problems if the number of increments are too big, and long run times; and making them too large (by dividing by 1.1 instead of 2, say) which would increase run time to reach convergence.

Line 610 This line is the end of the accuracy iteration REPEAT_UNTIL loop. Execution is returned to line 280 unless the condition, that FLAG4 is non-zero, is met. FLAG4 is set to one when accuracy conditions are met in procedure TEST_AC, line 1320.

Line 620 This calls procedure NEW_TBPd if FLAG5 is zero. FLAG5 will be zero until the TBPd used for the current TBPd iteration is within the tolerance as determined in procedure NEW_TBPd line 4500. FLAG5 is initially set to

zero at line 160.

PROCNEW_TBPd (lines 4450-4570) This procedure checks the validity of the TBPd value chosen and calculates the value for the next iteration of the TBPd iterative loop. The current value of TBPd is stored as TBPdO. Hydrostatic pressure (HSP) due to the height of column calculated is evaluated in line 4470 by the formula "HSP = ρ g h". Then DP boiling point at this pressure is calculated by linear interpolation of values between maximum and minimum experimental column heights in line 4480 (this formula would need to be changed if column height was increased above 90 cm, and linear interpolation may not be sufficiently accurate in the case of a large increase). This value is called "interp". The mean TBPd is then calculated as the average of interp the value of full hydrostatic head, and the value at zero head i.e. atmospheric pressure (27.88 °C). This value of TBPd will be the new value in any subsequent iteration. Line 4500 tests to see if the variation between the new TBPd and the previous value TBPdO is small enough (less than 0.05 °C) to be acceptable, and if it is sets the final convergence FLAG5 to one. To accelerate TBPd convergence in the case of a large predicted MEH giving large variations in TBPd, line 4510 moves the new value of TBPd in the "right direction" by a further half of the difference in successive values. This acceleration is only invoked if the variation in TBPd is greater than 0.5 °C, which is rare but possible. If FLAG5 has not been set to one and a further iteration is required then lines 4520 to 4550 print a screen message to show iteration, with a hard copy if this has been specified. FLAG6 is used to toggle printer on / off commands. Finally to cut down round off error, TBPd is rounded to 2 decimal places using the user defined function ROUNDDP before calling the procedure ZERO_TOTS.

FNROUNDDP (lines 1060-1070) This function takes 2

parameters: the variable name to have its value rounded and a number specifying the number of decimal places. The function returns the variable rounded off to that number of places.

PROCZERO_TOTS (lines 2810-2280) This procedure sets variables (with names ending in "tot") used to record totals in PROCCALC_AVES back to zero in readiness for another TBPd iteration.
Line 630 This is the terminator for the TBPd iterative loop initiated at line 210. Execution is returned to line 210 unless FLAG5 = 1 i.e. TBPd convergence has occurred as determined in procedure NEW_TBPd. The program calculations are essentially complete when this condition is met, and the latest execution of procedure PRINTOUTF will form the final printout of the answers.
Line 640 Causes the computer to emit a "beep" to signal program completion.
Line 650 Evaluates and prints out program run time on the screen.
Line 660 Marks the end of the main program.
Two additional procedures are not executed by the main program but can be called up after program end by keyboard command. Procedure F_KEYS has defined function keys to simplify these calls. The procedures are both to produce an increment by increment printout of important parameters - a "column profile". PROCPROFILE can be used on screen or hardcopy. PROCCOND_PRO uses the condensed print format of an Epson printer to "squeeze in" more values on a line and thus can only be used for hardcopy. It prints out 12 values per increment rather than 7 for PROCPROFILE. Both procedures use the variable CHRT to keep track of a column height running total so that the total height at each increment can be printed out for ease of analysis.

6.5.6 Typical Program Outputs

Two types of program output are shown in the appendices and detailed below. These are shown for program runs with the standard data set with Tc1 at 42°C.

A. Standard Output

See appendix 14. This run shows the printout for the two TBPd iterations which were required: the initial value of 28.6°C and the final value of 28.62°C . This final printout is divided by lines into three sections. The top section contains TBPd and a reprint of input data for run identification. The second section starts with the major results, MEH or column height in metres at the given Tc1 value. This is followed by a print of program internal variables i.e. final increment size, final number of increments, number of iterations for accuracy convergence and final values of accuracy measurement. Important calculated temperatures (in °C) are then output.

The last section is a print of column mean values of important variables.

B. Profile Output

See appendix 15. This appendix shows only the first part of the 1187 line long profile printout produced by procedure COND_PRO. The first line is a set of titles for each of the important variables in the profile, followed by a tabulated list of their values for each increment. N counts the increment number and CHRT the cumulative column height in metres. All numbers are printed in the "4 figure plus exponent" format to ensure layout and accuracy. With small increments this means some changes are too small to show up on a single increment change since the changes are less than the 3dp accuracy of the pre-exponent number. Note that in the region shown, boiling has yet to occur.

6.6 Computing Symbols Used In All 3 Models

These are presented in tabular form, in order of their assignment in program 115VAMODEL.

Variable Name in Program	Equivalent Symbols Used in Text	Description (Units)
Any name ending in lower case c	Affix c	Refers to continuous phase (in cases where symbol may be ambiguous
Any name ending in lower case d	Affix d	Refers to discontinuous phase (in cases where symbol may be ambiguous)
ASURFd( )		Array to store profile of ASURFd
ASURFd		Surface area of drop (m^2)
AC		Convergence accuracy between 2 successive MEH calculation runs
CHINC( )		Array to store profile of CHINC
Cpc Cpd	Cpc Cpd	Specific heat capacities (at constant pressure) of relevant phase ($J\ kg^{-1}K^{-1}$)
COLHT	MEH	Column height - a running total of heights of increments (m)
CHINC		Height equivalent to the current calculated time increment (m)
CSATUBE		Column cross sectional area (m2)
COLHTOLD		Variable to store last MEH value between successive iterations (m)
CHINCtot	(MEH)	Total of CHINCs to enable calculation of average

		value (=MEH) (m)
CHINCA		Average CHINC over all the increments in an iteration (m)
D( )		Array to store profile of changing drop diameter (m)
D	D	Liquid drop diameter for the dispersed phase (m)
Dlv	Dlv	Diameter of combined liquid droplet and vapour bubble attached (m)
Dtc	ΔTc	Overall temperature drop for the continuous phase (K)
DT	ΔT	Increment temperature driving force for heat transfer from continuous phase to droplet (K)
DF1	ΔT1	True countercurrent temperature difference for calculation of LMTD at top of first increment (K)
DF2	ΔT2	As DF1 but for bottom of first increment (K)
DtcINC01	ΔTc01	DT for the first increment (K)
Dtot		Sum of D values for each increment in an iteration (m)
DA	Dave	Average D value per increment for an iteration (m)
FLAG5		Flag which is set when program has converged to an acceptable TBPd
FLAG1		Flag which is set at end of first iteration to allow 2 iterations to be carried out before convergence testing

FLAG4		Flag which is set when program has converged to an acceptable accuracy for the given TBPd
Fc	Fc	Volumetric flowrate of continuous phase (m^3 s^{-1})
FLAG2		Flag which is set to avoid continuous printing of fixed parameters
FLAG3		Flag which is set when pinch temperature driving force is calculated
FLAG6		Flag which controls printout of TBPd iteration message
FLAG7		Flag which controls the increment in which modification of heat transfer area takes place
HTAREAd( )		Array storing profile of HTAREAd
HTAREAd	A	Liquid surface area of droplet available for heat transfer (m^2)
HSP	ΔP	Pressure due to hydrostatic head at column bottom (N m-2)
J		Program loop terminator variable, equal to N-1
K		Program loop counting variable
LATHTd	λ	Specific latent heat of vaporisation of dispersed phase, J kg^{-1}
LMAC		Fractional variation between log mean temperature difference and simple temperature difference for an increment

M		Program variable to set maximum number of increments and hence array sizes
MASSvapd		Mass of droplet evaporated to the vapour phase
MASSliqd		Mass of droplet remaining in liquid phase
MUc	μc	Absolute viscosity of continuous phase ($kg\ m^{-1}\ s^{-1}$)
MEVAPDROP		Mass of drop evaporated to vapour over current increment ($kg\ drop^{-1}$)
MEVAP		Mass of drop evaporated to vapour per second per drop ($kg\ s^{-1}\ drop^{-1}$)
NOIT		Number of iterations taken for current value of TBPd
NDROPPSd		Number of drops entering column per second (s^{-1})
N		Loop counter which counts number of increments
Nu	Nu	Nusselt number for increment
PCOPY$		String variable determining type of printout
Pr( )		Array storing profile of Pr
PINCHDT	ΔTpinch	Minimum approach driving force occurring at onset of boiling (K)
Pr	Pr	Prandtl number for increment
Prtot		Total of incremental Pr
PrA	Prave	Average Pr for iteration

QINC( )		Array to store profile of QINC (W)
QINC		Heat transfer rate for the increment (W)
Qoverall	Q	Heat transfer rate over the whole column (W)
QDROPcd		Heat transfer rate to a single drop (W drop^{-1})
QINCtot		Sum of QINC for the iteration (W)
QINCA		Average value of QINC over the column for the current iteration (W)
Redc( )		Array to store profile of Redc
Rec( )		Array to store profile of Rec
ROc	ρc	Density of continuous phase (kg m^{-3})
ROdI	ρdI	Initial density of dispersed phase (kg m^{-3})
ROdV	ρdV	Density of vapour dispersed phase
ROd	ρd	Density of dispersed phase (kg m^{-3})
R	R	Drag coefficient acting on drops (drag force / unit projected area) (N m^{-2})
ReFACT		Factor in calculation of Re (s m^{-1})
Redc	Redc	Reynolds number for drop movement through continuous phase
Rec	Rec	Reynolds number for the continuous phase flow in the column
ROdIv	ρdIv	Mean density of attached

		vapour bubble and liquid drop in dispersed phase (kg m^{-3})
Rectot		Sum of all Rec values for iteration
Redctot		Sum of all Redc values for iteration
RedcA		Average Redc for iteration
RecA	Recave	Average Rec for iteration
S		Increment size for iteration (s)
Smax		Maximum calculable value of increment (s)
TBPd		Boiling point temperature at column average pressure for dispersed phase
Tc1	Tc1	Continuous phase inlet temperature (°C)
Tc( )		Array to store temperature of continuous phase at each increment (°C)
TDROPd( )		Array to store dispersed phase drop temperature at each increment (°C)
TDROPd		Dispersed phase drop temperature of current increment (°C)
T		Dummy variable representing temperature (°C)
TDROPdO		Variable to store old value of TDROPd (°C)
TGAINd		Gain in drop temperature due to sensible heat transfer (°C)
TBPdO	TBPd	Variable to store old value of TBPd (°C)

VOLvapd		Bubble volume of vapour / liquid attached bubble / droplet (m^3)
VOLliqd		Droplet volume of vapour / liquid attached bubble / droplet (m^3)
VOLlv		Combined volume of vapour and liquid for an attached bubble / droplet (m^3)
X Y		Dummy variables in "round off" functions
diag$		Program variable controlling printout detail
h( )		Array to store profile of h
h	h	Incremental (instantaneous) heat transfer coefficient for continuous- to- dispersed phase heat transfer ($W\ m^{-2}\ K^{-1}$)
htot		Sum of h values over one iteration ($W\ m^{-2}\ K^{-1}$)
hA	have	Average h over one iteration($W\ m^{-2}\ K^{-1}$)
interp		Interpolation factor in calculating TBPd (^{o}C)
kc	kc	Thermal conductivity of continuous phase ($W\ m^{-1}\ K^{-1}$)
lmtdINC01	ΔT, LMTD	Log mean temperature difference for first increment (^{o}C)
mdropremd( )		Array to store profile of mdropremd
mINJECTEDd	md	Mass flowrate of dispersed phase ($kg\ s^{-1}$)
mdropd		Mass of droplet of dispersed phase (kg)

mdropremd		Mass of droplet remaining in current increment as liquid phase after evaporation (kg)
mdropremdO		Variable to store old value of mdropremd
mINJECTEDc	mc	Mass flowrate of continuous phase (kg s^{-1})
mdropretot		Sum of mdropremd values for each increment in an iteration (kg)
mdropreA	mdropreave	Average value of mdropremd per increment over an iteration (kg)
sizeAR		Variable setting size of profile arrays for dimensioning
sumQINC		Running total of QINC values for an iteration (W)
tf		Minimum liquid film thickness for droplet / bubble attachment (m)
ud( )		Array to store profile of ud over an increment (m s^{-1})
uc	uc	Velocity of continuous phase (m s^{-1})
ud	ud	Velocity of dispersed phase relative to continuous phase (m s^{-1})
udtot		Sum of increment ud values over one iteration (m s^{-1})
udA	udave	Average of increment ud values over one iteration (m s^{-1})

Additional symbols used in 38S0MODEL only:

Variable name in Program	Equivalent Symbol Used in Text	Description (Units)
COLEVAPHT	MEH	Predicted minimum evaporation column height (m)
FLAG		Flag which is set after initial calculation of Tc1
Qcd		Total heat transfer rate from continuous to dispersed phases (W)
TcMEAN		Mean value of inlet and outlet temperatures for continuous phase (°C)
timeed		Predicted time taken to evaporate dispersed phase (s)
waterdist		Distance travelled by drops through the continuous phase (m)

7. Discussion Of Results And Model Analysis

7.1 General

7.1.1 Introduction

MEH results and the development of the computer model are discussed in this section. Drop size analysis results are not further discussed as these are self-explanatory. After having developed a model which is a fair fit to the experimental data it is possible to examine the effects of many parameters on the model ad infinitum. The parameters considered are those of significance from the point of view of testing the model or of comparative theoretical interests. Having proven out the model it remains as a tool for future work.

In the main, graphs pertinent to chapter 7 are found in appendix 17, and spreadsheet analysis in appendix 16.

7.1.2 Graphical Presentation

MEH vs Tc1 graphs (see appendix 17) form a curve for which it is very difficult to fit a polynomial. It is desirable to take advantage of least squares to fit to the data, in order to cut out decision based on judgement alone. This can be achieved by using a log linear plot for which a second order polynomial fit gives good characteristics. Due to the coarsening effect of the log-linear fit at higher MEH values, which reduces scatter, where appropriate a linear graph is presented. For these graphs no curve is generated.

7.2 Experimental Results

7.2.1 Reproducibility

In order to determine reproducibility of MEH measurements, run 1 was performed in triplicate, A, B and C. Tc1 values vary due to different thermostat setting so a graphical analysis is appropriate. A linear graph of the results in fig 5.3 shows the scatter and distribution of points. It can be seen that runs 1A, B and C follow the same general shape showing good reproducibility within experimental error.

Fig 5.4 shows a log linear plot of the points with a 2nd order polynomial fitted to all the points, to show scatter around the mean. This shows that there is a fair amount of scatter around the mean but no particular bias in any run which would indicate lack of reproducibility. Analysis of the least squares regression data gives the following sum error squared values for the graph:

A 0.0365

B 0.0459

C 0.0338

Mean line 0.1017

This shows that run B is the worst representation of the mean, with little to choose between A and C. All values are sufficiently close to indicate a good level of reproducibility.

7.2.2 Selection Of Typical Data

In order to simplify analysis, run 1A was selected to represent run 1 in analysis and model fitting. The reasons for choosing run 1 have already been

discussed (section 5.2.1). For convenience this is reduced further to eight data points. A is selected on the following basis:

1. It is a good fit to the mean data as measured by least squares.

2. Although C is a slightly better fit, examination of the data for both shows that A has one deviation from a progressive decrease in MEH as Tc1, whereas C has two such points which are of questionable validity.

3. On further examination of A, the Tc1 = 42.7°C point is discarded as it gives an error squared deviation from the log-linear mean fit which is an order of magnitude greater than all other points. Printout from the spreadsheet used to determine this analysis can be seen in fig 7.1 If left in use this point would skew all numerical fits towards itself. It is quite clear that scatter is responsible for this point being erroneous.

Thus the eight remaining points of run 1A are used to typify run 1 data. Since it is obviously impractical to utilise all 54 experimental runs, most analysis is carried out on this run and extended to other runs for comparison where appropriate.

7.2.3 General Form

It can also be seen that lower Tc1 values with higher MEH values are more sensitive than higher Tc1 values, where the curve tends to level out into a near asymptote. This shape of curve is typical of all experimental runs and suggests the existence of a minimum column height value below which increase in temperature driving force has little effect on MEH. This occurs at a value of 14 cm MEH for run 1 and for other runs (see figs 5.5 to 5.31) where the

near - asymptote is clearly established it generally occurs in the range 10 to 30 cm. Since the experimental results do not extend below 10 cm it is impossible to be conclusive about values below this region. These near-asymptotes suggests the existence of a minimum length of column for which heat transfer is not very dependent on imposed driving force. In this initial region droplet temperature is rising prior to evaporation. When the bubble point is reached, the driving force for heat transfer will be at its minimum value. The existence of this pinch in the driving force which can be seen in fig 2.7, appendix 1, would tend to constrain the heat transfer. If the pinch became too small for appreciable heat transfer the drop would rise past this point at constant temperature until the driving force increased sufficiently above the pinch value to resume heat transfer to the drop. This will depend on hydrostatic effects on boiling point. This effect of limiting ΔT on height would be most significant at low MEH values. The CP temperature profile would contain a region of constant temperature first above the pinch, which would be generally insensitive to increases in Tc1. Pinch temperature is not experimentally measured but can be evaluated from the computer model and this is studied later (see section 7.8).

7.2.4 Corroboration Of Results

No published results have been found which directly compare with the flow configuration and refrigerant used in this work. Sideman and Taitel's [2] work is widely used in comparative studies since it is the most comprehensively reported. However Sideman's data is for a static column and his evaporative height analysis is for evaporative height only (not including a sensible heat measurement) and used the mean temperature difference (Tc-Td) as dependent variable. This temperature difference will differ markedly for a counter current column. In the absence of any direct comparison the best that

can be achieved is to compare the expression of Sideman and Taitel for overall heat transfer coefficient with that produced from the computer model which is the best fit to my data. This analysis is carried out in section 7.4 and does corroborate my findings. It can be said in addition that MEH values for my work are of the same order of magnitude as for Sideman and Taitel's [2].

7.3 Computer Model And Heat Transfer Correlation

7.3.1 Introduction

To obtain the best computer model simulation of the experimental results the procedure is as follows. Firstly, the best fit of the three experimental models, overall, vapour detachment and vapour attachment versions, is determined.

Secondly, the best correlation for instantaneous heat transfer coefficient is determined. This is based on determining by running the best version of the computer model with various published correlations for Nusselt number to determine the best fit.

Thirdly, the best of these fits is modified to give the best possible values of coefficients in the correlation to fit the data.

These three stages were all based on run 1A and a trial and error procedure was followed to incorporate the results of the second stage in the first stage. Finally, having arrived at a good model for run 1A it is used to produce values for graphical comparisons to other experimental runs.

Where graphical comparison is not sufficiently sensitive to determine closest fit, a least squares analysis is calculated using a spreadsheet to determine

best fit i.e. lowest sum error squared.

7.3.2 Best Fit Model Basis

Figs 7.2 and 7.3 show comparative plots for the three models bases 38SOMODEL the overall model 77VDMODEL, the vapour disengagement incremental model and 115VAMODEL, the vapour attachment incremental model. These are compared to run 1A results in a linear - linear plot to show undistorted scatter, and on a curve fitted log linear plot which gives a better comparison. The correlation for heat transfer coefficient in all three models is that recommended by Rowe et al, equation 2.2.6, using a value for the constant B of 0.79 appropriate for water.

Examination of fig 7.3 clearly shows that both incremental models are better fits to the data than the 38SOMODEL. The 38SOMODEL consistently under predicts MEH which implies if we accept that the Re and Pr exponents are realistic since they are widely reported, that the value B is too high for an overall calculation, but is better for an incremental model which relies on an instantaneous value of heat transfer coefficient.

38SOMODEL is ruled out but it is less clear from graphical inspection which incremental model is the better. Both are reasonable fits to the data. Therefore a numerical analysis is performed, see spreadsheet fig 7.4.This shows that the best fit is given by the 115VAMODEL program.This is to be expected as the 115VAMODEL is the most sophisticated model, and implies that vapour attachment to the liquid droplet is the mechanism involved in a counter current column system. What is surprising is that the vapour attachment / disengagement basis makes such relatively little difference. The implications of this are that firstly a model based on disengagement which is much simpler to

derive would still give good results. Secondly, the assumption of 25% of total bubble / drop area being available for heat transfer made in the VA model (β =135° on average) compensates to a large extent for the vapour insulating of the droplet, so that heat transfer area becomes similar to that of a single phase liquid droplet.

Since the best fit is obtained with the 115VAMODEL, this version is used in subsequent development work.

7.3.3 Best Fit Heat Transfer Correlation Form

In order to determine the form of heat transfer correlation which fits the data, a selection of seven of the most pertinent from the literature survey were selected. However, these correlations are with the exception of equation 2.2.15, derived for overall heat transfer coefficient, and all apply to a different flow configuration. This analysis cannot therefore be considered to be a testing of other workers' correlations since they are out of context. Instead these seven correlations serve as first approximations to indicate which of them deserves further development as an instantaneous heat transfer correlation. All forms of relationship predict Nusselt number.

Each correlation in turn was coded, together with appropriate supportive calculation, into the program for 115VAMODEL. The program was then run to generate MEH predictions. The following correlations were considered:

Equation No	Reference
2.3.1	Sideman and Taitel [2]
2.2.7	Prakash and Pinder [34]
2.2.10	Adams and Pinder [37]

2.2.13	Battya et al [44]
2.2.14	Raina and Wanchoo [30]
2.2.15	Shimizu and Mori [48]
2.2.6	Rowe et al [11]

Fig 7.3 (graphs 3 and 4) already seen, show the fit of equation 2.2.6 which is reasonably close. The other models are shown comparatively in figure 7.5. Of the others the best fit is equation 2.3.1 in terms of shape and position, but all are poorer than equation 2.2.6 in terms of position. The other six equations give a much higher predicted MEH, indicating that predicted Nu is too low. The reason that equation 2.2.6 provides a better fit is that the coefficient multiplying the right hand side of the equation is much higher than for the other six equations. This is true even of equation 2.2.15 which is derived for instantaneous heat transfer coefficients.

Therefore it is apparent that, accepting the assumption in my model, the instantaneous heat transfer coefficients are higher than would be expected from comparisons with overall average heat transfer coefficients. Equation 2.2.6 is therefore used as the basis for determining best heat transfer correlation coefficient values to 'fine tune' the fit to the data.

No further conclusions about the heat transfer correlation and mechanism can be drawn from this analysis since the equations are being used out of context and as such their basis for theoretical derivation does not apply.

7.3.4 Best Fit Heat Transfer Correlation Coefficients

The values of the coefficients to best fit experimental data in the form of equation 2.2.6 can now be determined. The equation as it stands is:

$$Nu = 2 + B\ Re^{1/3}\ Pr^{1/2} \qquad \{eqn\ 2.2.6\}$$

The relationship is not particularly sensitive to exponent values and many workers prefer to use Peclet number i.e. use the same exponent for Re and Pr. The constant value of 2 is not very significant at reasonable Re values but is retained as it has a theoretical validity.

The value of B is dependent on the system. A value of B = 0.79 is recommended for water, and this has been used so far, but this tends to over predict Nu and then under predict MEH when applied to instantaneous heat transfer coefficient in the 115VAMODEL program. To establish the correct value of B for the water / evaporating isopentane system modelled, trial computer runs were carried out with different values of B to determine which gave the best fit to run 1A. Graphical analysis was not sufficiently sensitive so recourse was made to a least squares numerical fit, the final stages of which is shown on spreadsheet in fig 7.6. This analysis shows that based on sum error squared deviation B = 0.76 is the best value, though it is not particularly sensitive to plus or minus 0.01. Graphical comparison of the B = 0.79 and B = 0.76 models were made in graphical figures 7.7 and 7.8. These again show that the model is not very sensitive to small variations in B, and that it fits the run 1A data quite well. The fit is better in the more sensitive low Tc1 region, which is appropriate for the potential acid recovery operation which will operate at a Tc1 value of 42°C. fig 7.8 however as a log-linear plot tends to magnify the deviation at the high Tc1 end which is not apparent in the linear plot of fig 7.7.

Thus the best correlation for instantaneous heat transfer coefficient in Nusselt number which corresponds to the assumptions made in the 115VAMODEL is:

$$Nu = 2 + 0.76\ Re^{1/3}\ Pr^{1/2} \qquad \{eqn\ 7.3.1\}$$

for the data in run 1. Before commenting on its relevance it is necessary to compare the 115VAMODEL with this correlation to the other experimental runs.

7.3.5 Best Model Fit To All Experimental Runs

Graphs representing the best model fit i.e. the 115VAMODEL program with equation 7.3.1 are plotted alongside experimental runs 2 to 54 in figures 5.5. to 5.31. In general it can be seen that the model is a reasonable fit to experimental data. Results are generally reproduced within experimental error. This shows that the errors due to assumption in the model, as discussed in section 6 and summarised in section 6.5.4 are comparable to the estimated experimental error of within 22%. This accuracy is fairly typical for heat transfer correlations.

Some runs do appear to give anomalous results. These are dealt with below:

In run 5, fig 5.6 the curve fit gives an apparent minimum for MEH, with an apparent increase in MEH with increasing Tc1 above $\sim$ 65°C. This is a function of the polynomial curve fit and is not thought to be a realistic representation. Extrapolation of any polynomial outside data range is dangerous so a conclusion based on such extrapolation would not be relevant anyway. Similar apparent behaviour is markedly shown in the following runs:

Run 8, fig 5.8

Run 10, fig 5.9

Run 23, fig 5.15

Run 25, fig 5.16

Run 29, fig 5.18

in all cases the conclusion is the same, as this is a function of the curve fit program not of the data. The line of fit is quite good to the left of the apparent minima, and should be ignored to the right of these.

No common factor can be found between the runs which exhibit this curve characteristic, other than it is more common where data is limited, as one would expect.

Run 14, fig 5.11, run 32, fig 5.20 and run 36, fig 5.22, are interesting in that the points form near straight lines. This however is not supported by other run data so it is probable that these are anomalies produced by experimental scatter combined with a log linear plot. A curve would of course be produced on a linear plot. These phenomena in isolation may be considered evidence for a simple exponential relationship between Tc1 and MEH, but this would not be generally justified. This straight line is somewhat apparent in a few other runs, but there it is obviously a result of too few data points.

Run 43, fig 5.25 produces a curve of inverted shape on a log linear plot. This is a more distorted curve of the straight line behaviour discussed previously, and curves for similar reasons. The data is obviously anomalous in the trend it produces and cannot be readily explained. This run is therefore of little value in further consideration.

With relatively few exceptions then the model based on the correlation in 7.3.1 combined with the 115VAMODEL assumption, provides reasonable prediction of MEH values for a given Tc1 over the wide range of flowrates and temperatures examined. The relationship is recommended originally for heat

transfer to rigid spheres above 12.8 mm diameter for Reynolds numbers in the range $10 < Re < 10^4$. However, it delivers good instantaneous prediction for fluid drops with the mean diameter range 2.8 to 6.2 mm and CP Reynolds numbers in the range 50 to 12200. This correlation is based on CP values and its accuracy levels support for the assumption that the controlling resistance to heat transfer lies in the CP film. The B value of 0.76 lies between the values recommended for water of 0.79 and air of 0.69. Conclusions drawn about the significance of this value must be tentative due to the novel application of the correlation. The most that can be said is that the coefficient is similar to that of a pure water based system but is potentially lower due to the presence of the DP vapour phase.

When drawing conclusions about the final version of the model the whole program must be reviewed as a package. It is inappropriate to draw conclusions from the form of equation 7.3.1 in isolation from the rest of the assumptions implicit in the model. Film coefficient calculation is interrelated in particular with assumptions made about heat transfer area and droplet / bubble velocity. When quoting conclusions about equation 7.3.1 then it is important to qualify these with reference to the other assumptions inherent in the computer model as a whole. Nevertheless the whole model provides a useful and reasonably accurate prediction tool which should find general application.

7.4 Comparison Of Model With Other Work

As previously explained,no similar model work exists for direct comparison. However, it is useful to compare models as far as possible to determine the degree of corroboration. Corroboration between model predictions will by extension provide some corroboration of experimental data if both models fit

the data on which they are based.

The main problem in corroborative study is the absence of published data for a countercurrent flowing CP. Comparison is made therefore for a fairly low CP flowrate.

Of the many forms of relationship published, many are based on the experimental work of Sideman and Taitel [2]. Sideman and Taitel's own relationship is of the form:

$$Nu = f\,(Pe)$$

which is similar to that of many other workers. For these reasons comparison is made by taking overall values of Nu and Pe for run 1 and finding the mean value of C in the equation below over the range of Tc1 values:

$$Nu = C\ Pe^{0.5} \qquad \{eqn\ 7.4.1\}$$

The value of C ranges from 0.185 to 0.198 with a mean value of 0.189. This compares with values of 0.272 quoted by Sideman and Taitel [2] and 0.169 quoted by Shimizu and Mori [48]. The latter is less applicable since it is quoted for considerably different circumstances.

In general this shows the coefficient is of the correct order of magnitude and is quite close in value to that of other workers. This finding tends to corroborate the model and experimental results. The value of C is lower than that of Sideman and Taitel which is unexpected since this suggests that heat transfer coefficients in the countercurrent system employed are lower than those found in a static system. One would normally expect increased turbulence to improve heat transfer. Bearing in mind that too close a comparison is not valid, the discrepancy can possibly be tentatively explained by the fact that Sideman and

Taitel's work was derived for wholly evaporative heat transfer whereas my work also includes heating the DP droplet to its bubble point. Evaporative heat transfer coefficients are generally higher than liquid-liquid values.

Practically speaking, should the 115VAMODEL later prove to be under predicting film coefficients then it would tend to under predict MEH. As a design program this would lead to a degree of over design. A conservative design which will work is more desirable than an undersized unit which is inoperable. For this reason it is better to adopt a conservative approach to the model for use in practical design work, and the practical value of the model would not be obviated.

7.5 Different Form Of Heat Transfer Correlation

Since the form of equation in 7.4.1 is so widely reported, it is interesting to see whether this form of correlation would give a better fit to experimental results than equation 7.3.1. To examine this, equation 7.4.1 was coded into 115VAMODEL to predict instantaneous Nusselt number. Several runs of the model were made with different values for the constant C, which was found to require a much higher value than that used for overall average calculations. This is because overall average work is based on initial drop diameter rather than its instantaneous value.

The data for various values of C was compared numerically on a least squares basis, with run 1A data to find the best fit. fig 7.9 shows the spreadsheet of this analysis. The best fit is obtained with a value of C of 0.61. Sum error squared is 102.1 for this value, compared to 83.7 for equation 7.3.1 (see fig 7.6).

Equation 7.3.1 gives therefore a better fit than the best form of equation 7.4.1.

7.6 Effect Of CP Reynolds Number

Values of MEH at a Tc1 of 60°C are determined by interpolation of experimental results. Interpolation is necessary since Tc1 is rarely fixed at exactly 60°C because of experimental variation. 60°C is chosen for Tc1 as this gives a good range of determinable values for MEH. CP Reynolds number, Rec, is calculated from the final version of the 115VAMODEL, since this provides the best estimation of values of the physical constants averaged over the column.

This MEH is plotted against Rec in fig 7.10. In assessing this graph it should be noted that points at low and high Rec are less accurate than the mid range values, as already explained.

This analysis is made to determine if CP turbulence has an independent effect on MEH. Such an effect might be to introduce vapour disengagement, mixing effects, or effects on sloshing and thus heat transfer area. If the effect were independent of the effect of bubble / droplet size and velocity, and if it were of sufficient magnitude then it would be expected to manifest around the transition zone for laminar to turbulent flow. The transition zone of 2000 to 3000 for Rec is shown in fig 7.10. Points are well defined around this region and no noticeable step change deviation can be seen. Therefore it is concluded that CP turbulence has no significantly large effect which is independent of DP properties at least in the better defined range of Rec from 200 to 4000.

The fact that the model, which fits experimental data well, was a combined CP and DP Reynolds number correlation, is evidence that the CP velocity does

effect heat transfer as a contribution towards the net Reynolds number of the droplet / bubble, Redc.

7.7 Effect Of Heat Transfer Area Assumptions

The assumption in 115VAMODEL of a mean value of vapour opening angle, 2β of 135° has already been discussed in section 2.3.1. Because this assumption is linked so closely with the determination of the heat transfer correlation (equation 2.3.1), the effect of changing this assumption is investigated. Fig 7.11shows the effect of assuming an average vapour opening angle suggested by Battya [45] of 180° (i.e. $\beta = 90^{\circ}$) which gives an area of 50% of the total bubble and droplet. The $2\beta = 135^{\circ}$ case is labelled 25% area and experimental results for run 1A, the data basis for the model runs is included as a datum.

It can be seen that the assumption has a marked effect on the position of the graph, yet the shape remains similar. It is likely then that an increase in the value of B in equation 2.2.6 is likely to be able to compensate for this increase in area. It is therefore confirmed that equation 7.3.1 should only be considered in the context of the area assumption on which its deviation is based.

7.8 Relationship Between MEH And ΔT

Other workers have analysed the relationship between average rate of heat transfer and driving force ΔT [32] [34]. A brief analysis is therefore included to determine any simple relationship between MEH and ΔT.

Firstly, a graph was plotted of MEH versus ΔT for run 1A, where ΔT is defined in this case as mean CP temperature - mean DP boiling point. No simple

correlation was found to apply. Fig 7.12 shows the best relationship is a second order polynomial curve MEH vs 1 / ΔT.

There exists a pinch on the CP-DP temperature profile (see fig 2.7). The driving force at the pinch was next investigated to see if a simple correlation could be made. ΔTpinch values calculated in the computer model were compared with MEH data for run 1A. In this case a good straight line was found to exist for the MEH vs reciprocal ΔTpinch plot, see fig 7.13. A confirmatory plot was made for a different set of parameters using run 12, see fig 7.14. This also gave a good straight line. Coefficients for the best fit straight line equations are:

run 1A intercept = 2.36, slope = 0.460

run 12 intercept = 0.128, slope = 0.497

both have mean error of fit within 9%.

This suggests a relationship of the form:

$$MEH \propto \Delta Tpinch^{-0.5} \qquad \{eqn\ 7.8.1\}$$

applies as an approximate or short cut method which may be useful in determining the approximate effects of an increase in Tc on MEH. This would be an approximate method only, it being preferable by far to run the computer model in any predictive work.

Sideman and Taitel [2] concluded for their static column work that evaporative height was proportional to (mean bulk Tc - mean DP boiling temperature) -see section 2.2.2. The work leading to equation 7.8.1 confirms that a similar relationship exists when extended to the pinch driving force in a counter-current column.

8. Conclusions

Experimental results on evaporation of isopentane droplets in water have been obtained for 54 runs of different counter current flowrates, temperature and drop initial diameters. The results give rise to information of practical importance and allow a computer model based on finite difference increments in the time domain to be developed. Specific significant conclusions arising from the discussion in chapter 7 are given below.

1. The major result of this research is the computerised program which models the relationship between column minimum evaporation height and continuous phase inlet temperature. The program produced is accurate to within the 22% experimental error over the wide range of countercurrent flowrates studied experimentally for the water / isopentane direct contact evaporative heat transfer system.

The model shows that the following major assumptions can be made with a fair degree of accuracy:

a) DP velocity can be calculated from terminal velocity correlations.

b) DP behaviour can be typified by relationships for rigid spheres.

c) A mean value of vapour half opening angle, β, of 135°, can be used to characterise the heat transfer area of the two phase droplet.

2. Assumption 1c is strongly interrelated with an appropriate expression for instantaneous heat transfer coefficient. The best correlation for this in the model is expressed thus in terms of dimensionless groups:

$$Nu = 2 + 0.76\ Re^{1/3}\ Pr^{1/2}$$

which is similar to an expression given by Rowe et al [11]. This applies for $3.8 \times 10^4 < Redc < 8.3 \times 10^4$, where Redc is Re based on combined CP and DP velocities.

3. The best form of correlation for overall heat transfer based on Peclet number which fits experimental data is:

$$Nu = 0.189\ Pe^{0.5}$$

The pre Peclet constant is lower than that of Sideman and Taitel [2] and higher than that of Shimizu and Mori [48]. The computer model is recommended for use rather than this relationship which is less rigorous in basis and of lower accuracy.

4. An approximate relationship of the form:

$$MEH\ \alpha\ \Delta Tpinch^{-0.5}$$

is proposed for use as a 'short cut' calculation tool. ΔTpinch is the pinch temperature difference between highest DP column temperature and the CP temperature at this point. Use of the provided computer model with the heat transfer correlation given in conclusion 2 is preferable.

In addition to these analytical conclusions is the further practical point that the process of direct contact heat transfer has proven successful in producing cooling in an analogous situation to that proposed industrially, and it is recommended that further work on the industrial application proceeds.

9. Recommendations For Further Work

The work undertaken in this study constitutes a foundation upon which to base future work. It is therefore useful to suggest areas which might receive attention should further research on the topic be undertaken. This is in addition to the recommendation to proceed with industrial development stated at the end of chapter 8.

Application of the computer model program to other systems by simply entering different physical property data would show if the model assumptions are of general utility. This is of particular interest in the acid recovery operation which is the potential practical application of this research. In any future research involving the pertinent acid / refrigerant system it is recommended that the experimental apparatus be sufficiently instrumented to allow comparison with computer model prediction. If the model can be adapted successfully then it will be of great value in design studies.

The computer model can be developed to incorporate an instantaneous value of heat transfer surface area. To obtain information about which of the various theoretical models for bubble / drop behaviour gives the best heat transfer results, the computer model can be modified to calculate an area for heat transfer which is more sophisticated than the assumption of constant opening angle. Such models could involve sloshing effects in more detail for example. This would be of theoretical interest mainly since the current model gives results which are adequate in a practical context.

APPENDICES

Appendix 1: Drawings Used In Theory Development.

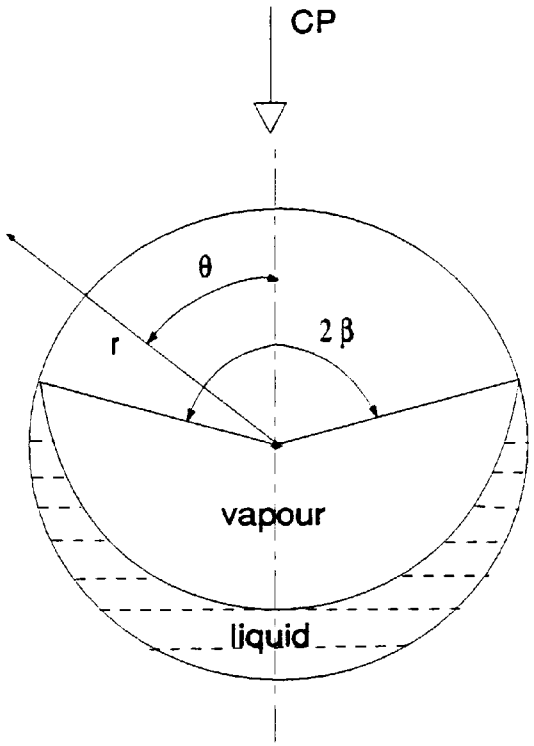

Fig.2.1 Two-phase Bubble Model

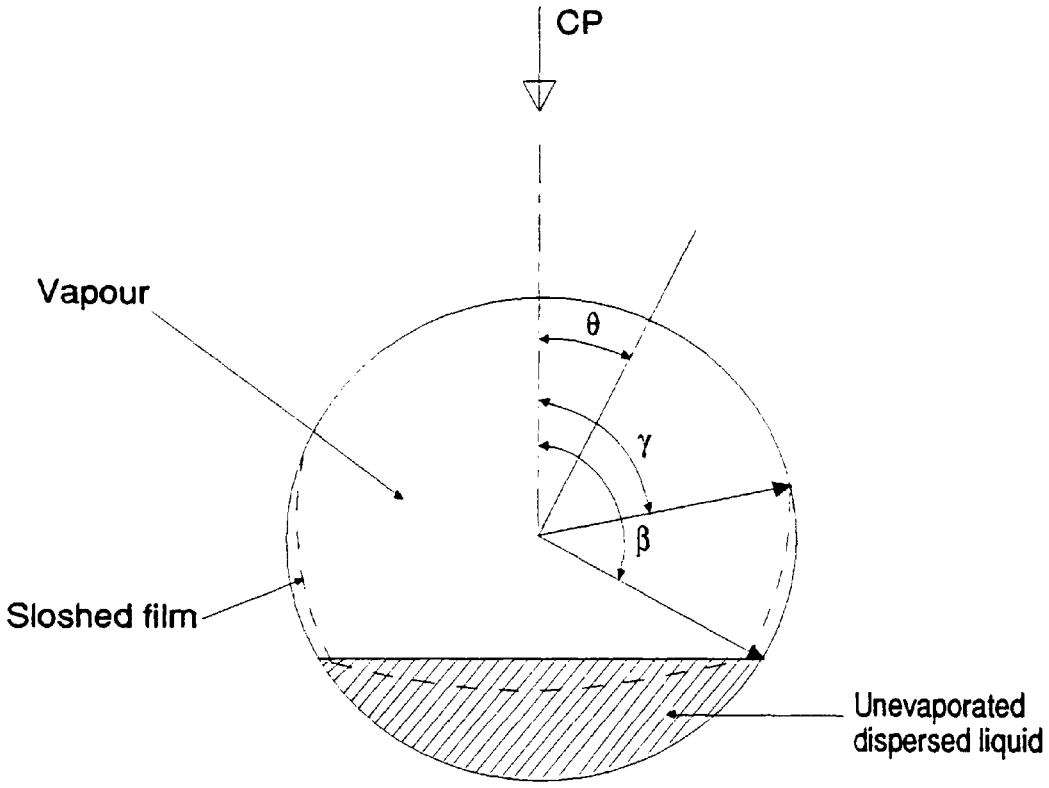

Fig.2.2 Two-phase Bubble Sloshing Model

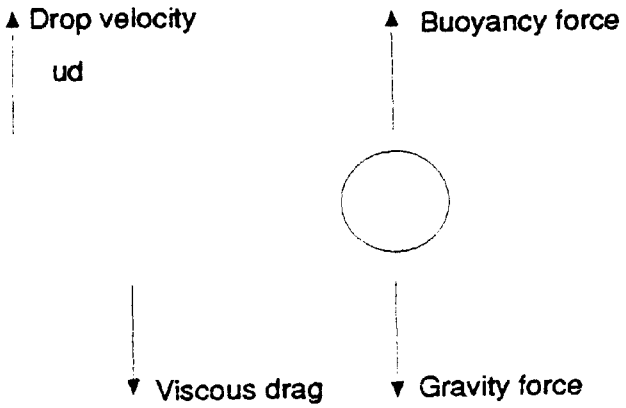

Fig.2.3 Bubble Forces

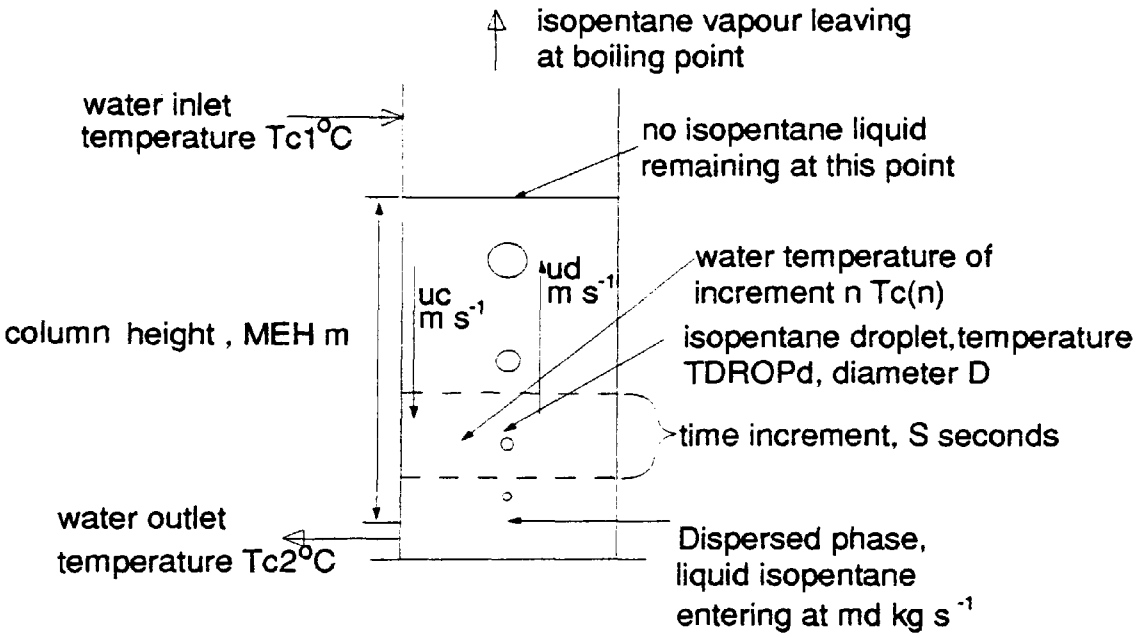

Fig.2.4 Incremental Model Basis

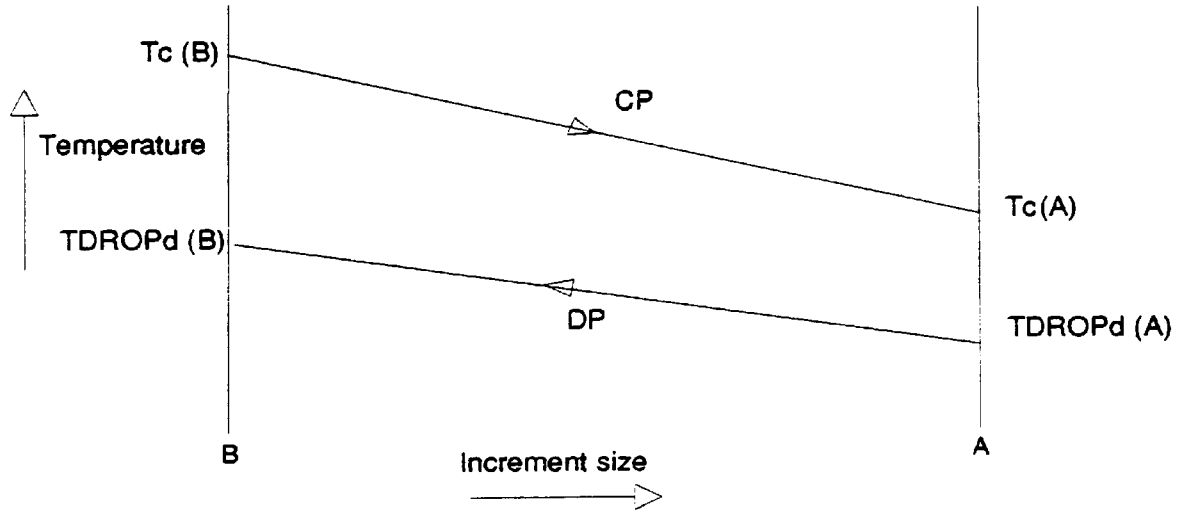

Fig. 2.5 Temperature Profile for Large Increment Size

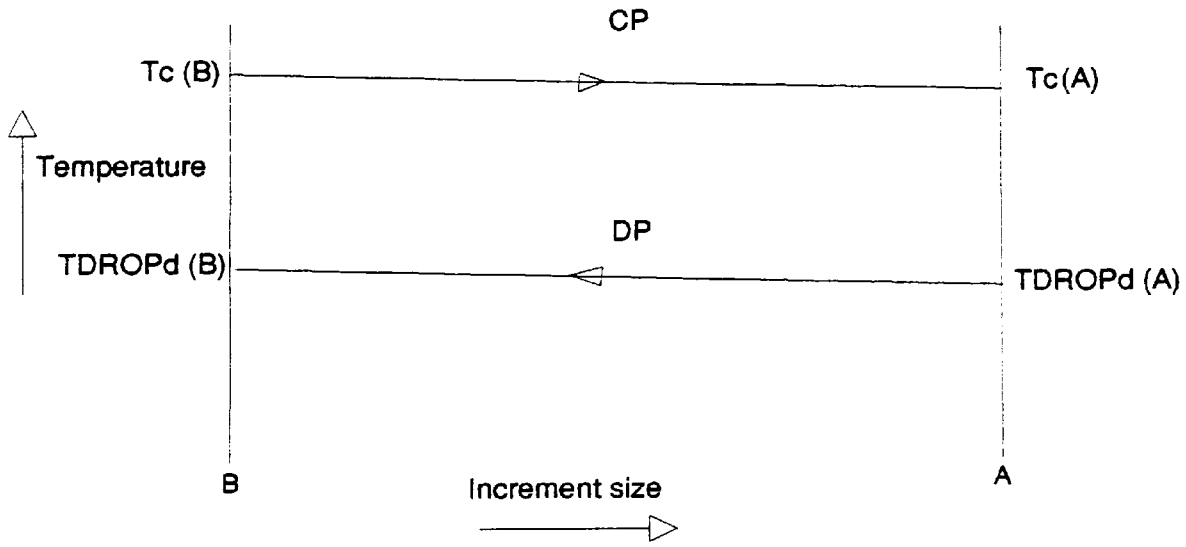

Fig. 2.6 Temperature Profile for Small Increment Size

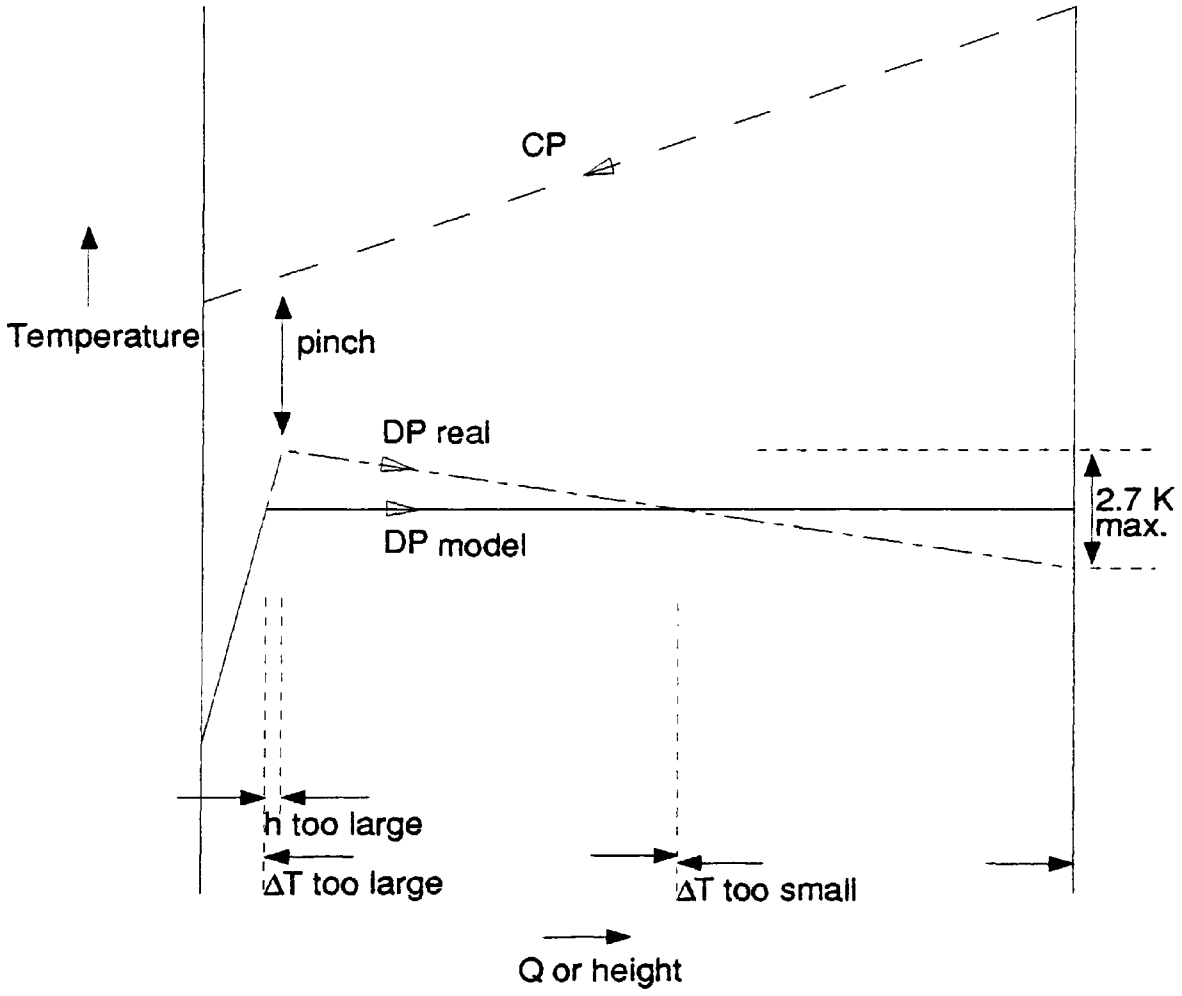

Not to scale. Comments refer to model.

Fig.2.7 Temperature Profile Analysis of Column

Appendix 2: References.

1. Jenkins D P, British Steel Welsh Laboratory Technical Note, 1984.

2. Sideman S and Taitel Y, Direct-Contact Heat Transfer with Change of Phase; Evaporation of Drops in an Immiscible Liquid Medium, Int J Heat Mass Transfer Vol 7, pp 1273-1289, 1964.

3. Sideman S and Shabtai H, Direct Contact Heat Transfer Between a Single Drop and an Immiscible Liquid Medium, Can. J. Chem.Eng., pp 107-115, 1964.

4. Coulson J M and Richardson J F, Chemical Engineering Vol 1, Revised Third Edition (SI units) p 248-249, Pergamon Press, 1977.

5. Perry R H and Chilton C H, Chemical Engineers Handbook, 5th Edition, pp 21-15 to 21-16, McGraw Hill, 1973.

6.Ito R, Hirata Y, Inoue K, and Kitagawa Y, Formation of a Liquid Drop at a Single Nozzle in a Uniform Stream, Int Chem Eng Vol 20 No 4, pp 616-620, 1980.

7. Nat. Eng. Lab. and I. Chem. E., Physical Property Data Service Computer Program Version 9-07 (see Appendix 5).

8.Chen J J, Heat Transfer in Bubble Columns- Application of the Ruckenstein-Smigelschi Model, Chemical Engineering Research and Design Vol 65, No 2, pp 115-119, 1987.

9. Hughmark G A, Heat and Mass Transfer for Spherical Particles in a Fluid Field, Ind Eng Chem Fundam Vol 19, No 2, 1980.

10. Gilson C D, Thomas A, and Hawkes F R, Drop Formation at a Nozzle; Calcium Alginate Bead Manufacture with and without immobilised yeast, to be published, plus personal consultation with C D Gilson.

11. Rowe P N , Claxton K T and Lewis J B, Heat and Mass Transfer from a single sphere in an Extensive Flowing Fluid , Trans Inst Chem Engrs Vol 43, 1965.

12. Coulson J M and Richardson J F, Chemical Engineering Vol 2, Third Edition (SI Units) pp 89-116, Pergamon Press,1983.

13. Buchholz R, Zakrzewski W, and Schugerl K, Techniques for Determining the Properties of Bubbles in Bubble Columns, Int Chem Eng Vol 21, No 2, 1981.

14. Field R W and Rahimi R, Hold Up and Heat Transfer in Bubble Columns, Inst Chem Eng Symp Ser, 108 (Fluid mixing 3) pp 257-270, 1988.

15. Chen B H, Heat Transfer in a Continuous Bubble Column, Can J Chem Eng Vol 67, pp 678-681, 1989.

16. Editorial, Reverse Osmosis on Top, The Chemical Engineer, p 6, 25 April, 1991.

17. Wilke C R, Cheng C T, Ledesma V L, and Porter J W, Direct Heat Transfer for Sea Water Evaporation, Chem. Eng. Prog. Vol 59, No 12, 1963.

18. Wiegandt H F, Saline Water Conversion by Freezing, Advances in Chemistry Series Vol 27, p 82-89, 1960.

19.Denton W H, Hall Taylor, N S, Klaschka J T, Smith M J S, Diffey H R and Rumary C H, Experimental Studies on the Immiscible Refrigerant (Butane) Freezing Process, Proc 3rd Int Symp Freshwater from the Sea, Vol 3, p 51-69, 1970.

20. Denton W H, Smith M J S, Klaschka J T, Forgan R, Diffey H R, Rumary C H, and Dawson R W, Experimental Studies on Washing and Melting Ice Crystals in the Immiscible Refrigerant Freezing Process, Proc. 4th Int. Symp. Freshwater from the Sea, Vol 3, p 291-311, 1973.

21. Fowles P E and Tsoung Y Y, Direct Cooling Crystallization, U S Patent No 4452621 June 5, 1984.

22. Kisaburek B,Uysal B Z and Dikmen K, Direct Contact Heat Transfer Between Two Immiscible Liquids, Chem Eng Commun Vol 20, Part 3-4 pp 157-172, 1983.

23. Sideman S and Hirsch G, Direct Contact Heat Transfer with Change of Phase; Condensation of Single Vapour Bubbles in an Immiscible Liquid Medium - Preliminary Studies, A I Ch E J Vol 11, No 6, pp 019-1025, 1965.

24. Sideman S and Moalem-Maron D, Direct Contact Condensation, Advances in Heat Transfer Vol 15, pp 227-281, 1982.

25.Tamir A, Taitel Y and Schlunder E U, Direct Contact Condensation of Binary Mixtures, Int J Heat Mass Transfer Vol 17, pp 1253 1260, 1974.

26. Pattantyus-h E, Temperature Variation and Collapse Time at the Condensation of Vapour Bubble, Int J Heat Mass Transfer Vol 15, pp 2419-2426, 1972.

27. Hendrix L T, Refrigerated Crystallizer System, U S Patent No 3486848, December 30, 1969.

28. Porteus A, Saline Water Distillation Processes, p 11, Longmans, 1975.

29. Raina G K and Wanchoo R K, Direct Contact Heat Transfer with Phase Change; Theoretical Expression for Instantaneous Velocity of a Two Phase Bubble, Int Commun Heat Mass Transfer Vol 11, pp 227-237, 1984.

30. Raina G K and Wanchoo R K, Direct Contact Heat Transfer with Phase Change: Bubble Growth and Collapse, Can J Chem Eng Vol 64, 1986.

31. Raina G K and Grover P D, Direct Contact Heat Transfer with Change of Phase: Experimental Technique, A I Ch E J Vol 34, No 8, pp 1376-1380, 1988.

32. Klipstein D H, Heat Transfer to a Vaporizing Immiscible Drop, D Sc Thesis, M I T, Cambridge Ma, 1963.

33. Moore G R, Vaporization of Superheated Drops in Liquids, A I Ch E J Vol 5, No. 458, 1959.

34. Prakash C B and Pinder K L, Direct Contact Heat Transfer Between Two Immiscible Liquids During Vaporization, Can J Chem Eng Vol 45, pp 210-220, 1967.

35. Bird R B, Stewart W E and Lightfoot E N, Transport Phenomena, International Edition, p 409, John Wiley and Sons, 1960.

36. Wakeshima H and Takata K On the Limit of Superheat, J Phys Soc Japan 13, p 1398, 1958.

37. Adams A E S and Pinder K L, Average Heat Transfer Coefficient during the Direct Evaporation of a Liquid Drop, Can J Chem Eng Vol 50, pp 707- 713, 1972.

38. Simpson H C, Beggs G C and Nazir M, Evaporation of Butane Drops in Brine, Desalination Vol 15, pp 11-23, 1974.

39. Pinder K L, Surface Area Prediction for Two Phase Drops in an Immiscible Liquid, Can J Chem Eng Vol 58, 1980.

40. Raina G K and Grover P D, Direct Contact Heat Transfer with Change of Phase: Theoretical Model, A I Ch E J Vol 28, No 3, pp 515-517, 1982.

41. Raina G K and Grover P D, Direct Contact Heat Transfer with Change of Phase; Theoretical Model Incorporating Sloshing Effects, A I Ch E J Vol 31, pp 507-509,1985.

42. Sideman S and Isenberg J, Direct Contact Heat Transfer with Change of Phase: Bubble Growth in Three-Phase Systems, Desalination Vol 2, p207, 1967.

43. Tochitani Y , Nakagawa T, Mori Y H and Komotori K, Vaporization of Single Liquid Drops in an Immiscible Lliquid, Part II: Heat Transfer Characteristics, Warme und Stoffuber-tragung, Vol 10, p 71, 1977.

44. Battya P, Raghavan V R and Seetharamu K N, Parametric Studies on Direct Contact Evaporation of an Immiscible Liquid, Int J Heat Mass Transfer Vol 27, No 2, pp 263-272, 1984.

45. Battya P, Raghavan V R and Seetharamu K N, A Theoretical Correlation for the Nusselt Number in Direct Contact Evaporation of a Moving Drop in an Immiscible Liquid, Warme und Stoffubertragung 19, pp 61-66, 1985.

46. Smith R C,Rohsenow W M and Kazimi M S, Volumetric Heat Transfer Coefficients for Direct Contact Evaporation, Trans A S M E Journal of Heat Transfer, Vol 104, pp 264-270, 1982.

47. Tadrist L, Shehu Diso I,Santini R and Pantaloni J, Vaporisation of a Liquid by Direct Contact in Another Immiscible Liquid , Int J Heat Mass Transfer, Vol 30, No 9, pp 1773-1785, 1987.

48. Shimizu Y and Mori Y H, Evaporation of Single Liquid Drops in an Immiscible Liquid at Elevated Pressures: Experimental Study with n-pentane and R113 drops in water, Int J Heat Mass Transfer Vol 31, No 9, pp 1843-1851, 1988.

49. Coulson J M and Richardson J F, Chemical Engineering, Vol 1, Revised Third Edition (SI Units), pp 169-171 and 192-205, Pergamon Press, 1977.

50. Mann R, Gas-Liquid Contacting in Mixing Vessels, I Chem E Industrial Research Fellowship Report, I Chem E, 1983.

51. Mochizuki T, Mori Y H and Kaji N, Augmentation of Direct Contact Heat Transfer to a Train of Drops through Application of a Transverse Electric Field, J Chem Eng of Japan, Vol 20, No 6, 1987.

52. Mori Y M, Classification of Configurations of Two Phase Vapour / Liquid Bubbles in an Immiscible Liquid in Relation to Direct Contact Evaporation and Condensation Processes, Int J Multiphase Flow Vol 11, No 4, pp 571-576, 1985.

53. Raina G K, Wanchoo R K and Grover P D, Direct Contact Heat Transfer with Phase Change: Motion of Evaporating Droplets, A I Ch E J Vol 30, No 5, pp 835-837, 1984.

54. Clift R, Bubbles, Drops and Particles, pp 203- 212, New York, Academic, 1978.

55. Wohlk W and Hofman G, Types of Crystallisers, Int Chem Eng Vol 27, No 2, 1987.

Appendix 3: Nomenclature.

Dimensionless groups

Bo	Bond number ((ρc - ρd) D^{*2} g / σ)
Fo	Fourier number (a x time / D^2)
Gr	Grashof number (D^3 g ρ Δρ / μ^2)
Ja	Jakob number of system
	(ρc Cpc (Tc-Td) / ρdv λ)
K	log mean partition coefficient [3]
L	Geometrical Factor [3]
Nu	Nusselt number (h D / k)
Pe	Peclet number (u D / a)
Pe'	viscosity modified Peclet number
	(Pe (1 / (1+(μd / μc))))
Pr	Prandtl number (Cp μ / k)
Re	Reynolds number (D u ρ / μ)
We	Weber number (ρ u^2 D / σ)

Dimensional symbols used in equation 2.2.16

do	orifice diameter,ft
F	empirical coefficient
Vo	velocity through orifice,ft / s
vp	droplet volume,cu ft
Δρ	density difference, lb / cu ft
μc	viscosity of continuous phase,
	lb / h ft
ρd	density of dispersed phase,lb / cu ft
σ	interfacial tension, dynes / cm

Other symbols

A	heat exchange area
a	thermal diffusivity
B	constant, equation 2.2.6; 0.69 in air and 0.79 in water.
C	a constant
Cp	specific heat capacity
D	diameter (of droplet / bubble unless specified)
D*	initial drop diameter
F	volume flowrate
g	acceleration due to gravity
h	film coefficient of heat transfer
k	thermal conductivity
l	length
MEH	minimum column height for complete evaporation of dispersed phase
m	mass flowrate
P	pressure
Q	heat transfer rate
R	drag force coefficient
r	radial coordinate
T	temperature
TBP	bubble point temperature
U	overall heat transfer coefficient
u	velocity
x	exponent equation 2.2.11
y	wall thickness

β	vapour half opening angle-see fig 2.1
ΔT	(no affix) temperature driving force for heat transfer
ΔT	(with affix) temperature difference for single medium
γ	sloshed film angle defined in fig 2.2
λ	specific latent heat of vaporisation (dispersed phase unless specified)
μ	fluid absolute viscosity
ρ	fluid density
θ	spherical / polar coordinate

Subscripts / affixes

1	inlet conditions
2	outlet conditions
(A), (B)	increment boundary conditions
ave	average value
b	bulk value
c	continuous phase
col	column
d	dispersed phase
i	inside
max	maximum
min	minimum
(n), (N)	increment number
o	outside
t	tube
v	vapour phase

	w	wall

Abbreviations

AMTD	arithmetic mean temperature difference
CP	continuous phase
DP	dispersed phase
LMTD	log mean temperature difference

Appendix 4: ADC Program.

```
10 DIMA(15):DIMT(15)
20 PRINT"■"
30 A=12
40 IF A(4 OR A)14 THEN30
50 PRINT"■"
60 GOSUB5000
70 GOSUB2000
80 OPEN3,4
90 FOR B=0TO15
100 GOSUB1000
110 NEXTB
120 GOSUB4000
130 GOSUB3000
140 GOSUB1500
150 GOTO90
160 CLOSE3:STOP
170 END
1000 REM
1010 REM
1020 REM
1030 OPEN1,A,B
1040 GET#1,J$,K$
1050 REM
1060 K=ASC(K$)-224
1070 IFK<0THENO=(K+32)*-1
1080 IFK=0THENO=K
1090 REM
1100 O=O*256
1110 REM
1120 IFJ$=""THENJ=0:GOTO1140
1130 J=ASC(J$)
1140 IFK<0THENJ=J*-1
1150 REM
1160 A(B)=J+O
1170 CLOSE1
1180 RETURN
1500 PRINT"■KEY S TO STOP, SPACE TO CONTINUE,C TO   RECALIBRATE T/CS"
1510 GET2$:IF2$=""THEN 1510
1520 IF 2$="S"THEN 160
1530 IF 2$="C"THEN GOSUB2000
1540 RETURN
2000 INPUT"INPUT  COLD REF TEMP (CHANNEL 0) DEG C ";CR
2010 INPUT"INPUT  HOT REF TEMP (CHANNEL 1) DEG C ";HR
2020 RETURN
3000 M=(HR-CR)/(A(1)-A(0))
3010 C=HR-M*A(1)
3020 PRINT#3,"DATE=";D$;" SOR TIME=";T$
3030 FORB=0TO15
3040 T(B)=M*A(B)+C
3050 T(B)=INT(T(B)*100+.50)/100
3060 PRINT"CHANNEL =";B;"TEMP DEG C=";T(B)
3070 PRINT#3,"CHANNEL =";B;"TEMP DEG C=";T(B)
3080 NEXTB
3090 RETURN
4000 IF ABS(A(15))<3THEN GOTO4050
4010 PRINT
4020 PRINT"■CHATTER >2 VALUE =";A(15)
4030 PRINT
4040 GOSUB1500
4050 RETURN
5000 INPUT"INPUT DATE (MAX 10 CHAR)";D$
5010 INPUT"INPUT SOR TIME (MAX 10 CHAR)";T$
5020 RETURN
10000 CLOSE3:OPEN4,4:CMD4:LIST
10010 PRINT#4
10020 CLOSE4
10030 STOP
```

```
10 DIMA(16):DIMT(16)
20 PRINT"□"
30 A=12
40 IF A<4 OR A>14 THEN30
50 PRINT"□"
60 GOSUB5000
70 GOSUB2000
80 OPEN3,4
90 FOR B=0TO15
100 GOSUB1000
110 NEXTB
120 GOSUB4000
130 GOSUB3000
140 GOSUB1500
150 GOTO90
160 CLOSE3:STOP
170 END
1000 REM
1010 REM
1020 REM
1030 OPEN1,A,B
1040 GET#1,J$,K$
1050 REM
1060 K=ASC(K$)-224
1070 IFK<0THEND=(K+32)*-1
1080 IFK>=0THEND=K
1090 REM
1100 D=D*256
1110 REM
1120 IFJ$=""THENJ=0:GOTO1140
1130 J=ASC(J$)
1140 IFK<0THENJ=J*-1
1150 REM
1160 A(B)=J+D
1170 CLOSE1
1180 RETURN
1500 PRINT"■KEY S TO STOP, SPACE TO CONTINUE,C TO   RECALIBRATE T/CS"
1510 GETZ$:IFZ$=""THEN 1510
1520 IF Z$="S"THEN 160
1530 IF Z$="C"THEN GOSUB2000
1540 RETURN
2000 INPUT"INPUT  COLD REF TEMP (CHANNEL 0) DEG C ";CR
2010 INPUT"INPUT  HOT REF TEMP (CHANNEL 1) DEG C ";HR
2020 RETURN
3000 M=(HR-CR)/(A(1)-A(0))
3010 C=HR-M*A(1)
3020 PRINT#3,"DATE=";D$;" SOR TIME=";T$
3030 FORB=0TO15
3040 T(B)=M*A(B)+C
3050 T(B)=INT(T(B)*100+.5)/100
3060 PRINT"CHANNEL =";B;"TEMP DEG C=";T(B)
3070 PRINT#3,"CHANNEL =";B;"TEMP DEG C=";T(B)
3080 NEXTB
3090 RETURN
4000 IF ABS(A(15))<3THEN GOTO4050
4010 PRINT
4020 PRINT"■CHATTER >2 VALUE =";A(15)
4030 PRINT
4040 GOSUB1500
4050 RETURN
5000 INPUT"INPUT DATE (MAX 10 CHAR)";D$
5010 INPUT"INPUT SOR TIME (MAX 10 CHAR)";T$
5020 RETURN
10000 CLOSE3:OPEN4,4:CMD4:LIST
10010 PRINT#4
10020 CLOSE4
10030 STOP
```

ADC23 Program Output.

```
DATE=15/8/89 SOR TIME=1000
CHANNEL = 0 TEMP DEG C= 0
CHANNEL = 1 TEMP DEG C= 42.1
CHANNEL = 2 TEMP DEG C= 30.1
CHANNEL = 3 TEMP DEG C= 18.04
CHANNEL = 4 TEMP DEG C= 32.09
CHANNEL = 5 TEMP DEG C= 18.15
CHANNEL = 6 TEMP DEG C= 26.88
CHANNEL = 7 TEMP DEG C= 27.83
CHANNEL = 8 TEMP DEG C= 26.98
CHANNEL = 9 TEMP DEG C= 28.08
CHANNEL = 10 TEMP DEG C= 27.88
CHANNEL = 11 TEMP DEG C= 30.8
CHANNEL = 12 TEMP DEG C= 27.58
CHANNEL = 13 TEMP DEG C= 28.38
CHANNEL = 14 TEMP DEG C= 27.18
CHANNEL = 15 TEMP DEG C= 25.5
```

Appendix 5: PPDS Example Program Output.

STREAM CONSTANTS: MJLENCH_ISOPENTANE

	COMPONENT		42
1	MOLECULAR WEIGHT		72.150
2	CRITICAL TEMPERATURE	DEG K	460.430
3	CRITICAL PRESSURE	N/SQ.M	0.3383E+07
4	CRITICAL VOLUME	M3/KGMOLE	0.3057
5	MELTING POINT	DEG K	113.000
6	BOILING POINT	DEG K	301.030
7	PARACHOR	ST-4/KMOLE	229.400
8	VAP. HT. OF FORMATN.	MJ/KGMOLE	-154.473
9	LIQ. HT. OF FORMATN.	MJ/KGMOLE	-178.945
10	FLASH POINT	DEG K	217.000
11	LOWER FLAMM. LIMIT	PERCENT	1.400
12	UPPER FLAMM. LIMIT	PERCENT	7.600
13	AUTOIGNITION TEMP.	DEG K	693.000
14	SOLUBILITY PARAMETER	RT(CAL/CC)	6.750
15	ACENTRIC FACTOR		0.2270
16	VAPOUR ENTROPY	KJ/KGMOLE K	343.600
17	A.F. OF HOMOMORPH		0.000
18	DIPOLE MOMENT	DEBYES	0.1000

STREAM VARIABLES. MJLENCH_ISOPENTANE

TEMPERATURE	DEG K	293.150
PRESSURE	N/SQ.M	101325.
MOLECULAR WEIGHT		72.150

1	VAP.HEAT CAPACITY	KJ/KG K	1.625*
	IDEAL GAS VALUE.	KJ/KG K	1.625
	ADJUSTED RATIO CP/CV		1.076
	IDEAL RATIO CP/CV		1.076
2	VAPOUR VISCOSITY	CENTIPOISE	0.6858E-02*
	IDEAL GAS VALUE.	CENTIPOISE	0.6858E-02
3	VAPOUR CONDUCTIVITY	W/M K	0.01398*
	IDEAL GAS VALUE.	W/M K	0.01398
4	VAPOUR ENTHALPY	MJ/KGMOLE	-0.5906*
	IDEAL GAS VALUE.	MJ/KGMOLE	-0.5906
5	LIQUID HEAT CAPACITY	KJ/KG K	2.274
6	LIQUID CONDUCTIVITY	W/M K	0.1095
7	LIQUID DENSITY	KG/CU.M	620.281
8	LIQ.CU.EXPAN. COEFF.	1/K	0.1714E-02
9	LIQUID ENTHALPY	MJ/KGMOLE	-25.647
10	LIQUID LATENT HEAT	MJ/KGMOLE	24.751
11	LIQ. SURFACE TENSION	N/M	0.01498
12	LIQ. VAPOUR PRESSURE	N/SQ.M	76532.3
13	LIQUID VISCOSITY	CENTIPOISE	0.2254
14	VAPOUR DENSITY	KG/CU.M	2.999*
	IDEAL GAS VALUE.	KG/CU.M	2.999
	COMPRESSIBILITY		1.000
15	TOT.HEAT OF FORMATN.	MJ/KGMOLE	-179.771*
16	VAPOUR ENTROPY	KJ/KGMOLE K	341.603*
	IDEAL GAS VALUE.	KJ/KGMOLE K	341.603
17	LIQUID ENTROPY	KJ/KGMOLE K	259.503
18	ENTROPY OF EVAPORTN.	KJ/KGMOLE K	84.432
19	VAPOUR FREE ENERGY	MJ/KGMOLE	-0.5023E-02*
	IDEAL GAS VALUE.	MJ/KGMOLE	-0.5023E-02
20	LIQUID FREE ENERGY	MJ/KGMOLE	-0.9938

STREAM CONSTANTS: MJLENCH_ISOPENTANE

	COMPONENT		42
1	MOLECULAR WEIGHT		72.150
2	CRITICAL TEMPERATURE	DEG K	460.430
3	CRITICAL PRESSURE	N/SQ.M	0.3383E+07
4	CRITICAL VOLUME	M3/KGMOLE	0.3057
5	MELTING POINT	DEG K	113.000
6	BOILING POINT	DEG K	301.030
7	PARACHOR	ST-4/KMOLE	229.400
8	VAP. HT. OF FORMATN.	MJ/KGMOLE	-154.473
9	LIQ. HT. OF FORMATN.	MJ/KGMOLE	-178.945
10	FLASH POINT	DEG K	217.000
11	LOWER FLAMM. LIMIT	PERCENT	1.400
12	UPPER FLAMM. LIMIT	PERCENT	7.600
13	AUTOIGNITION TEMP.	DEG K	693.000
14	SOLUBILITY PARAMETER	RT(CAL/CC)	6.750
15	ACENTRIC FACTOR		0.2270
16	VAPOUR ENTROPY	KJ/KGMOLE K	343.600
17	A.F. OF HOMOMORPH		0.000
18	DIPOLE MOMENT	DEBYES	0.1000

STREAM VARIABLES. MJLENCH_ISOPENTANE

	TEMPERATURE	DEG K	293.150
	PRESSURE	N/SQ.M	101325.
	MOLECULAR WEIGHT		72.150
1	VAP.HEAT CAPACITY	KJ/KG K	1.625*
	IDEAL GAS VALUE.	KJ/KG K	1.625
	ADJUSTED RATIO CP/CV		1.076
	IDEAL RATIO CP/CV		1.076
2	VAPOUR VISCOSITY	CENTIPOISE	0.6858E-02*
	IDEAL GAS VALUE.	CENTIPOISE	0.6858E-02
3	VAPOUR CONDUCTIVITY	W/M K	0.01398*
	IDEAL GAS VALUE.	W/M K	0.01398
4	VAPOUR ENTHALPY	MJ/KGMOLE	-0.5906*
	IDEAL GAS VALUE.	MJ/KGMOLE	-0.5906
5	LIQUID HEAT CAPACITY	KJ/KG K	2.274
6	LIQUID CONDUCTIVITY	W/M K	0.1095
7	LIQUID DENSITY	KG/CU.M	620.281
8	LIQ.CU.EXPAN. COEFF.	1/K	0.1714E-02
9	LIQUID ENTHALPY	MJ/KGMOLE	-25.647
10	LIQUID LATENT HEAT	MJ/KGMOLE	24.751
11	LIQ. SURFACE TENSION	N/M	0.01498
12	LIQ. VAPOUR PRESSURE	N/SQ.M	76532.3
13	LIQUID VISCOSITY	CENTIPOISE	0.2254
14	VAPOUR DENSITY	KG/CU.M	2.999*
	IDEAL GAS VALUE.	KG/CU.M	2.999
	COMPRESSIBILITY		1.000
15	TOT.HEAT OF FORMATN.	MJ/KGMOLE	-179.771*
16	VAPOUR ENTROPY	KJ/KGMOLE K	341.603*
	IDEAL GAS VALUE.	KJ/KGMOLE K	341.603
17	LIQUID ENTROPY	KJ/KGMOLE K	259.503
18	ENTROPY OF EVAPORTN.	KJ/KGMOLE K	84.432
19	VAPOUR FREE ENERGY	MJ/KGMOLE	-0.5023E-02*
	IDEAL GAS VALUE.	MJ/KGMOLE	-0.5023E-02
20	LIQUID FREE ENERGY	MJ/KGMOLE	-0.9938

Appendix 6: Apparatus Figures.

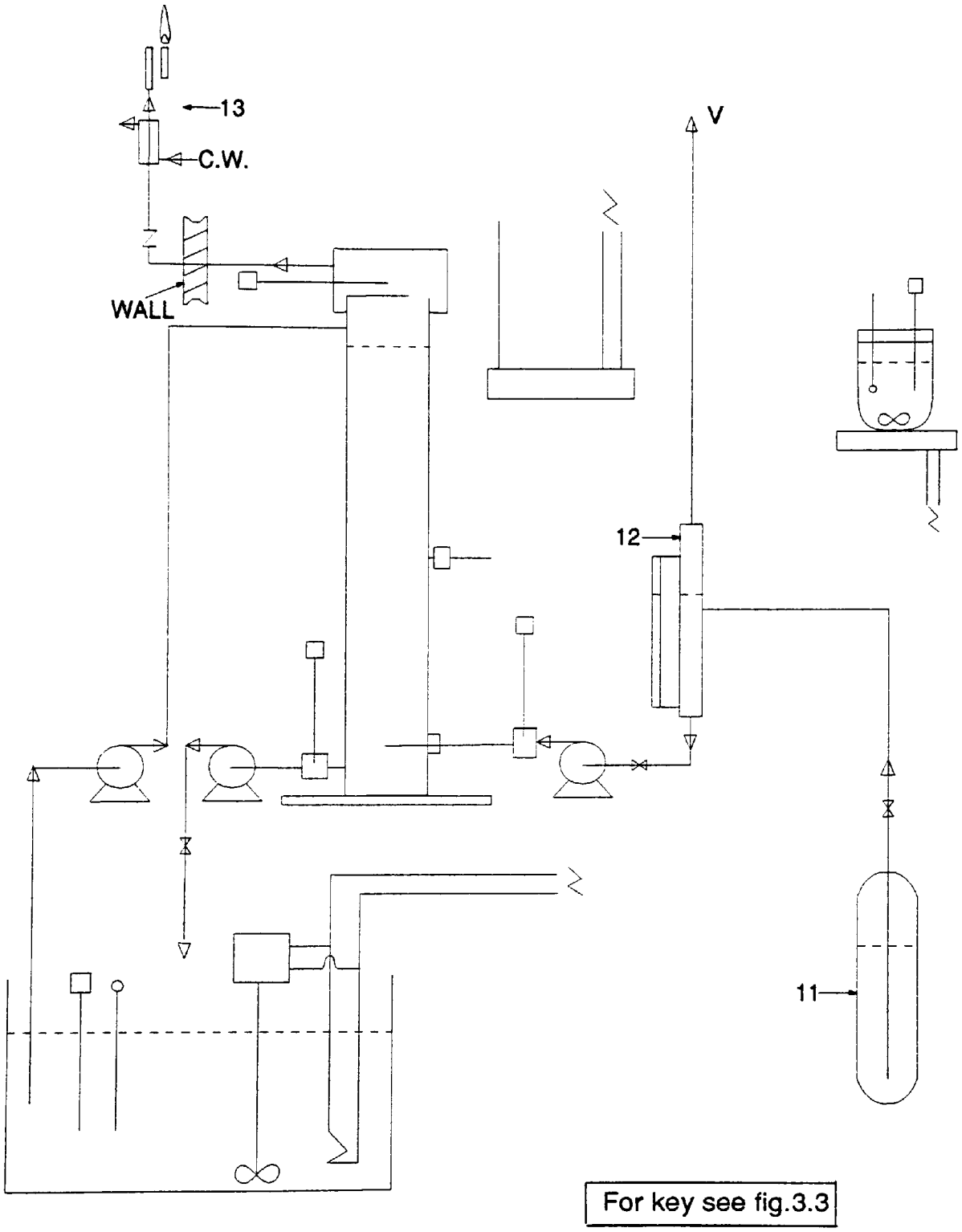

Fig. 3.1 n-butane Apparatus.

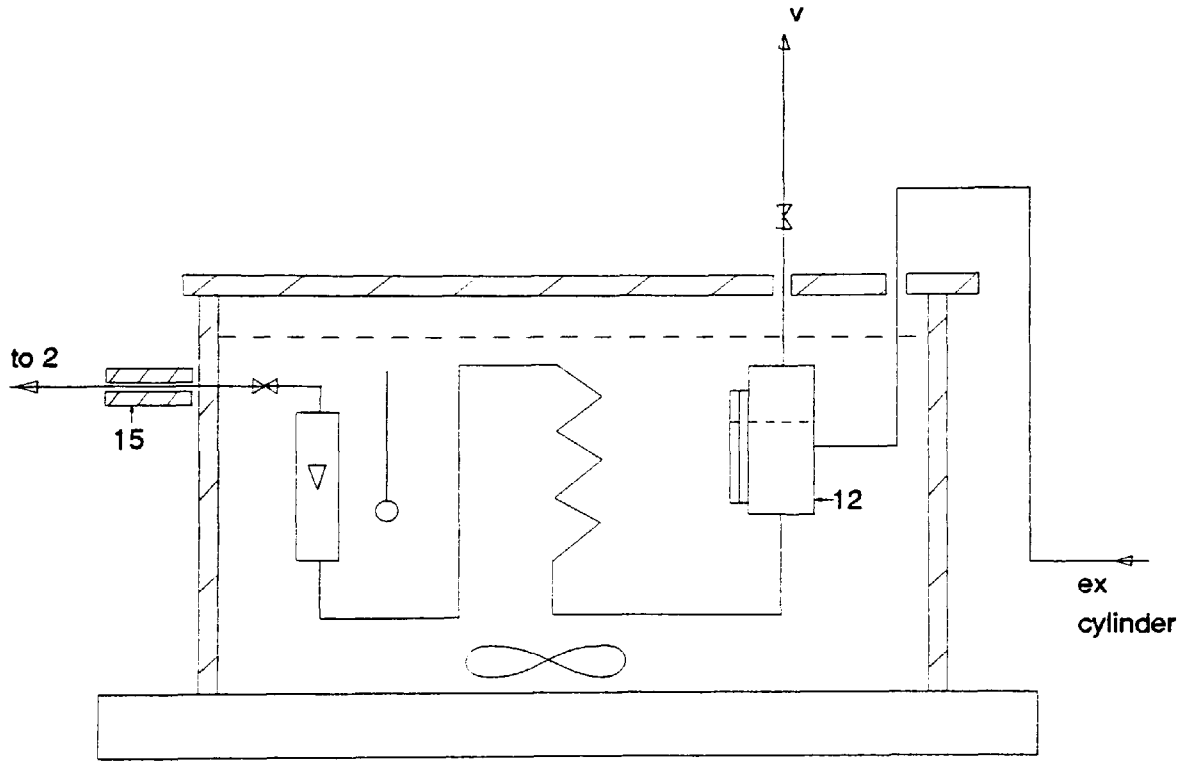

For key see fig.3.3

Fig. 3.2 Cooling Bath Apparatus

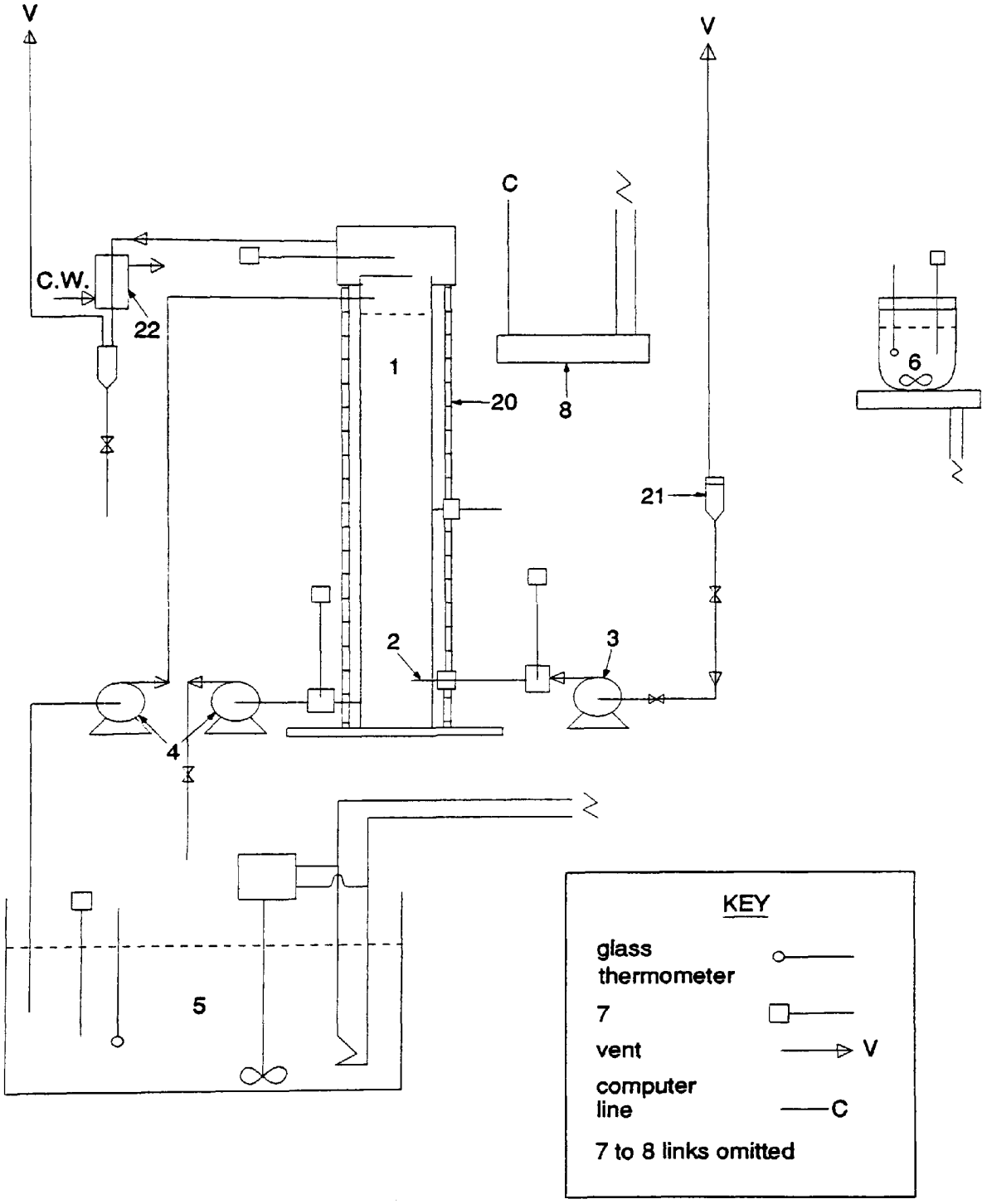

Fig. 3.3 Isopentane Apparatus

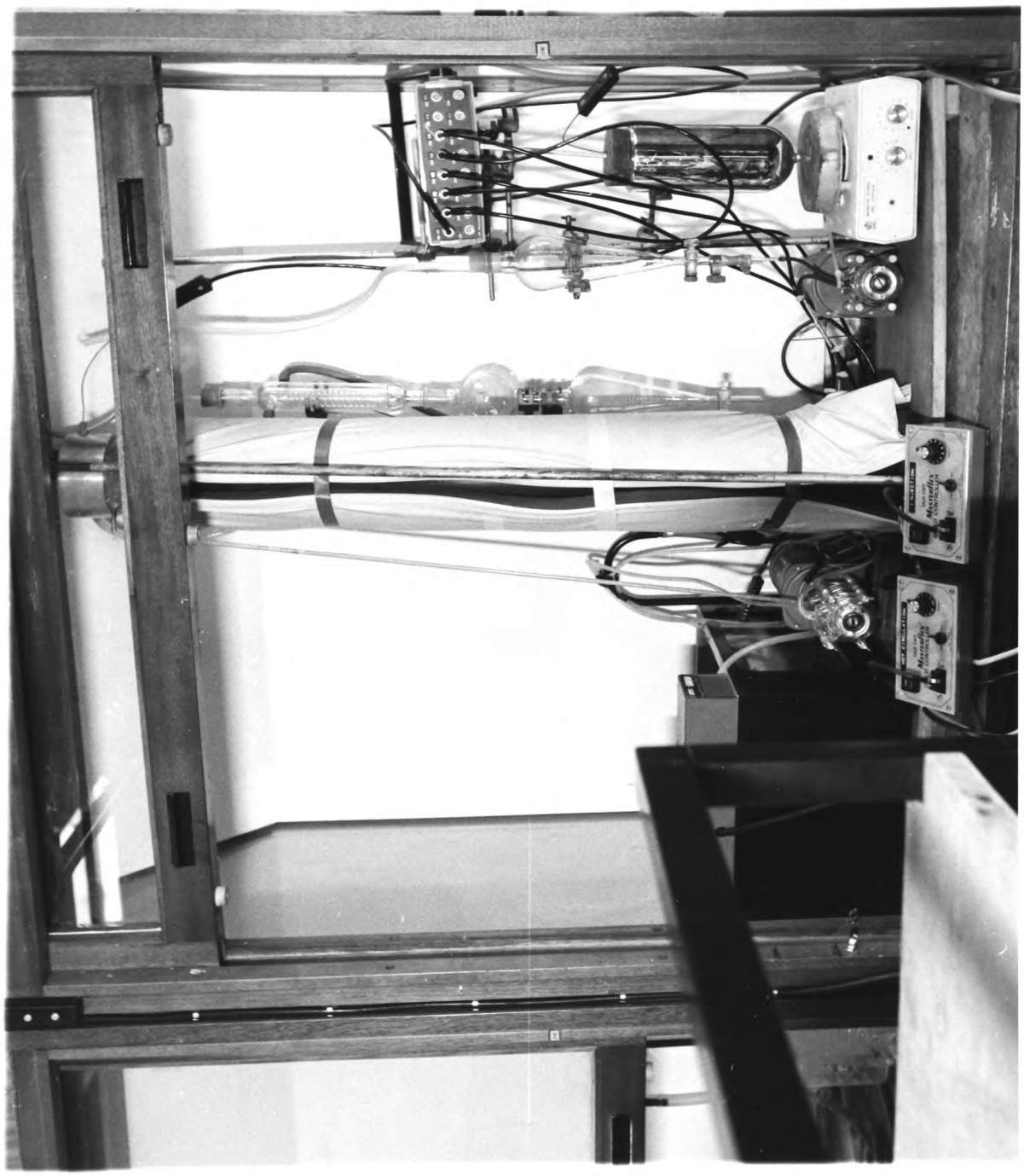

Fig. 3.4 Heat Transfer Apparatus

Fig. 3.5 Computer Apparatus

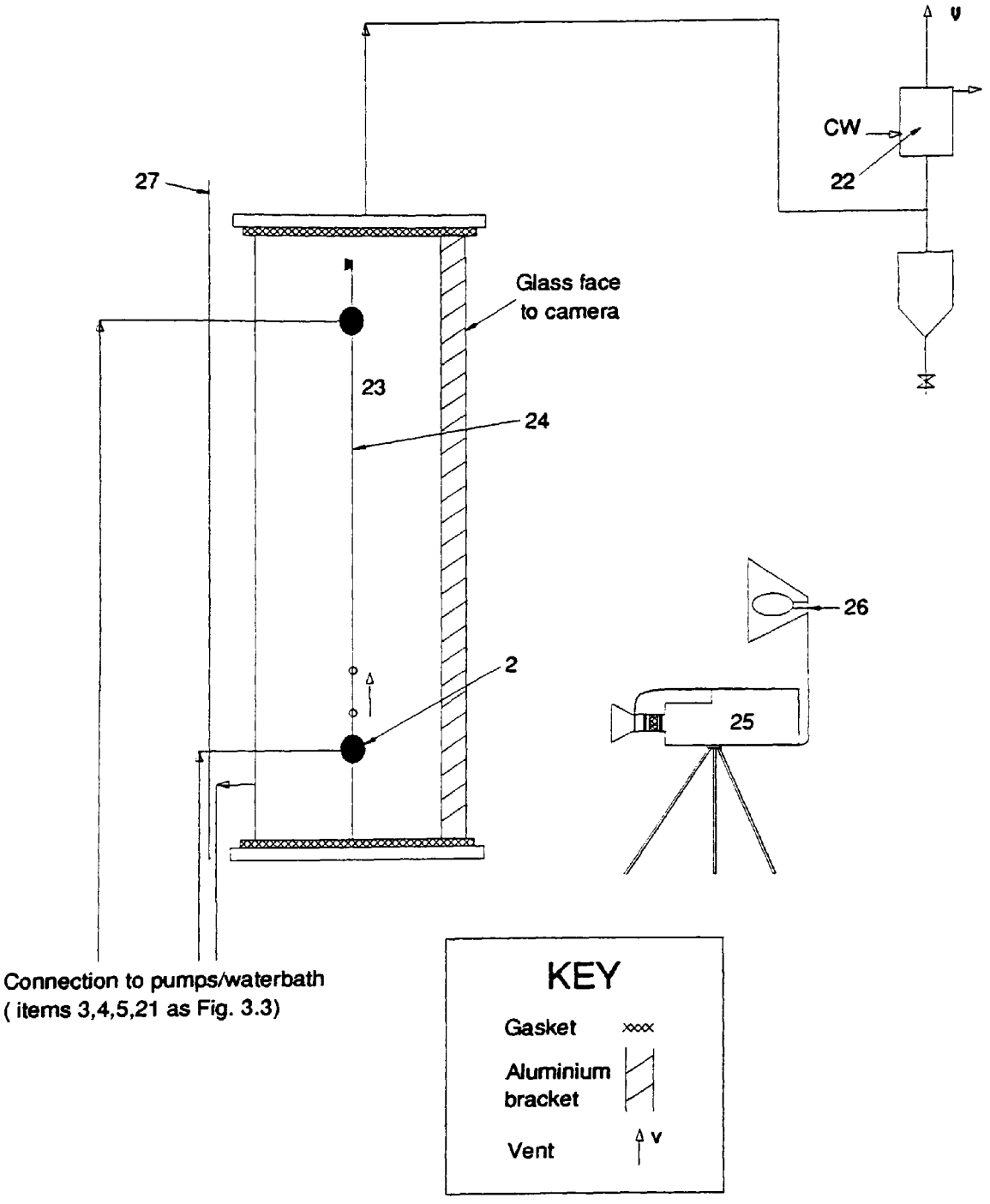

Fig.3.6 Diagram of Photographic Apparatus

Fig. 3.7 Photographic Apparatus (1)

A6.8

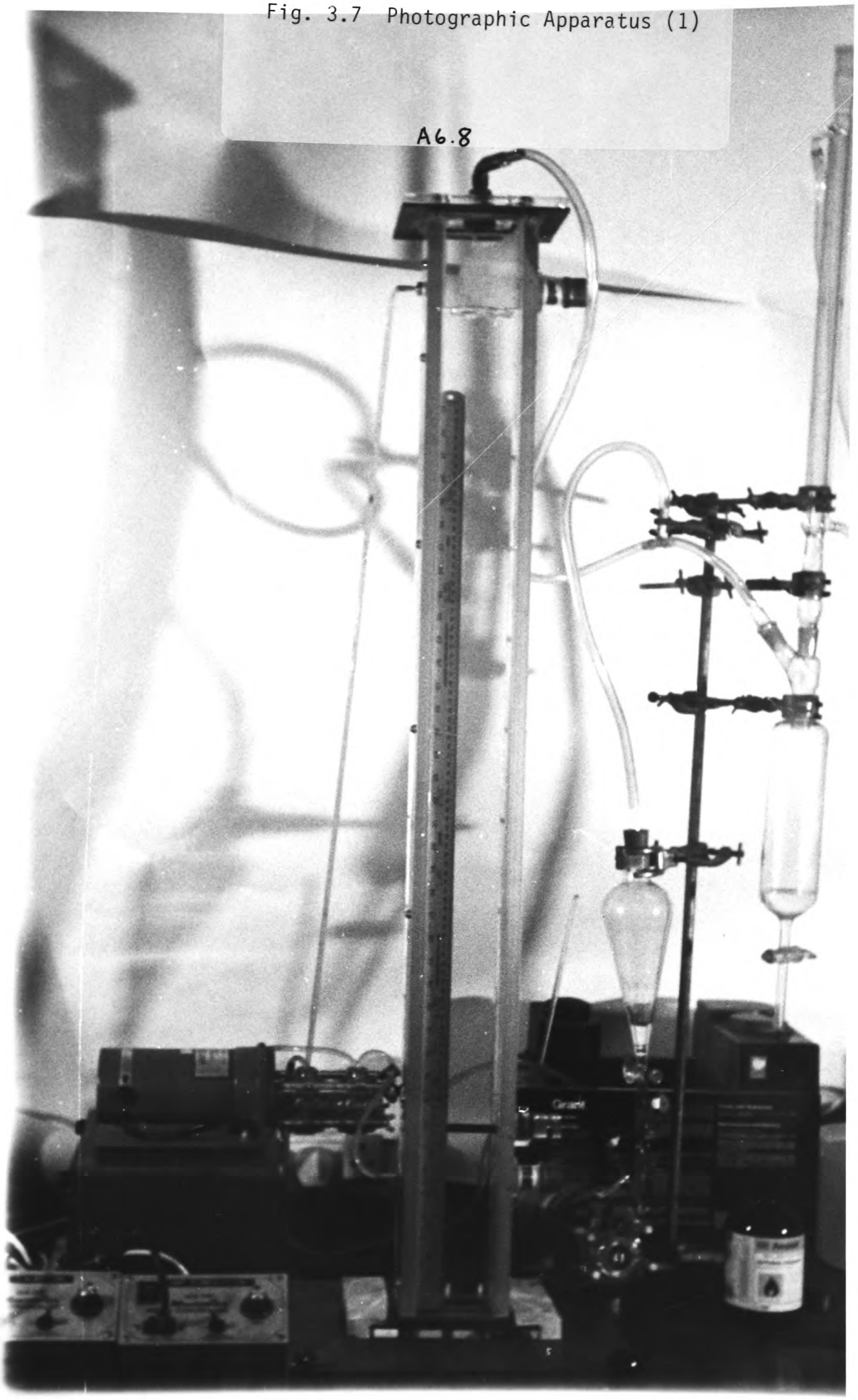

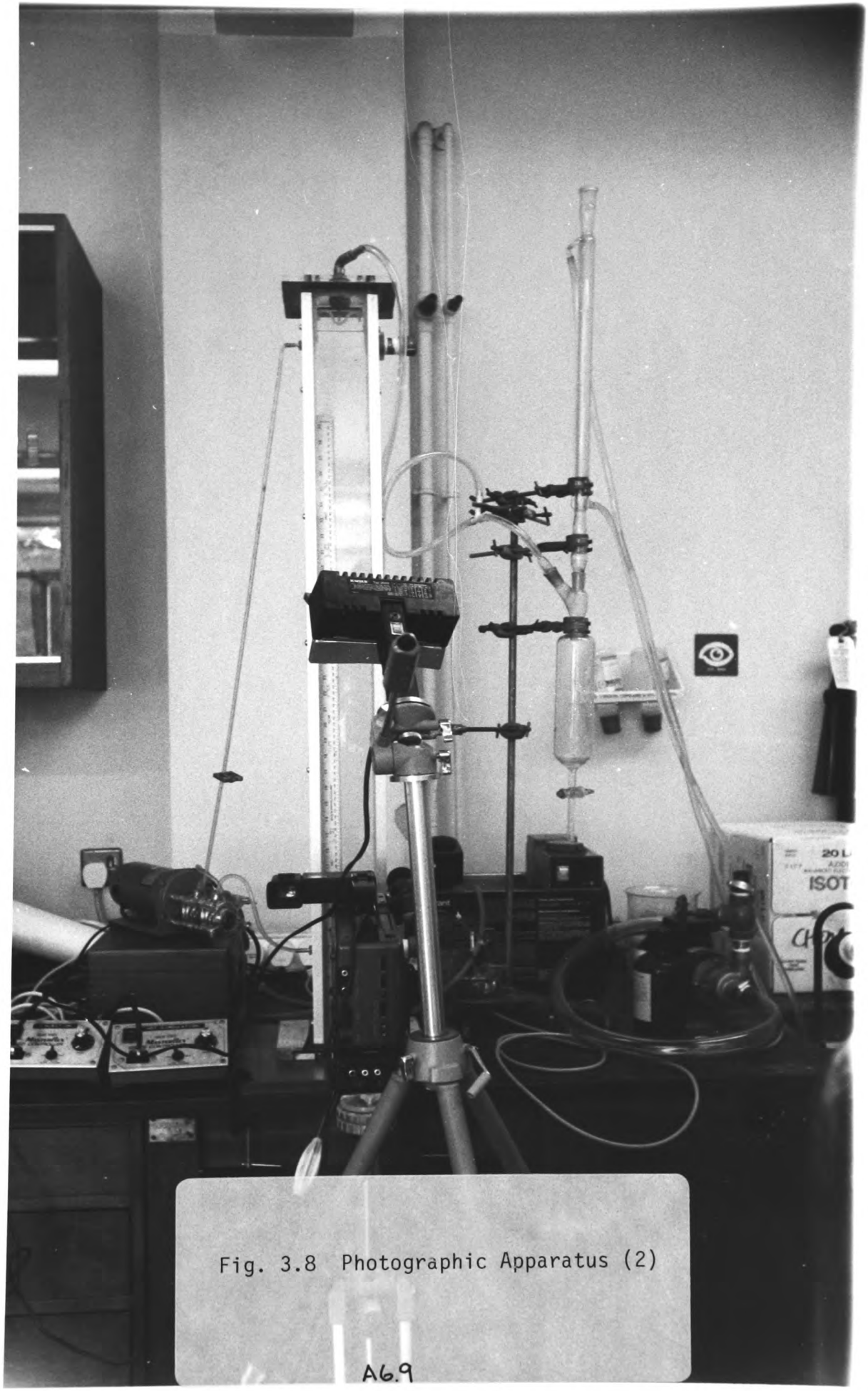

Fig. 3.8 Photographic Apparatus (2)

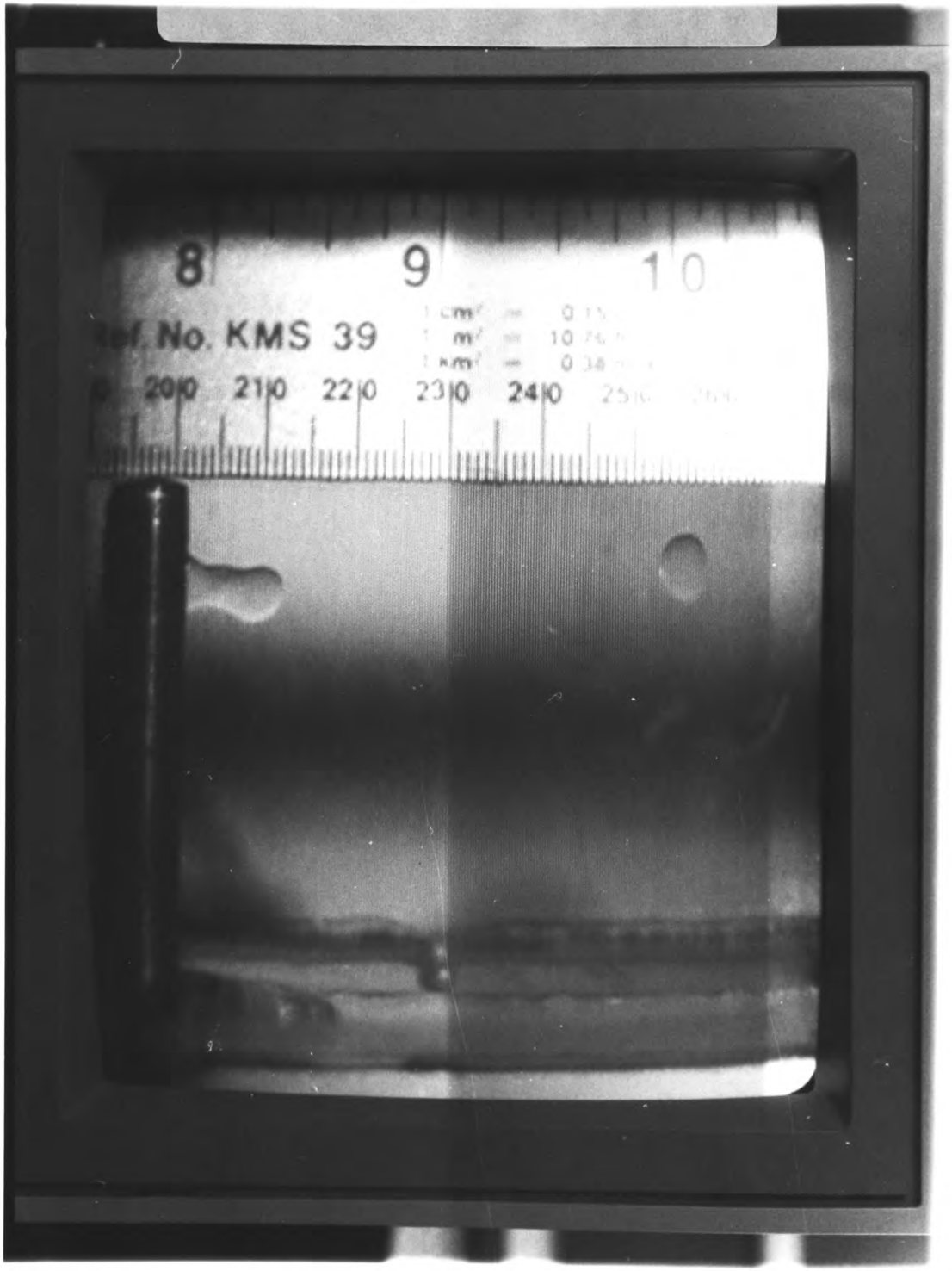
8
9
10
Ref. No. KMS 39
20
21
22
23
24

Appendix 7: 38SOMODEL Listing.

```
10 REM >38SOMODEL
20 REM INITIAL OVERALL MODEL FOR SENSITIVITY ANALYSIS
30 REM  ROc,ROd,D,MUc,Fc,Cpc,kc,mINJECTEDd,Tc1
100 DATA 994,612.3,5E-3,718E-6,7.59E-6,4.178E3,625E-3,8.6E-4,42
110 PROCREAD_DATA
120 PROCFALLING_V
130 PROCFORCE_BAL
140 PROChCALC
150 PROCO_HEAT_BAL
160 PROCMASS_EVAP
170 PROCTIME_HT
180 PRINT
190 PRINT"ud=";ud," Tc1=";Tc1
200 PRINT"h=";h," C HT=";COLEVAPHT
210 PRINT"WATER TEMP DROP=";Dtc
220 END
230 :
1000 DEFPROCREAD_DATA
1010 READ ROc,ROd,D,MUc,Fc,Cpc,kc,mINJECTEDd,Tc1
1020 ENDPROC
1030 :
1040 DEFPROCFORCE_BAL
1050 R=(ROc-ROd)*D*9.807*2/3
1060 ud=SQR(R/(ROc*.22))
1070 Redc=D*ud*ROc/MUc
1080 IFRedc>1E4 OR Redc<500 THEN PRINT"Redc=";Redc;" outside
limit!":STOP
1090 Redc=Redc*(ud+uc)/ud :REM ReFOR ROWE-NET VELOCITY
1100 ENDPROC
1110 :
1120 DEFPROCFALLING_V
1130 CSATUBE=PI*4.7E-2^2
1140 uc=Fc/CSATUBE
1150 ENDPROC
1160 :
1170 DEFPROChCALC
1180 Pr=Cpc*MUc/kc
1190 Nu=2+.79*Pr^(1/3)*Redc^.5
1200 h=Nu*kc/D
1210 ENDPROC
1220 :
1230 DEFPROCO_HEAT_BAL
1240 LATHTd=.3347E6
1250 Qoverall=mINJECTEDd*LATHTd
1260 mINJECTEDc=Fc*ROc
1270 Dtc=Qoverall/Cpc/mINJECTEDc
```

```
1280 ENDPROC
1290 :
1300 DEFPROCMASS_EVAP
1310 ASURFd=PI*D^2
1320 TcMEAN=Tc1-Dtc/2
1330 DT=TcMEAN-30.6
1340 Qcd=h*ASURFd*DT
1350 MEVAP=Qcd/LATHTd
1360 ENDPROC
1370 :
1380 DEFPROCTIME_HT
1390 mdropd=4*PI*ROd*(D/2)^3/3
1400 timeed=mdropd/MEVAP
1410 waterdist=ud*timeed
1420 COLEVAPHT=(ud-uc)*timeed
1430 ENDPROC
1440 :
```

Appendix 8: 38SOMODEL Typical Output.

```
ud=0.238871319          Tc1=42
h=7038.87786            C HT=0.844161882
WATER TEMP DROP=9.13182474
>
```

Appendix 9: Graphical Figure For Water Properties.

Fig.6.1

Viscosity and Thermal Conductivity vs Temperature for Water
800
755
710
665
620
575
530
485
440
395
350
30
35
40
45
50
55
60
65
70
75
80
Water Temperature (deg.C)
1
2
1.Viscosity(1/1000000 kg/m s) 2.Thermal con.(1/1000 W/m k

Fig.6.1

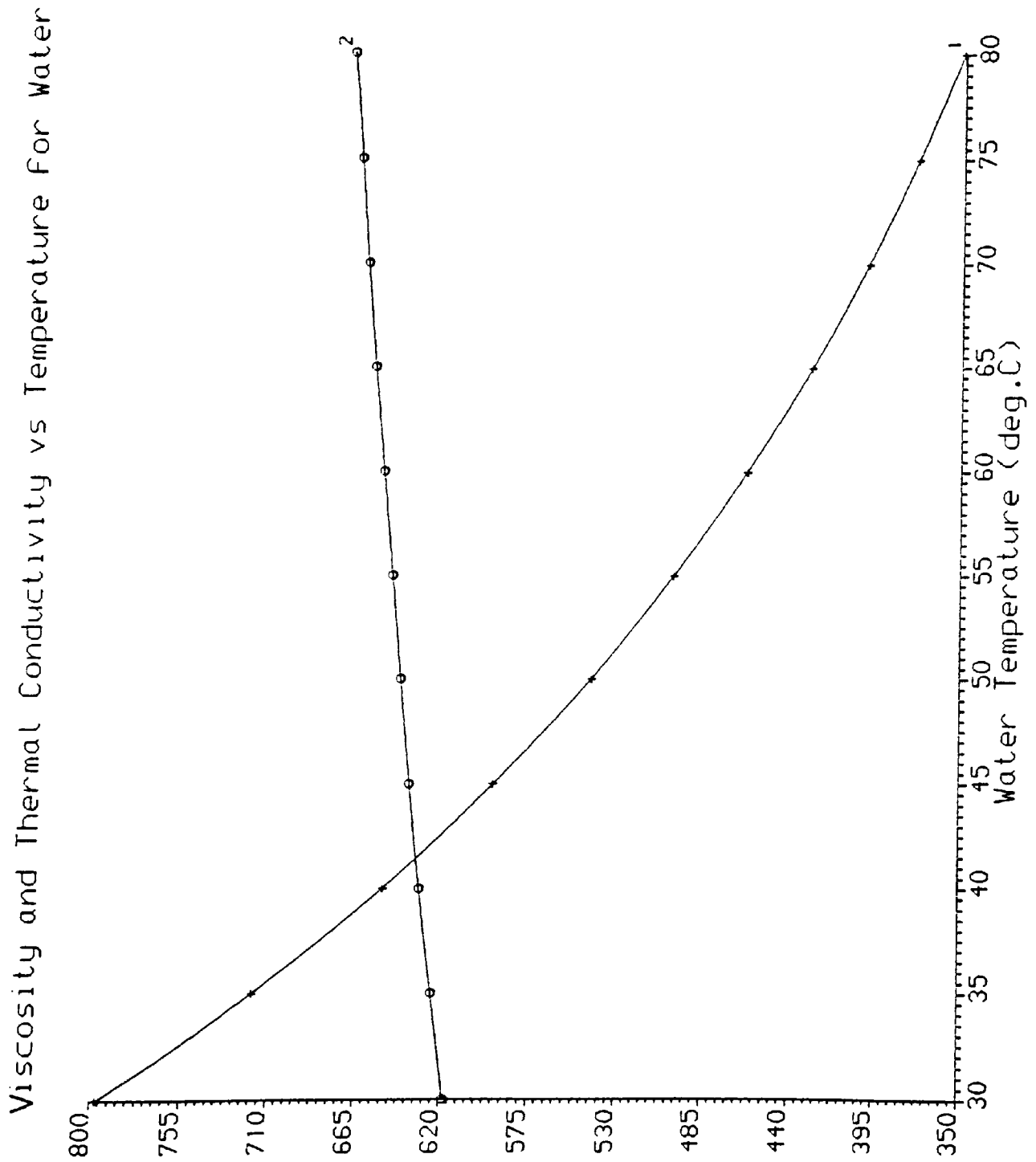

1.Viscosity(1/1000000 Kg/m s) 2.Thermal con.(1/1000 W/m K)

Appendix 10: Ploter Curve Fit Coefficients.

Fig.6.2

COEFFICIENTS OF THE BEST POLYNOMIAL FOR SET 1 (VISCOSITY)

(Y = A + B*X + C*X**2 + D*X**3 +...)

A = 1720.3111572266
B = -50.498462677002
C = 0.90706968307495
D = -0.10014014318585E-01
E = 0.60950915212743E-04
F = -0.15382987328394E-06

TABLE OF RESIDUALS

X	Y	Y(CALC)	DIFF	WEIGHT
30.00000	797.0000	796.9738	0.2626467E-01	1.000000
35.00000	718.0000	718.0594	-0.5946767E-01	1.000000
40.00000	651.0000	651.0693	-0.6936345E-01	1.000000
45.00000	594.0000	593.7203	0.2797001	1.000000
50.00000	544.0000	544.1818	-0.1818390	1.000000
55.00000	501.0000	501.0186	-0.1856869E-01	1.000000
60.00000	463.0000	463.1329	-0.1329051	1.000000
65.00000	430.0000	429.7064	0.2936167	1.000000
70.00000	400.0000	400.1428	-0.1427942	1.000000
75.00000	374.0000	374.0105	-0.1050055E-01	1.000000
80.00000	351.0000	350.9846	0.1541853E-01	1.000000

SUM OF ERRORS SQUARED = 0.24529256

REMEMBER THAT EXTRAPOLATION BEYOND THE DATA POINTS IS ALWAYS DANGEROUS, PARTICULARLY SO WITH HIGH ORDER POLYNOMIALS.

Fig.6.3

COEFFICIENTS OF THE BEST POLYNOMIAL FOR SET 2 (THERMAL CONDUCTIVITY)
(Y = A + B*X + C*X**2 + D*X**3 +...)

A = 1177.0633544922
B = -74.129554748535
C = 3.8318984508514
D = -0.10044516623020
E = 0.14375972095877E-02
F = -0.10697965080908E-04
G = 0.32418064677131E-07
H = 0.00000000000000E+00
I = 0.00000000000000E+00
J = 0.00000000000000E+00

TABLE OF RESIDUALS

X	Y	Y(CALC)	DIFF	WEIGHT
30.00000	618.0000	617.9917	0.8281708E-02	1.000000
35.00000	625.0000	625.0278	-0.2779734E-01	1.000000
40.00000	632.0000	631.9891	0.1090616E-01	1.000000
45.00000	638.0000	637.9249	0.7510373E-01	1.000000
50.00000	643.0000	643.0863	-0.8628467E-01	1.000000
55.00000	648.0000	648.0123	-0.1226410E-01	1.000000
60.00000	653.0000	652.9863	0.1365304E-01	1.000000
65.00000	658.0000	657.8515	0.1485221	1.000000
70.00000	662.0000	662.1947	-0.1947131	1.000000
75.00000	666.0000	665.8903	0.1097605	1.000000
80.00000	670.0000	670.0101	-0.1006699E-01	1.000000

SUM OF ERRORS SQUARED = 0.86503394E-01

REMEMBER THAT EXTRAPOLATION BEYOND THE DATA POINTS IS ALWAYS DANGEROUS, PARTICULARLY SO WITH HIGH ORDER POLYNOMIALS.

Appendix 11: 77VDMODEL Listing.

```
10 REM >77VDMODEL
20 REM VAPOUR DISENGAGEMENT AND SENSIBLE HEAT VERSION WIT
H TBP SETTING TO CORRECT AVERAGE
30 REM  ROc,ROd,D,Fc,Cpc,mINJECTEDd,Cpd
100 DATA 994,609.4,4.3E-3,10E-6,4.178E3,8.6E-4,2293
110 M=5000:REM MAX NO. OF INCREMENTS
120 PCOPY$="N":REM SET TO Y IF HARDCOPY OF FINAL RESULTS REQ
UIRED
130 TBPd=28.6:REM INITIAL AVERAGE VALUE OF B PT
140 *KEY1PROCPROFILE
150 FLAG5=0:REM FLAGS NEED TO REPEAT TO ESTABLISH TBPd
160 INPUT" Tc1",Tc1
170 INPUT"FULL PRINTOUT (Y/N)";diag$
180 PROCDIM_ARRAYS
190 REPEAT
200 PROCZERO_ARRAYS
210 S=.005:REM INCREMENT SIZE IN SECS
220 FLAG1=0:REM FLAGS FIRST ITERATION OF INITIAL RUN
230 FLAG4=0:REM FLAGS PROGRAM HAS CONVERGED TO A RESULT
240 A%=@%
250 @%=&90A:REM SETS PRINT FORMAT
260 NOIT=0
270 IF LEFT$(diag$,1)<>"Y" AND LEFT$(diag$,1)<>"y" THEN GOTO 300
280 PRINT"....."
290 PRINT NOIT
300 NOIT+=1
310 PROCREAD_DATA
320 PROCINITIALISE
330 OFF
340 PRINT
350 FOR N=0 TO M
360 IF LEFT$(diag$,1)="Y" OR LEFT$(diag$,1)="y" THEN GOTO 400
370 VDU3
380 PRINTTAB(10)"COMPUTING,ITERATION NO ";NOIT;" INCREMENT NO.
";N
390 VDU11
400 Tc(0)=Tc1-Dtc
410 IF Tc(0)<=TBPd THEN PRINT"TOTAL EVAPORATION NOT POSSIBLE,
Tc(0)=";Tc(0);" <=";TBPd:STOP
420 MUc=FNVISCOc(Tc(N))
430 kc=FNTHERMKc(Tc(N))
440 PROCFORCE_BAL
450 IF FLAG1=0 AND NOIT=1 THEN PROCCHECK_S
460 TDROPdO=TDROPd
470 IF TDROPd<TBPd THEN PROChCALC_SH ELSE PROChCALC_EV
480 IF TDROPd<TBPd THEN PROCDROP_TEMP ELSE PROCMASS_EVAP
```

```
490 mdropremd=mdropremd-MEVAPDROP
500 PROCQ_VALUES
510 PROCPRINTOUTI
520 PROCSET_ARRAYS
530 IF mdropremd<=0 THEN GOTO 560
540 PROCNEW_PARAMS
550 NEXT N
560 IF N=M+1 AND mdropremd>0 THEN PRINT"NO. OF ITERATIONS EXCE
EDS M (";M;")":STOP
570 IF FLAG1=0 THEN GOTO 590
580 PROCTEST_AC
590 IF FLAG1=0 THEN FLAG1=1
600 IF FLAG4=1 THEN PROCFINAL:GOTO 640
610 PROCSTORE_VAR
620 S=S/2
630 IF FLAG4=0 THEN GOTO 270
640 IF FLAG5=0 THEN PROCNEW_TBPd
650 UNTIL FLAG5=1
660 END
670 :
1000 DEFPROCFINAL
1010 PROCCALC_AVES
1020 PROCPRINTOUTF
1030 ENDPROC
1040 :
1050 DEFPROCSTORE_VAR
1060 COLHTOLD=COLHT
1070 ENDPROC
1080 :
1090 DEFPROCTEST_AC
1100 AC=ABS(COLHT-COLHTOLD)/COLHT
1110 IF AC>.003 THEN GOTO  1190
1120 DF1=Tc(1)-TDROPd(1)
1130 DF2=Tc(0)-TDROPd(0)
1140 lmtdINC01=(DF1-DF2)/LN(DF1/DF2)
1150 DtcINC01=Tc(0)-TDROPd(0)
1160 LMAC=ABS(lmtdINC01-DtcINC01)/lmtdINC01
1170 IF LMAC>.01 THEN GOTO  1190
1180 FLAG4=1:REM FLAGS ACCURRACIES OK
1190 ENDPROC
1200 :
1210 DEFPROCPRINTOUTF
1220 ON
1230 PRINT
1240 PRINT
1250 IF PCOPY$="Y"THEN VDU2
1260 PRINT"++++++++++++++++++++++++++++++++++++++++++++++++++++++
+"
```

```
1270 PRINT"uc=";uc,"mINJECTEDd=";mINJECTEDd,"TBPd=";TBPd
1280 PRINT"WATER FLOW,Fc=";Fc,"D INITIAL=";D(0)
1290 PRINT"----------------------------"
1300 PRINT"COLUMN HT=";CHINCtot;" m  at Tc1=";Tc1" <<<<<"
1310 PRINT"S=";S,,"N=";N,"NO.ITERATS=";NOIT
1320 PRINT"iterative accuracy,AC=";AC*100;" %"
1330 PRINT"lmtd accuracy,LMAC=";LMAC*100" %"
1340 PRINT"pinch delta T=";PINCHDT
1350 PRINT"cont phase delta T=";Tc1-Tc(0),"Tc(0)=";Tc(0)
1360 PRINT
1370 PRINT"MEAN VALUES:"
1380 PRINT"ud=";udA,"Pr=";PrA
1390 PRINT"mass of drop remaining=";mdropreA
1400 PRINT"Redc=";RedcA,"Rec=";RecA
1410 PRINT"h=";hA,"drop D=";DA
1420 PRINT"incremental col ht =";CHINCA
1430 PRINT"incremental heat transfered =";QINCA
1440 PRINT
1450 IF PCOPY$="Y"THEN VDU3
1460 ENDPROC
1470 :
1480 DEFPROCPRINTOUTI
1490 IF LEFT$(diag$,1)<>"Y" AND LEFT$(diag$,1)<>"y" THEN GOTO 1680
1500 IF FLAG2=1 THEN GOTO 1560
1510 PRINT"++++++++++++++++++++++++++++++++++"
1520 PRINT" Tc1=";Tc1,"mINJECTEDd=";mINJECTEDd
1530 PRINT"WATER FLOW,Fc=";Fc,"D INITIAL=";D
1540 PRINT"uc=";uc,"INITIAL DROP MASS=";mdropd
1550 PRINT"**************************"
1560 PRINT"S=";S,,"N=";N
1570 PRINT"ud=";ud,"Pr=";Pr
1580 PRINT"Redc=";Redc,"Rec=";Rec
1590 PRINT"h=";h,"D=";D
1600 PRINT"Tc(";N;")=";Tc(N),"C HT=";COLHT
1610 PRINT"-------------------------"
1620 PRINT"DROP TEMP=";TDROPd
1630 PRINT"MDROPREM=";mdropremd
1640 PRINT"QT";sumQINC,"QINC";QINC
1650 PRINT"**************************"
1660 PRINT
1670 FLAG2=1:REM FIRST PRINTOUT FLAG PER CYCLE
1680 ENDPROC
1690 :
1700 DEFPROCZERO_ARRAYS
1710 FOR Y% = 0 TO INT(sizeAR)
1720 mdropremd(Y%)=0
1730 TDROPd(Y%)=0
1740 ud(Y%)=0
```

```
1750 ud(Y%)=0
1760 Pr(Y%)=0
1770 Redc(Y%)=0
1780 Rec(Y%)=0
1790 h(Y%)=0
1800 D(Y%)=0
1810 CHINC(Y%)=0
1820 QINC(Y%)=0
1830 NEXT Y%
1840 ENDPROC
1850 :
1860 DEFPROCSET_ARRAYS
1870 mdropremd(N)=mdropremd
1880 TDROPd(N)=TDROPdO
1890 ud(N)=ud
1900 Pr(N)=Pr
1910 Redc(N)=Redc
1920 Rec(N)=Rec
1930 h(N)=h
1940 D(N)=D
1950 CHINC(N)=CHINC
1960 QINC(N)=QINC
1970 ENDPROC
1980 :
1990 DEFPROCZERO_TOTS
2000 CHINCtot=0
2010 Dtot=0
2020 htot=0
2030 Rectot=0
2040 Redctot=0
2050 Prtot=0
2060 udtot=0
2070 mdropretot=0
2080 QINCtot=0
2090 ENDPROC
2100 :
2110 DEFPROCCALC_AVES
2120 J=N-1
2130 FOR K=0 TO J
2140 CHINCtot=CHINCtot+CHINC(K)
2150 Dtot=Dtot+D(K)
2160 htot=htot+h(K)
2170 Rectot=Rectot+Rec(K)
2180 Redctot=Redctot+Redc(K)
2190 Prtot=Prtot+Pr(K)
2200 udtot=udtot+ud(K)
2210 mdropretot=mdropretot+mdropremd(K)
2220 QINCtot=QINCtot+QINC(K)
```

```
2230 IF FLAG3=1 THEN GOTO 2250
2240 IF TDROPd(K)>=TBPd THEN PINCHDT=Tc(K)-TBPd :FLAG3=1
2250 NEXT K
2260 QINCA=QINCtot/N
2270 mdropreA=mdropretot/N
2280 udA=udtot/N
2290 PrA=Prtot/N
2300 RedcA=Redctot/N
2310 RecA=Rectot/N
2320 hA=htot/N
2330 DA=Dtot/N
2340 CHINCA=CHINCtot/N
2350 ENDPROC
2360 :
2370 DEFPROCDIM_ARRAYS
2380 sizeAR=M+1
2390 DIMTc(sizeAR)
2400 DIMCHINC(sizeAR)
2410 DIMmdropremd(sizeAR)
2420 DIMud(sizeAR)
2430 DIMPr(sizeAR)
2440 DIMRedc(sizeAR)
2450 DIMRec(sizeAR)
2460 DIMh(sizeAR)
2470 DIMD(sizeAR)
2480 DIMQINC(sizeAR)
2490 DIMTDROPd(sizeAR)
2500 ENDPROC
2510 :
2520 DEFPROCQ_VALUES
2530 QINC=QDROPcd*NDROPPSd*S
2540 sumQINC=QINC+sumQINC
2550 ENDPROC
2560 :
2570 DEFPROCREAD_DATA
2580 RESTORE
2590 READ ROc,ROd,D,Fc,Cpc,mINJECTEDd,Cpd
2600 ENDPROC
2610 :
2620 DEFPROCFORCE_BAL
2630 R=(ROc-ROd)*D*9.807*2/3
2640 REM ASSUME 500<=Re<=10000
2650 ud=SQR(R/(ROc*.22))
2660 ReFACT=D*ROc/MUc
2670 Redc=ud*ReFACT
2680 IF Redc >1E4 THEN PRINT"Redc=";Redc;" outside limit!":STOP
2690 IF Redc >=500 THEN GOTO 2770
2700 REM ASSUME 0.2<=Re<500
```

```
2710 ud=(ReFACT^.6*R/9/ROc)^(1/1.4)
2720 Redc=ud*ReFACT
2730 IF Redc >=.2 THEN GOTO 2770
2740 REM ASSUME Re<0.2
2750 ud=R*D/12/MUc
2760 Redc=ud*ReFACT
2770 Redc=Redc*(ud+uc)/ud :REM ReFOR ROWE-NET VELOCITY
2780 Rec=.094*uc*ROc/MUc
2790 ENDPROC
2800 :
2810 DEFPROCFALLING_V
2820 CSATUBE=PI*4.7E-2^2
2830 uc=Fc/CSATUBE
2840 ENDPROC
2850 :
2860 DEFPROChCALC_EV
2870 Pr=Cpc*MUc/kc
2880 Nu=2+.79*Pr^(1/3)*Redc^.5
2890 h=Nu*kc/D
2900 ENDPROC
2910 :
2920 DEFPROChCALC_SH
2930 Pr=Cpc*MUc/kc
2940 Nu=2+.79*Pr^(1/3)*Redc^.5
2950 h=Nu*kc/D
2960 ENDPROC
2970 :
2980 DEFPROCO_HEAT_BAL
2990 LATHTd=.3347E6
3000 Qoverall=mINJECTEDd*(LATHTd+Cpd*(TBPd-18))
3010 mINJECTEDc=Fc*ROc
3020 Dtc=Qoverall/Cpc/mINJECTEDc
3030 ENDPROC
3040 :
3050 DEFPROCMASS_EVAP
3060 ASURFd=PI*D^2
3070 DT=Tc(N)-TBPd
3080 QDROPcd=h*ASURFd*DT
3090 MEVAP=QDROPcd/LATHTd
3100 MEVAPDROP=MEVAP*S
3110 ENDPROC
3120 :
3130 DEFPROCDROP_TEMP
3140 ASURFd=PI*D^2
3150 MEVAPDROP=0
3160 DT=Tc(N)-TDROPd
3170 QDROPcd=h*ASURFd*DT
3180 TGAINd=S*QDROPcd/mdropd/Cpd
```

```
3190 TDROPd=TDROPd+TGAINd
3200 IF TDROPd>TBPd THEN TDROPd=TBPd
3210 ENDPROC
3220 :
3230 DEFPROCINITIALISE
3240 COLHT=0
3250 PINCHDT=0
3260 FLAG2=0
3270 FLAG3=0
3280 TDROPd=18
3290 sumQINC=0
3300 QINC=0
3310 CHINC=0
3320 PROCFALLING_V
3330 mdropd=4*PI*ROd*(D/2)^3/3
3340 mdropremd=mdropd
3350 NDROPPSd=mINJECTEDd/mdropd
3360 PROCO_HEAT_BAL
3370 ENDPROC
3380 :
3390 DEFFNVISCOc(T)
3400 =(1720.31-50.4985*T+.907070*T^2-.0100140*T^3+.609509E-4*T^4-.153
83E-6*T^5)*1E-6
3410 :
3420 DEFFNTHERMKc(T)
3430 =(1177.06-74.1296*T+3.8319*T^2-.100445*T^3+.0014376*T^4-.10698E-
4*T^5+.324181E-7*T^6)*1E-3
3440 :
3450 DEFPROCNEW_PARAMS
3460 D=(6*mdropremd/(PI*ROd))^(1/3)
3470 Tc(N+1)=Tc(N)+(QINC/(Cpc*ROc*uc*CSATUBE))
3480 CHINC=S*(ud-uc)
3490 IF uc>ud THEN CHINC=0
3500 COLHT=COLHT+CHINC
3510 ENDPROC
3520 :
3530 DEFPROCCHECK_S
3540 Smax=1/ud
3550 IF S>Smax THEN PRINT"RESET S TO A VALUE LOWER THAN Smax,
S=";S,"Smax=";Smax:STOP
3560 ENDPROC
3570 :
3580 DEFPROCPROFILE
3590 A%=@%
3600 @%=&10409
3610 diag2$="N":REM SET TO Y FOR CHINC PRINTOUT
3620 IF diag2$="Y" THEN PRINT"   N","   Tc","    D"," TDROPd","    h","
QINC","mdroprem","  CHINC":GOTO 3640
```

```
3630 PRINT"  N","  Tc","   D"," TDROPd","   h","  QINC","mdroprem","  CHRT
"
3640 FOR X%=0 TO N+1
3650 @%=&10409
3660 REM IF X%>3222 THEN VDU2
3670 IF diag2$="Y" THEN PRINTX%;Tc(X%);D(X%);TDROPd(X%);h(X%);QIN
C(X%);mdropremd(X%);" ";CHINC(X%):GOTO 3680
3680 CHRT=CHRT+CHINC(X%)
3690 PRINTX%;Tc(X%);D(X%);TDROPd(X%);h(X%);QINC(X%);mdropremd(
X%);" ";CHRT
3700 @%=A%
3710 NEXT X%
3720 @%=&10409
3730 IF diag2$="Y" THEN PRINT"  N","  Tc","   D"," TDROPd","   h","
QINC","mdroprem","  CHINC":GOTO 3750
3740 PRINT"  N","  Tc","   D"," TDROPd","   h","  QINC","mdroprem","  CHRT
"
3750 @%=A%
3760 REM IF X%>3222 THEN VDU3
3770 ENDPROC
3780 :
3790 DEFPROCPROFSECT
3800 VDU2
3810 @%=&90A
3820 PRINT"  N  ","  Tc  ","   D  ","  QINC  ","TDROPd ","  mdroprem","  CHI
NC"
3830 FOR X%=N-2 TO N+2
3840 PRINTX%;Tc(X%);D(X%);QINC(X%);TDROPd(X%);mdropremd(X%);"
";CHINC(X%)
3850 NEXT
3860 VDU3
3870 ENDPROC
3880 :
3890 DEFPROCNEW_TBPd
3900 *K.2PROCNEW_TBPd|MP.TBPd
3910 TBPdO=TBPd
3920 HSP=ROc*9.81*CHINCtot
3930 interp=27.88+HSP*2.79/10133
3940 TBPd=(27.88+interp)/2
3950 IF ABS(TBPd-TBPdO)<=.05 THEN FLAG5=1
3960 IF PCOPY$="Y"THEN VDU2
3970IF FLAG5=0 THEN PRINT:PRINT"NOW ITERATING FOR CORRECT M
EAN B PT":PRINT
3980 IF PCOPY$="Y"THEN VDU3
3990 TBPd=FNROUNDDP(TBPd,2)
4000 PROCZERO_TOTS
4010 ENDPROC
4020 :
```

```
4030 DEFFNROUNDDP(X,Y)
4040 =(INT(X*(10^Y)+.5))/(10^Y)
4050 :
```

Appendix 12: 77VDMODEL Typical Output.

```
++++++++++++++++++++++++++++++++++++++++++++++++++++++++++++
uc=1.44096825E-3     mINJECTEDd=8.6E-4    TBPd=28.6
WATER FLOW,Fc=1E-5  D INITIAL=4.3E-3
-----------------------------
COLUMN HT=0.699561287 m  at Tc1=42 <<<<<
S=2.5E-3  N=1792     NO.ITERATS=2
iterative accuracy,AC=0.0464767131 %
lmtd accuracy,LMAC=0.883602052 %
pinch delta T=6.47295784
cont phase delta T=7.43438584 Tc(0)=34.5656142

MEAN VALUES:
ud=0.157592637       Pr=4.36665149
mass of drop remaining=9.44069336E-6
Redc=725.719483      Rec=204.574125
h=8825.45776         drop D=2.63425959E-3
incremental col ht =3.90380183E-4
incremental heat transfered =0.172383656


NOW ITERATING FOR CORRECT MEAN B PT

++++++++++++++++++++++++++++++++++++++++++++++++++++++++++++
uc=1.44096825E-3     mINJECTEDd=8.6E-4    TBPd=28.82
WATER FLOW,Fc=1E-5  D INITIAL=4.3E-3
-----------------------------
COLUMN HT=0.71614182 m  at Tc1=42 <<<<<
S=2.5E-3  N=1832     NO.ITERATS=2
iterative accuracy,AC=0.0469141143 %
lmtd accuracy,LMAC=0.883556821 %
pinch delta T=6.25322334
cont phase delta T=7.44483232 Tc(0)=34.5551677

MEAN VALUES:
ud=0.15780301        Pr=4.36777967
mass of drop remaining=9.48446091E-6
Redc=727.677241      Rec=204.528284
h=8829.55007         drop D=2.63942414E-3
incremental col ht =3.90907107E-4
incremental heat transfered =0.168862702
```

Appendix 13: 115VAMODEL Listing.

```
10 REM >115VAMODEL
20 REM SENSIBLE HEAT VERSION WITH TBP SETTING TO CORRECT
AVERAGE AND VAPOUR  ATTACHMENT
30 REM  ROc,ROdl,D,Fc,Cpc,mINJECTEDd,Cpd,ROdv,tf
100 DATA 994,609.4,4.3E-3,10E-6,4.178E3,8.6E-4,2293,3.2,6E-10
110 M=5000:REM MAX NO. OF INCREMENTS
120 PCOPY$="N":REM SET TO Y IF HARDCOPY OF FINAL RESULTS
REQUIRED
130 TBPd=28.6:REM INITIAL AVERAGE VALUE OF B PT
140 PROCF_KEYS
150 A%=@%
160 FLAG5=0:REM FLAGS NEED TO REPEAT TO ESTABLISH TBPd
170 INPUT" Tc1",Tc1
180 INPUT"FULL PRINTOUT (Y/N)";diag$
190 TIME=0
200 PROCDIM_ARRAYS
210 REPEAT:REM START OF TBPd ITERATIVE LOOP
220 PROCZERO_ARRAYS
230 S=.00125:REM INCREMENT SIZE IN SECS
240 FLAG1=0:REM FLAGS FIRST ITERATION OF INITIAL RUN
250 FLAG4=0:REM FLAGS PROGRAM HAS CONVERGED TO A RESULT
260 @%=&90A:REM SETS PRINT FORMAT
270 NOIT=0
280 REPEAT:REM START OF ACCURACY ITERATIVE LOOP
290 IF LEFT$(diag$,1)="Y" OR LEFT$(diag$,1)="y" THEN PROCPRINT_LINE
300 NOIT+=1
310 PROCREAD_DATA
320 PROCINITIALISE
330 OFF
340 PRINT
350 FOR N=0 TO M:REM START OF STAGEWISE CALCS LOOP
360 IF LEFT$(diag$,1)<>"Y" AND LEFT$(diag$,1)<>"y" THEN
PROCPRINT_INC
370 Tc(0)=Tc1-Dtc
380 IF Tc(0)<=TBPd THEN PRINT"TOTAL EVAPORATION NOT POSSIBLE,
Tc(0)=";Tc(0);" <=";TBPd:STOP
390 MUc=FNVISCOc(Tc(N))
400 kc=FNTHERMKc(Tc(N))
410 PROCFORCE_BAL
420 IF FLAG1=0 AND NOIT=1 THEN PROCCHECK_S
430 TDROPdO=TDROPd
440 IF TDROPd<TBPd THEN PROChCALC_SH ELSE PROChCALC_EV
450 IF TDROPd<TBPd THEN PROCDROP_TEMP ELSE PROCMASS_EVAP
460 mdropremdO=mdropremd
470 mdropremd=mdropremd-MEVAPDROP
480 PROCQ_VALUES
490 IF LEFT$(diag$,1)="Y" OR LEFT$(diag$,1)="y" THEN PROCPRINTOUTI
```

```
500 PROCSET_ARRAYS
510 IF mdropremd<=0 THEN GOTO 540
520 PROCNEW_PARAMS
530 NEXT N:REM END OF STAGEWISE CALCS LOOP
540 IF N=M+1 AND mdropremd>0 THEN PRINT"NO. OF ITERATIONS
EXCEEDS M (";M;")":STOP
550 IF FLAG1=0 THEN GOTO 570
560 PROCTEST_AC
570 IF FLAG1=0 THEN FLAG1=1
580 IF FLAG4=1 THEN PROCFINAL:GOTO 610
590 PROCSTORE_VAR
600 S=S/2
610 UNTIL FLAG4<>0:REM END OF ACCURACY ITERATIVE LOOP
620 IF FLAG5=0 THEN PROCNEW_TBPd
630 UNTIL FLAG5=1:REM END OF TBPd ITERATIVE LOOP
640 VDU7
650 PRINT"RUNTIME=";TIME/100;" SECS"
660 END
670 :
1000 DEFFNVISCOc(T)
1010 =(1720.31-50.4985*T+.907070*T^2-.0100140*T^3+.609509E-4*T^4-.1538
3E-6 *T^5)*1E-6
1020 :
1030  DEFFNTHERMKc(T)
1040 =(1177.06-74.1296*T+3.8319*T^2-.100445*T^3+.0014376*T^4-.10698E-4
*T^5+.324181E-7*T^6)*1E-3
1050 :
1060 DEFFNROUNDDP(X,Y)
1070 =(INT(X*(10^Y)+.5))/(10^Y)
1080 :
1090 DEFPROCPRINT_INC
1100 PRINTTAB(10)"COMPUTING,ITERATION NO ";NOIT;" INCREMENT
NO. ";N
1110 VDU11
1120 ENDPROC
1130 :
1140 DEFPROCFINAL
1150 PROCCALC_AVES
1160 PROCPRINTOUTF
1170 ENDPROC
1180 :
1190 DEFPROCSTORE_VAR
1200 COLHTOLD=COLHT
1210 ENDPROC
1220 :
1230 DEFPROCTEST_AC
1240 AC=ABS(COLHT-COLHTOLD)/COLHT
1250 IF AC>.003 THEN GOTO  1330
```

```
1260 DF1=Tc(1)-TDROPd(1)
1270 DF2=Tc(0)-TDROPd(0)
1280 lmtdINC01=(DF1-DF2)/LN(DF1/DF2)
1290 DtcINC01=Tc(0)-TDROPd(0)
1300 LMAC=ABS(lmtdINC01-DtcINC01)/lmtdINC01
1310 IF LMAC>.01 THEN GOTO  1330
1320 FLAG4=1:REM FLAGS ACCURRACIES OK
1330 ENDPROC
1340 :
1350 DEFPROCPRINTOUTF
1360 ON
1370 PRINT
1380 PRINT
1390 IF PCOPY$="Y"THEN VDU2
1400 PRINT"++++++++++++++++++++++++++++++++++++++++++++++++++++++++++
+++"
1410 PRINT"uc=";uc,"mINJECTEDd=";mINJECTEDd,"TBPd=";TBPd
1420 PRINT"WATER FLOW,Fc=";Fc,"D INITIAL=";D(0)
1430 PRINT"----------------------------"
1440 PRINT"COLUMN HT=";CHINCtot;" m  at Tc1=";Tc1" <<<<<"
1450 PRINT"S=";S,,"N=";N,"NO.ITERATS=";NOIT
1460 PRINT"iterative accuracy,AC=";AC*100;" %"
1470 PRINT"lmtd accuracy,LMAC=";LMAC*100" %"
1480 PRINT"pinch delta T=";PINCHDT
1490 PRINT"cont phase delta T=";Tc1-Tc(0),"Tc(0)=";Tc(0)
1500 PRINT
1510 PRINT"MEAN VALUES:"
1520 PRINT"ud=";udA,"Pr=";PrA
1530 PRINT"mass of drop remaining=";mdropreA
1540 PRINT"Redc=";RedcA,"Rec=";RecA
1550 PRINT"h=";hA,"drop D=";DA
1560 PRINT"incremental col ht =";CHINCA
1570 PRINT"incremental heat transfered =";QINCA
1580 PRINT
1590 IF PCOPY$="Y"THEN VDU3
1600 ENDPROC
1610 :
1620 DEFPROCPRINTOUTI
1630 IF LEFT$(diag$,1)<>"Y" AND LEFT$(diag$,1)<>"y" THEN GOTO 1830
1640 IF FLAG2=1 THEN GOTO 1700
1650 PRINT"++++++++++++++++++++++++++++++++"
1660 PRINT" Tc1=";Tc1,"mINJECTEDd=";mINJECTEDd
1670 PRINT"WATER FLOW,Fc=";Fc,"D INITIAL=";D
1680 PRINT"uc=";uc,"INITIAL DROP MASS=";mdropd
1690 PRINT"**************************"
1700 PRINT"S=";S,,"N=";N
1710 PRINT"ud=";ud,"Pr=";Pr
1720 PRINT"Redc=";Redc,"Rec=";Rec
```

```
1730 PRINT"h=";h,"D=";D
1740 PRINT"ASURFd=";ASURFd,"HTAREAd=";HTAREAd
1750 PRINT"Tc(";N;")=";Tc(N),"C HT=";COLHT
1760 PRINT"-------------------------"
1770 PRINT"DROP TEMP=";TDROPdO
1780 PRINT"MDROPREM=";mdropremdO
1790 PRINT"QT";sumQINC,"QINC";QINC
1800 PRINT"**************************"
1810 PRINT
1820 FLAG2=1:REM FIRST PRINTOUT FLAG PER CYCLE
1830 ENDPROC
1840 :
1850 DEFPROCZERO_ARRAYS
1860 FOR Y% = 0 TO INT(sizeAR)
1870 mdropremd(Y%)=0
1880 TDROPd(Y%)=0
1890 ud(Y%)=0
1900 Tc(Y%)=0
1910 Pr(Y%)=0
1920 Redc(Y%)=0
1930 Rec(Y%)=0
1940 h(Y%)=0
1950 D(Y%)=0
1960 CHINC(Y%)=0
1970 QINC(Y%)=0
1980 ASURFd(Y%)=0
1990 HTAREAd(Y%)=0
2000 NEXT Y%
2010 ENDPROC
2020 :
2030 DEFPROCSET_ARRAYS
2040 HTAREAd(N)=HTAREAd
2050 ASURFd(N)=ASURFd
2060 mdropremd(N)=mdropremdO
2070 TDROPd(N)=TDROPdO
2080 ud(N)=ud
2090 Pr(N)=Pr
2100 Redc(N)=Redc
2110 Rec(N)=Rec
2120 h(N)=h
2130 D(N)=D
2140 CHINC(N)=CHINC
2150 QINC(N)=QINC
2160 ENDPROC
2170 :
2180 DEFPROCZERO_TOTS
2190 CHINCtot=0
2200 Dtot=0
```

```
2210  htot=0
2220 Rectot=0
2230 Redctot=0
2240 Prtot=0
2250 udtot=0
2260 mdropretot=0
2270 QINCtot=0
2280 ENDPROC
2290 :
2300 DEFPROCCALC_AVES
2310 J=N-1
2320 FOR K=0 TO J
2330 CHINCtot=CHINCtot+CHINC(K)
2340 Dtot=Dtot+D(K)
2350 htot=htot+h(K)
2360 Rectot=Rectot+Rec(K)
2370 Redctot=Redctot+Redc(K)
2380 Prtot=Prtot+Pr(K)
2390 udtot=udtot+ud(K)
2400 mdropretot=mdropretot+mdropremd(K)
2410 QINCtot=QINCtot+QINC(K)
2420 IF FLAG3=1 THEN GOTO 2440
2430 IF TDROPd(K)>=TBPd THEN PINCHDT=Tc(K)-TBPd :FLAG3=1
2440 NEXT K
2450 QINCA=QINCtot/N
2460 mdropreA=mdropretot/N
2470 udA=udtot/N
2480 PrA=Prtot/N
2490 RedcA=Redctot/N
2500 RecA=Rectot/N
2510 hA=htot/N
2520 DA=Dtot/N
2530 CHINCA=CHINCtot/N
2540 ENDPROC
2550 :
2560 DEFPROCF_KEYS
2570 *KEY1PROCPROFILE
2580 *KEY3PROCCOND_PRO
2590 ENDPROC
2600 :
2610 DEFPROCPRINT_LINE
2620 PRINT"....."
2630 PRINT NOIT+1
2640 ENDPROC
2650 :
2660 DEFPROCDIM_ARRAYS
2670 sizeAR=M+1
2680 DIMTc(sizeAR)
```

```
2690 DIMCHINC(sizeAR)
2700 DIMmdropremd(sizeAR)
2710 DIMud(sizeAR)
2720 DIMPr(sizeAR)
2730 DIMRedc(sizeAR)
2740 DIMRec(sizeAR)
2750 DIMh(sizeAR)
2760 DIMD(sizeAR)
2770 DIMQINC(sizeAR)
2780 DIMTDROPd(sizeAR)
2790 DIMASURFd(sizeAR)
2800 DIMHTAREAd(sizeAR)
2810 ENDPROC
2820 :
2830 DEFPROCQ_VALUES
2840 QINC=QDROPcd*NDROPPSd*S
2850 sumQINC=QINC+sumQINC
2860 ENDPROC
2870 :
2880 DEFPROCREAD_DATA
2890 RESTORE
2900 READ ROc,ROdl,D,Fc,Cpc,mINJECTEDd,Cpd,ROdv,tf
2910 ENDPROC
2920 :
2930 DEFPROCFORCE_BAL
2940 R=(ROc-ROd)*D*9.807*2/3
2950 REM ASSUME Re>10000
2960 ud=SQR(R/(ROc*.05))
2970 ReFACT=D*ROc/MUc
2980 Redc=ud*ReFACT
2990 IF Redc >1E4 THEN GOTO 3110
3000 REM ASSUME 500<=Re<=10000
3010 ud=SQR(R/(ROc*.22))
3020 Redc=ud*ReFACT
3030 IF Redc >=500 THEN GOTO 3110
3040 REM ASSUME 0.2<=Re<500
3050 ud=(ReFACT^.6*R/9/ROc)^(1/1.4)
3060 Redc=ud*ReFACT
3070 IF Redc >=.2 THEN GOTO 3110
3080 REM ASSUME Re<0.2
3090 ud=R*D/12/MUc
3100 Redc=ud*ReFACT
3110 Redc=Redc*(ud+uc)/ud :REM ReFOR ROWE-NET VELOCITY
3120 Rec=.094*uc*ROc/MUc
3130 ENDPROC
3140 :
3150 DEFPROCFALLING_V
3160 CSATUBE=PI*4.7E-2^2
```

```
3170 uc=Fc/CSATUBE
3180 ENDPROC
3190 :
3200 DEFPROChCALC_EV
3210 Pr=Cpc*MUc/kc
3220 Nu=2+.79*Pr^(1/3)*Redc^.5
3230 h=Nu*kc/D
3240 ENDPROC
3250 :
3260 DEFPROChCALC_SH
3270 Pr=Cpc*MUc/kc
3280 Nu=2+.79*Pr^(1/3)*Redc^.5
3290 h=Nu*kc/D
3300 ENDPROC
3310 :
3320 DEFPROCO_HEAT_BAL
3330 LATHTd=.3347E6
3340 Qoverall=mINJECTEDd*(LATHTd+Cpd*(TBPd-18))
3350 mINJECTEDc=Fc*ROc
3360 Dtc=Qoverall/Cpc/mINJECTEDc
3370 ENDPROC
3380 :
3390 DEFPROCMASS_EVAP
3400 ASURFd=PI*D^2
3410 DT=Tc(N)-TBPd
3420 MEVAP=QDROPcd/LATHTd
3430 MEVAPDROP=MEVAP*S
3440 MASSliqd=MASSliqd-MEVAPDROP
3450 MASSvapd=MASSvapd+MEVAPDROP
3460 VOLvapd=MASSvapd/ROdv
3470 VOLliqd=MASSliqd/ROdl
3480 VOLlv=VOLvapd+VOLliqd
3490 ROdlv=mdropd/VOLlv
3500 Dlv=2*(VOLlv*.75/PI)^(1/3)
3510 IF FLAG7=0 THEN FLAG7=1:GOTO 3530
3520 IF (VOLliqd/tf) < (ASURFd/4) THEN HTAREAd=(VOLliqd/tf) ELSE
HTAREAd=(ASURFd/4)
3530 QDROPcd=h*HTAREAd*DT
3540 ROd=ROdlv
3550 ENDPROC
3560 :
3570 DEFPROCDROP_TEMP
3580 ASURFd=PI*D^2
3590 HTAREAd=ASURFd
3600 MEVAPDROP=0
3610 DT=Tc(N)-TDROPd
3620 QDROPcd=h*HTAREAd*DT
3630 TGAINd=S*QDROPcd/mdropd/Cpd
```

```
3640 TDROPd=TDROPd+TGAINd
3650 IF TDROPd>TBPd THEN TDROPd=TBPd
3660 ENDPROC
3670 :
3680 DEFPROCINITIALISE
3690 Dlv=D
3700 VOLvapd=0
3710 VOLliqd=0
3720 MASSvapd=0
3730 VOLlv=0
3740 ROd=ROdl
3750 COLHT=0
3760 PINCHDT=0
3770 sumQINC=0
3780 QINC=0
3790 CHINC=0
3800 TDROPd=18
3810 FLAG2=0:REM FIRST PRINTOUT FLAG PER CYCLE
3820 FLAG3=0:REM FLAGS PINCH DT HAS BEEN CALCULATED
3830 FLAG6=0:REM PRINTOUT FLAG FOR TBPd ITERATION
3840 FLAG7=0:REM FLAGS TIME FOR HTAREA TO BE MODIFIED
3850 mdropd=4*PI*ROdl*(D/2)^3/3
3860 MASSliqd=mdropd
3870 mdropremd=mdropd
3880 mdropremdO=0
3890 NDROPPSd=mINJECTEDd/mdropd
3900 PROCFALLING_V
3910 PROCO_HEAT_BAL
3920 ENDPROC
3930 :
3940 DEFPROCNEW_PARAMS
3950 D=Dlv
3960 Tc(N+1)=Tc(N)+(QINC/(Cpc*ROc*uc*CSATUBE))
3970 CHINC=S*(ud-uc)
3980 IF uc>ud THEN CHINC=0
3990 COLHT=COLHT+CHINC
4000 ENDPROC
4010 :
4020 DEFPROCCHECK_S
4030 Smax=1/ud
4040 IF S>Smax THEN PRINT"RESET S TO A VALUE LOWER THAN Smax,
S=";S,"Smax=";Smax:STOP
4050 ENDPROC
4060 :
4070 DEFPROCPROFILE
4080 A%=@%
4090 @%=&10409
4100 diag2$="N":REM SET TO Y FOR CHINC PRINTOUT
```

```
4110 IF diag2$="Y" THEN PRINT"  N","  Tc","  D"," TDROPd","
h","mdroprem","  CHINC":GOTO 4130
4120 PRINT"  N","  Tc","  D"," TDROPd","  h","mdroprem","  CHRT"
4130 FOR X%=0 TO N+1
4140 @%=&10409
4150 IF diag2$="Y" THEN
PRINTX%,Tc(X%),D(X%),TDROPd(X%),h(X%),mdropremd(X%),CHINC(X%):
GOTO 4160
4160 CHRT=CHRT+CHINC(X%)
4170 PRINTX%,Tc(X%),D(X%),TDROPd(X%),h(X%),mdropremd(X%),"
";CHRT
4180 @%=A%
4190 NEXT X%
4200 @%=&10409
4210 IF diag2$="Y" THEN PRINT"  N","  Tc","  D"," TDROPd","
h","mdroprem","  CHINC":GOTO 4230
4220 PRINT"  N","  Tc","  D"," TDROPd","  h","mdroprem","  CHRT"
4230 @%=A%
4240 ENDPROC
4250 :
4260 DEFPROCCOND_PRO
4270 VDU2
4280 VDU1,15
4290 CHRT=0
4300 @%=&1040A
4310 PRINT"  N","  Tc","  D"," TDROPd","  h","mdroprem","  CHRT","  ud","
ASURFd","HTAREAd"," Redc","  QINC"
4320 FOR X%=0 TO N+1
4330 @%=&1040A
4340 CHRT=CHRT+CHINC(X%)
4350 PRINTX%,Tc(X%),D(X%),TDROPd(X%),h(X%),mdropremd(X%),CHRT;
ud(X%),ASURFd(X%),HTAREAd(X%),Redc(X%),QINC(X%)
4360 @%=A%
4370 NEXT X%
4380 @%=&1040A
4390 PRINT"  N","  Tc","  D"," TDROPd","  h","mdroprem","  CHRT","  ud","
ASURFd","HTAREAd"," Redc","  QINC"
4400 @%=A%
4410 VDU1,18
4420 VDU3
4430 ENDPROC
4440 :
4450 DEFPROCNEW_TBPd
4460 TBPdO=TBPd
4470 HSP=ROc*9.81*CHINCtot
4480 interp=27.88+HSP*2.79/10133
4490 TBPd=(27.88+interp)/2
4500 IF ABS(TBPd-TBPdO)<.05 THEN FLAG5=1
```

```
4510 IF ABS(TBPd-TBPdO)>.5 THEN TBPd=TBPd+(TBPd-TBPdO)*.5:REM
ACCELERATOR
4520 IF PCOPY$="Y"THEN VDU2:FLAG6=1
4530 IF FLAG5=0 THEN PRINT:PRINT"ITERATING FOR CORRECT MEAN B
PT":PRINT
4540 IF FLAG6=1 THEN VDU3:FLAG6=0
4550 TBPd=FNROUNDDP(TBPd,2)
4560 PROCZERO_TOTS
4570 ENDPROC
4580 :
```

Appendix 14: 115VAMODEL Typical Output.

```
++++++++++++++++++++++++++++++++++++++++++++++++++++++++++++
uc=1.44096825E-3     mINJECTEDd=8.6E-4    TBPd=28.6
WATER FLOW,Fc=1E-5   D INITIAL=4.3E-3
----------------------------
COLUMN HT=0.700557892 m   at Tc1=42 <<<<<
S=6.25E-4 N=1152     NO.ITERATS=2
iterative accuracy,AC=0.136339253 %
lmtd accuracy,LMAC=0.218963379 %
pinch delta T=6.46954372
cont phase delta T=7.43438584 Tc(0)=34.5656142

MEAN VALUES:
ud=0.975993664       Pr=4.65736597
mass of drop remaining=2.03521822E-5
Redc=21648.1396      Rec=192.900573
h=8887.31911         drop D=0.0115958048
incremental col ht =6.0812317E-4
incremental heat transfered =0.268223055


ITERATING FOR CORRECT MEAN B PT

++++++++++++++++++++++++++++++++++++++++++++++++++++++++++++
uc=1.44096825E-3     mINJECTEDd=8.6E-4    TBPd=28.82
WATER FLOW,Fc=1E-5   D INITIAL=4.3E-3
----------------------------
COLUMN HT=0.719899638 m   at Tc1=42 <<<<<
S=6.25E-4 N=1187     NO.ITERATS=2
iterative accuracy,AC=0.174139565 %
lmtd accuracy,LMAC=0.218949836 %
pinch delta T=6.2498574
cont phase delta T=7.44483232 Tc(0)=34.5551677

MEAN VALUES:
ud=0.973329452       Pr=4.65837559
mass of drop remaining=2.03866635E-5
Redc=21540.5394      Rec=192.861727
h=8886.64258         drop D=0.0115605503
incremental col ht =6.06486637E-4
incremental heat transfered =0.26076467
```

Appendix 15: 115VAMODEL Example Page Of Profile Output.

N	Tc	D	TDROPd	h	mdroprem	CHRT	ud	ASURFd	HTAREAd	Redc	QINC
0000E0	3.456E1	4.300E-3	1.800E1	7.345E3	2.537E-5	0000E0	2.224E-1	5.809E-5	5.809E-5	1.320E3	1.496E-1
1.000E0	3.456E1	4.300E-3	1.808E1	7.345E3	2.537E-5	1.381E-4	2.224E-1	5.809E-5	5.809E-5	1.320E3	1.490E-1
2.000E0	3.456E1	4.300E-3	1.815E1	7.345E3	2.537E-5	2.761E-4	2.224E-1	5.809E-5	5.809E-5	1.320E3	1.484E-1
3.000E0	3.457E1	4.300E-3	1.823E1	7.345E3	2.537E-5	4.142E-4	2.224E-1	5.809E-5	5.809E-5	1.321E3	1.477E-1
4.000E0	3.457E1	4.300E-3	1.830E1	7.345E3	2.537E-5	5.523E-4	2.224E-1	5.809E-5	5.809E-5	1.321E3	1.471E-1
5.000E0	3.457E1	4.300E-3	1.838E1	7.345E3	2.537E-5	6.904E-4	2.224E-1	5.809E-5	5.809E-5	1.321E3	1.464E-1
6.000E0	3.458E1	4.300E-3	1.845E1	7.346E3	2.537E-5	8.284E-4	2.224E-1	5.809E-5	5.809E-5	1.321E3	1.458E-1
7.000E0	3.458E1	4.300E-3	1.852E1	7.346E3	2.537E-5	9.665E-4	2.224E-1	5.809E-5	5.809E-5	1.321E3	1.452E-1
8.000E0	3.458E1	4.300E-3	1.860E1	7.346E3	2.537E-5	1.105E-3	2.224E-1	5.809E-5	5.809E-5	1.321E3	1.445E-1
9.000E0	3.459E1	4.300E-3	1.867E1	7.346E3	2.537E-5	1.241E-3	2.224E-1	5.809E-5	5.809E-5	1.321E3	1.439E-1
1.000E1	3.459E1	4.300E-3	1.874E1	7.346E3	2.537E-5	1.381E-3	2.224E-1	5.809E-5	5.809E-5	1.321E3	1.433E-1
1.100E1	3.459E1	4.300E-3	1.882E1	7.346E3	2.537E-5	1.519E-3	2.224E-1	5.809E-5	5.809E-5	1.321E3	1.426E-1
1.200E1	3.460E1	4.300E-3	1.889E1	7.346E3	2.537E-5	1.657E-3	2.224E-1	5.809E-5	5.809E-5	1.321E3	1.420E-1
1.300E1	3.460E1	4.300E-3	1.896E1	7.346E3	2.537E-5	1.795E-3	2.224E-1	5.809E-5	5.809E-5	1.321E3	1.414E-1
1.400E1	3.460E1	4.300E-3	1.903E1	7.347E3	2.537E-5	1.933E-3	2.224E-1	5.809E-5	5.809E-5	1.322E3	1.408E-1
1.500E1	3.461E1	4.300E-3	1.910E1	7.347E3	2.537E-5	2.071E-3	2.224E-1	5.809E-5	5.809E-5	1.322E3	1.402E-1
1.600E1	3.461E1	4.300E-3	1.918E1	7.347E3	2.537E-5	2.209E-3	2.224E-1	5.809E-5	5.809E-5	1.322E3	1.396E-1
1.700E1	3.461E1	4.300E-3	1.925E1	7.347E3	2.537E-5	2.347E-3	2.224E-1	5.809E-5	5.809E-5	1.322E3	1.390E-1
1.800E1	3.462E1	4.300E-3	1.932E1	7.347E3	2.537E-5	2.485E-3	2.224E-1	5.809E-5	5.809E-5	1.322E3	1.384E-1
1.900E1	3.462E1	4.300E-3	1.939E1	7.347E3	2.537E-5	2.623E-3	2.224E-1	5.809E-5	5.809E-5	1.322E3	1.378E-1
2.000E1	3.462E1	4.300E-3	1.946E1	7.347E3	2.537E-5	2.761E-3	2.224E-1	5.809E-5	5.809E-5	1.322E3	1.372E-1
2.100E1	3.463E1	4.300E-3	1.953E1	7.347E3	2.537E-5	2.900E-3	2.224E-1	5.809E-5	5.809E-5	1.322E3	1.366E-1
2.200E1	3.463E1	4.300E-3	1.960E1	7.348E3	2.537E-5	3.038E-3	2.224E-1	5.809E-5	5.809E-5	1.322E3	1.360E-1
2.300E1	3.463E1	4.300E-3	1.966E1	7.348E3	2.537E-5	3.176E-3	2.224E-1	5.809E-5	5.809E-5	1.322E3	1.354E-1
2.400E1	3.464E1	4.300E-3	1.973E1	7.348E3	2.537E-5	3.314E-3	2.224E-1	5.809E-5	5.809E-5	1.322E3	1.348E-1
2.500E1	3.464E1	4.300E-3	1.980E1	7.348E3	2.537E-5	3.452E-3	2.224E-1	5.809E-5	5.809E-5	1.323E3	1.342E-1
2.600E1	3.464E1	4.300E-3	1.987E1	7.348E3	2.537E-5	3.590E-3	2.224E-1	5.809E-5	5.809E-5	1.323E3	1.336E-1
2.700E1	3.465E1	4.300E-3	1.994E1	7.348E3	2.537E-5	1.728E-3	2.224E-1	5.809E-5	5.809E-5	1.323E3	1.330E-1
2.800E1	3.465E1	4.300E-3	2.000E1	7.348E3	2.537E-5	3.866E-3	2.224E-1	5.809E-5	5.809E-5	1.323E3	1.324E-1
2.900E1	3.465E1	4.300E-3	2.007E1	7.348E3	2.537E-5	4.004E-3	2.224E-1	5.809E-5	5.809E-5	1.323E3	1.319E-1
3.000E1	3.466E1	4.300E-3	2.014E1	7.348E3	2.537E-5	4.142E-3	2.224E-1	5.809E-5	5.809E-5	1.323E3	1.313E-1

Appendix 16: Spreadsheet Sample Output Figures.

Fig.5.1 Spreadsheet Analysis of Mean D for Various Video Runs

INJECTION SPEED =3

VIDEO RUN:	3	13	66	72
D, mm:	5.0	4.5	5.0	5.0
	5.0	5.0	5.0	5.0
	5.0	5.0	5.0	5.0
	6.0	5.0	5.5	5.0
	6.0	6.0	6.0	5.0
	6.0	6.0	6.0	5.0
	6.0	6.0	6.0	5.5
	6.0	6.0	6.0	5.5
	6.0	6.0	6.0	5.5
	6.5	6.0	6.0	5.5
	6.5	6.5	6.5	6.0
	7.0	6.5	6.5	6.0
	7.0	7.0	7.0	6.0
	7.0	7.0	7.0	6.0
	7.0	7.0	7.5	7.0
	7.5	7.0	7.5	7.0
	7.5	7.5	7.5	7.0
	7.5	7.5	7.5	7.5
	8.0	7.5	7.5	7.5
	8.0	8.0	8.0	8.0
MEAN:	6.53	6.35	6.45	6.00
STD. DEV.:	0.94	0.97	0.94	0.99
OVERALL MEAN:		6.33		
OVERALL STD. DEV.:		0.964		

Fig.5.2 Spreadsheet Analysis of Mean D for Various Sample Sizes

Sample size: (Video Run 3 Inj. Speed 3)	10	20	30	40
	8.0	7.0	5.5	6.0
	5.0	5.0	5.0	5.0
	7.0	6.0	7.0	7.0
	6.0	6.0	7.5	6.0
	7.0	7.5	7.5	7.0
	6.0	7.5	5.0	7.5
	6.5	8.0	6.5	8.0
	7.0	6.5	6.5	6.0
	5.0	7.5	7.5	7.5
	6.0	6.0	6.0	5.5
Cumulative:				
MEAN:	6.35	6.53	6.48	6.50
STD.DEV.:	0.944	0.939	0.942	0.941

Fig.7.1 L2 Analysis of Run1A vs Fit to Runs1A,B,C

RUN1A	LOGLIN FIT	ERROR^2
82.4	73.2	84.6
82.2	67.0	231.0
48.7	55.2	42.2
30.0	38.2	67.2
30.6	30.5	0.0
22.1	21.5	0.4
18.8	17.8	1.0
14.4	16.5	4.4
14.3	15.1	0.6
SUMS:		431.6

Fig.7.4 L2 Analysis of VA and VD Models.

RUN1A	VD B=.79	ERROR^2	VA B=.79	ERROR^2
82.40	74.30	65.61	75.20	51.84
48.70	53.10	19.36	51.30	6.76
30.00	37.50	56.25	35.00	25.00
30.60	31.00	0.16	28.60	4.00
22.10	23.10	1.00	21.00	1.21
18.80	19.20	0.16	17.20	2.56
14.40	17.40	9.00	15.60	1.44
14.30	14.20	0.01	12.60	2.89
SUMS:		151.55		95.70

L2 Analysis of VA Model for Various B Values

RUN1A	B=.77	ERROR^2	B=.76	ERROR^2	B=.75	ERROR^2
82.4	77.4	25.0	78.5	15.2	79.6	7.8
48.7	52.7	16.0	53.3	21.2	54.1	29.2
30.0	36.0	36.0	36.4	41.0	36.9	47.6
30.6	29.4	1.4	29.7	0.8	30.1	0.2
22.1	21.5	0.4	21.8	0.1	22.1	0.0
18.8	17.6	1.4	17.9	0.8	18.1	0.5
14.4	16.0	2.6	16.2	3.2	16.4	4.0
14.3	13.0	1.7	13.1	1.4	13.3	1.0
SUMS:		84.5		83.7		90.4

Fig.7.6.

L2 Analysis Of C, Equation 7.4.1

RUN1A	C=0.60	ERROR^2	C=0.61	ERROR^2	C=0.62	ERROR^2
82.4	77.9	20.2	76.6	33.6	75.2	51.8
48.7	53.6	24.0	52.8	16.8	51.9	10.2
30.0	37.3	53.3	36.7	44.9	36.0	36.0
30.6	30.8	0.0	30.2	0.2	29.8	0.6
22.1	23.0	0.8	22.6	0.2	22.3	0.0
18.8	19.2	0.2	18.9	0.0	18.6	0.0
14.4	17.5	9.6	16.9	6.2	16.9	6.2
14.3	14.5	0.0	14.0	0.1	14.0	0.1
SUMS:		108.2		102.1		105.1

Appendix 17: Graphical Figures, Results And Model Analysis.

Fig.5.3

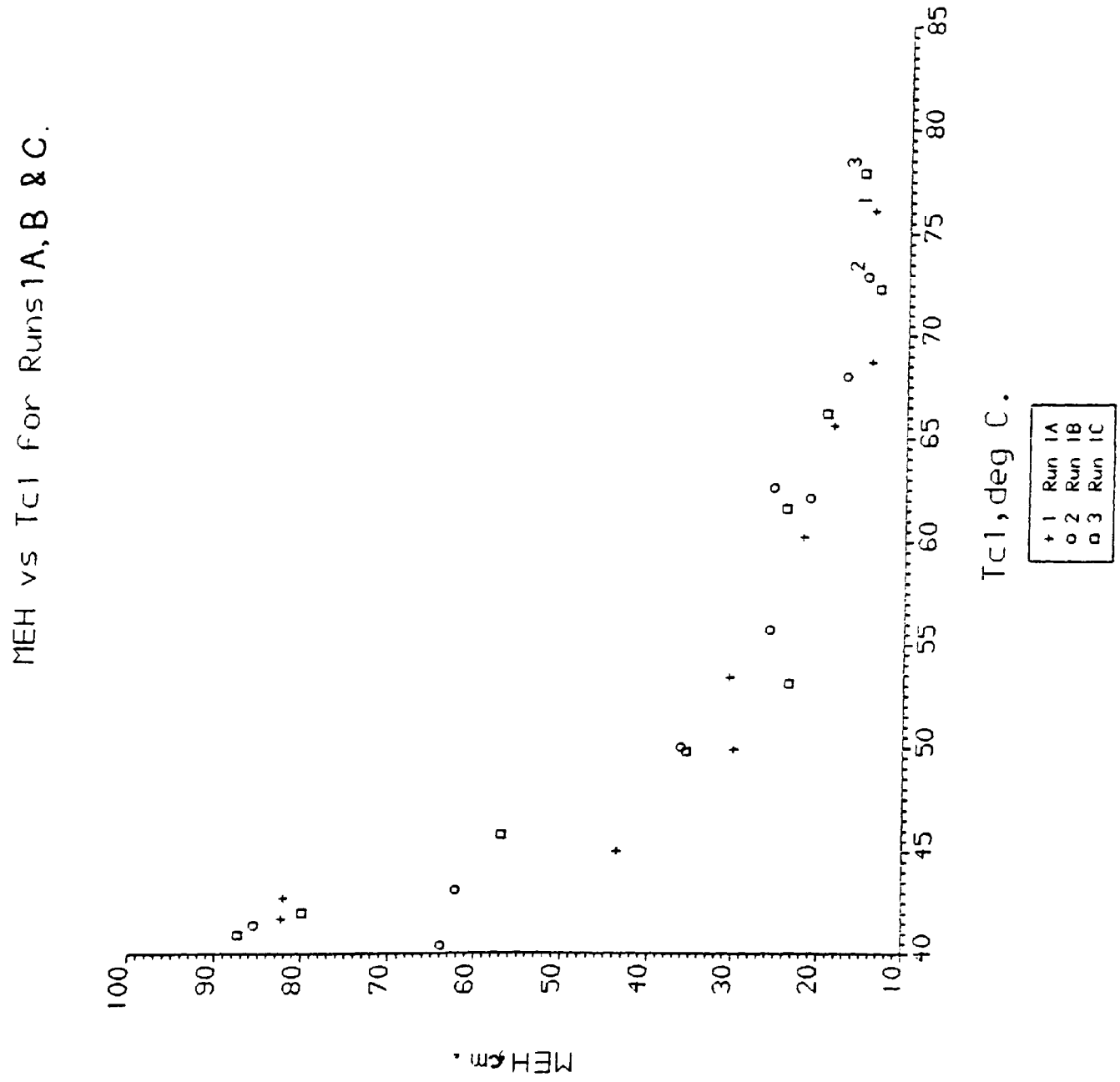
MEH vs Tc1 for Runs 1A, B & C.
MEH, %
Tc1, deg C.
+ 1 Run 1A
o 2 Run 1B
□ 3 Run 1C
100
90
80
70
60
50
40
30
20
10
40
45
50
55
60
65
70
75
80
85

Fig.5.4

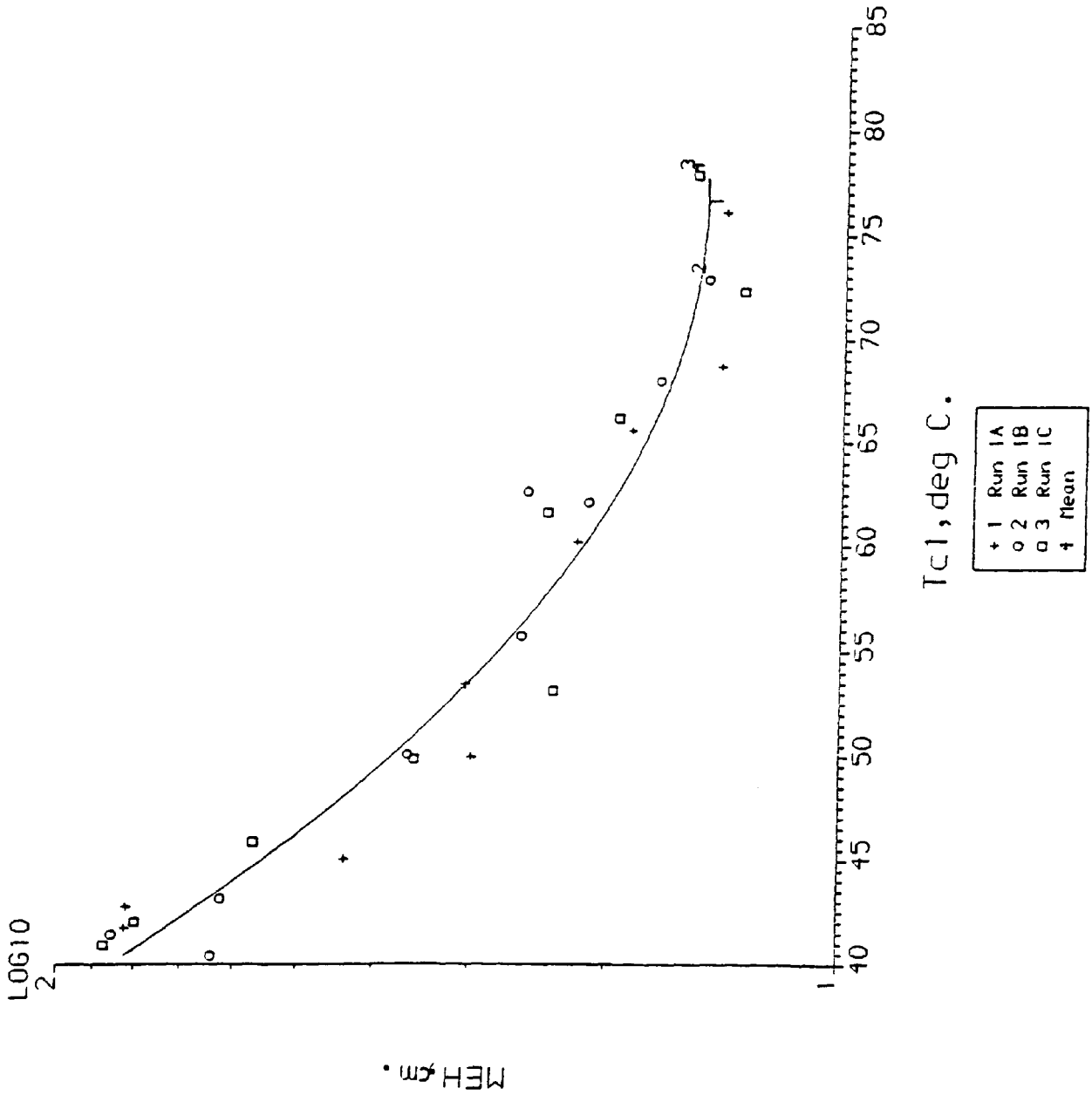
MEH vs Tc1 For Runs 1A, B & C.
LOG10
MEH, cm.
Tc1, deg C.
40
45
50
55
60
65
70
75
80
85
1
2
+ 1 Run 1A
o 2 Run 1B
□ 3 Run 1C
4 Mean

Fig.5.5

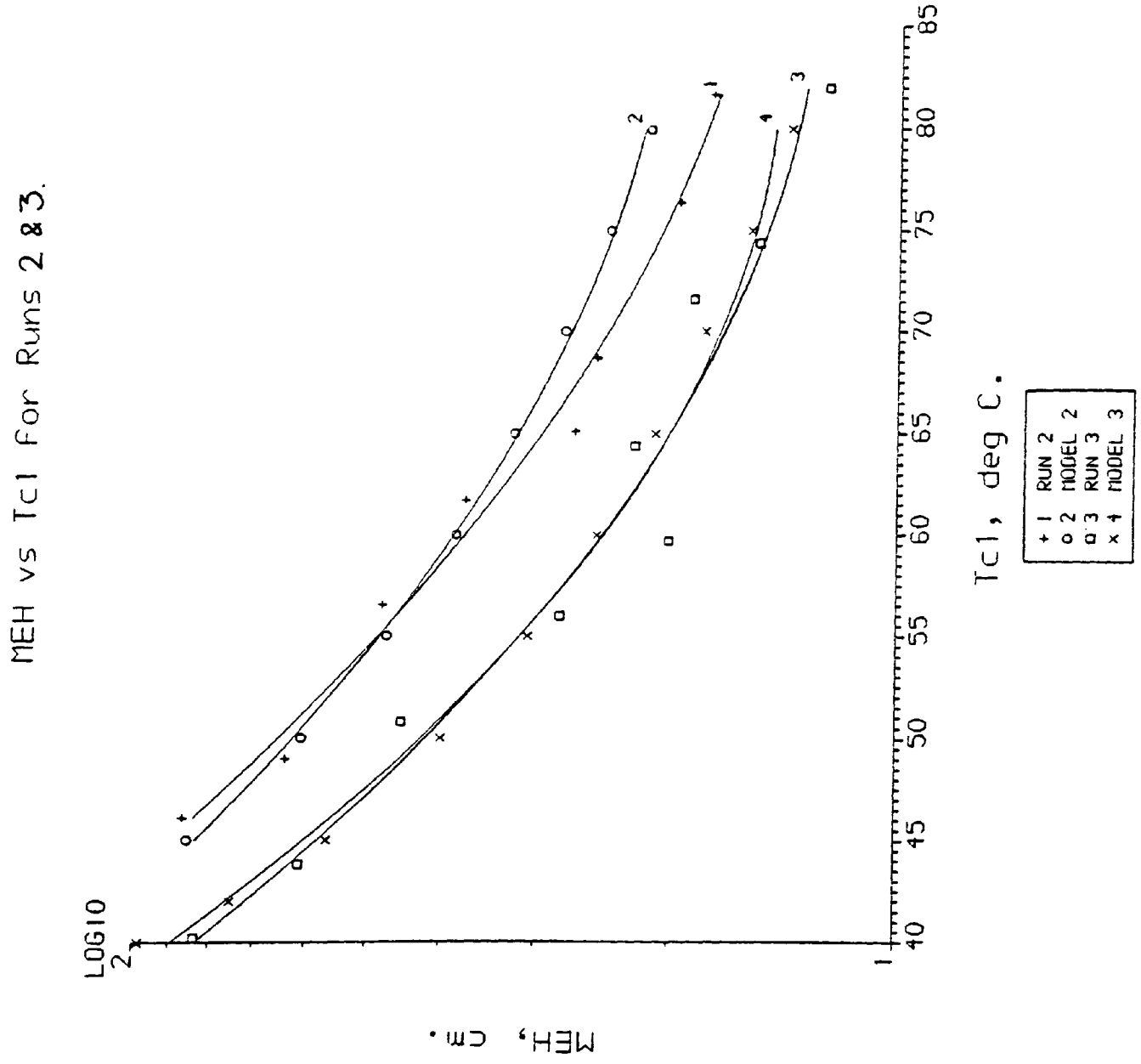
MEH vs Tc1 For Runs 2 & 3.
LOG10
2
1
MEH, cm.
40
45
50
55
60
65
70
75
80
85
Tc1, deg C.
+ 1 RUN 2
o 2 MODEL 2
□ 3 RUN 3
× 4 MODEL 3

Fig.5.6

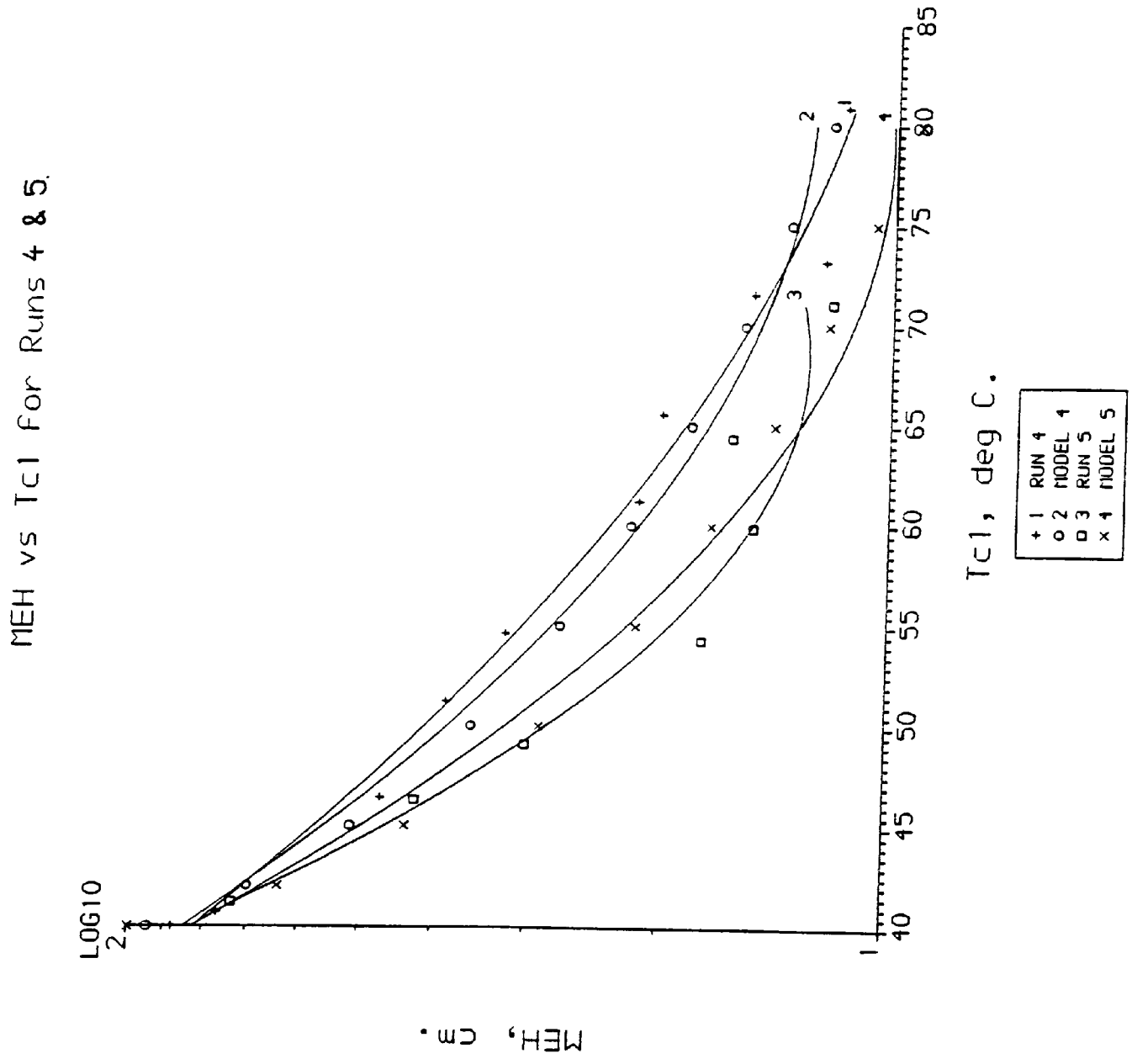
MEH vs Tc1 For Runs 4 & 5
LOG10
MEH, cm.
Tc1, deg C.
40
45
50
55
60
65
70
75
80
85
1
2
+ 1 RUN 4
o 2 MODEL 4
□ 3 RUN 5
× 4 MODEL 5

Fig.5.7

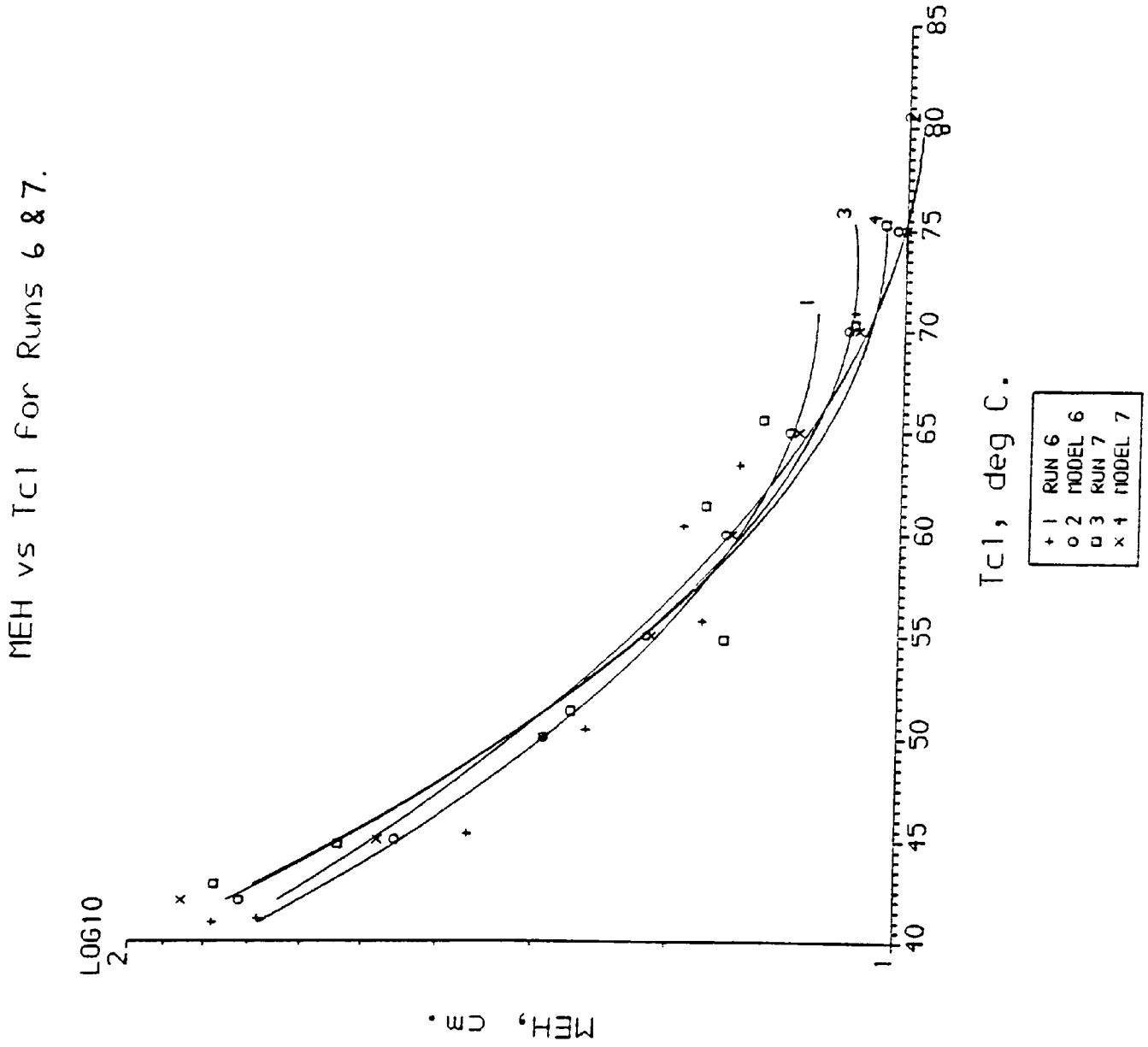
MEH vs Tc1 For Runs 6 & 7.
LOG10
MEH, cm.
Tc1, deg C.
+ 1 RUN 6
o 2 MODEL 6
□ 3 RUN 7
× 4 MODEL 7

Fig.5.8

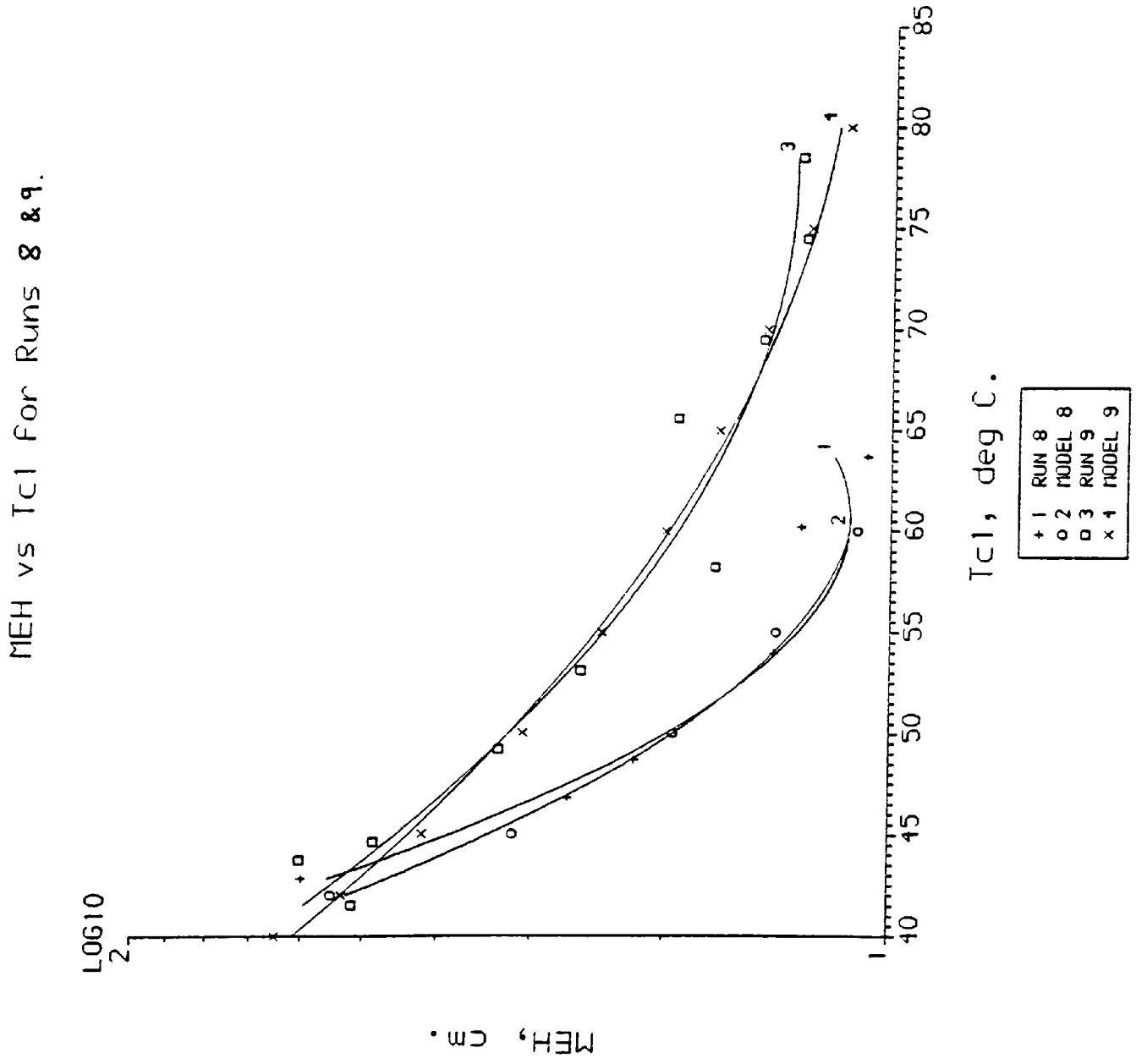
MEH vs Tc1 For Runs 8 &9.
LOG10
MEH, cm.
Tc1, deg C.
+ 1 RUN 8
o 2 MODEL 8
□ 3 RUN 9
× 4 MODEL 9

Fig.5.9

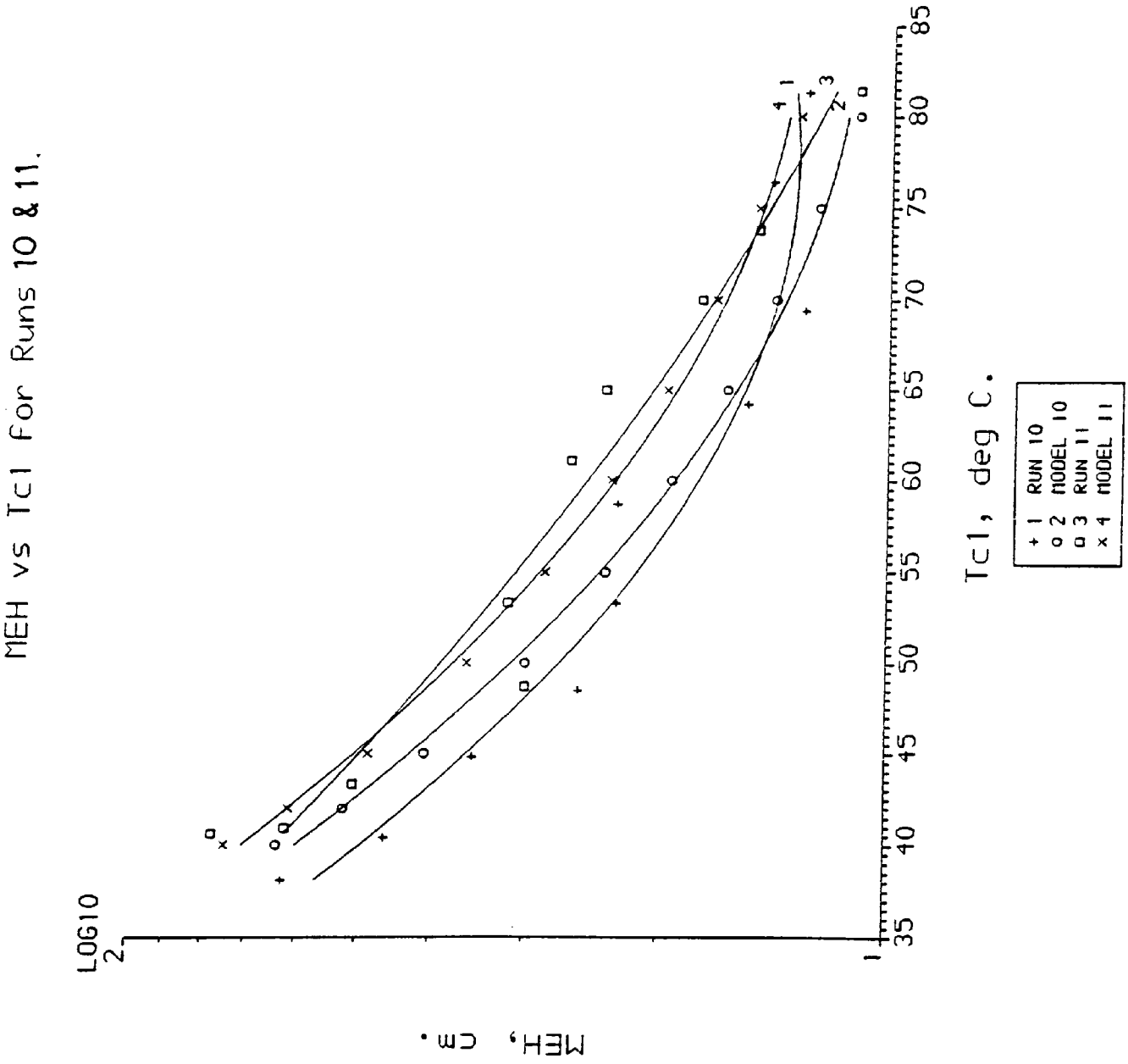
MEH vs Tc1 For Runs 10 & 11.
LOG10
MEH, cm.
2
1
35
40
45
50
55
60
65
70
75
80
85
Tc1, deg C.
+ 1 RUN 10
o 2 MODEL 10
□ 3 RUN 11
× 4 MODEL 11

Fig.5.10

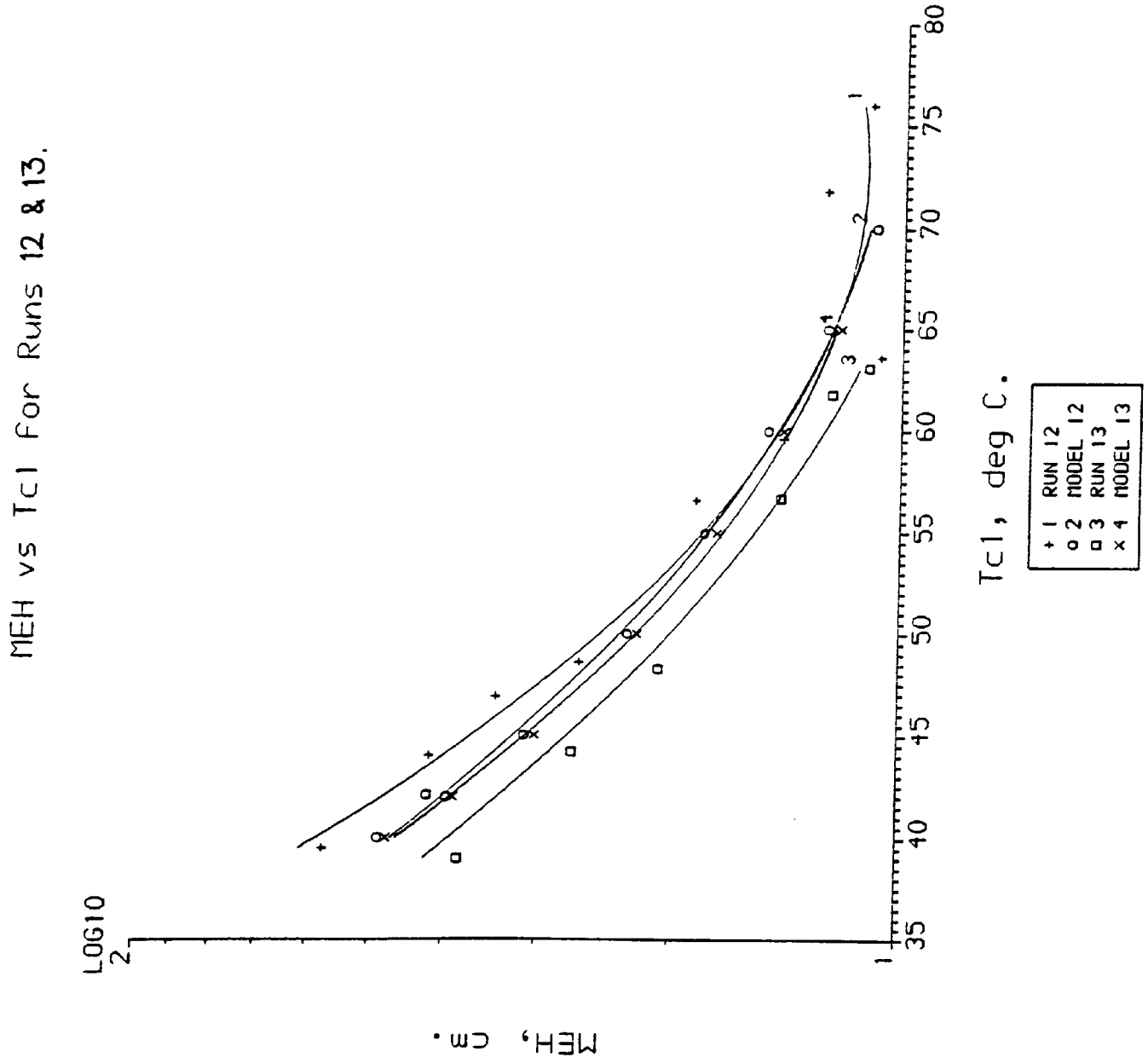
MEH vs Tc1 For Runs 12 & 13.
LOG10
MEH, cm.
Tc1, deg C.
35
40
45
50
55
60
65
70
75
80
1
2
+ 1 RUN 12
o 2 MODEL 12
□ 3 RUN 13
× 4 MODEL 13

Fig.5.11

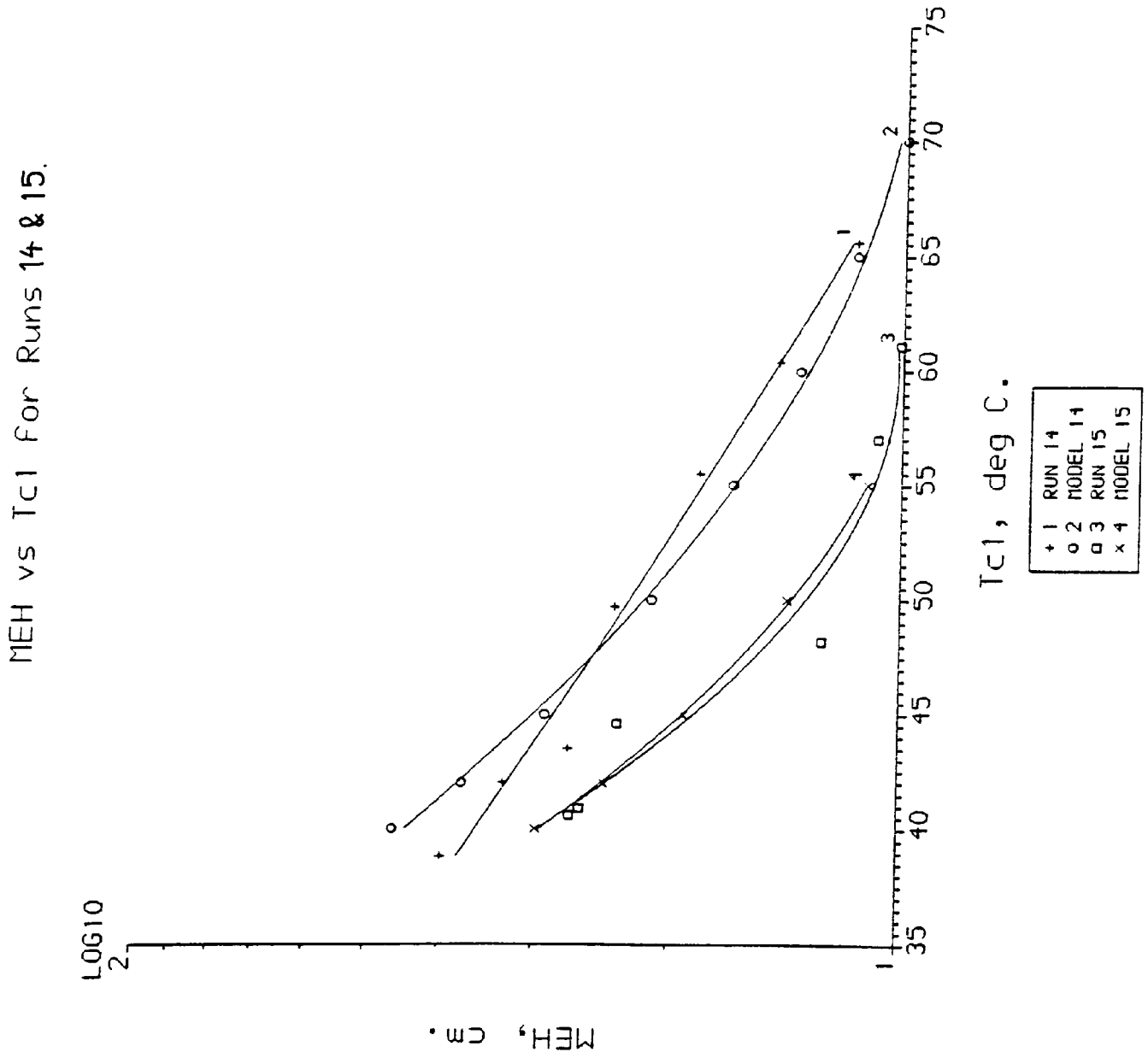
MEH vs Tc1 For Runs 14 & 15.
LOG10
MEH, cm.
Tc1, deg C.
35
40
45
50
55
60
65
70
75
1
2
+ 1 RUN 14
o 2 MODEL 14
□ 3 RUN 15
× 4 MODEL 15

Fig.5.12

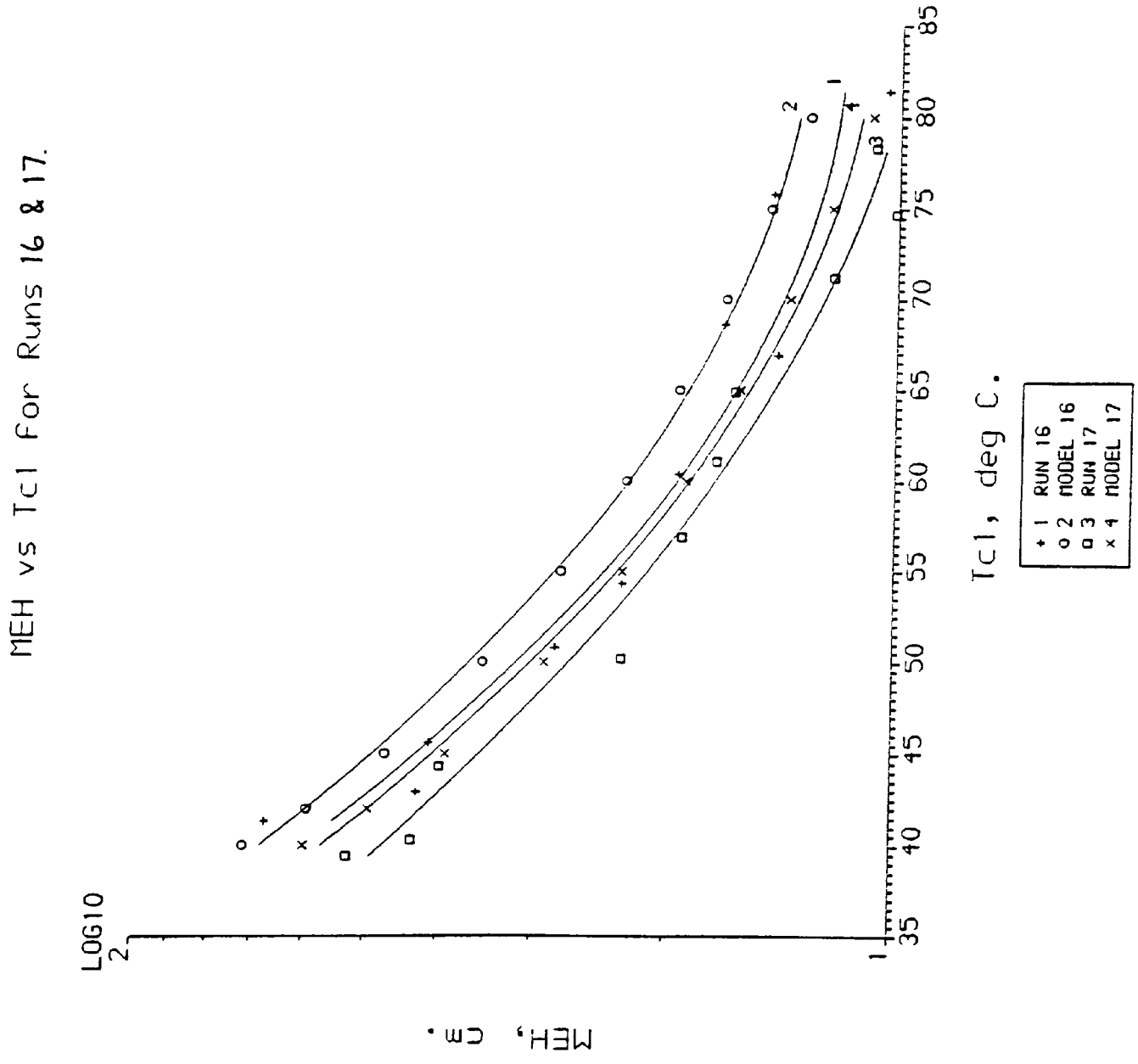
MEH vs Tc1 For Runs 16 & 17.
LOG10
2
1
MEH, cm.
35
40
45
50
55
60
65
70
75
80
85
Tc1, deg C.
+ 1 RUN 16
o 2 MODEL 16
□ 3 RUN 17
× 4 MODEL 17

Fig.5.13

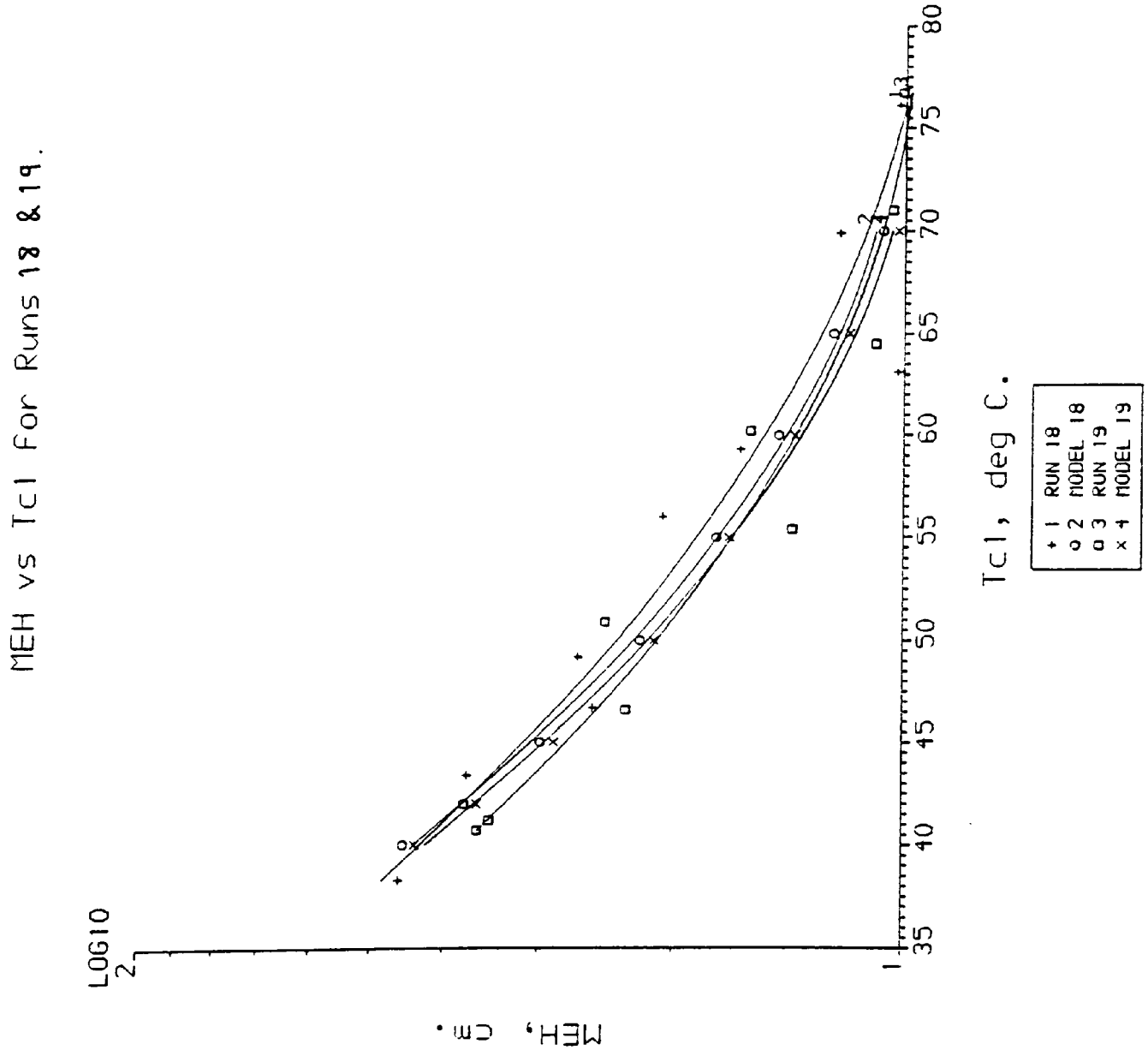
MEH vs Tc1 For Runs 18 & 19.
LOG10
MEH, cm.
Tc1, deg C.
35
40
45
50
55
60
65
70
75
80
1
2
+ 1 RUN 18
o 2 MODEL 18
□ 3 RUN 19
× 4 MODEL 19

Fig.5.14

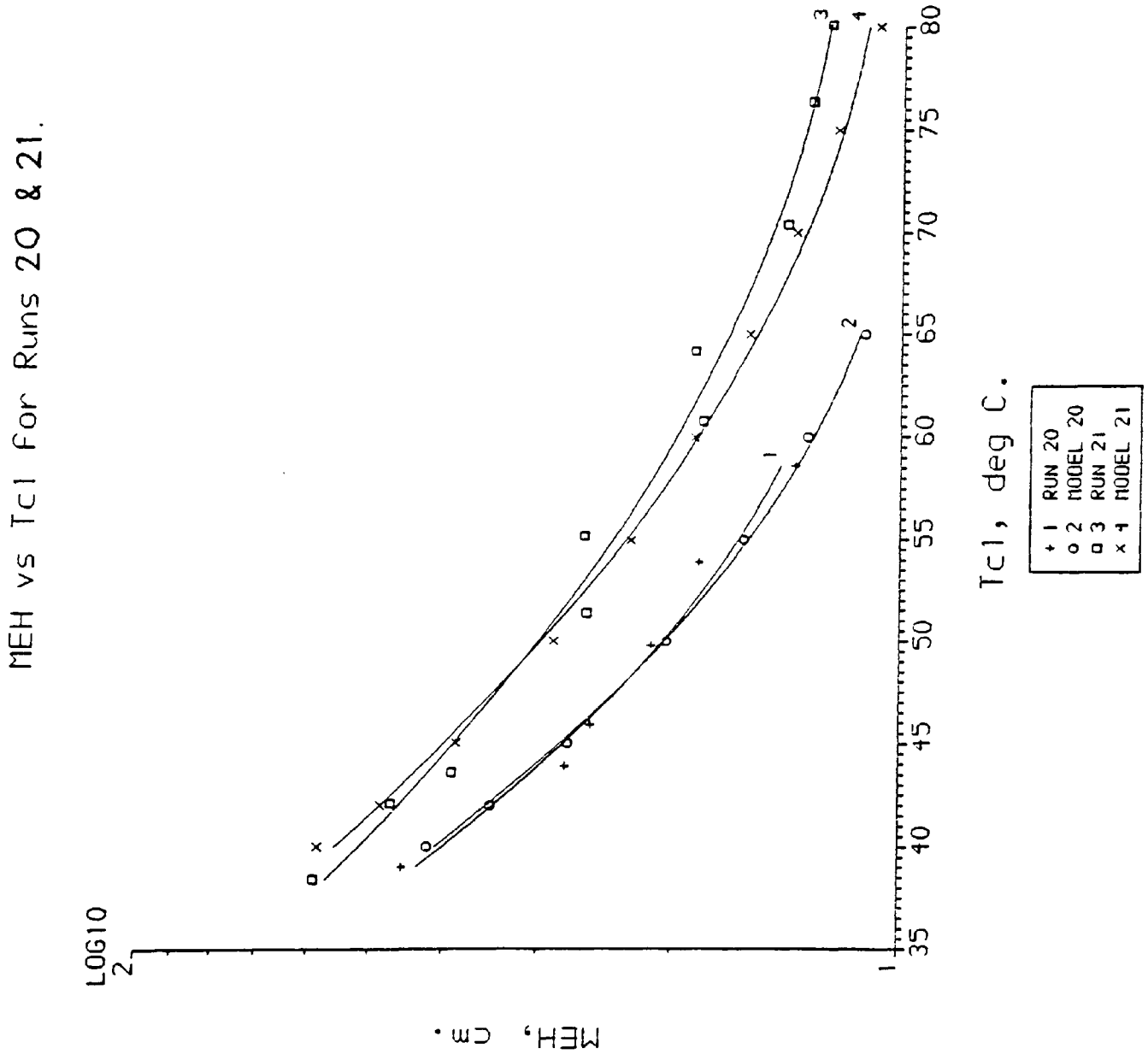
MEH vs Tc1 For Runs 20 & 21.
LOG10
MEH, cm.
2
1
35
40
45
50
55
60
65
70
75
80
Tc1, deg C.
+ 1 RUN 20
o 2 MODEL 20
□ 3 RUN 21
× 4 MODEL 21

Fig.5.15

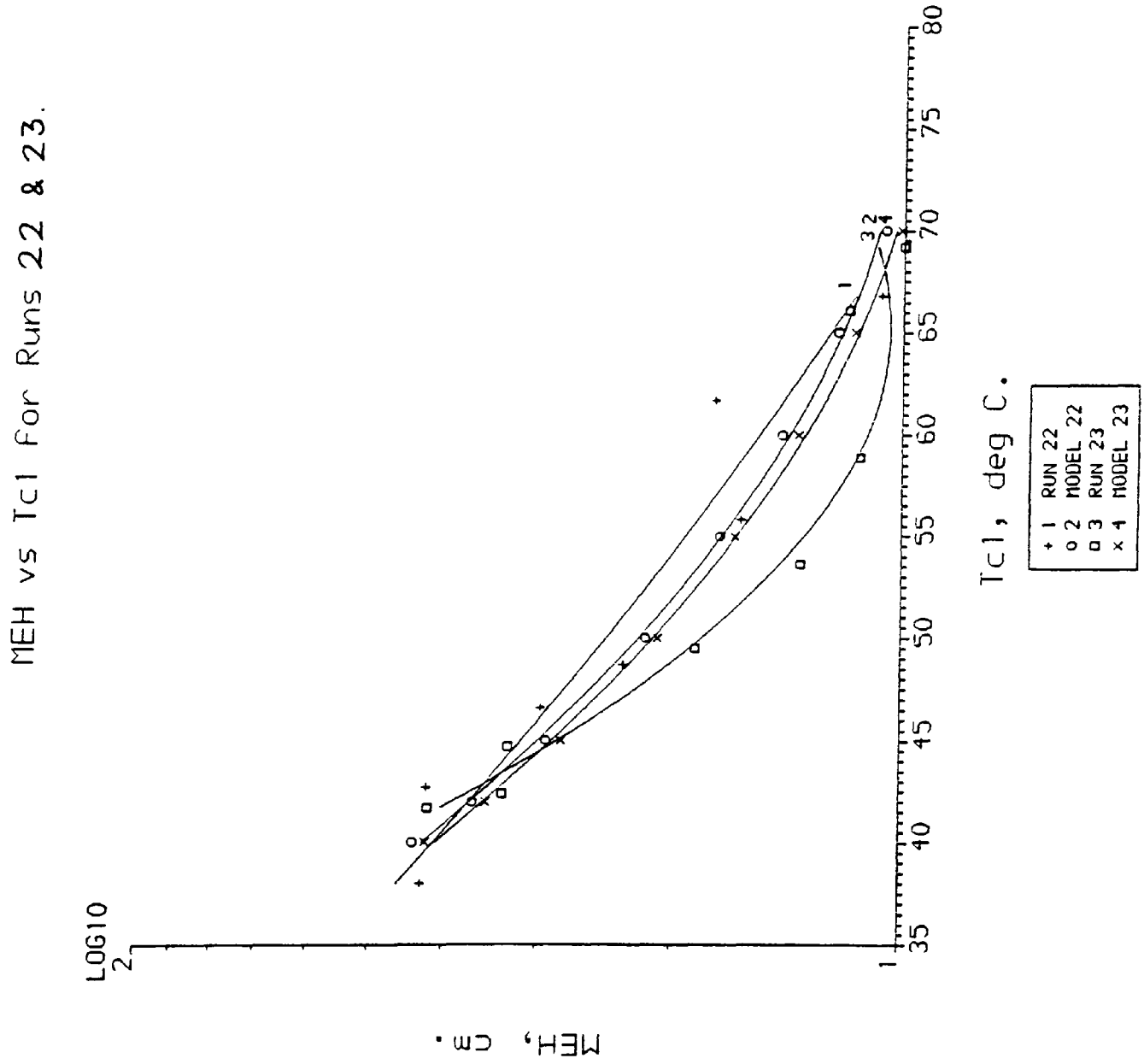
MEH vs Tc1 For Runs 22 & 23.
LOG10
MEH, cm.
Tc1, deg C.
+ 1 RUN 22
o 2 MODEL 22
□ 3 RUN 23
× 4 MODEL 23
35
40
45
50
55
60
65
70
75
80
1
2

Fig.5.16

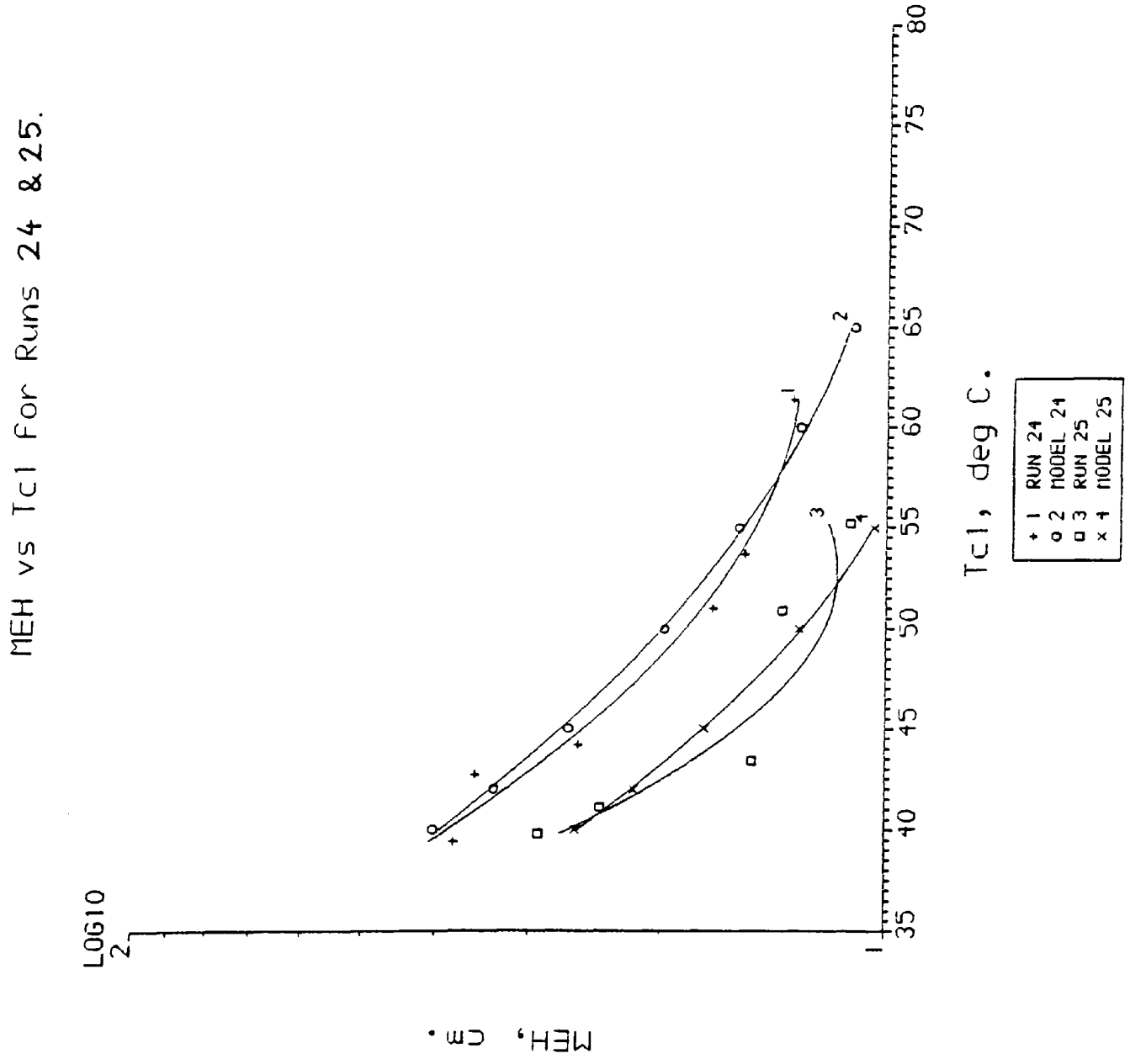
MEH vs Tc1 For Runs 24 & 25.
LOG10
2
1
MEH, cm.
35
40
45
50
55
60
65
70
75
80
Tc1, deg C.
+ 1 RUN 24
o 2 MODEL 24
□ 3 RUN 25
× 4 MODEL 25

Fig.5.17

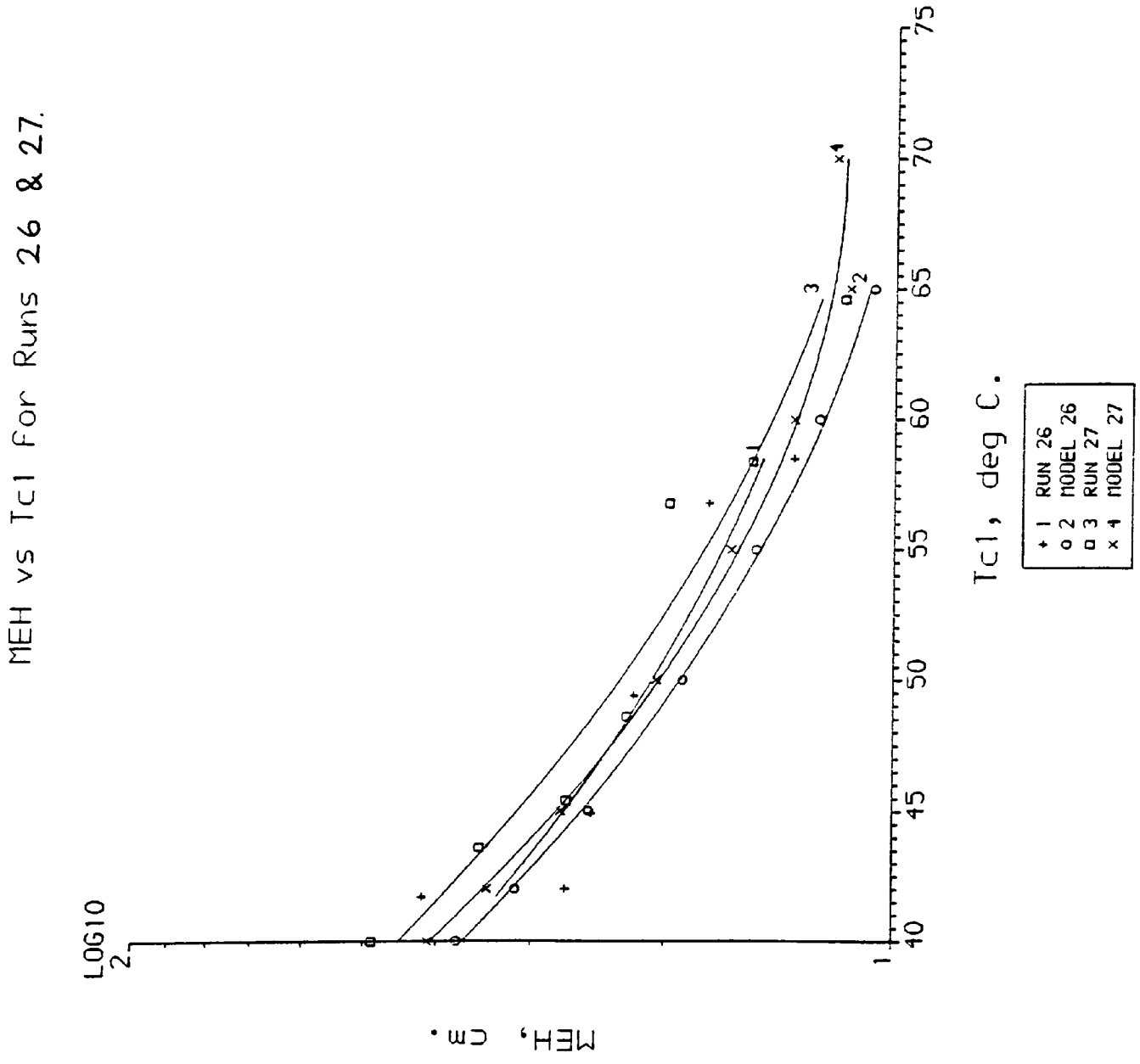
MEH vs Tc1 For Runs 26 & 27.
LOG10
MEH, cm.
Tc1, deg C.
40
45
50
55
60
65
70
75
1
2
3
x1
x2
+ 1 RUN 26
o 2 MODEL 26
□ 3 RUN 27
× 4 MODEL 27

Fig.5.18

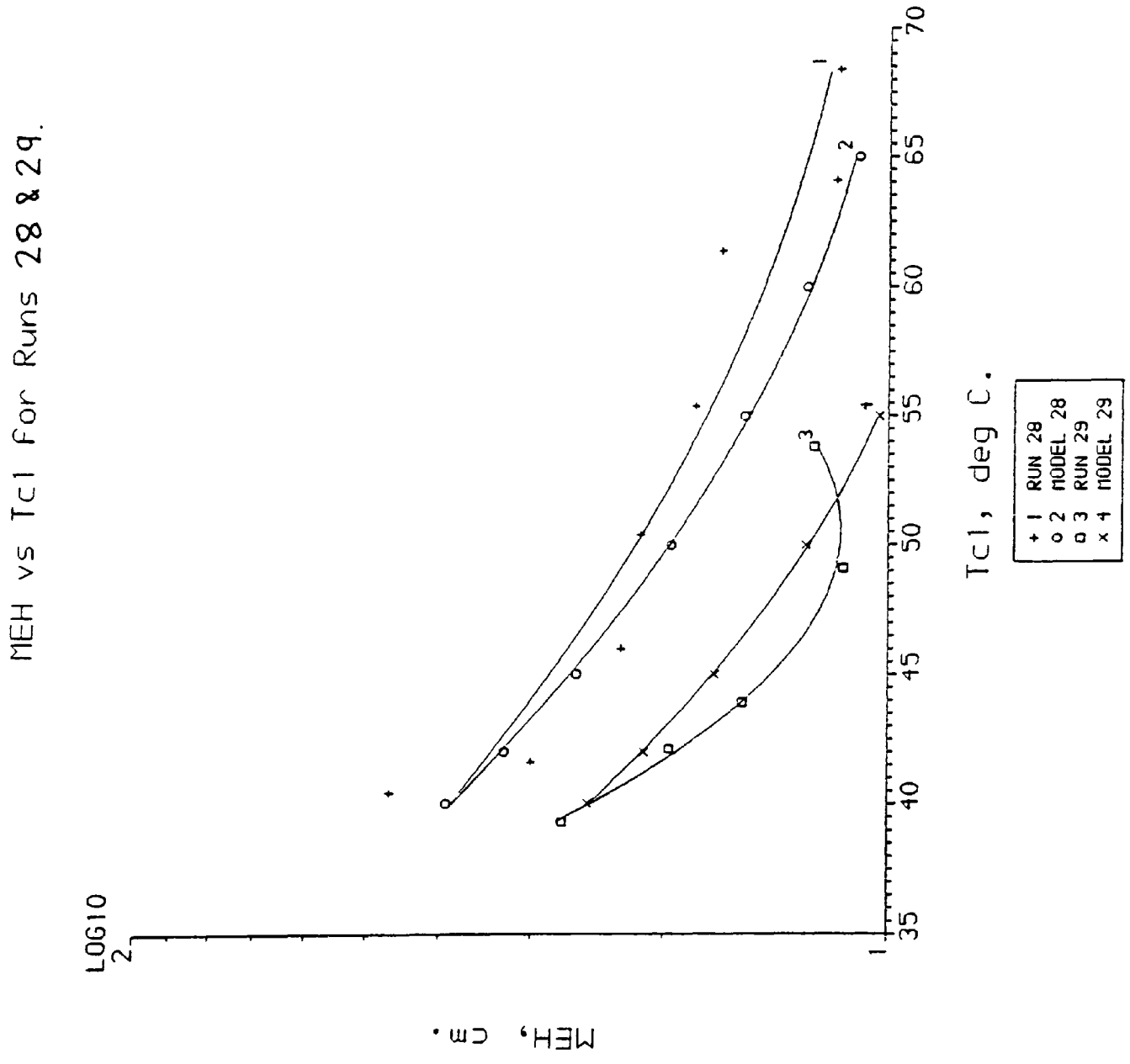
MEH vs Tc1 For Runs 28 & 29.
LOG10
2
1
MEH, cm.
35
40
45
50
55
60
65
70
Tc1, deg C.
+ 1 RUN 28
o 2 MODEL 28
□ 3 RUN 29
× 4 MODEL 29

Fig.5.19

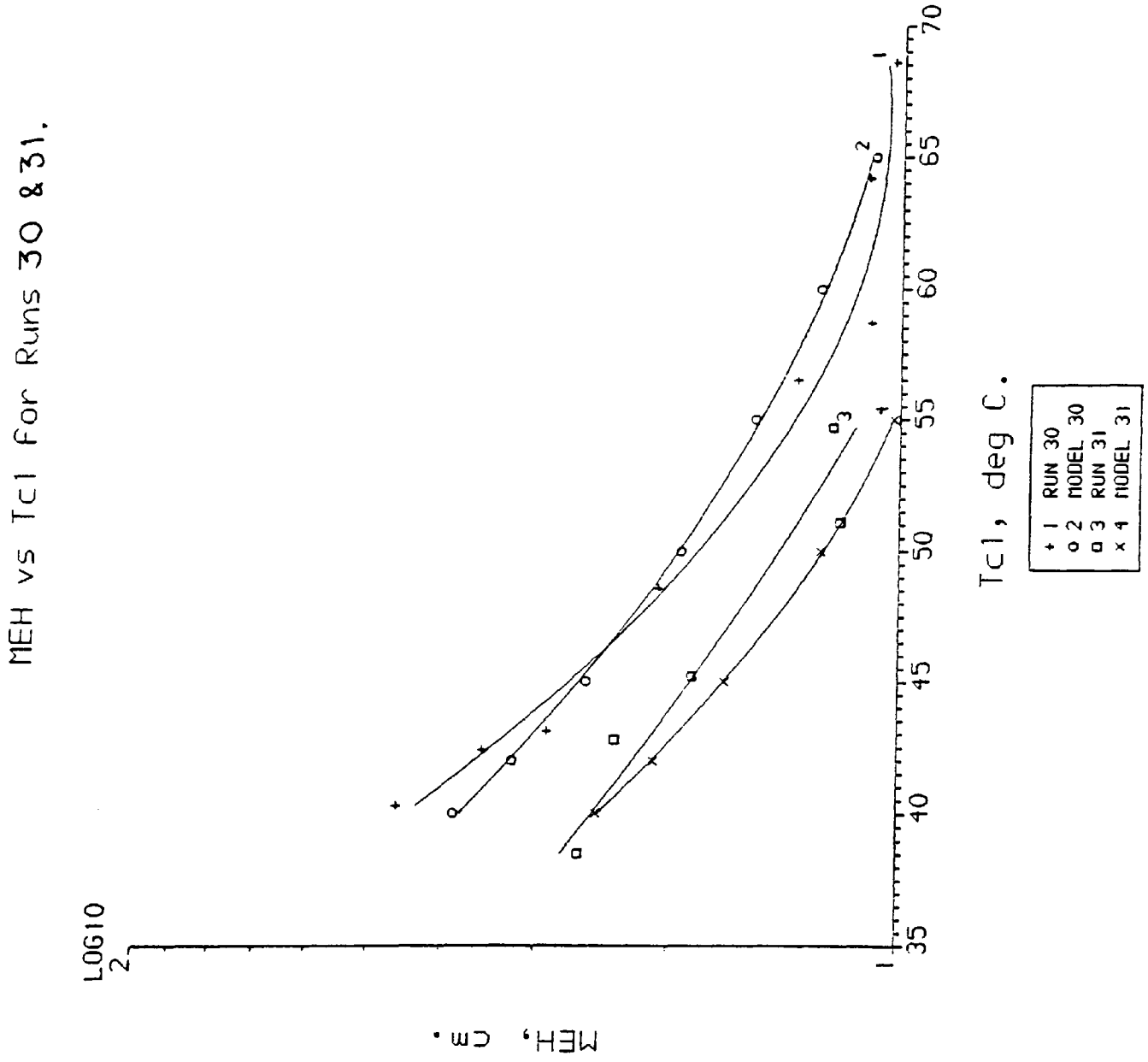
MEH vs Tc1 For Runs 30 &31.
LOG10
MEH, cm.
Tc1, deg C.
35
40
45
50
55
60
65
70
1
2
+ 1 RUN 30
o 2 MODEL 30
□ 3 RUN 31
× 4 MODEL 31

Fig.5.20

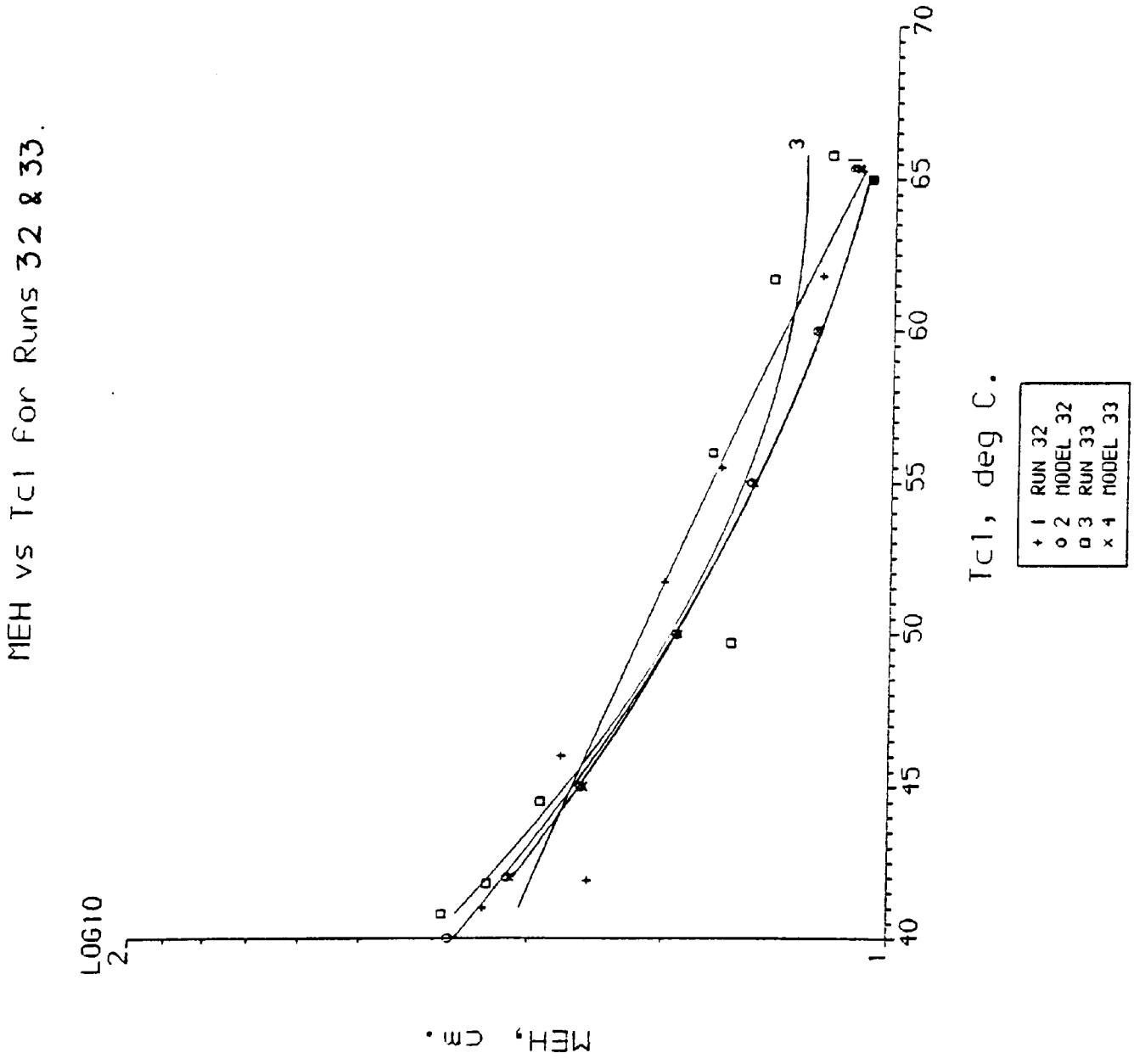
MEH vs Tc1 For Runs 32 & 33.
LOG10
MEH, cm.
Tc1, deg C.
+ 1 RUN 32
o 2 MODEL 32
□ 3 RUN 33
× 4 MODEL 33

Fig.5.21

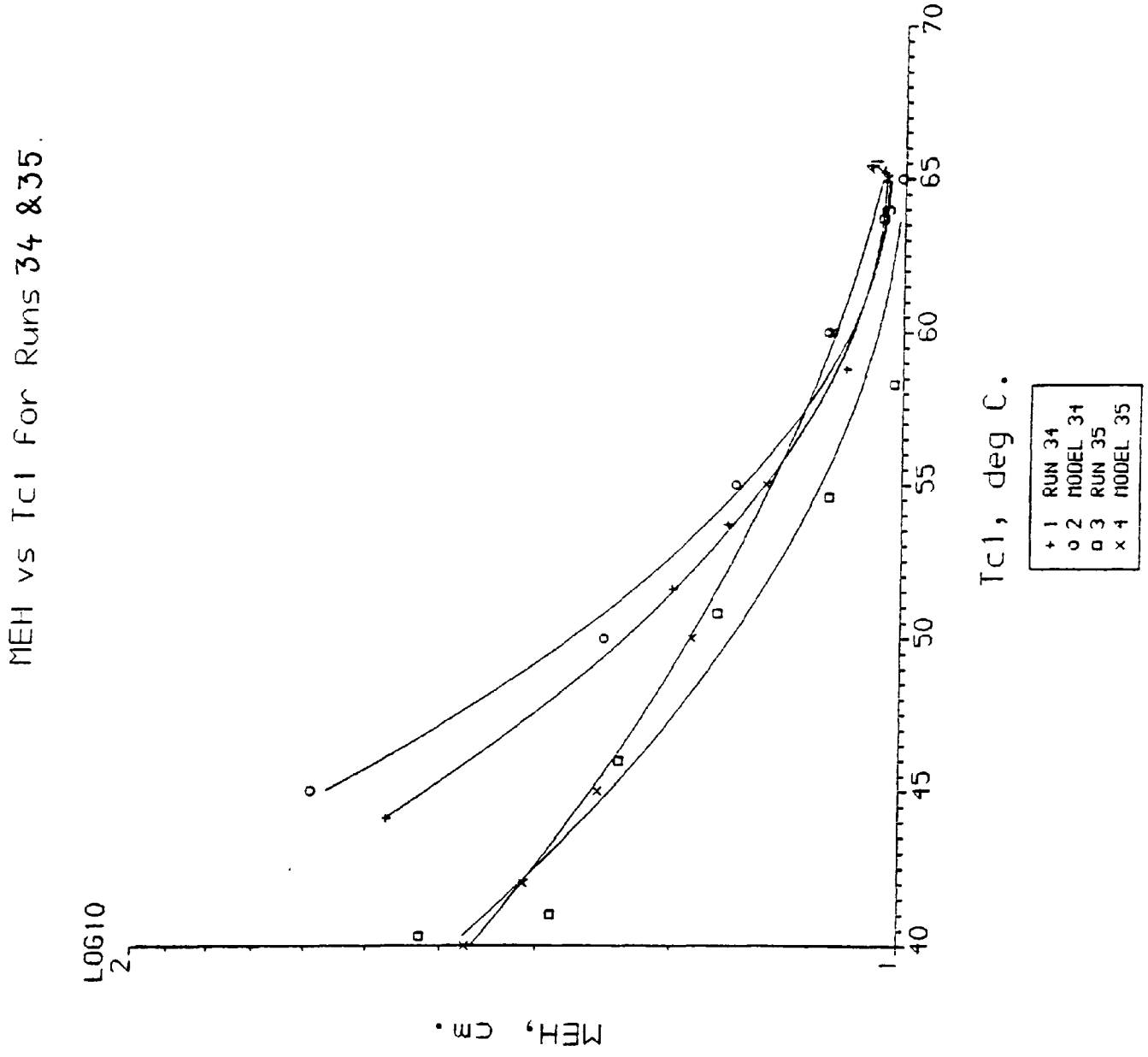
MEH vs Tc1 For Runs 34 &35.
LOG10
MEH, cm.
2
1
40
45
50
55
60
65
70
Tc1, deg C.
+ 1 RUN 34
o 2 MODEL 34
□ 3 RUN 35
× 4 MODEL 35

Fig.5.22

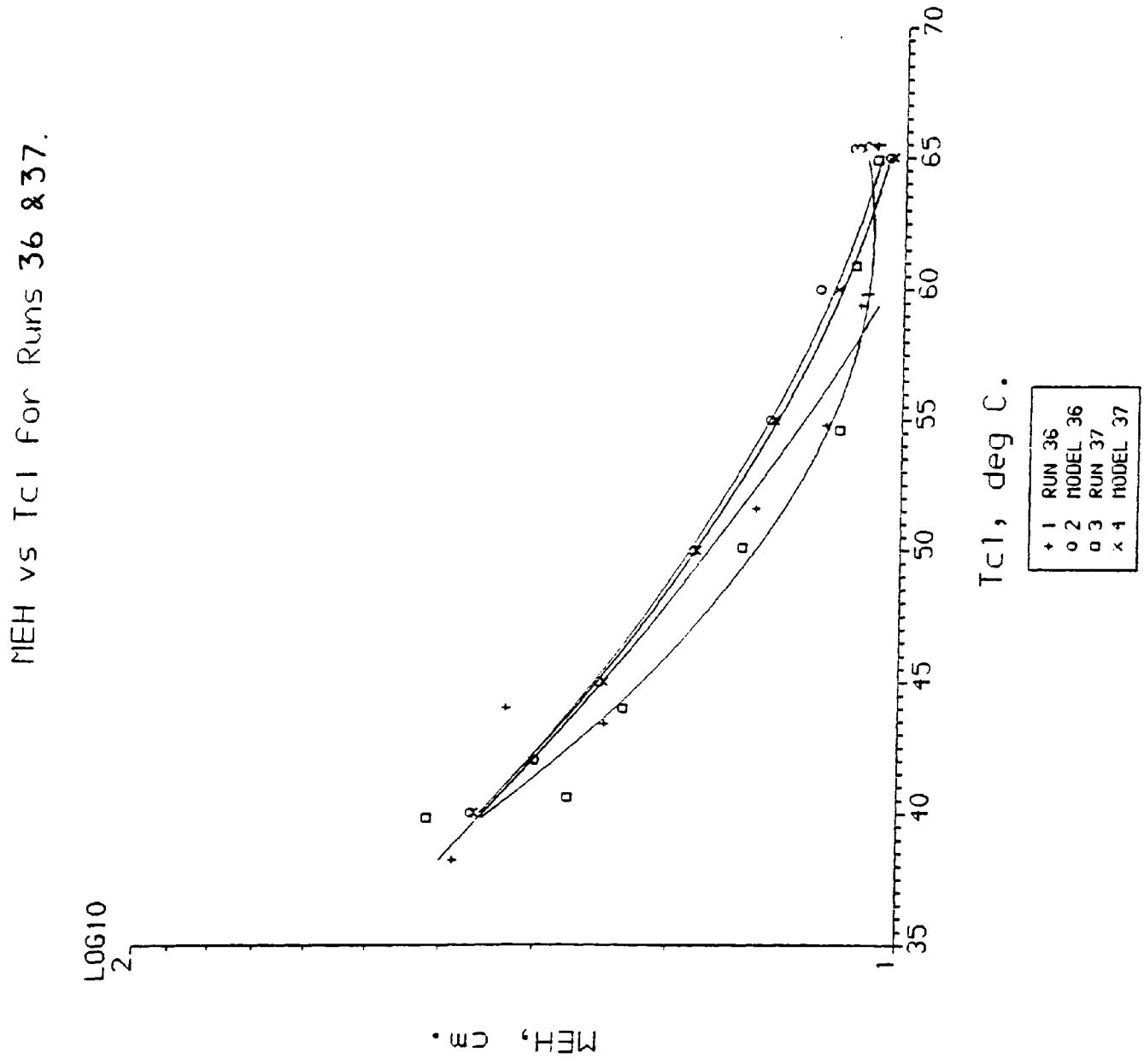
MEH vs Tc1 For Runs 36 &37.
LOG10
2
1
MEH, cm.
35
40
45
50
55
60
65
70
Tc1, deg C.
+ 1 RUN 36
o 2 MODEL 36
□ 3 RUN 37
× 4 MODEL 37

Fig.5.23

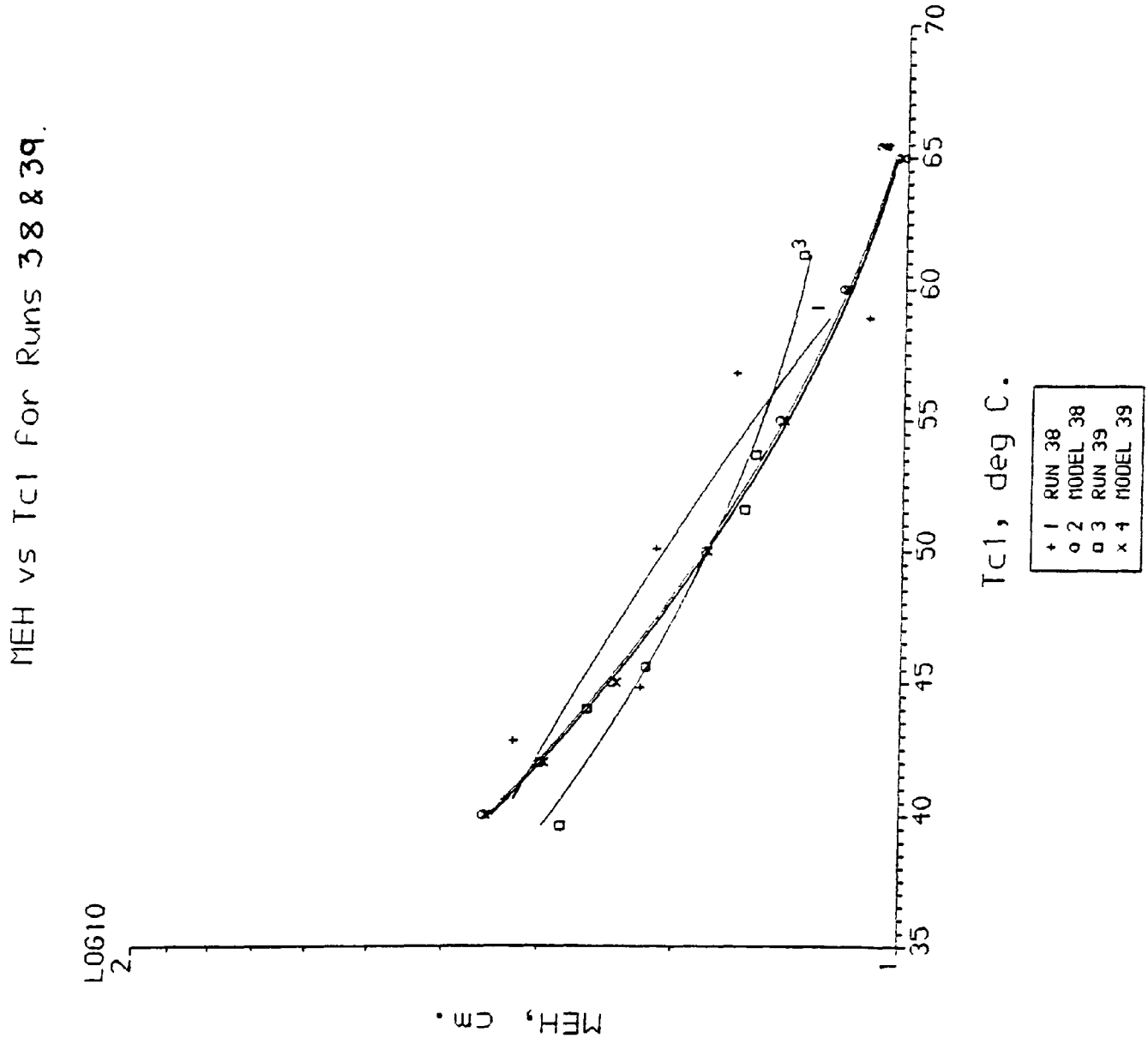
MEH vs Tc1 For Runs 38 & 39.
LOG10
MEH, cm.
Tc1, deg C.
35
40
45
50
55
60
65
70
1
2
+ 1 RUN 38
o 2 MODEL 38
□ 3 RUN 39
× 4 MODEL 39

Fig.5.24

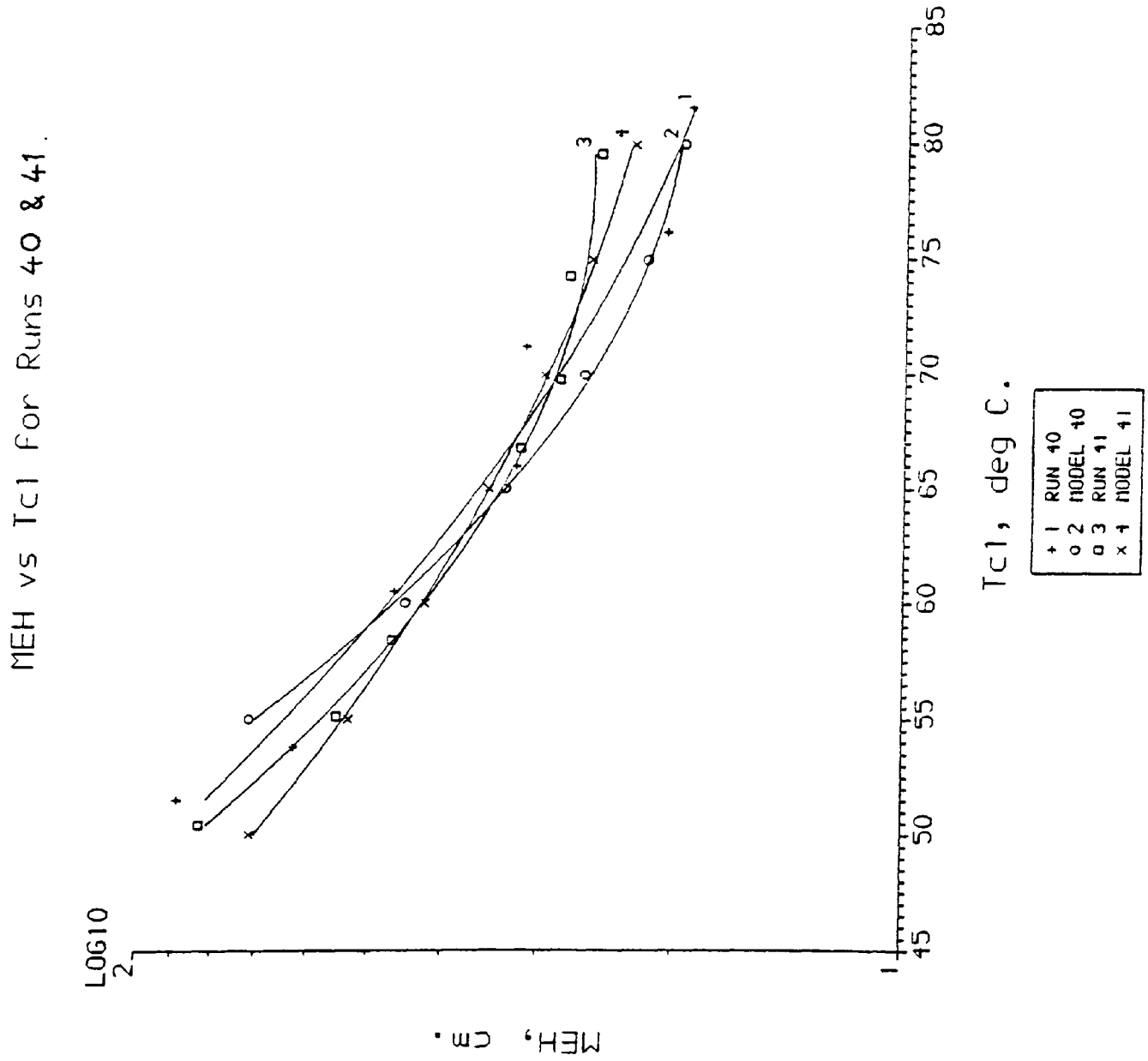
MEH vs Tc1 For Runs 40 & 41.
LOG10
2
1
MEH, cm.
45
50
55
60
65
70
75
80
85
Tc1, deg C.
+ 1 RUN 40
o 2 MODEL 40
□ 3 RUN 41
× 4 MODEL 41

Fig.5.25

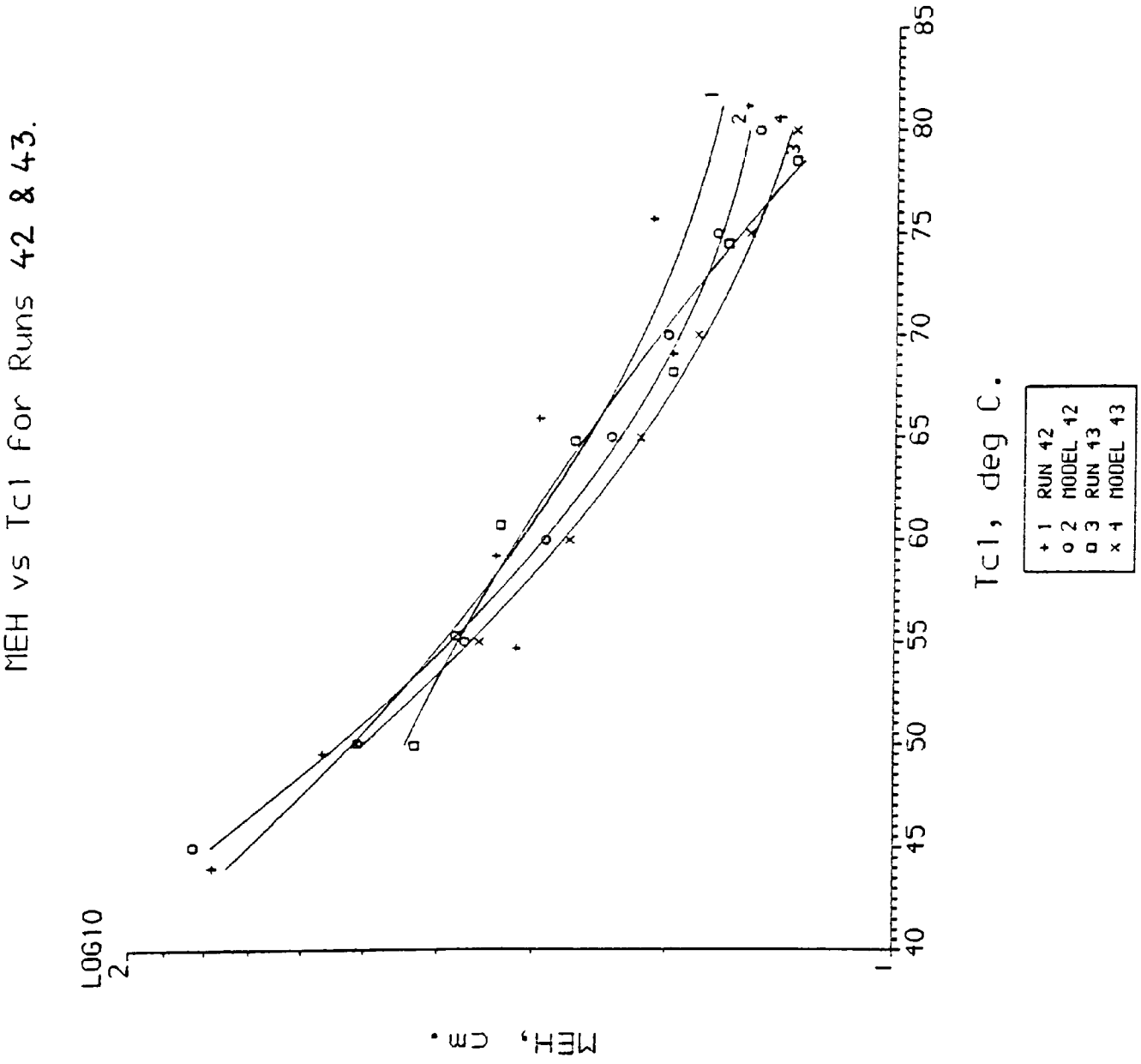
MEH vs Tc1 for Runs 42 & 43.
LOG10
2
1
MEH, cm.
40
45
50
55
60
65
70
75
80
85
Tc1, deg C.
+ 1 RUN 42
o 2 MODEL 42
□ 3 RUN 43
× 4 MODEL 43

Fig.5.26

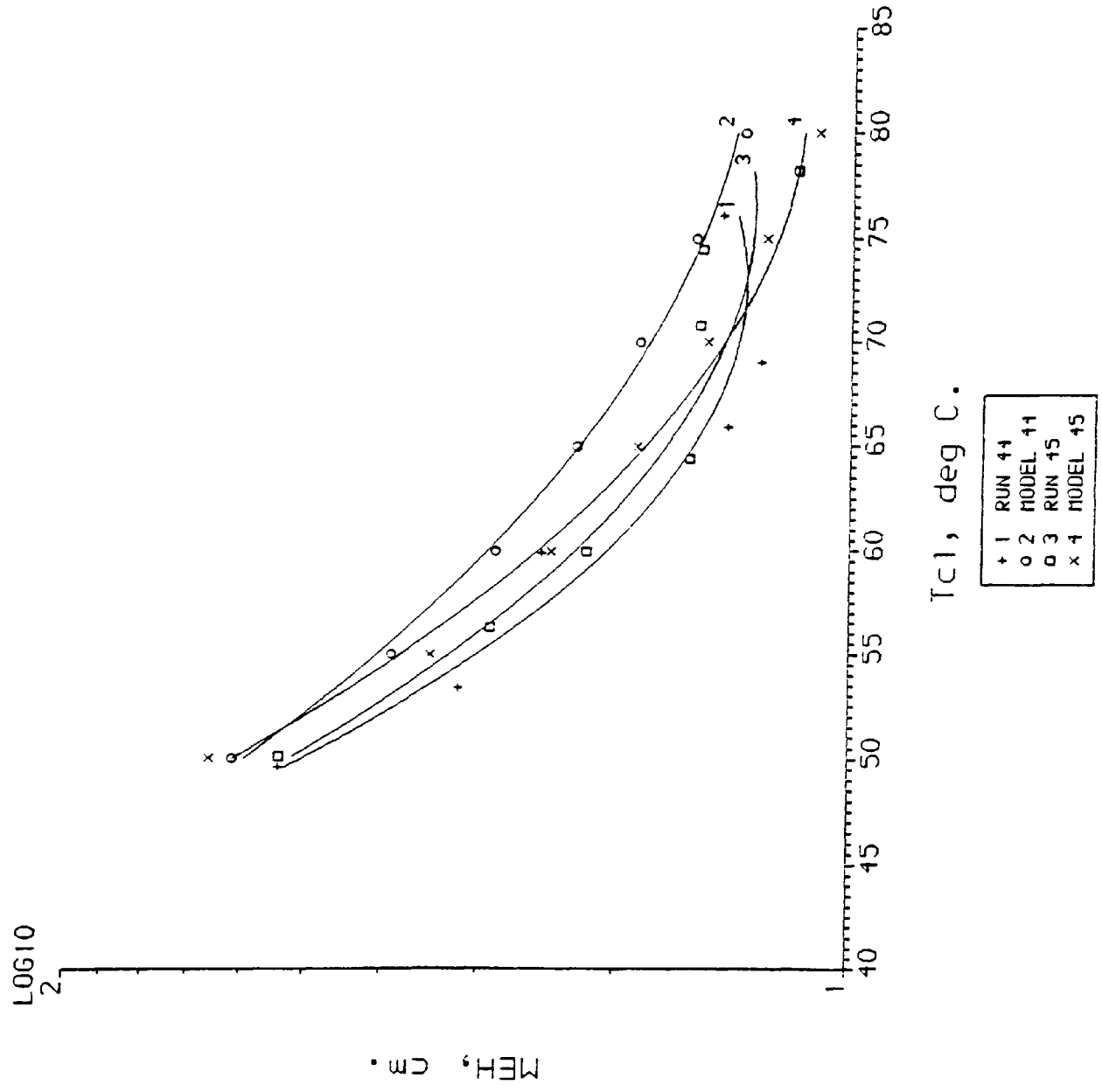
MEH vs Tc1 For Runs 44 & 45.
LOG10
2
1
MEH, cm.
40
45
50
55
60
65
70
75
80
85
Tc1, deg C.
+ 1 RUN 44
o 2 MODEL 44
□ 3 RUN 45
× 4 MODEL 45

Fig.5.27

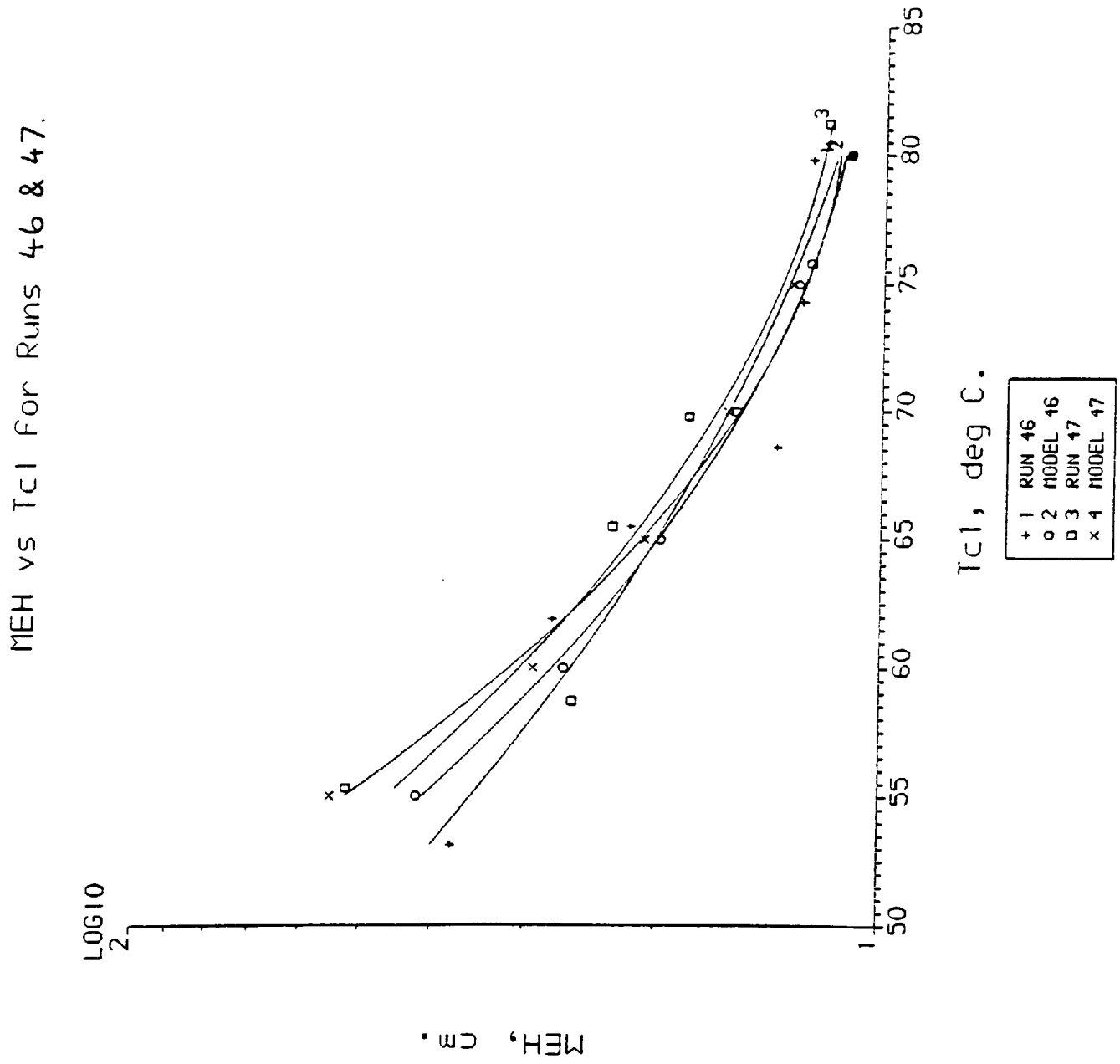
MEH vs Tc1 For Runs 46 & 47.
LOG10
MEH, cm.
Tc1, deg C.
+ 1 RUN 46
o 2 MODEL 46
□ 3 RUN 47
× 4 MODEL 47

Fig.5.28

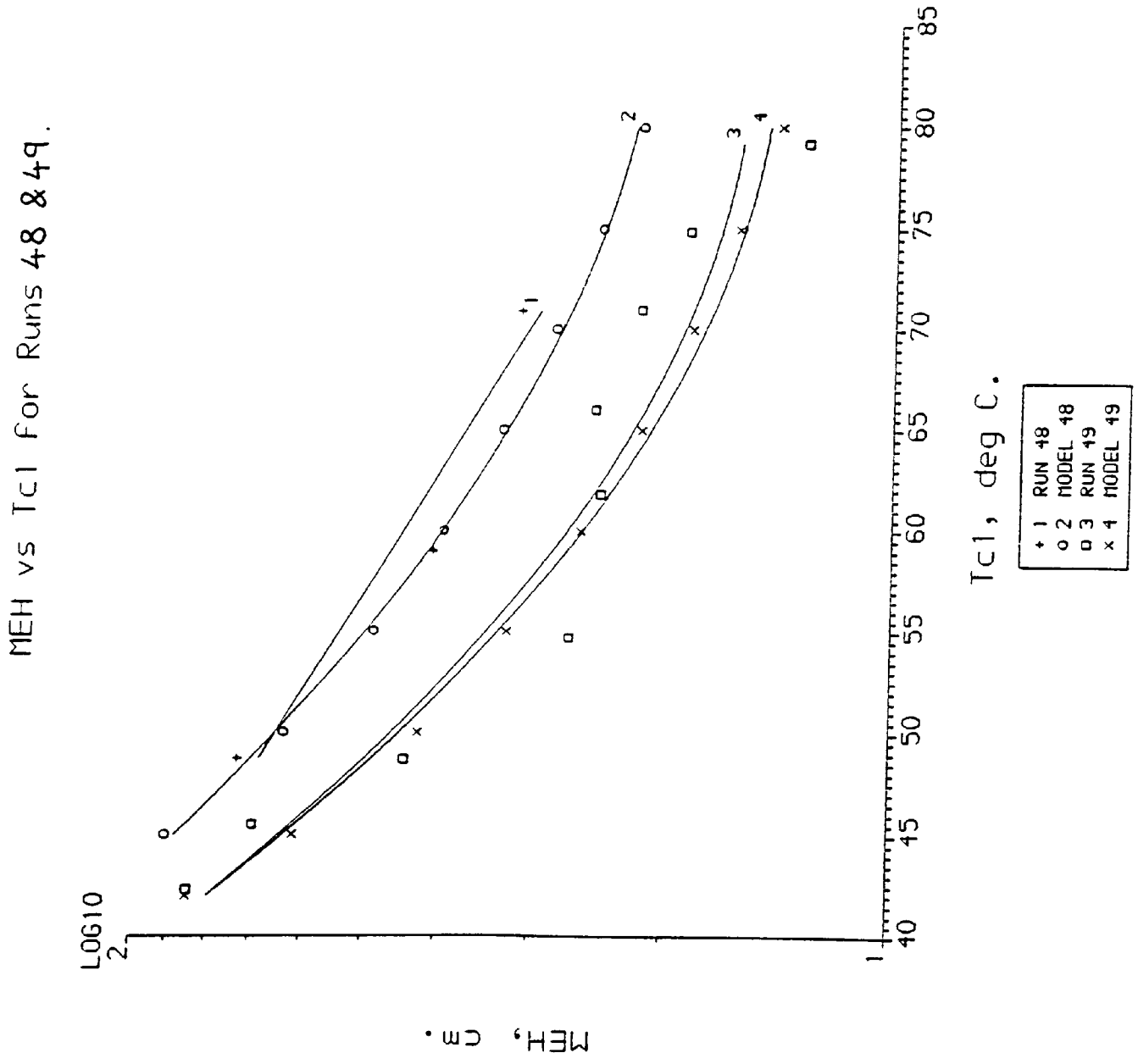
MEH vs Tc1 For Runs 48 & 49.
LOG10
MEH, cm.
Tc1, deg C.
+ 1 RUN 48
o 2 MODEL 48
□ 3 RUN 49
× 4 MODEL 49

Fig.5.29

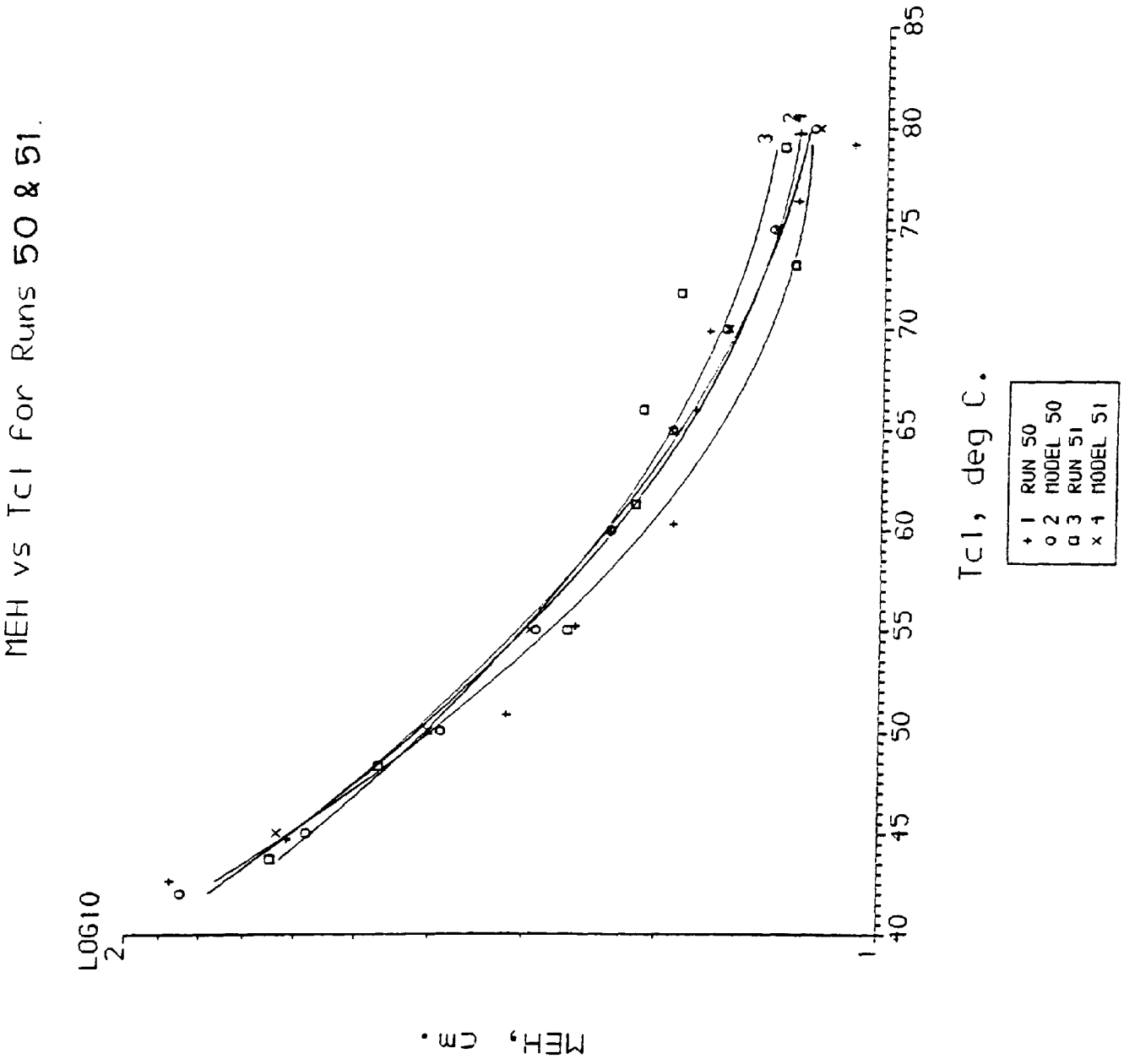
MEH vs Tc1 For Runs 50 & 51.
LOG10
MEH, cm.
Tc1, deg C.
40
45
50
55
60
65
70
75
80
85
1
2
3
4
+ 1 RUN 50
o 2 MODEL 50
□ 3 RUN 51
× 4 MODEL 51

Fig.5.30

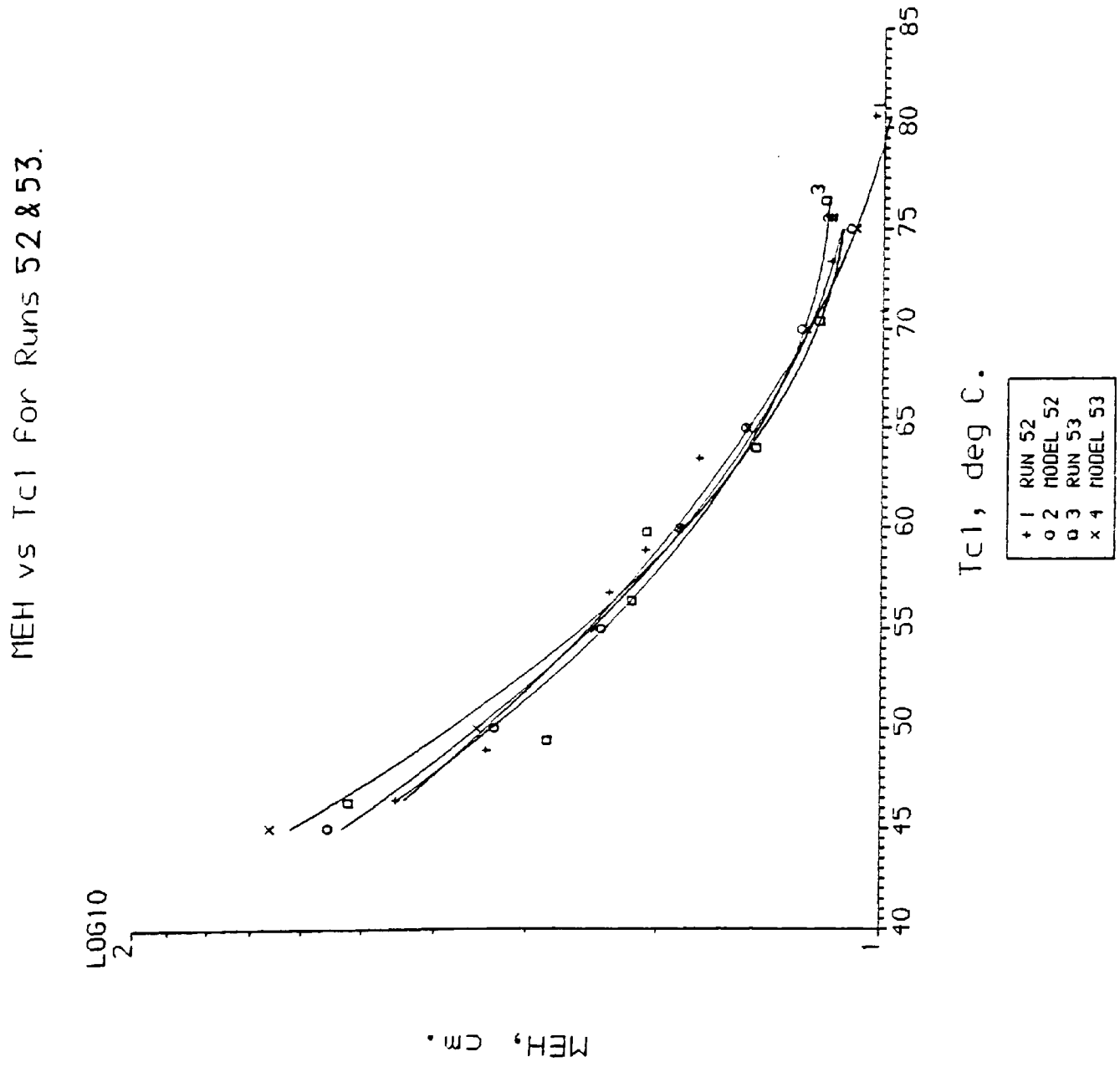
MEH vs Tc1 For Runs 52 & 53.
LOG10
MEH, cm.
Tc1, deg C.
40
45
50
55
60
65
70
75
80
85
1
2
+ 1 RUN 52
o 2 MODEL 52
□ 3 RUN 53
× 4 MODEL 53

Fig.5.31

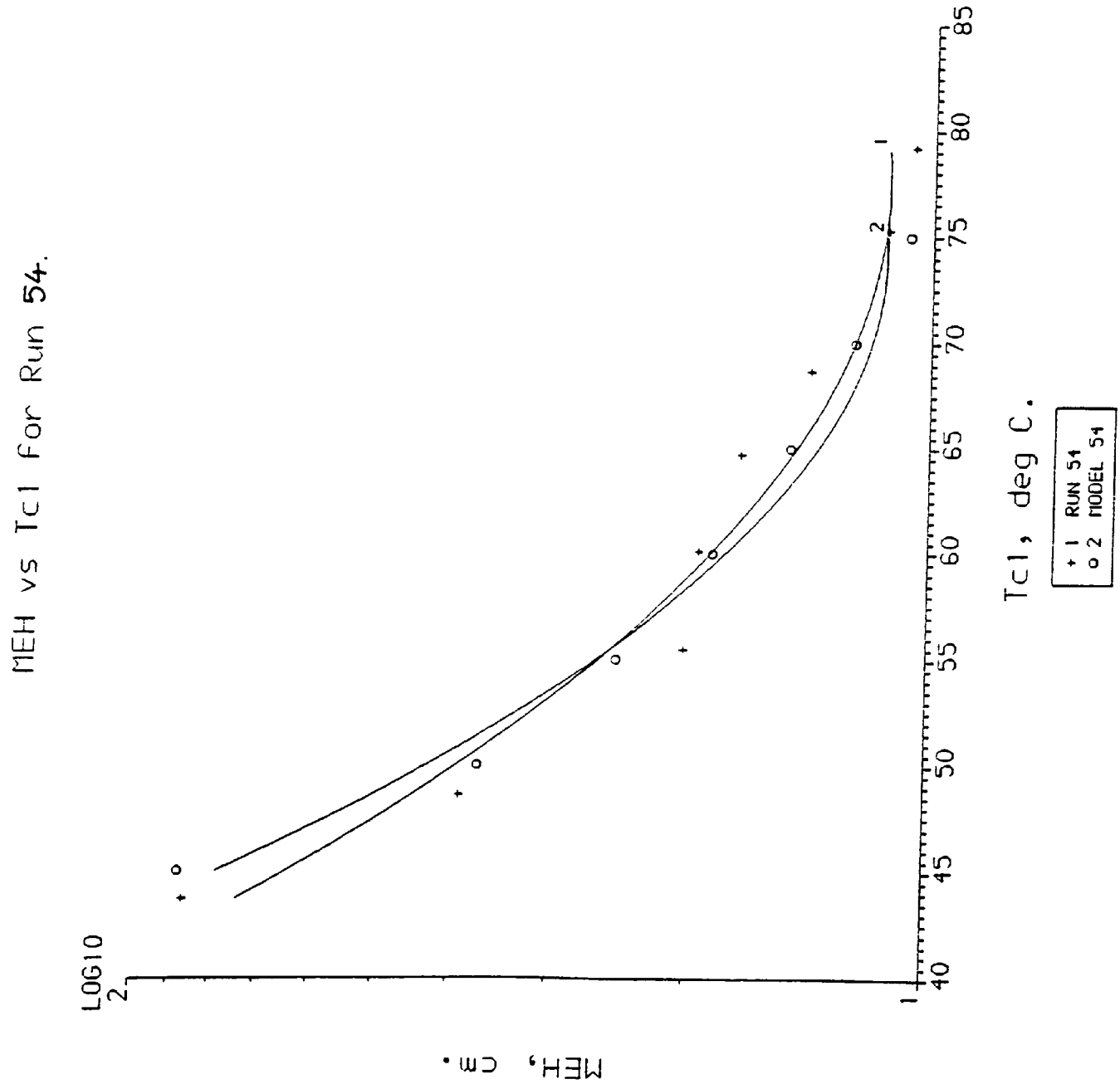
MEH vs Tc1 For Run 54.
LOG10
MEH, cm.
Tc1, deg C.
+ 1 RUN 54
o 2 MODEL 54
40
45
50
55
60
65
70
75
80
85
1
2

Fig.7.2

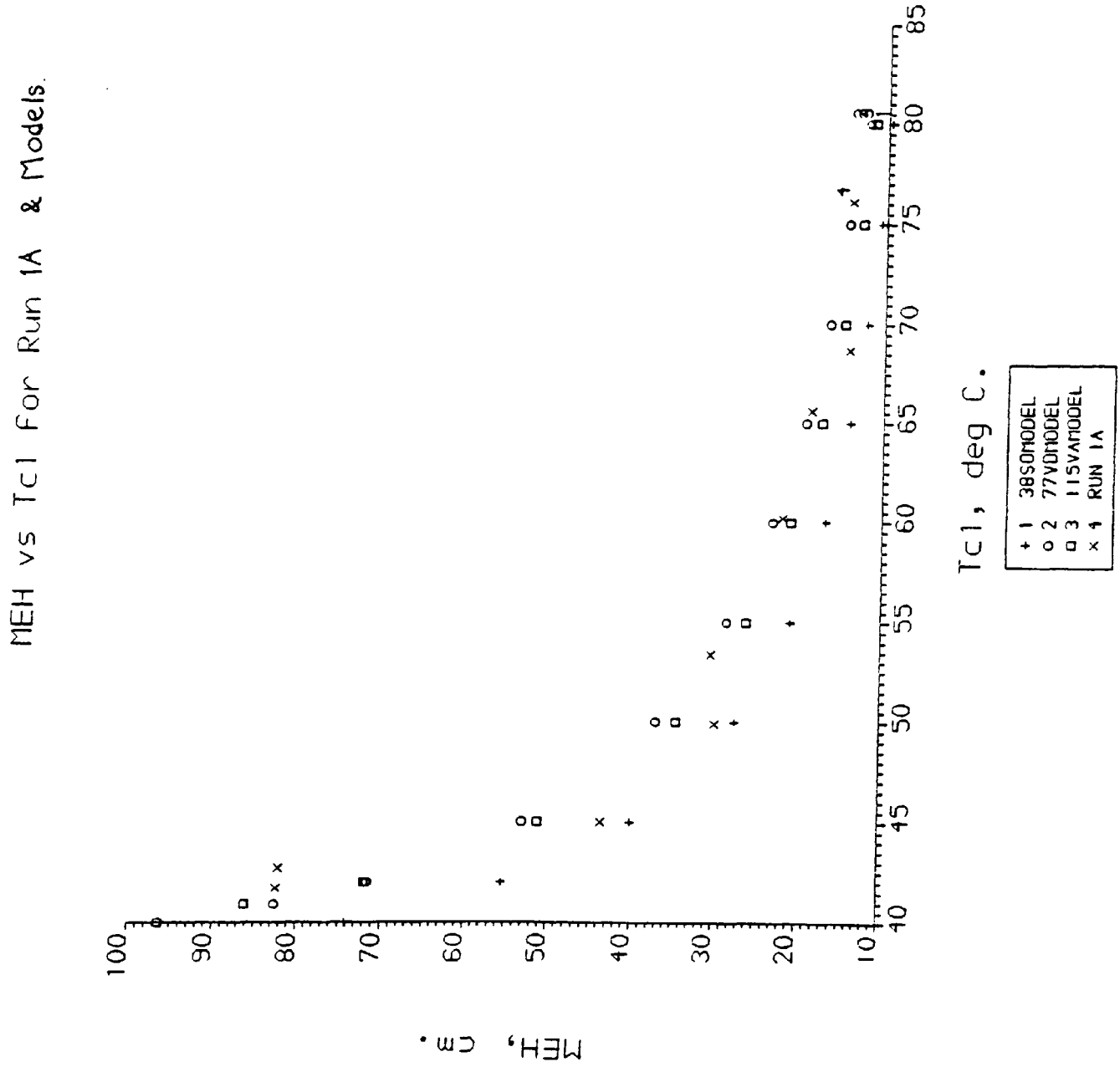
MEH vs Tc1 For Run 1A & Models
MEH, cm.
Tc1, deg C.
+ 1 38SOMODEL
o 2 77VOMODEL
□ 3 115VAMODEL
× 4 RUN 1A

Fig.7.3

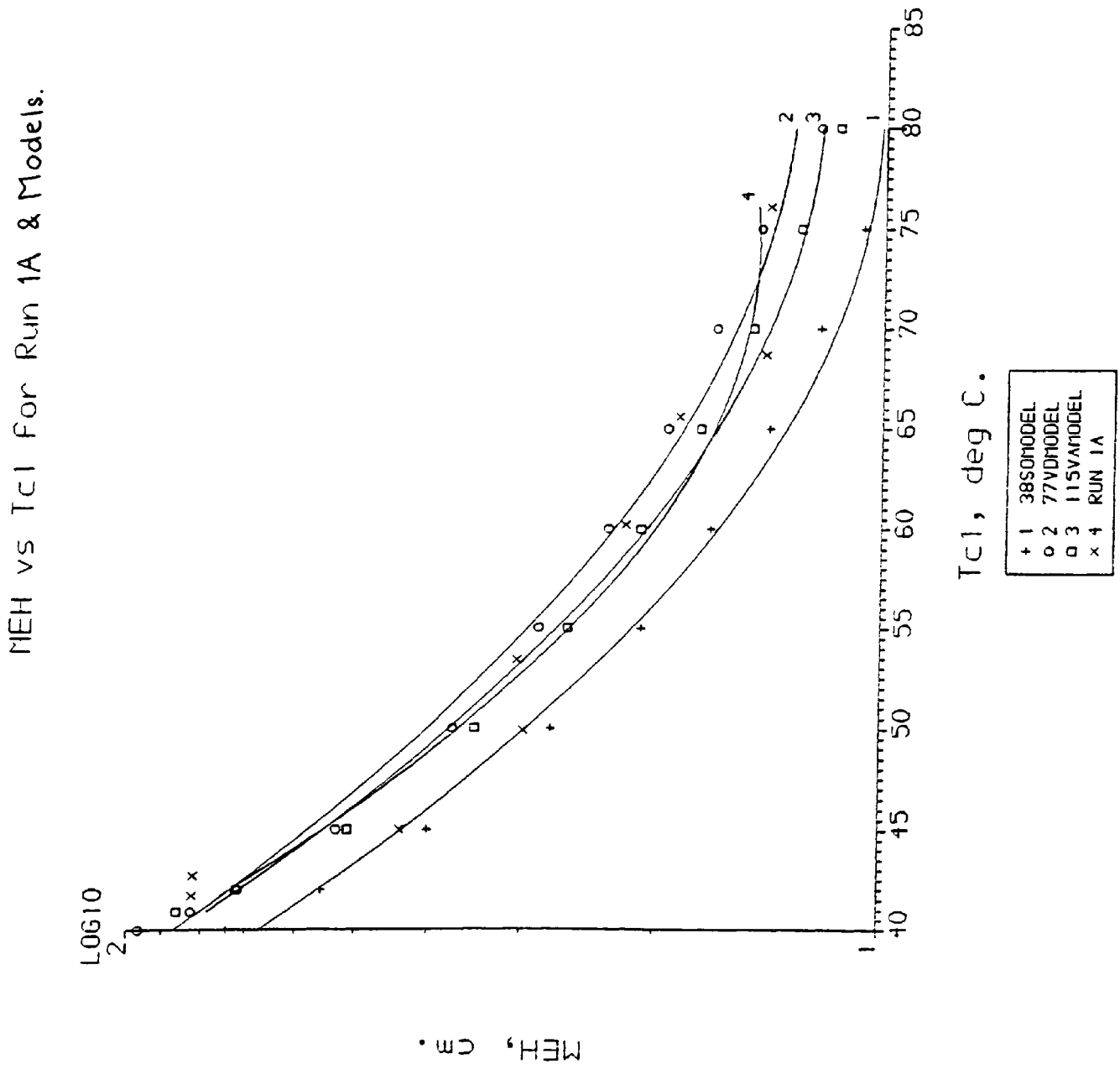
MEH vs Tc1 For Run 1A & Models.
LOG10
MEH, cm.
Tc1, deg C.
+ 1 38SONODEL
o 2 77VDNODEL
□ 3 115VANODEL
× 4 RUN 1A

Fig.7.5

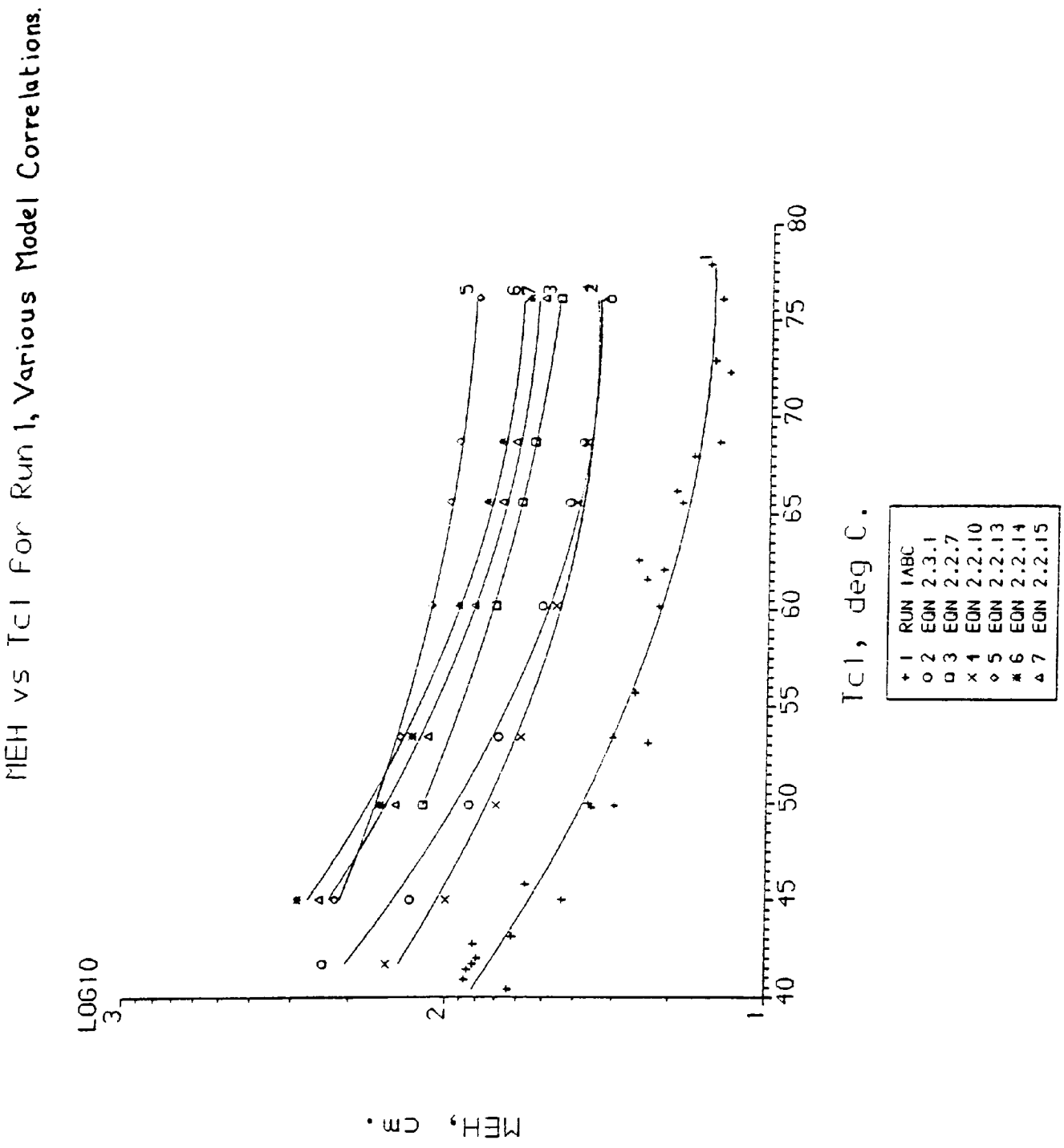
MEH vs Tc1 For Run 1, Various Model Correlations.
LOG10
MEH, cm.
Tc1, deg C.
3
2
1
40
45
50
55
60
65
70
75
80
+ 1 RUN 1ABC
o 2 EQN 2.3.1
□ 3 EQN 2.2.7
× 4 EQN 2.2.10
◇ 5 EQN 2.2.13
✱ 6 EQN 2.2.14
△ 7 EQN 2.2.15

Fig.7.7

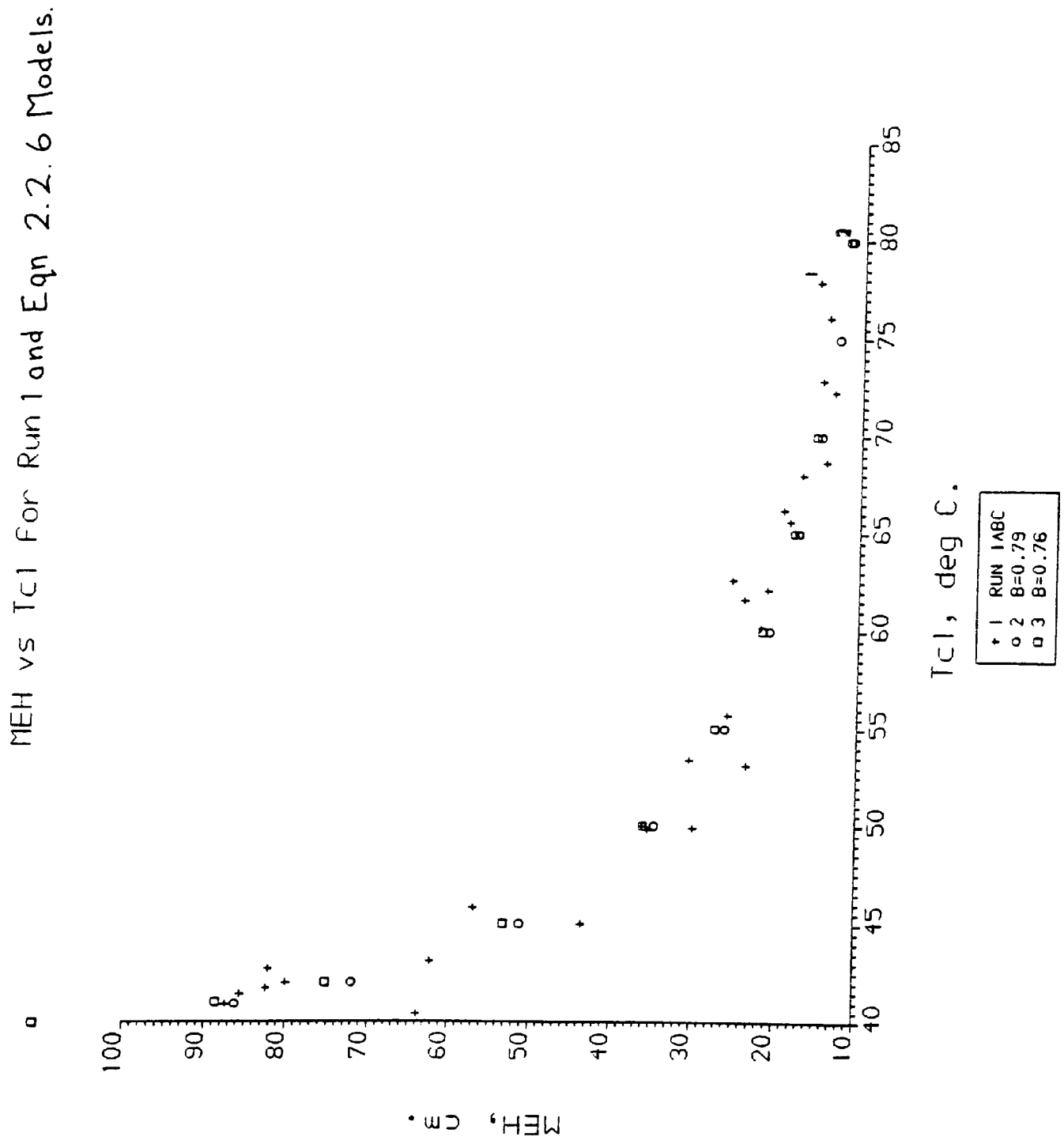
MEH vs Tc1 For Run 1 and Eqn 2.2.6 Models.
MEH, cm.
Tc1, deg C.
1 RUN 1ABC
2 B=0.79
3 B=0.76

Fig.7.8

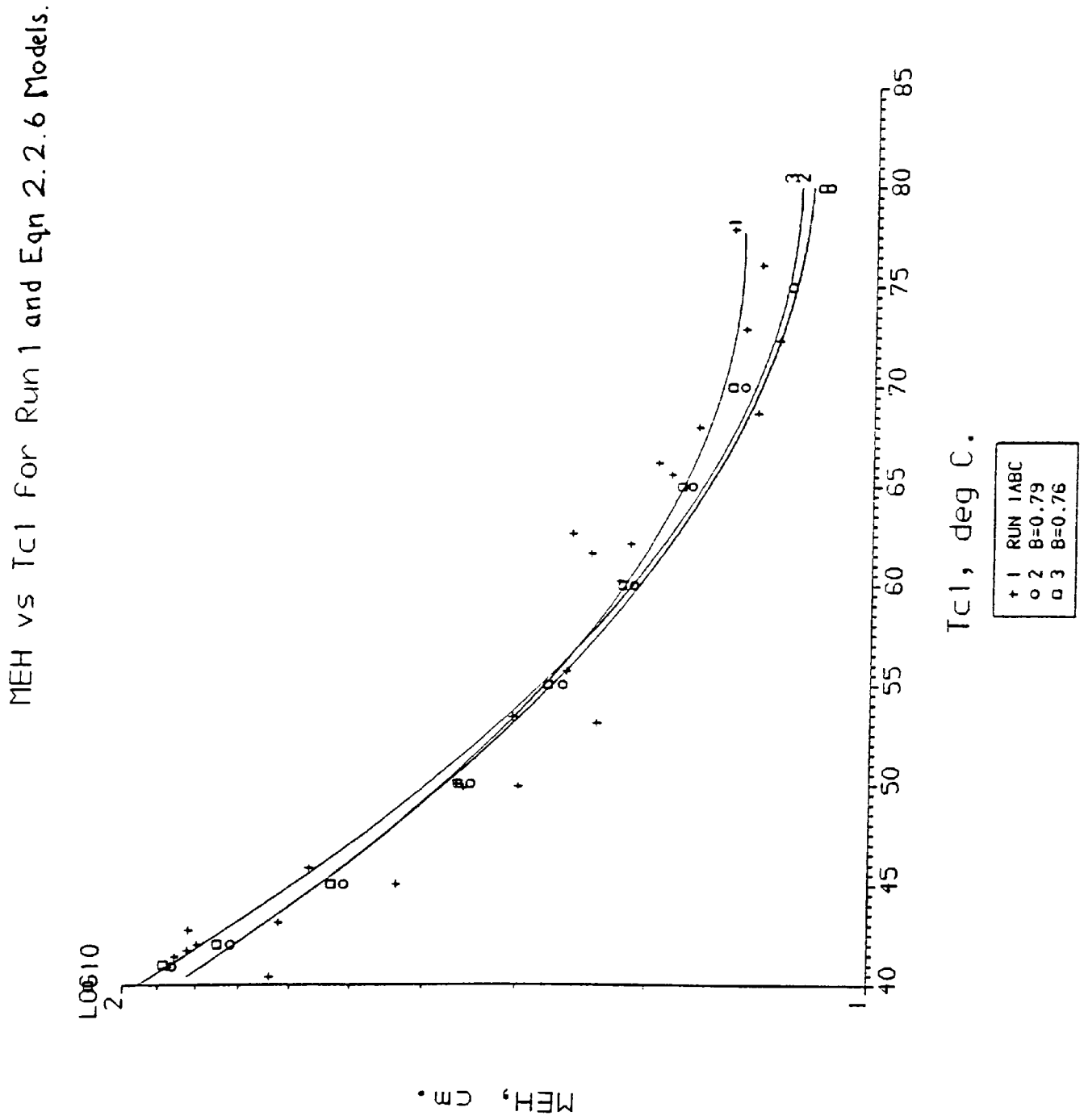
MEH vs Tc1 For Run 1 and Eqn 2.2.6 Models.
LOG10 MEH, cm.
2
1
40
45
50
55
60
65
70
75
80
85
Tc1, deg C.
+ 1 RUN 1ABC
o 2 B=0.79
□ 3 B=0.76

Fig.7.10

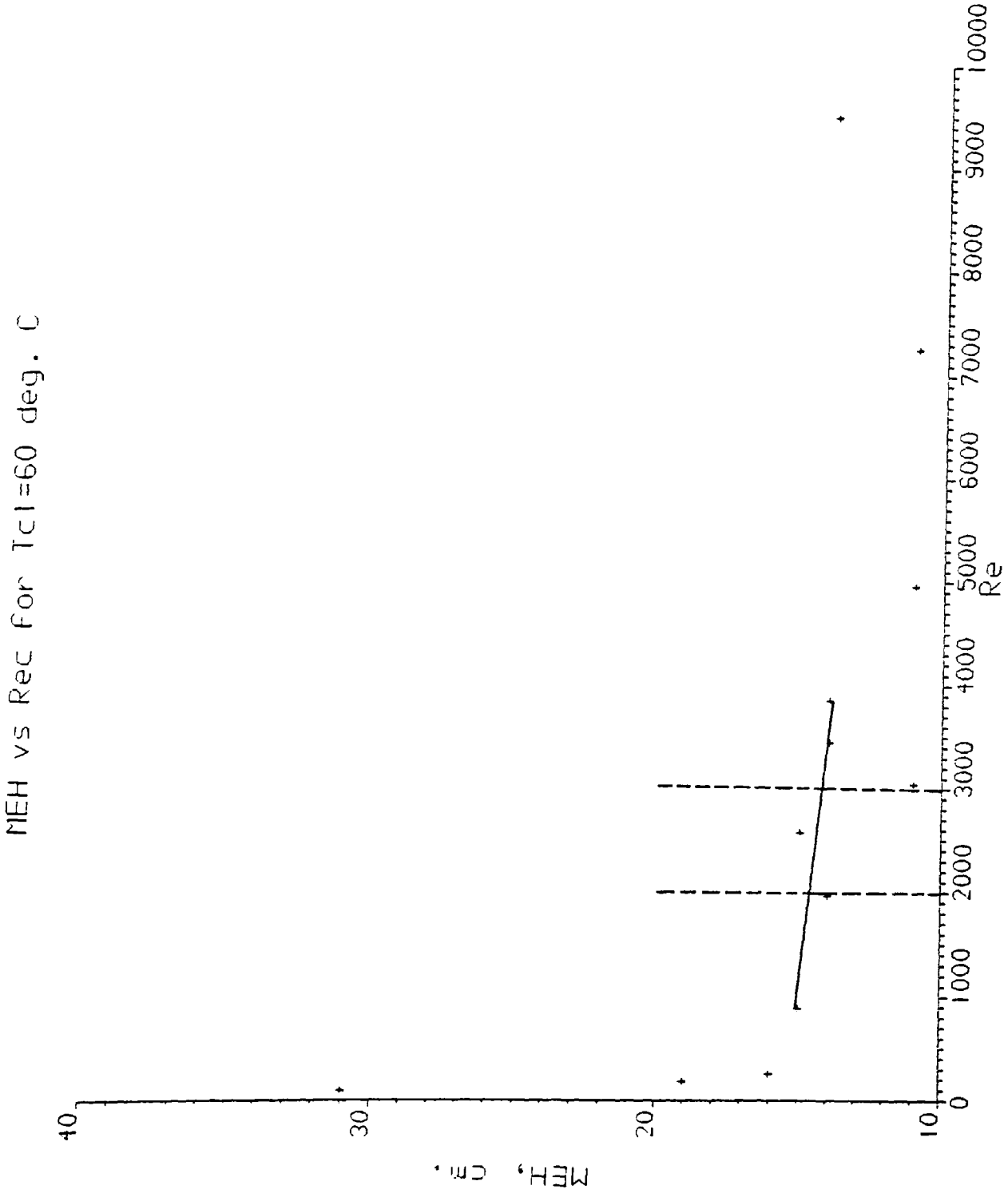
MEH vs Rec For Tc1=60 deg. C
MEH, cm.
Re
10
20
30
40
0
1000
2000
3000
4000
5000
6000
7000
8000
9000
10000

Fig.7.11

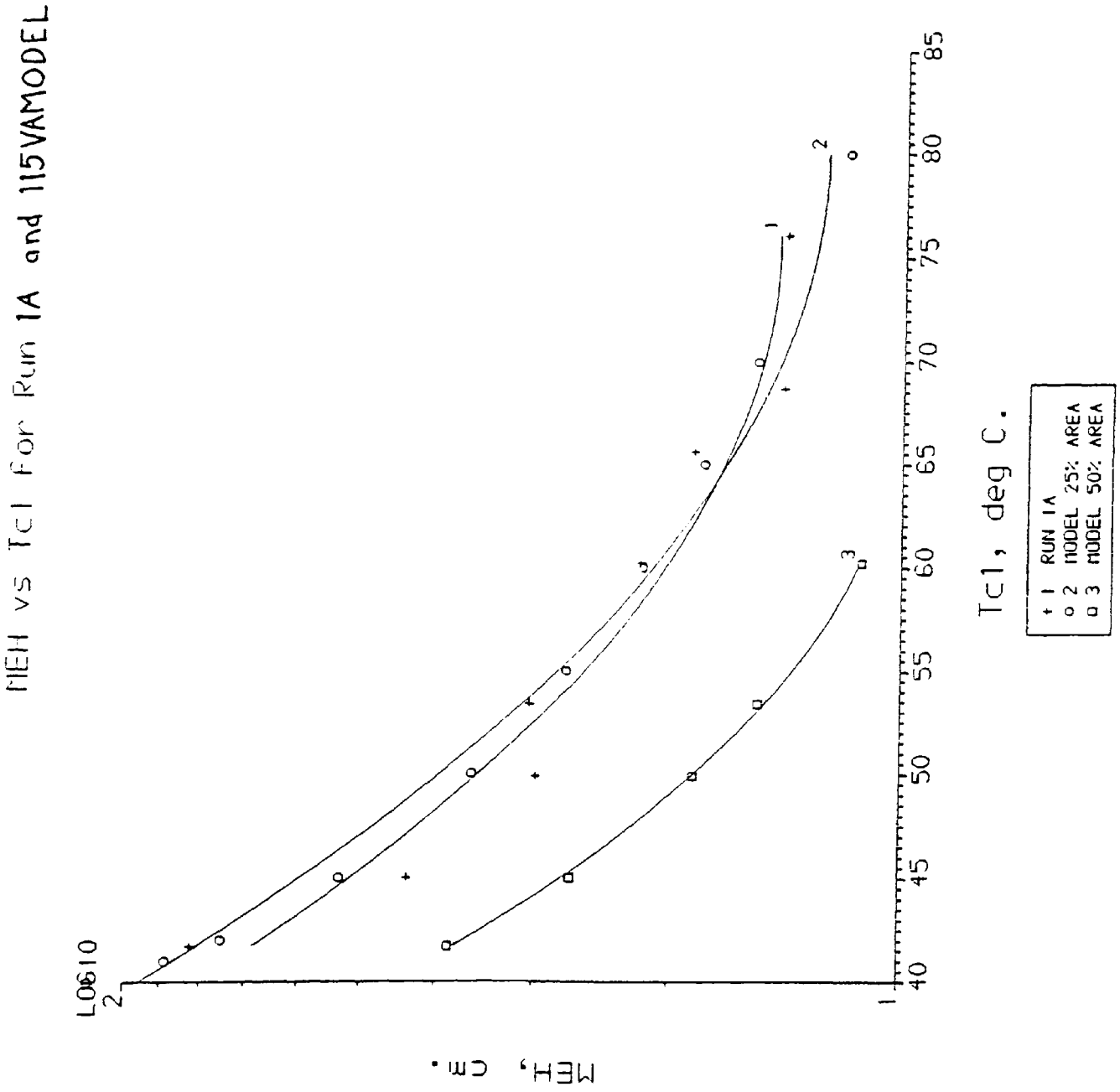
MEH vs Tc1 For Run 1A and 115VAMODEL
LOG10
2
1
40
45
50
55
60
65
70
75
80
85
MEH, cm.
Tc1, deg C.
+ 1 RUN 1A
o 2 MODEL 25% AREA
□ 3 MODEL 50% AREA

Fig.7.12

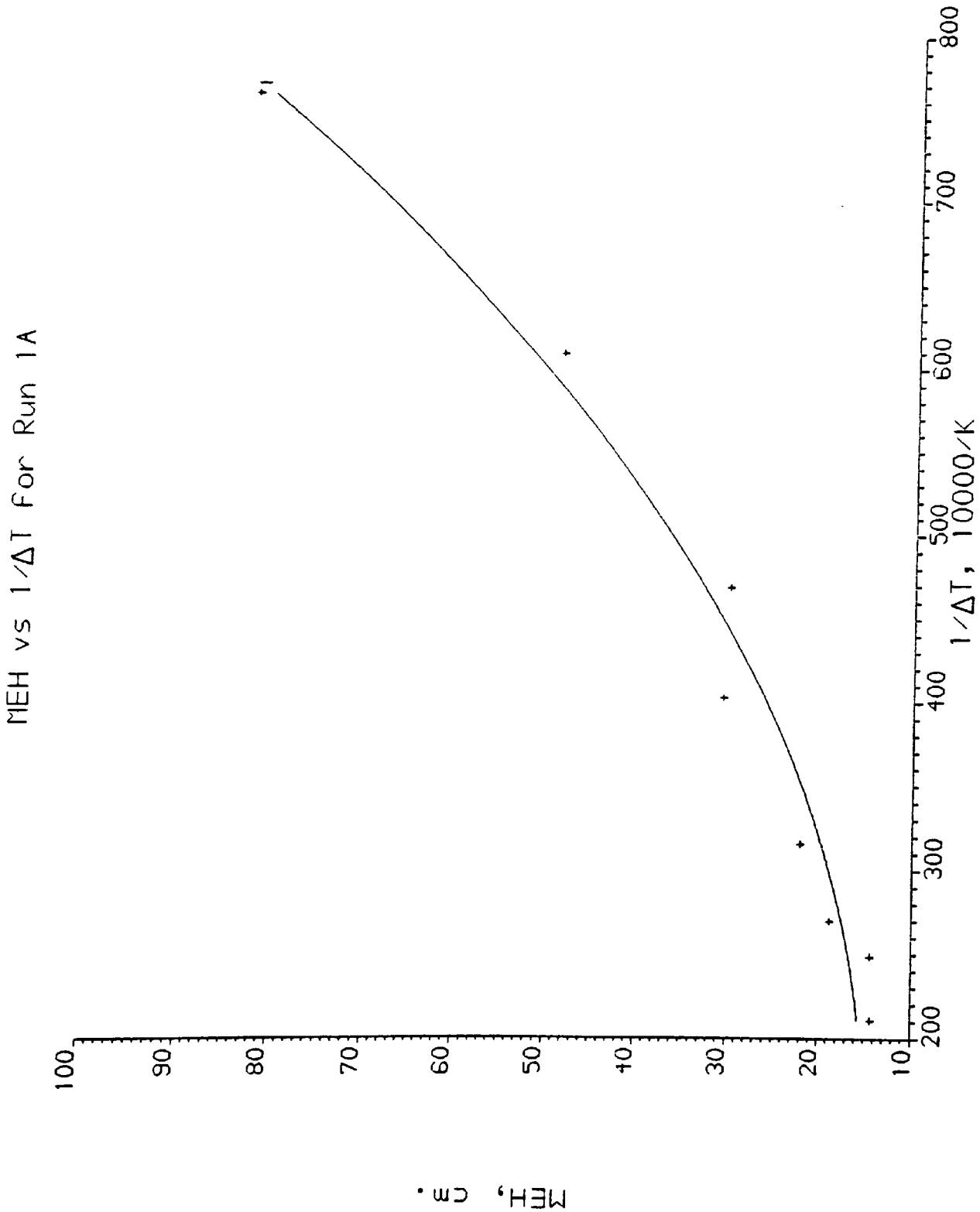
MEH vs 1/ΔT For Run 1A
MEH, cm.
100
90
80
70
60
50
40
30
20
10
200
300
400
500
600
700
800
1/ΔT, 10000/K

Fig.7.13

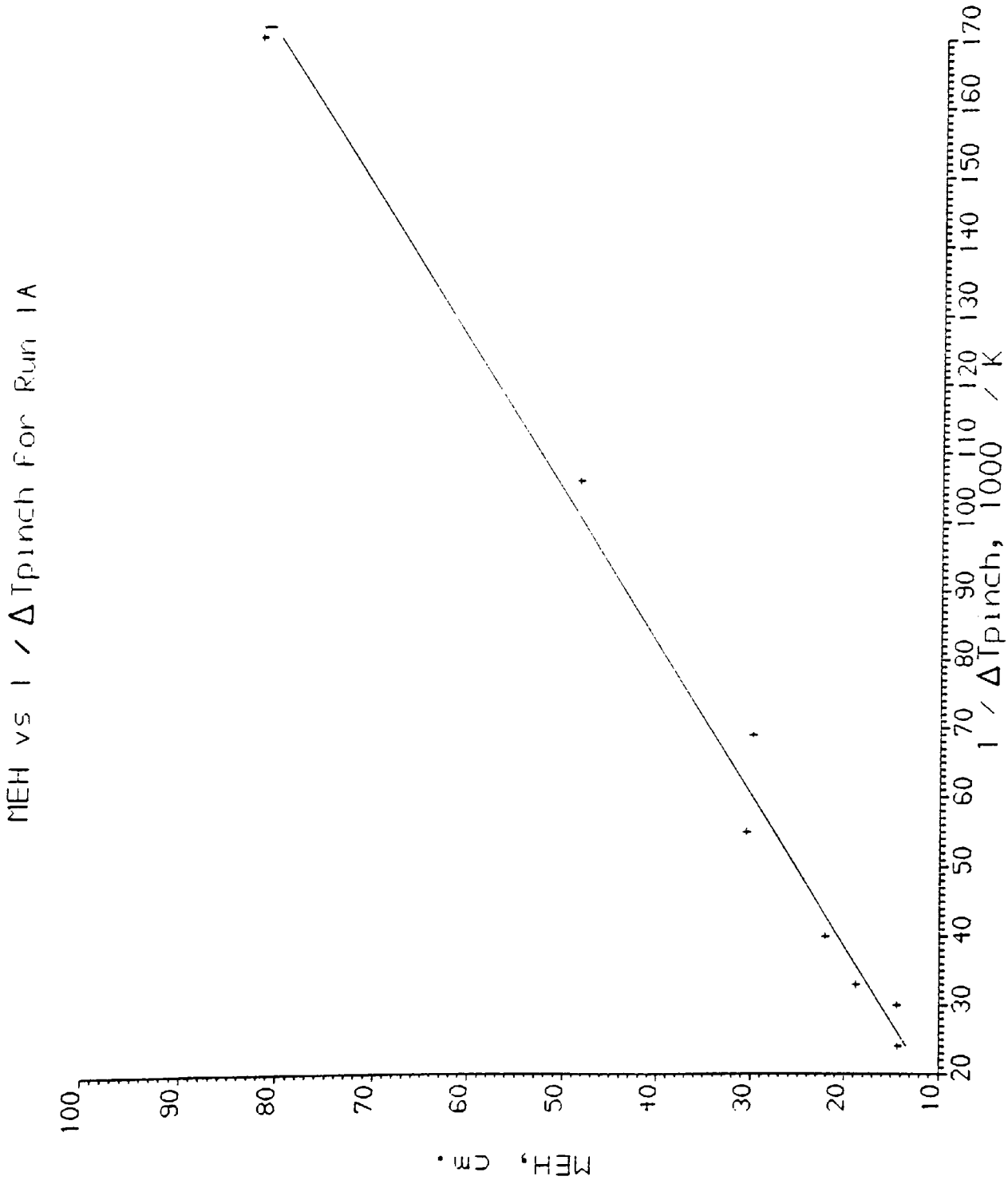
MEH vs 1 / ΔTpinch For Run 1A
ΣEH, cm.
100
90
80
70
60
50
40
30
20
10
20
30
40
50
60
70
80
90
100
110
120
130
140
150
160
170
1 / ΔTpinch, 1000 / K

Fig.7.14

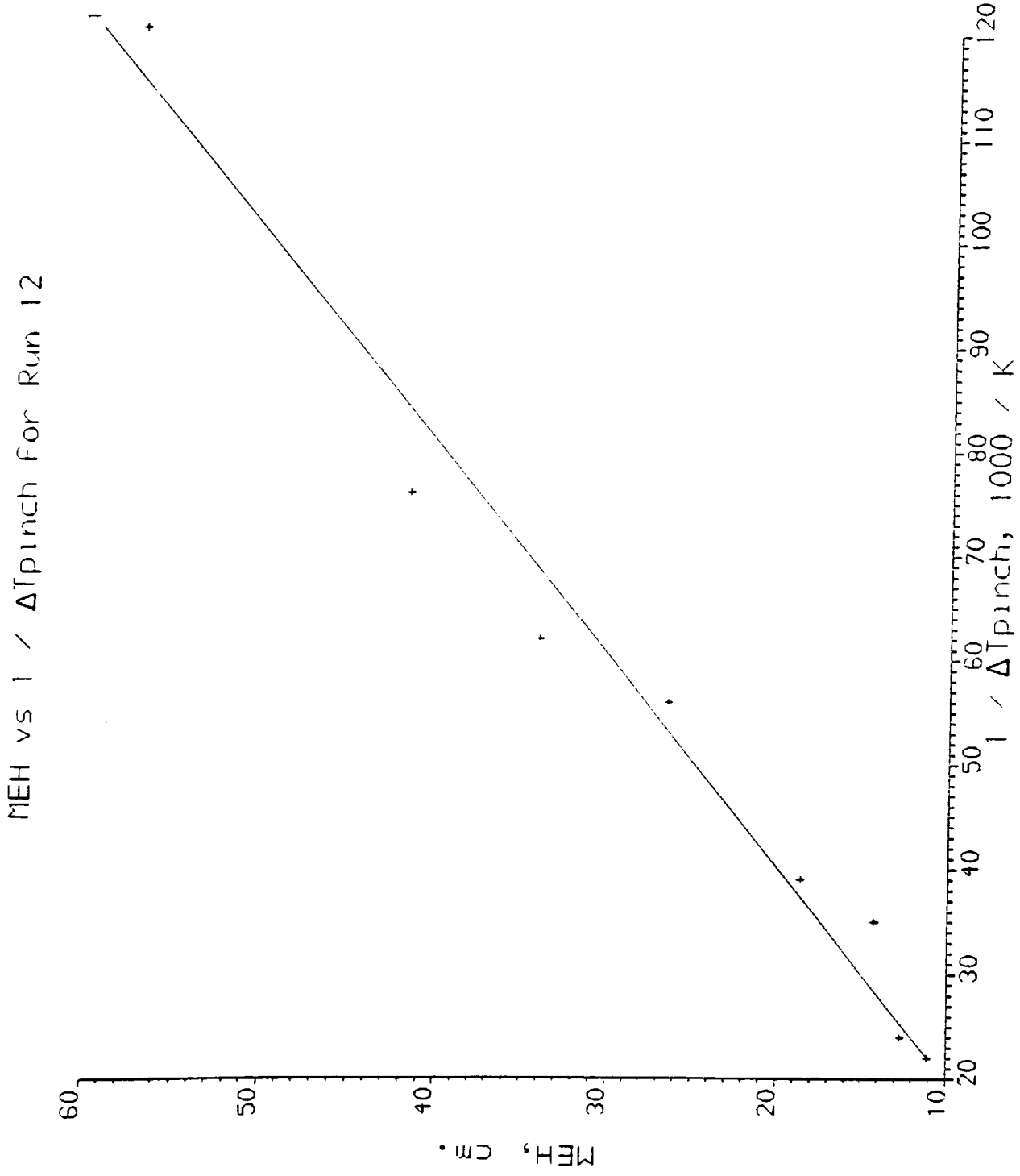
MEH vs 1 / ΔTpinch for Run 12
MEH, cm.
1 / ΔTpinch, 1000 / K
10
20
30
40
50
60
70
80
90
100
110
120

Appendix 18: 115VAMODEL Flowchart.

This is a simplified flowchart for the 115VAMODEL program.

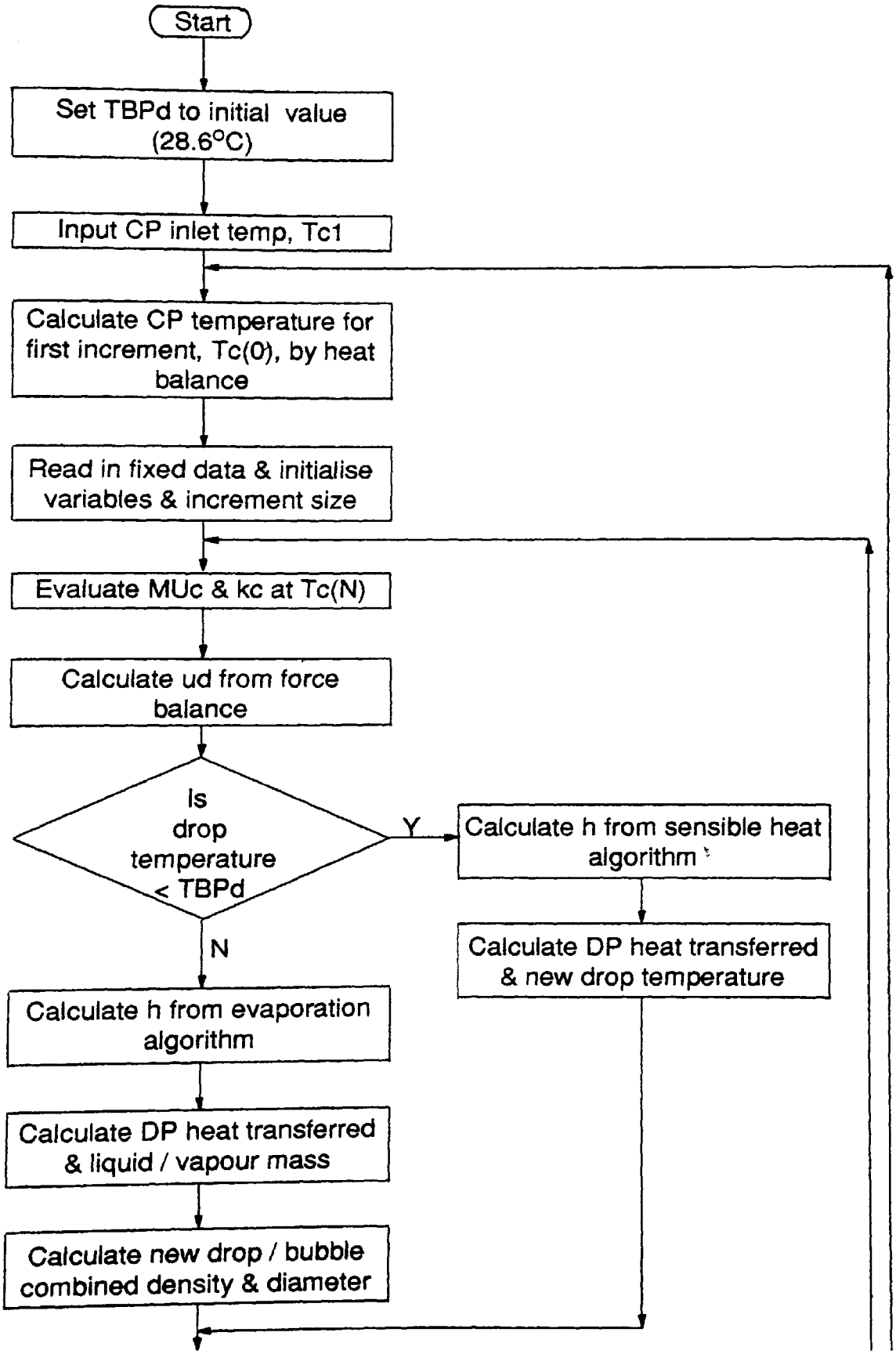

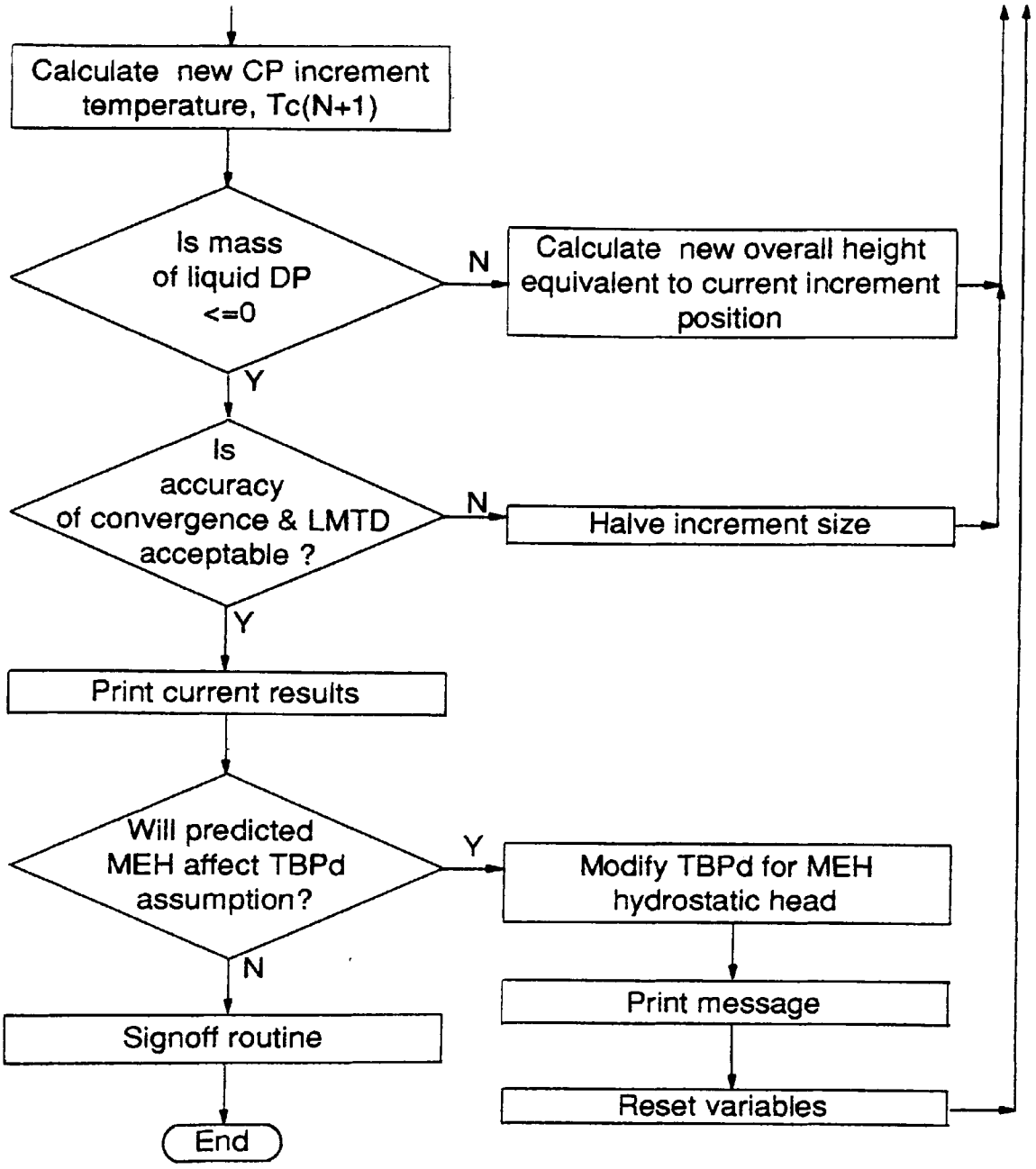
Calculate new CP increment temperature, Tc(N+1)
Is mass of liquid DP <=0
N
Calculate new overall height equivalent to current increment position
Y
Is accuracy of convergence & LMTD acceptable ?
N
Halve increment size
Y
Print current results
Will predicted MEH affect TBPd assumption?
Y
Modify TBPd for MEH hydrostatic head
N
Print message
Signoff routine
Reset variables
End